

rec'd user letter
dtd. 3/5/93

Channel and Hillslope Processes in a Semiarid Area New Mexico

By LUNA B. LEOPOLD, WILLIAM W. EMMETT, and ROBERT M. MYRICK
EROSION AND SEDIMENTATION IN A SEMIARID ENVIRONMENT

GEOLOGICAL SURVEY PROFESSIONAL PAPER 352-G



UNITED STATES GOVERNMENT PRINTING OFFICE, WASHINGTON : 1966

9303110396 930305
PDR WASTE PDR
WT-11

102-8

UNITED STATES DEPARTMENT OF THE INTERIOR

STEWART L. UDALL, *Secretary*

GEOLOGICAL SURVEY

William T. Pecora, *Director*

For sale by the Superintendent of Documents, U.S. Government Printing Office
Washington, D.C. 20402 - Price 50 cents (paper cover)

CONTENTS

	Page		Page
Abstract.....	193	Headcut enlargement.....	229
Acknowledgments.....	193	Fence Line Headcut.....	229
Alluvial fills in western valleys.....	193	Coyote C. Arroyo Headcut.....	230
Geographic setting.....	195	Movement of large particles in headwater rills.....	232
Valley alluvium.....	195	Slopewash Tributary.....	232
The local bedrock.....	198	Gunshot Arroyo.....	232
Relation of valley alluvium and colluvium to headwater areas.....	199	Morning Walk Wash.....	234
Study areas.....	201	Sedimentation in channels and reservoirs.....	235
Methods of study.....	201	Analysis of sediment budget.....	236
Magnitude and frequency of rainfall and streamflow, 1958-64.....	202	Climatological observations during aggradation.....	240
Channel form and bed materials.....	203	References.....	243
Spacing of gravel bars.....	207	Summary of data:	
Movement of coarse particles.....	209	A, Nonrecorded rain-gage data, Arroyo de los Frijoles, 159-63.....	247
Scour and fill.....	215	B, Recorded rain-gage data at Main Project Reach, 1959-62.....	247
Hillslope erosion.....	220	C, Erosion-pin plot in Slopewash Tributary, 1959-64.....	248
Erosion plot on Slopewash Tributary.....	220	D, Slope-retreat pins in Slopewash Tributary, 1959-64.....	249
Slope-retreat pins on Slopewash Tributary.....	222	E, Iron-pin lines in Slopewash Tributary, 1958-64..	250
Other measurements of slope erosion on Slopewash Tributary.....	227	F, Erosion nail lines in Coyote C. Arroyo, 1961-64..	250
Erosion nails on Coyote C. Arroyo.....	227	G, Nail sections A-J in Slopewash Tributary, 1959-64.....	251
Tracing of fluorescent sand.....	227	H, Mass-movement line in Slopewash Tributary, 1959-64.....	251
Channel enlargement on Slopewash Tributary.....	228	I, Mass-movement line in Coyote C. Arroyo, 1961-64..	251
Deep or mass movement.....	228	J, Movement of coarse particles in Morning Walk Wash, 1961-64.....	252
Slopewash Tributary.....	228		
Coyote C. Arroyo.....	229		

ILLUSTRATIONS

	Page
FIGURE 138. Location map.....	195
139. Detailed area map.....	196
140. Photographs showing typical aspects of valleys and terraces.....	197
141. Diagrammatic cross section of alluvial valley.....	198
142. Stratigraphic cross sections of minor tributaries.....	200
143. Topographic map of Arroyo de los Frijoles.....	202
144. Topographic map of Slopewash Tributary.....	204
145. Sketch map of Coyote C. Arroyo.....	205
146. Photographs of several study areas.....	207
147-150. Graphs showing:	
147. Magnitude and frequency of streamflows, Arroyo de los Frijoles.....	208
148. Relation of channel width and drainage area to channel length.....	209
149. Bed-material grain-size analyses.....	210
150. Distribution of coarsest particles along length of channel.....	211
151. Sections showing spacing and composition of gravel bars.....	212
152. Photographs of painted rock experiments.....	214
153-156. Graphs showing:	
153. Effect of spacing and particle size on ability of flows to move rocks.....	215
154. Summary of data relating discharge, size, and spacing for painted rock experiments.....	216
155. Transport distance of rocks as function of particle weight.....	217
156. Transport distance of rocks as function of discharge.....	219

FIGURE		Page
	157. Photograph of scour chain.....	220
	158-161. Graphs showing:	220
	158. Downstream pattern of scour and fill for different time periods.....	221
	159. Depth of scour as function of discharge.....	222
	160. Scour and fill, Main Project Reach.....	223
	161. Accumulative net changes in bed elevation, Arroyo de los Frijoles.....	224
	162. Photographs of erosion pins.....	225
	163. Sketch map showing slope-retreat pins, Slopewash Tributary.....	226
	164. Graph showing 6-year net erosion, Slopewash Tributary.....	227
	165. Photograph of Fence Line Headcut.....	229
	166. Photographs of headcuts and valley alluvium.....	230
	167. Topographic map and profile, Coyote C. Arroyo headcut.....	231
	168. Photograph of Green Rock Gulch.....	232
	169. Profile of Gunshot Arroyo showing movement of coarse particles.....	233
	170. Topographic map of dam and reservoir, Coyote C. Arroyo.....	235
	171-174. Graphs of:	
	171. Precipitation parameters, 1853-1962, for station at Santa Fe, N. Mex.....	241
	172. Individual summer rains.....	241
	173. Individual nonsummer rains.....	242
	174. Average annual intensity of rainfall.....	243

TABLES

TABLE		Page
1.	Characteristics of locations studied.....	201
2.	Summary of flows at three locations along Arroyo de los Frijoles, 1958-63.....	203
3.	Relation of transport distance to flow discharge.....	218
4.	Mean depth of scour as a function of discharge.....	220
5.	Summary of particle movement, Morning Walk Wash, 1961-62.....	234
6.	Observed sedimentation in reservoir behind dam on Coyote C. Arroyo, 1961-64.....	232
7.	Observed rates of channel changes in Coyote C. Arroyo, 1961-64.....	236
8.	Data on measured rates of erosion and deposition.....	237
9.	Average rates of erosion and deposition.....	238

EROSION AND SEDIMENTATION IN A SEMIARID ENVIRONMENT

CHANNEL AND HILLSLOPE PROCESSES IN A SEMIARID AREA, NEW MEXICO

By LUNA B. LEOPOLD, WILLIAM W. EMMETT, and ROBERT M. MYRICK

ABSTRACT

Ephemeral washes having drainage areas from a few acres to 5 square miles are shown by actual measurement to be accumulating sediment on the streambed. This aggradation is not apparent to the eye but is clearly shown in 7 years of annual remeasurement.

A similar aggradation was in progress in the same area some 3000 years ago as evidenced by an alluvial terrace later dissected by the present channel system. At that time as well as at present, aggradation occurred even in tributary areas draining a few acres. Colluvial accumulations merge with channel deposits and blanket the valleys and tributary basins even up to a few hundred feet of the drainage divides.

The present study concerned the amounts of sediment produced by different erosion processes in various physiographic positions in the drainage basins. Measurements show that by far the largest sediment source is sheet erosion operating on the small percentage of basin area near the basin divides.

Channel movement, gully head extension, and channel enlargement are presently small contributors of sediment compared with sheet erosion on unrilled slopes. As in previous studies, not all of the erosion products could be accounted for by accumulations on colluvial slopes and on beds of channels. The discrepancies are attributed primarily to sediment carried completely out of the basins studied and presumably deposited somewhere downstream.

Aggradation of alluvial valleys of 5 square miles area and smaller both in the present epicycle, and in prehistorical but post-glacial times in this locality, cannot be attributed to gully- or rill extension in the headwater tributaries but to sheet erosion of the most upstream margins of the basins.

Studies of rainfall characteristics of the 7 years of measurement compared with previous years in the 100-year record do not provide a clear-cut difference which would account for the presently observed aggradation of channels. Longer period of measurement of erosion and sedimentation will be necessary to identify what precipitation parameters govern whether the channels aggrade or degrade.

ACKNOWLEDGMENTS

This study was conceived and initiated by Dr. John P. Miller and the senior author in the summer of 1958, and fieldwork was continued during each successive summer for periods of 1-3 weeks. Immediately following the field season of 1961 Dr. Miller died from bubonic plague contracted during that fieldwork. We resolved to execute the work thereafter with especial diligence.

An important part of the observations made during the first 5 years consisted of the data on the movement of the hundreds of individual cobbles which had been painted for identification. Emphasis was gradually shifted to the observations on rates of erosion and sediment movement which had been begun as only an auxiliary part of the original investigation. It is with these observations that the present paper is primarily concerned.

For permission to work on the property known as Las Dos and for many other courtesies we are grateful to the late Mrs. Adelina Otero-Warren. Dr. Bergere Kenney has kindly encouraged the work to continue on that property.

The slope-area measurements of discharge and many other observations when we were not in the area were made under the direction of Wilbur L. Heckler, district engineer for the U.S. Geological Survey in Santa Fe. Louis J. Reiland, Leo G. Stearns, Charlie R. Sieber, Leon A. Wiard, and others of the Santa Fe office contributed materially to these observations.

Field assistants and technical associates during various seasons included Brandis Marsh, Peter Sparks, Macklin Smith, Olav Slaymaker, Thomas Detwyler, Garnett Williams, and Lehn Franke.

The C¹⁴ analysis of the charcoal sample was run by Dr. Meyer Rubin in the laboratory of the Geological Survey in Washington, D.C.

For their review, comments, and suggestions, we are indebted to Stafford C. Happ, Asher P. Schick, George H. Dury, S. A. Schumm, R. F. Hadley, M. R. Collings, W. L. Heckler, and L. J. Reiland.

ALLUVIAL FILLS IN WESTERN VALLEYS

To cross any valley in the foothills of a large part of the western conterminous United States is to traverse a flat floor of stream-deposited alluvium. Many such floors, once smooth and undissected, are now trenched by arroyos or troughlike gullies. Abandoned flood plains or alluvial terraces can be seen in many such valleys, representing the surfaces of previous valley fills.

A large literature describes the local sequences of alluviation and erosion in such valleys, and there appears to be considerable contemporaneity in the timing of these alterations in post-Pleistocene time over an area that stretches from Wyoming to Texas. When grazing by cattle reached peak intensity about 1880, the most recent epicycle of valley trenching began in what is now believed to be a coincidence of climatic conditions conducive to erosion and degradation of the vegetative cover by overuse.

The alluvium which now fills these valleys and which is being trenched is usually similar in texture to that representing the fills of previous epicycles, though in some places the recent fill material is somewhat coarser. This alluvium is predominantly silt, often fine sandy silt, sometimes silty fine sand. The amount of clay is generally not great. The fills may be only a few feet deep in ephemeral tributaries draining several acres, and can be at least 50-feet thick through long distances. The latter figure applies to the alluvial valley, 150 miles in length, of the Rio Puerco, a tributary to the Rio Grande.

Three periods of late Pleistocene and recent alluviation are recognized in many places in Western States. The most recent fills now being eroded are less deep than those of previous periods of aggradation represented by the terraces which stand above the present valley floors, so even larger amounts of alluvium were stored in valleys in the past than are now observed.

Thus an immense amount of silty and fine-sandy alluvium has been produced by ephemeral drainage basins in the five states—Arizona, New Mexico, Utah, Colorado, and Wyoming—and has been deposited in valleys. When a period of valley trenching occurred, much was eroded out, carried downstream, and the process repeated.

It is logical to suppose that the source of sediment which would contribute to such aggradation during the periods of alluviation would be rill and gully erosion in the headwater tributaries. Deposits in the valley must have been derived from the basin upstream. But alluviation, when it occurred in the main valleys or master streams, also affected minor tributaries as well. The ground surface seems to sweep from valley floor up to the adjacent hills and up tributary valleys in concave-to-the-sky profiles. The topography of the adjacent hills seems to have been drowned in a sea of alluvium, softening and smoothing the surface configuration of the whole landscape. This phenomenon occurs widely and is the general rule in Nebraska, Kansas, Missouri, and the driftless area as well as in New Mexico, Wyoming and other parts of the Rocky Mountain area.

So widespread has been the phenomenon of valley aggradation with silty alluvium and so large are the volumes of sediment involved that the geomorphologist may wish to see examples of present-day streams currently undergoing such alluviation, and to discern the areal sources of the material being deposited. But, interestingly, it is difficult to designate channels undergoing such a process—at least any that are identifiable by visual or qualitative criteria. The processes which were so important even in the historic past cannot easily be observed at present.

Furthermore, if Leopold and Miller (1954) were correct in their assertion that the source of the valley alluvium was not in channel and gully erosion of the headwaters, then the processes of such sediment production must have been mass wasting and sheet erosion. The first of these is a process little studied and the second is a process studied far more on agricultural than on grazing or uncultivated areas. Little is known about rates of such processes on nonagricultural land, nor have the effects of relief, land slope, vegetation density, or other relevant factors been observed.

The present investigation was initiated to study both process and rate of aggradation and degradation in the channels, rills, and on the hillslopes of a drainage basin typical of many parts of the semiarid West. This paper is a progress report on that study.

Investigations of the kind described here involve the operation of field stations and specific experiments over a period of several years. Results can be obtained only at infrequent intervals because of the sporadic character of the precipitation. The general method, then, was to establish observation stations which could be visited for resurvey during a period of a few weeks in summer each year, and to maintain a more restricted number of observations after each important storm. The area chosen, Arroyo de los Frijoles near Santa Fe, N. Mex., was one in which previous work had been done by Leopold and Miller (1956), and for this reason it provided a familiar geographic and geologic background on which to base further investigations.

Our objective was to integrate several aspects of fluvial processes operating in the area: specifically, to study sheet erosion on the divide and interstream areas, slope retreat adjacent to steep-walled gullies that prevail in the uplands, and in particular, the movement of coarse and fine sediment down the arroyos of various dimensions. To this end, various kinds of measuring devices were gradually developed and installed. The results reported here represent information collected during 7 years of observation, but some measurements have been made for only a part of the 7-year period.

GEOGRAPHIC SETTING

Arroyo de los Frijoles and the other ephemeral channels discussed here are a few miles west-northwest of Santa Fe, N. Mex. (figs. 138 and 139). They are typically many small arroyos or dry channels in the lowlands of the Rio Grande Depression at the base of the Sangre de Cristo Range. As one approaches Santa Fe from the west, the Sangre de Cristo Mountains appear to be abutted by a broad sloping surface underlain by poorly consolidated sand and gravel. There are actually several surfaces differing but slightly in elevation. However, the local relief is considerable, with rolling hills dissected by gullies, rills, and broad sandy-floored washes. As is typical of arid regions everywhere, these channels present almost endless variety. They range from tiny rills near the drainage divide to deep, wide arroyos incised in flat alluvial valleys. Vegetation is sparse, both adjacent to the channels and on the interfluvies between them. In general the area is a woodland association, including juniper, piñon, sage, and a low-density understory of grasses.

Because of its geological character and climate, the area studied is characterized by huge amounts of both fine and coarse sediment readily available for transportation. During runoff sediment may be derived from the unconsolidated country rock or from recent alluvium adjacent to the channels.

An arroyo discharges water only when a moderately heavy rain falls on the drainage basin. This is a summertime phenomenon because heavy rains fall only from thunderstorms. No flow occurs during the winter. Ordinarily during a summer there are about three rainstorms of sufficient magnitude to produce runoff. However, only exceptional rains affect an entire drainage

basin the size of the Arroyo de los Frijoles at Sand Plug Reach (drainage area = 3.75 sq mi).

VALLEY ALLUVIUM

Many widely separated areas in southwestern United States have undergone three periods of alluviation followed by erosion, and there is evidence of approximate simultaneity of the respective events from one area to another. That some or all of these events should have occurred in the study area would be a logical supposition.

Arroyo de los Frijoles through most of its length is incised into an alluvial fill of silty sand which at present has a surface configuration characterized by two terraces, and paired remnants of each are common along the principal drainage ways. The higher terrace stands about 5 feet above the channel bed in upper tributaries and tends to remain about the same height downstream along the 7-mile reach which we have studied in detail. The terrace tread is uniform and flat, and vegetated, as are the hills, with piñon and juniper and an understory of grass. Along much of the stream length the terrace is bounded by a vertical wall, at least on one side of the channel, but elsewhere it slopes down to the lower terrace in a subdued S-shaped profile which may have a maximum slope of 1:5. Such a rounded scarp is generally vegetated with bunch grasses of low density. The terrace tread grades in a smooth curve to the adjacent hills, and its whole width seldom is more than 300 feet.

The low terrace averages about 1-2 feet above the present streambed and is seldom bounded by vertical banks. Its surface tends also to be somewhat irregular and can usually be recognized by the occurrence of rabbit brush, locally called chamiso [*Chrysothamnus nauseosus* (Pall.) Britt.], which occurs neither on the higher terrace nor on the presently active point bars.

Typical aspects of the valleys and the terraces are shown in figure 140.

The stratigraphic relation of the alluvium of the high terrace to the bedrock underlying the adjacent hills is commonly seen in the vertical banks. The valley fill was laid in a shallow U-shaped trough cut into the friable and poorly consolidated bedrock, and the bed of the present channel lies very near the bottom of this trough in the smaller valleys and probably close to it even in the main stream. That is to say, the present stream has cut nearly through the valley alluvium and most of the depth of alluvium can be seen in the cut banks or vertical walls.

The relation of the alluvium underlying the tread of the lower terrace to that of the upper terrace is difficult to decipher. So nearly the same is the alluvium under the two terrace treads that even when a vertical bank

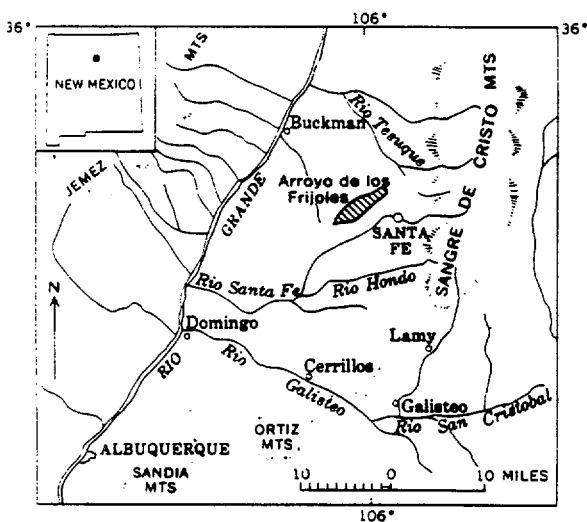


FIGURE 138.—Area in New Mexico where detailed studies were made.

cuts through both, no stratigraphic contact is obvious, though an inset relation is suggested by the contacts seen. The same difficulty is often observed in alluvial fills of western valleys. We have concluded after inspection of many sections, that the lower terrace represents the top of an inset fill and that Arroyo de los Frijoles is an example of a two-fill, two-terrace alluvial valley (see Leopold and Miller, 1954, p. 5, for a discus-

sion of the classification of terraces and fills). A diagrammatic cross section is presented of this valley in figure 141. We here apply the name Coyote terrace deposits to the alluvial deposit under the higher terrace so prominent along streams in the vicinity which will be referred to as the Coyote terrace.

The type locality for the Coyote terrace deposits will be along the Arroyo de los Frijoles at what we will

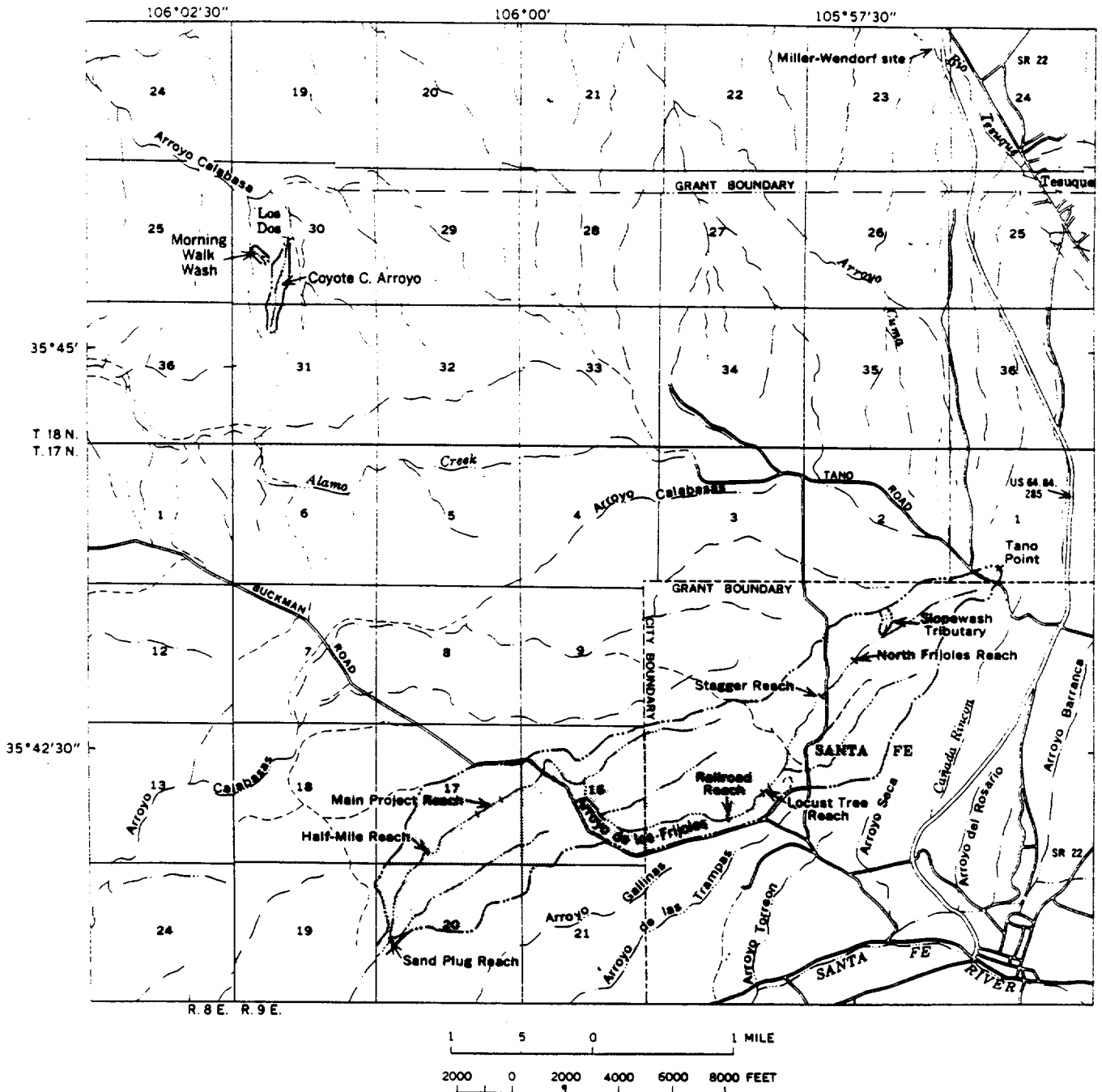


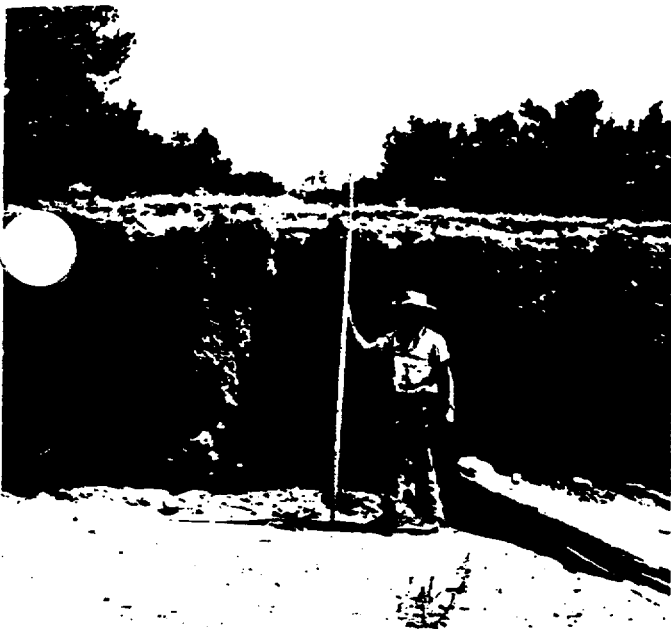
FIGURE 139.—Drainage basins of Arroyo de Los Frijoles, Coyote C. Arroyo, and Morning Walk Wash. Named reaches are locations where detailed studies were made. Also included are principal stream channels and roadways within the area.



A



B



C

FIGURE 140.—Typical aspects of the valleys and the terraces. A, Drainage basin of Coyote C. Arroyo; the man is standing on a flat surface of alluvium or colluvium. B, Two terrace levels along Arroyo de los Frijoles; the lower terrace, about 18 inches above the channel bed, is in the foreground; at the tree near the channel edge, the upper terrace stands 5 feet above the present bed and grades smoothly to adjacent hills. C, Arroyo de los Frijoles; the channel is cutting into the upper terrace material that here stands 8 feet above the present bed elevation; the view is on the left bank just downstream from Fence Line Headcut; bedrock crops out in the channel bed at this place, dipping downstream.

of fine gravel. When dry, the cut banks stand vertically and are hard to dig with a shovel. The alluvium is 5–10 feet thick and rests on bedrock, which here is unconsolidated sand and gravel. The top several inches may contain more fine sand or silt than at greater depths. No soil zonation is apparent though the upper 6 inches are slightly darker from the admixture of humus and incipient soil development.

The Coyote terrace forms a curving surface as it rises away from the valley floor and joins the hillslopes underlain by the Santa Fe Group. The alluvium inter-fingers with colluvium at the valley sides and extends upstream in minor tributary valleys, where the distinction between valley alluvium and colluvium at the base of the slope often cannot be made.

In the Tesuque Valley just 4 miles to the north, similar alluvial terraces have been studied by Miller and Wendorf (1958) at a location shown on figure 139. There, two terraces occur at 18–20 feet and 8–10 feet above the present channel; the alluvium underlying the higher one contains dateable artifacts and charcoal. A C^{14} date of charcoal lying 130 inches below the surface of the upper terrace was 2230 ± 250 years. Between the

describe here as our main-project reach, in the NW $\frac{1}{4}$ SE $\frac{1}{4}$ sec. 17, T. 17N., R. 9E., 4.2 miles from Santa Fe. The name is derived from Coyote C. Arroyo at Las Dos (see p. 205), where a sample of charcoal buried in this deposit gave a date of 2800 ± 250 years B.P. (USGS sample W1328).

Coyote terrace deposit is alluvium consisting of red-brown, slightly indurated silty sand or fine sand, sometimes fine sandy silt, with occasional discontinuous lenses

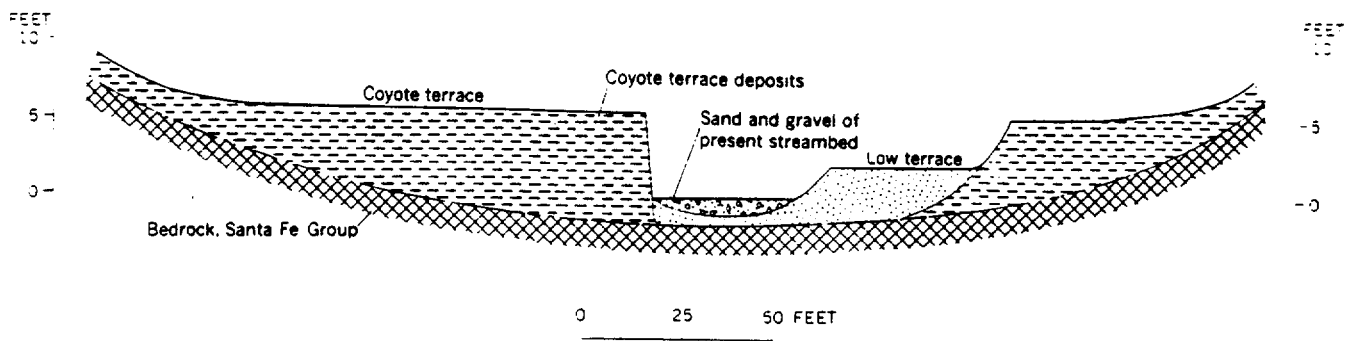


FIGURE 141.—Diagrammatic cross section, Coyote terrace deposits.

Tesuque area and Arroyo de los Frijoles, the agreement of dates, the similarity in form, the comparable character of the alluvial materials, and the geographic proximity of the areas suggest that the respective periods of deposition and erosion in the valleys of the whole area are correlative and may be considered Coyote terrace deposits.

Though the terrace heights and the depth of alluvium of the Coyote terrace deposits differ somewhat from valley to valley as indicated by the comparison between Arroyo de los Frijoles and Tesuque Creek, such a valley fill is ubiquitous in all the ephemeral valleys in the area. It typifies all the drainages rising in the foothills which lie west of the Sangre de Cristo Range and east of the escarpment of La Bajada, a distance of 11 miles or more in most places, and extending north-south at least from Cuyamungue, 12 miles north of Santa Fe, to San Cristobal, 25 miles south of the city. This area of more than 100 square miles has been seen, at least in reconnaissance, during this study, and our impression is that similar relations would be observed over a much larger area in central New Mexico. The Coyote terrace deposits correspond to Deposition 2 in the regional alluvial chronology of Kirk Bryan. (See Leopold and Miller, 1954, p. 58.)

THE LOCAL BEDROCK

The hills being drained by the network of ephemeral channels are composed of the upper beds of Santa Fe Group. The whole group is at least several thousands of feet thick, but that part with which we are concerned includes the upper zones only, principally the Tesuque and Ancha Formations (Miller, and others, 1963, especially p. 50-51 and pl. 1). The geologic map by these authors includes similar landscape 3 miles north of our study area which they mapped as Tesuque Formation described as follows (p. 50):

The Tesuque Formation of the Santa Fe Group, as defined here, consists of poorly consolidated, water-laid silt, sand, and gravel, mostly tan in color. . . . Abrupt changes in texture, both

vertically and horizontally, are the rule. Bedding is locally distinct, but few beds can be traced more than a mile or two. Some of the sandstone beds are fairly well sorted and locally cross-bedded. Their coherence is due to cementation by calcium carbonate. At most places, even in unconsolidated materials, the sediments are highly calcareous.

The Tesuque Formation was derived from Paleozoic and Precambrian rocks of the mountains. The presence of a considerable quantity of quartzite pebbles, for example near Tesuque, indicates drainage southward from Rio Santa Cruz or Rio de Truchas, which requires a radical difference from the present drainage pattern.

Miller, Montgomery, and Sutherland (1963) consider the Tesuque Formation to be Tertiary. They identify a Pleistocene or upper Pliocene Ancha Formation consisting of remnants of a once-continuous sheet of unconsolidated gravel which extended originally from the western part of the Sangre de Cristo range to the Rio Grande. The gravels were considered to be laid down as fan deposits derived from glacial action and carried out to cover the older Tesuque beds as glacial outwash deposits.

Those workers did not map as Ancha Formation any of the deposits in the area just to the north; the bedrock materials with which we deal are probably entirely Tesuque Formation. Because, as Miller, Montgomery, and Sutherland stated (1963, p. 51), 100-300 feet of dissection has occurred since deposition of the fan gravel comprising the Ancha Formation, the concentration of gravel on many hilltops which we observe in our study area may represent a lag concentrate of gravel derived from Ancha beds which now have been removed.

Other than the gravel concentrate on hilltops, the description given by Miller and his associates fits the bedrock materials. Those authors, as well as we, observed many places where the upper surface of the Santa Fe beds is weathered. A zone of caliche, 2-3 feet thick locally, permeates the sandy, or elsewhere the gravelly, bedrock materials. This caliche where it crops out does not affect the alluvium or colluvium and indicates processes of soil formation and weathering related to events prior to the deposition of the Coyote alluvium.

RELATION OF VALLEY ALLUVIUM AND COLLUVIUM TO HEADWATER AREAS

The surface of the Coyote terrace can be followed as remnants along the main valley of Arroyo de los Frijoles and other washes upstream to where the present channel is a few feet wide. Similarly, the surface can be followed up lateral tributaries where it grades to the adjacent hills. Colluvium deposited by rills and unconcentrated wash merges and interfingers with alluvial deposits of the main valleys and tributaries. Excavation by shovel in the bed of any small, even any steep, tributary reveals alluvial-colluvial material within a few hundred feet of the watershed divide. The same relation of alluvium to headwater slopes was found in eastern Wyoming by Leopold and Miller (1954) who summarized their findings in these words (p. 83):

The terraces of master streams can be traced directly into many tributaries of moderate size, indicating that erosion of alluvium in the master streams was accompanied by gully erosion in tributaries, even the ephemeral ones.

... likewise, aggradation in the main stream valleys was accompanied by deposition in tributary valleys and draws. Probably these deposits were derived by mass movement and sheet erosion on upland slopes.

It seems logical that the shift in relations between runoff and vegetation which caused erosion of all major streams would also affect the smallest tributary valleys in a similar way at the same time. . . . As the deposit in the main valley gradually increased . . . the wash slopes that were graded to the main river accumulated material which blanketed all except the most prominent hills and uplands. The area of upland from which alluvial materials were being derived by erosion shrank, and the area of deposition increased.

percentage of area of a small basin blanketed with alluvium-colluvium is exemplified in Coyote C. Arroyo. (See fig. 139 for location.) This typical drainage basin has an area of 0.064 sq mi (40.8 acres) of which 0.022 sq mi (14.4 acres) is covered by alluvium-colluvium, the remainder being hillslope and hilltop area of Tesuque Formation. In this example, then, 34 percent of the surface area was alluviated, and the average distance from the head of deposition in small swales to the watershed divide was 190 feet. The alluviation extends headward astonishingly close to the drainage divides. The proximity of the colluvial-alluvial deposits to drainage divide can be seen in figure 140A.

The relation of the small tributary draws to the headwater slopes may be typified by the two examples in figure 142. Profiles of the surface of the alluvium-colluvium merge smoothly into the unrilled hillslope underlain by bedrock. Cross profiles drawn nearly parallel to the contours of the side hills demonstrate, in conjunction with the stratigraphic evidence seen in the channel walls and in pits dug in the plane of the

profile, that alluvial and colluvial material fill a former channel system cut into the bedrock and that subsequently the present channels have reevacuated parts of the earlier system. The present channel network incised into the alluvium makes a present topography similar to that existing before the Coyote terrace deposition.

This conclusion is supported by observations of the extent of gravel which more or less covers many of the rounded hilltops of the area. In the Slopewash Tributary example in figure 142, section B-B' crosses from west to east a gravel-covered hilltop, a gravel-free area, and again a gravel-covered hilltop. At the base of the channel on the right bank the bedrock is permeated with a white cement, presumably CaCO_3 .

Exposures elsewhere also indicate that hilltops covered with lag gravel are usually underlain by bedrock. Thus the deep layers of silt exposed in present channel walls were deposited in channels which dissected the bedrock. The alluvium lapped up against the gravel-covered slopes and in places covered the gravel.

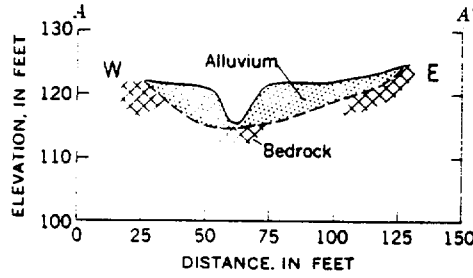
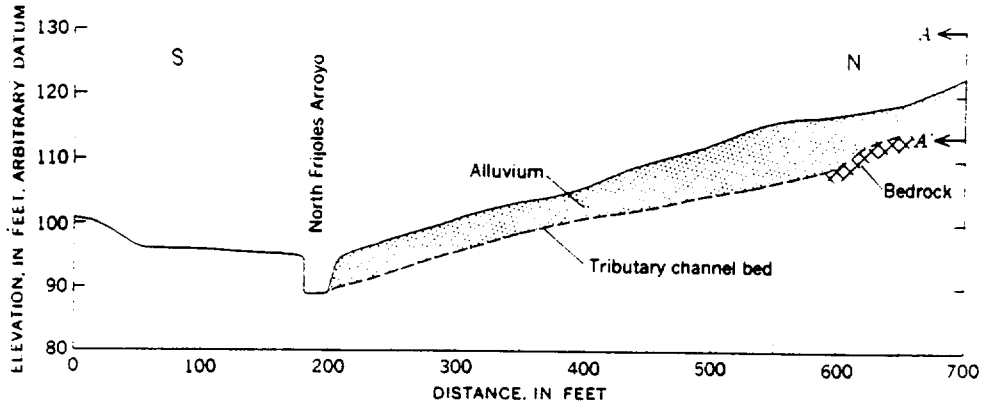
Investigations of the relation of the alluvium to the bedrock topography showed that the underlying Tesuque Formation generally appears no more weathered at the contact than elsewhere. In some places, however, alluvium was deposited over a surface heavily cemented with caliche. The caliche appears as a hard cement where the Tesuque was gravel, and where the Tesuque was silty, as a whitish calcification of a zone extending 3-4 feet below the contact, and especially concentrated on fracture planes. Hard nodules of caliche in the silt are seldom seen, but amorphous soft masses without sharp boundaries are common.

These facts support the conclusion reached by Miller, Montgomery, and Sutherland (1963), that a long period of weathering under subhumid conditions was followed by a semiarid climate during which caliche permeated an undulating topographic surface. Our observations add the additional postulation that, subsequently, this topography was first alluviated and later erosion developed a drainage network similar to and about the same depth as the present one; the erosion removed part but not all of the materials which had undergone calichefication.

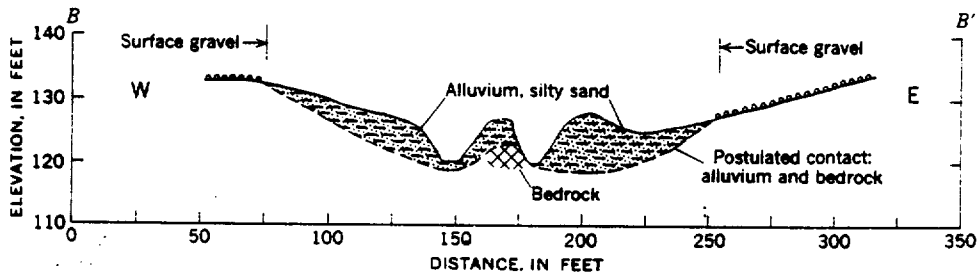
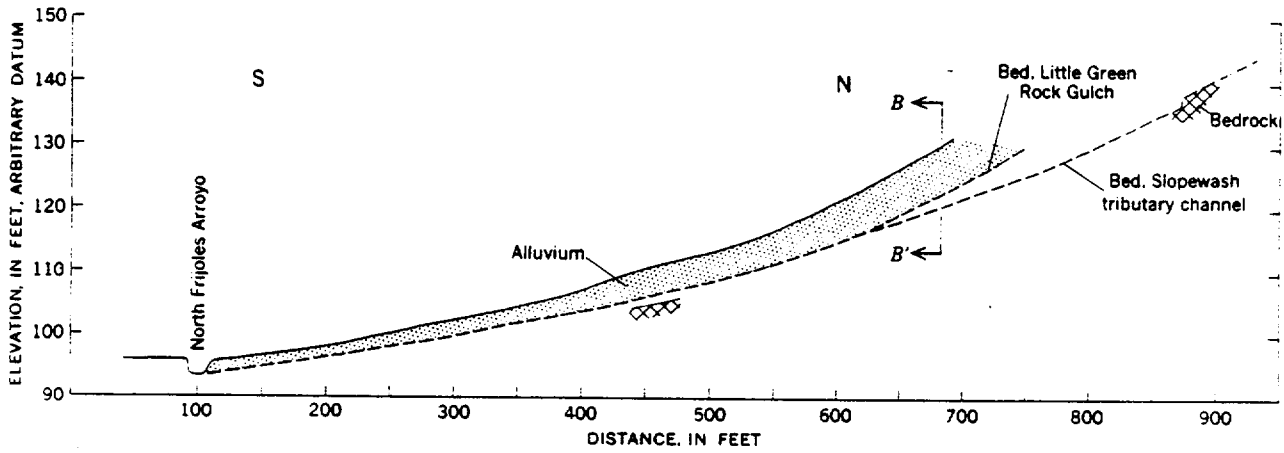
To summarize, alluviation during Coyote terrace time aggraded not only the main valleys but small tributary draws as well. Post-Coyote terrace erosion reexcavated much of the earlier topography. The problem posed by this sequence of events is the following:

If alluviation took place in all the headwater draws at the time the main valleys were being aggraded, where did all the debris come from, and by what processes?

EROSION AND SEDIMENTATION IN A SEMIARID ENVIRONMENT



A.—UNNAMED TRIBUTARY TO NORTH FRIJOLES ARROYO AT STAGGER REACH



B.—SLOPEWASH TRIBUTARY TO NORTH FRIJOLES ARROYO

FIGURE 142.—Two examples of small tributaries showing stratigraphic and topographic relation of alluvium to bedrock.

Clearly, the sediment was derived from the hills above the areas of alluviation but not from rills or gullies on these hills, as evidenced by the absence of gullies or rills of any depth or importance outside of those which were alluviated. Thus the sediment must have been derived from processes other than rill and gully erosion, specifically, sheet erosion or mass movement. This hypothesis attributes to the latter processes greater efficiency than we at least would have supposed. We were led, then, to devise methods of measurement which would allow the construction of a sediment budget, however approximate, to ascertain whether relative importance of present processes would shed light on these events of the past.

Another problem is highlighted by the postulates stated. It is usual to suppose that alluviation of a master stream would provide a rising base level for the tributaries which enter into it. Then the aggradation in the tributary would similarly provide a rising base level for its own subtributaries. Though this scheme is a simple one and would lead to field relations here observed, it also implies that the alluviation of the headwater tributaries would lag in time that of the main stem. But these inferences do not agree with field observations in the Arroyo Frijoles area.

It seems much more likely that in our study area the relation of runoff to vegetation which would lead a main stream to aggrade would similarly have the same result on the tributaries. We believe that control by base level is a relatively minor factor in alluviation of the valleys.

The remainder of this paper is organized around the measurement program instituted to investigate these questions. The sample areas studied will be described, the measurement methods outlined, and the results summarized. These measurements will then be discussed in terms of the problems outlined (see p. 236). We begin with a discussion of the study areas.

STUDY AREAS

The areas of special study shown in figure 139 include Arroyo de los Frijoles through its uppermost 7 miles and some smaller basins of several acres in an area 4 miles distant, near Las Dos. The principal basin, Arroyo de los Frijoles, has a channel width which ranges from the smallest recognizable rills a few inches wide to an arroyo 100–200 feet wide. All channels more than a foot wide have a flat predominantly sandy surface dotted in places with scattered gravel.

Larger scale maps, figures 143–45, show details of the areas of intensive study and will be referred to in later discussions.

Figure 146 illustrates the character of the country and the aspect presented by main and tributary chan-

nels. Figure 146, *A* and *B*, shows a small tributary within a few hundred feet of the headwater divide, a subbasin we called Slopewash Tributary.

At a point 1.1 miles from the furthest divide the North Frijoles Reach is typical, figure 146. One mile farther downstream the channel is larger, as shown at Locust Tree Reach (fig. 146*D*). Main Project Reach, 4.9 miles from the headwater divide and at a place where the drainage area is 2.87 sq mi, is illustrated in figures 146*E* and *F*.

Some characteristics of each of the study areas are indicated in table 1.

TABLE 1.—Characteristics of locations studied

Location	Drainage area (sq mi)	Elevation (ft above msl)		Relief (ft)	Length (ft)
		At headwater	At downstream point		
Arroyo de los Frijoles:					
Slopewash Tributary.....	0.05	7,280	7,200	80	1,200
North Frijoles Arroyo:		7,388			
At gaging station.....	.56		7,159	229	5,800
At Stagger Reach.....	.70		7,111	277	8,200
At mouth.....	1.36		7,048	340	11,750
At Locust Tree Reach.....	1.49		7,037	351	12,400
At Railroad Reach.....	1.61		6,987	401	15,400
At Main Project Reach.....	2.87		6,790	598	28,000
Sand Plug Reach:					
At Stump section.....	3.18		6,696	692	33,600
At Rocky Nose section.....	3.75		6,672	716	34,800
Gunshot Tributary, at mouth.....		6,798	6,723	75	1,150
Arroyo Falta.....	.12	6,800	6,620	180	5,000
Coyote Cr. Arroyo, at dam.....	.064	6,735	6,550	185	3,600
Morning Walk Wash:					
South gully.....		6,633	6,540	93	700
North gully.....		6,615	6,540	75	870

METHODS OF STUDY

Observations of nearly all the types described here began in the period 1958–61 and are continuing as this paper is written. Water stages of flow are measured by recorders at gaging stations installed on North Frijoles Arroyo and at Main Project. The duration of individual flows is generally two hours or less and current-meter measurements for the construction of stage-discharge rating curves are impracticable without a full-time resident hydrographer. Stage-time hydrographs are obtained from the stage recorders, but maximum discharge for each flow is computed using a survey profile of high-water marks. This, combined with cross-sectional areas of flow determined by scour chains (described below), permits the computation of discharge using an estimated value of flow resistance.

A network of 12 nonrecording rain gages is observed after each significant summer rain.

Depths of scour and fill in channels are measured by chains set vertically in a dug hole in the streambed. At maximum depth of scour the chain is bent over by the flow and is usually covered by fill on the receding stage (Emmett and Leopold, 1964).

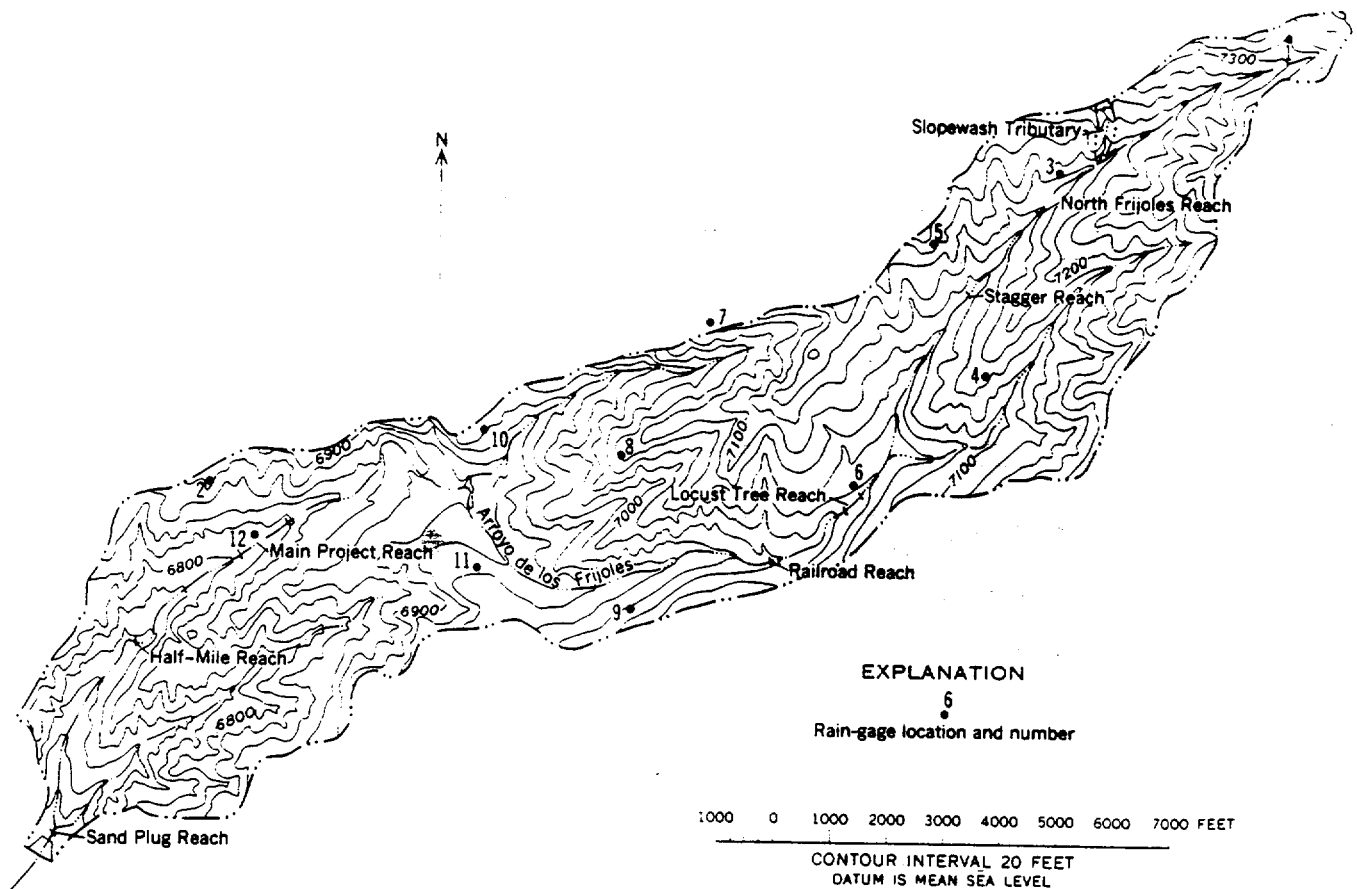


FIGURE 143.—Arroyo de los Frijoles.

Erosion pins, consisting of a 10-inch nail put through a washer, driven flush with the ground surface, are used to record increments of surface erosion. Some of these pins are arranged in a grid over certain plots, but generally the nails are in a line as a transect from hilltop to base or across a channel as a cross-section.

Mass-movement pins are set on a line between immovable bench marks, and are surveyed for alignment by transit.

Many rocks have been painted for identification and observed for movement after each flow.

The individual plants on some 3×3-ft quadrats have been mapped and are to be remapped periodically to observe changes with time.

Although the methods are simple, the labor after each storm (about 3 per summer) and during the annual resurvey of all observation points is rather great.

MAGNITUDE AND FREQUENCY OF RAINFALL AND STREAMFLOW, 1958-64

Rainfall has been measured since 1959 at 12 locations within the drainage basin, as shown in figure 143. Sum-

mary of data A (p. 247) contains a partial summary of the data collected from these sites.

The gages were not read after each shower, but efforts were made to read them at least after every flow-producing storm. The sporadic nature of storms is indicated by the unequal distribution of rainfall among stations.

At the Main Project Reach a recording rain gage has been installed at the location of the water-stage recorder. Precipitation data (summary of data B) collected here allow a better indication of the rainfall characteristics. The record is too incomplete to show the mean annual precipitation which at that location must be about 12 inches per year.

The 1,300 cfs (cubic feet per second) flow of July 25, 1962, the second highest flow recorded at the Main Project Reach, was caused by a storm which registered 1.5 inches in 25 minutes at the Main Project gage.

Channel discharge is measured or estimated at three places in Arroyo de los Frijoles: Main Project, Locust Tree, and North Frijoles. Gaging stations are installed at the Main Project and at North Frijoles reaches. During the period 1958-63, runoff occurred at the three

measuring stations on the dates indicated in table 2. in which are presented values of peak discharge. Spaces in the table usually refer to no flow; however, in a few instances some flow may have occurred but was of negligible magnitude. Flow data discussed in this report are peak values.

TABLE 2.—Summary of peak discharges, in cubic feet per second, at three locations along Arroyo de los Frijoles, 1958-63

(a) and (b) refer to separate flows or different peak flows occurring on the same day

Date	North Frijoles	Locust Tree	Main Project
1958			
August 18.....			20
September 6.....	15-20		10-15
September 13.....	194	1,320	3,060
1959			
May 23.....	140	50-75	3-5
June 15.....			2-4
July 23.....			10-15
August 17.....		20-25	20-25
August 24.....	50	15	
October 29.....	.5		1
1960			
July 14.....	67	380	35
August 4.....			152
September 15(a).....	1		10-20
(b).....			10-15
October 9.....	3-5		
October 16(a).....	5-7		
(b).....	9-10		10-15
October 17.....			10-15
1961			
June 26.....			1
July 8.....	58	498	98
August 12.....	85	300-400	80-90
August 23.....	3-5	3-5	3
September 18(a).....	10		40
(b).....			60
September 19.....	230	650	250
1962			
June 30.....	.3	30	
July 5.....	6-8	150	40
July 11.....	.3		10
5.....			3
85.....		450	1300
90.....		450	300
September 19.....	1		
1963			
July 20.....	10	5	15
September 21.....	5	391	316

Most storms are intense and so local that only a part of the drainage basin is affected by each. Only twice (September 13, 1958, and July 25, 1962) was there increasing discharge in the downstream direction due to heavy rainfall over the entire basin, and these two storms caused the greatest flows during the period of record.

For each of the three measurement locations, the peak flows experienced were arranged according to rank and recurrence intervals were computed. These are plotted against their corresponding discharge and are shown as dashed lines in figure 147. Recurrence intervals are determined by the U.S. Geological Survey method,

$T = \frac{n+1}{m}$, where T = recurrence interval in years, n = number of years of record, and m = magnitude or rank of flood, the highest being number one.

Excepting the two storms just mentioned, the spotty distribution of precipitation implies that data collected at each of the three reaches may be considered as inde-

pendent flows. If this were in fact true, a type of station-year analysis might be attempted by combining 5-years of record for each of three locations into a synthetic 15-year record. The solid line on figure 147 gives this average frequency of the three reaches. The solid circles on this graph represent all flows at the three stations, arranged in order of magnitude.

For small flows all moderate-size drainage areas are capable of receiving sufficient rainfall to produce a similarity in flow frequency. For drainage areas larger than some given size, further increases in area would not increase the size of flood of a given frequency. This feature is indicated by the fact that a flow of 2-year recurrence interval is about the same at Locust Tree and Main Project Reaches despite the fact that the drainage area of the latter is about twice that of the former.

The present data exceed by fivefold the values presented by Leopold and Miller (1956, fig. 21, p. 24). The latter values should not be considered applicable to the foothill area of ephemeral streams though they were so considered in that report. It is now obvious that flow frequencies of the gaged streams emanating from the high mountains are not comparable with and are smaller than values for ephemeral washes in the foothills, despite the lower mean annual precipitation of the latter areas.

The problem of flow frequency is of paramount importance to evaluation of erosion and sediment transport processes. Though the method of determining frequency is still open to further study in ephemeral basins, figure 147 expresses the occurrence of events in the studied basin during the period of observation.

CHANNEL FORM AND BED MATERIALS

A salient aspect of the change in channel characteristics downstream is the increase in width, shown in figure 148. As defined here, channel width refers only to the active channel which is swept free of vegetation except for annual plants. In some places the actual width between the steep banks is greater than indicated on figure 148. Such reaches usually include remnants of the lower terrace, which not only supports some vegetation but also stands 1-2 feet above the presently active bed.

The variability of channel width quite evident in figure 148 seems large, but one does not realize how large the variance is in the usual channel until he begins to make quantitative measurements. On a perennial eastern stream not much larger in drainage area than Arroyo de los Frijoles, the ratio of the standard deviation to mean channel width averages about 0.25 (data from Wolman, 1955, fig. 37), whereas for a reach of Arroyo

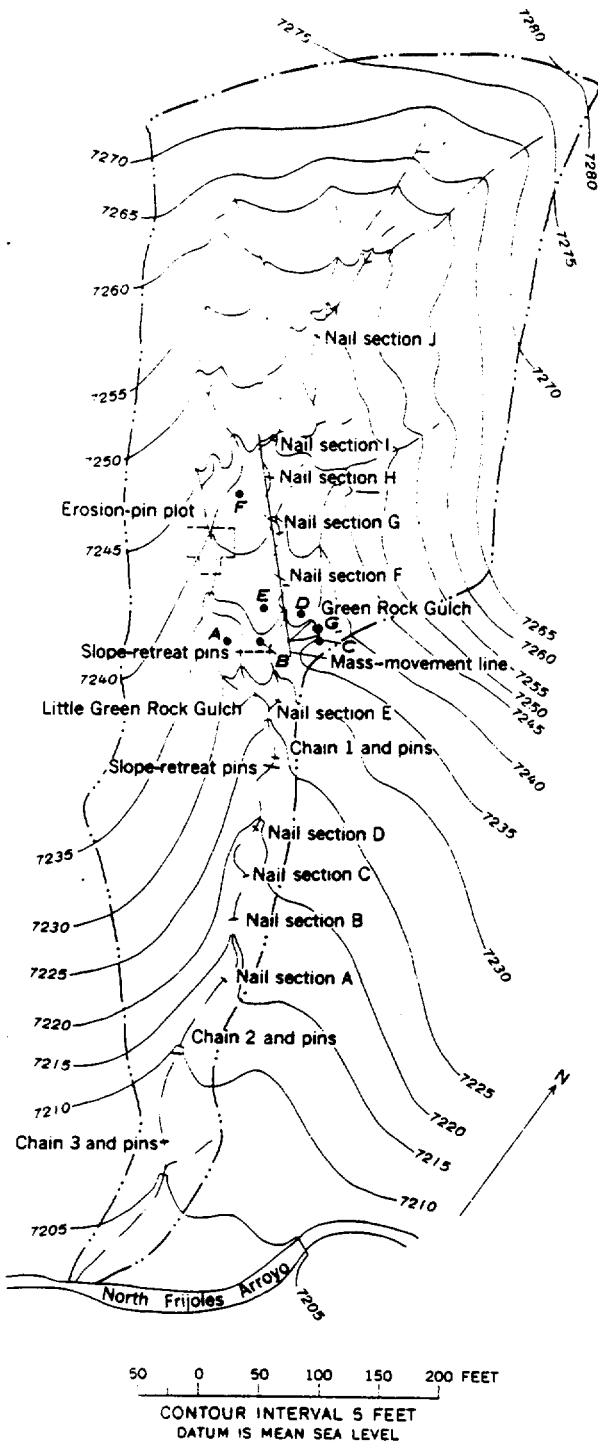


FIGURE 144.—Slopewash Tributary

de los Frijoles below the junction of North and South Frijoles it is about 0.39. Also, the variability of width is not so great above that junction where the drainage area is less than 1 sq mi. In an ephemeral basin, it appears that when the drainage area exceeds the size of the usual summer thunderstorm, only parts of the basin

contribute runoff. Thus different reaches of channel experience different sequences of flows, and this probably tends to increase the variance of channel width.

The increase in drainage area with channel length is shown in the top part of figure 148. At three places, sudden increases in drainage area occur where relatively large tributaries enter the main channel. However, as mentioned above, it appears that these increases in drainage area affect channel width only incidentally, as the size of a given storm may or may not extend over the whole contributing area.

The bed of Arroyo de los Frijoles is predominantly sandy with scattered fine gravel and cobbles, but there are local concentrations of rocks. Considering first the nongravelly areas which predominate, sieve analyses are shown in figure 149A. The median diameter for all surface samples are within the limits of medium to coarse sands.

Three samples from Arroyo de los Frijoles provide comparison of median grain diameter at points downstream in the same basin.

Location sampled	Drainage area (sq mi)	Median grain size (mm)
Slopewash Tributary.....	0.05	0.56
North Frijoles Reach.....	.56	.78
Main Project Reach.....	2.87	.72

Though a larger number of samples may have yielded a more uniform set of values, at least it can be said that there is no progressive decrease of the size of sand downstream.

Figure 149B illustrates the composition within the area of a gravel concentration or bar. Clearly, the majority of the larger particles are in the top 2 inches (discussed in more detail on p. 212) and the composition over the full depth of the concentration is more coarse than in a nonbar area. Downstream tips of gravel bars are characterized by material a little finer than in nonbar areas. This is an expected pattern and is observed in other depositional phenomena such as mudflows.

The largest particle occurring in each 100-foot segment of the channel of Arroyo de los Frijoles was measured, and the results are plotted in figure 150. The size of the material in the Slopewash Tributary is as large as that in North Frijoles and, indeed, almost as large as that anywhere in the whole length of the stream. Maximum particle size actually increases somewhat downstream, and local variations from section to section are commonly two to threefold.

In gravelly perennial streams the occurrence of pools and riffles is characterized by considerable bed relief.

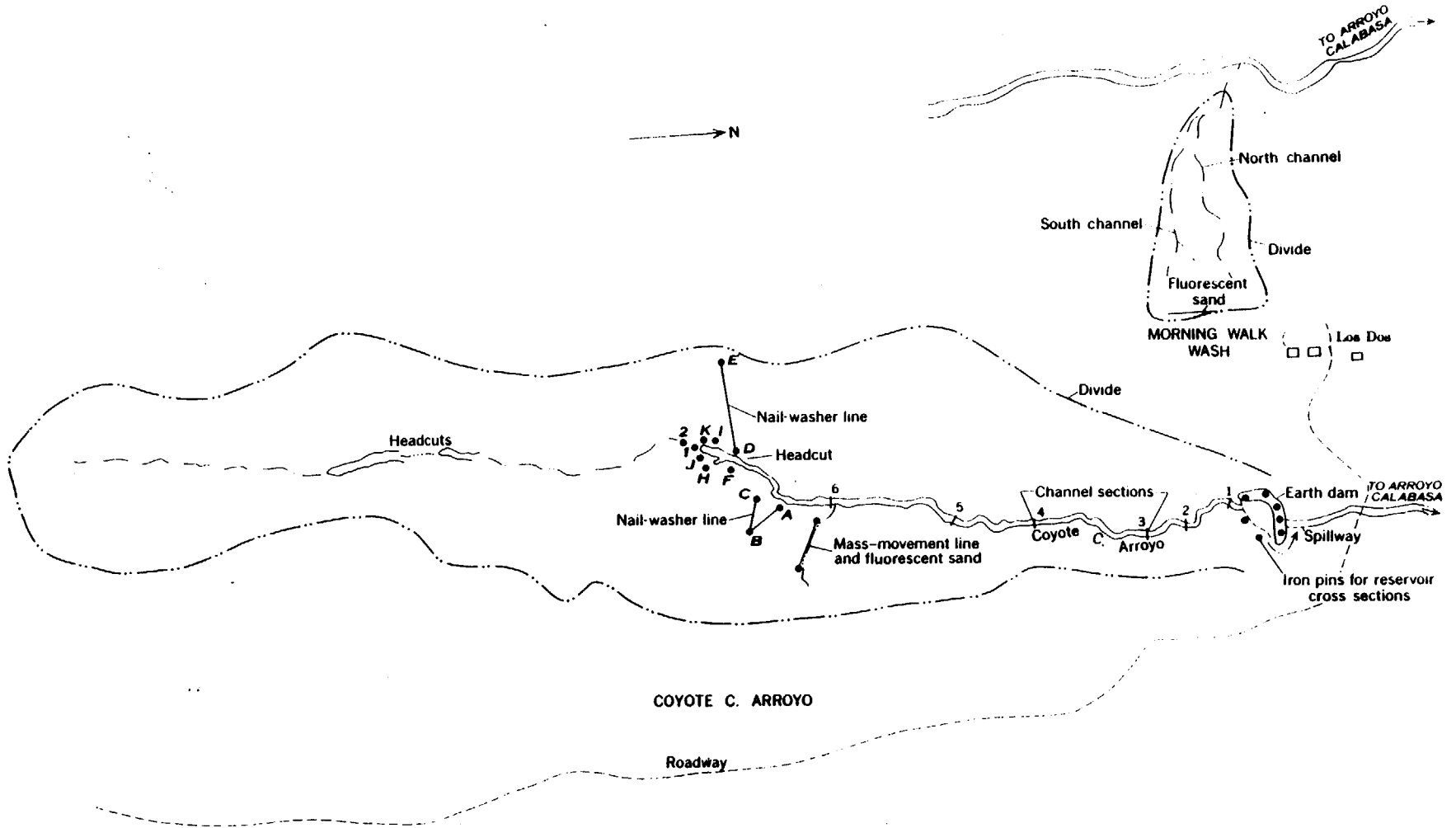


FIGURE 145.—Drainage basins of Coyote C. Arroyo and Morning Walk Wash; solid circles labelled in bold type are nail-and-washer observation points or iron pins for resurvey; channel cross-section locations are labeled 1-6.



A



B



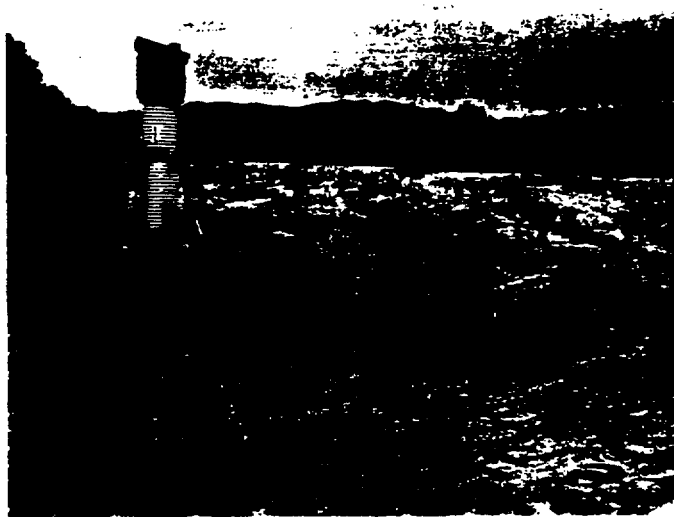
C



D



E



F

FIGURE 146 (Above and left).—Photographs illustrating several of the individual study areas. *A*, Slopewash Tributary; the area shown is along the mass-movement line (see fig. 144 for location). *B*, Slopewash Tributary; the area shown is within the erosion plot. *C*, North Frijoles Reach, Arroyo de los Frijoles; the view is downstream from above the gaging station. *D*, Locust Tree Reach, Arroyo de los

Frijoles; view upstream; visible in the foreground are rock groups from the painted rock experiments. *E*, Main Project Reach, Arroyo de los Frijoles; the view is downstream from above the gaging station. *F*, Main Project Reach, Arroyo de los Frijoles, looking upstream.

The riffle is a gravel bar or accumulation which is a topographic high, a feature which rises well above the mean bed elevation. The pool is a trough below mean elevation.

the larger ephemeral streams of the area here studied, there is no such relief on the dry streambed. In fact the bed is remarkably flat across its width and closely resembles a gently inclined plane, for the longitudinal profile is quite straight.

Only in detailed mapping did we become aware of the fact that local concentrations of gravel on the sand bed correspond in principle to the riffle of the perennial river. These bars, as we call them, are so slightly elevated above mean channel bed elevation that they would not be recognizable as a topographic high. Rather, we have mapped them merely by inspection of surface texture. Because some gravel particles occur everywhere, designation of a bar is rather subjective, but generally it implies individual cobbles spaced within several diameters; whereas in areas not called bars the spacing of cobbles would be 20–50 diameters or more. Typical gravel concentrations are illustrated in figure 152*D*.

SPACING OF GRAVEL BARS

The position of gravel bars in the vicinity of the Main Project Reach as mapped each summer during the

period 1958–63 is shown in figure 151. It seems apparent that the position of a gravel bar remains remarkably stable. This is true despite the fact that two or three flows of sufficient magnitude to move the material on the bars occurred between the successive mappings. For example, the largest flow measured during the entire period of study occurred between mappings in 1958 and 1959, and at that time scour to depths of 0.4–1.4 feet occurred. Thus all the material of the surface of the channel bed moved downstream, yet the bars were rebuilt in approximately the same places as before. However, with each annual mapping, a few bars are missing in the new map that were present in the old map, and also a few new bars appear.

Beginning in 1961, a more intensive effort was made to map gravel accumulations. It is this effort, rather than an actual increase, which, in figure 151, shows more extensive areas of gravel beginning in 1961.

In accordance with observations elsewhere the gravel bars are spaced on the average at a distance equal to five to seven times the channel width, and this ratio persists through all the years of record.

Measurements of gravel size and density on the surface of gravel bars were made at two different times separated by major flows. It was found that both the size distribution and density of particles greater than 1 inch in diameter remained almost the same.

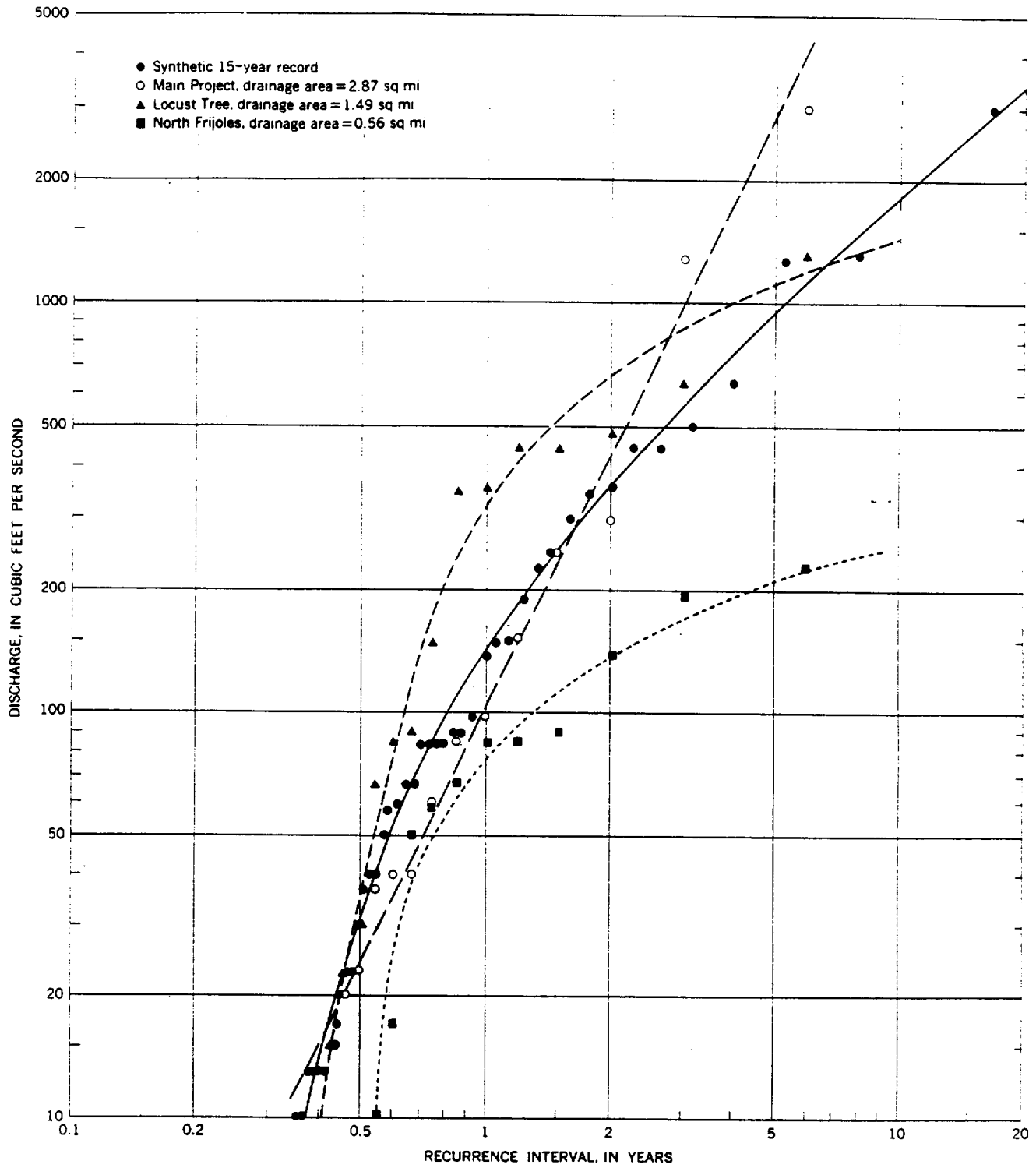


FIGURE 147.—Magnitude and frequency of flows, Arroyo de los Frijoles, 1958-62.

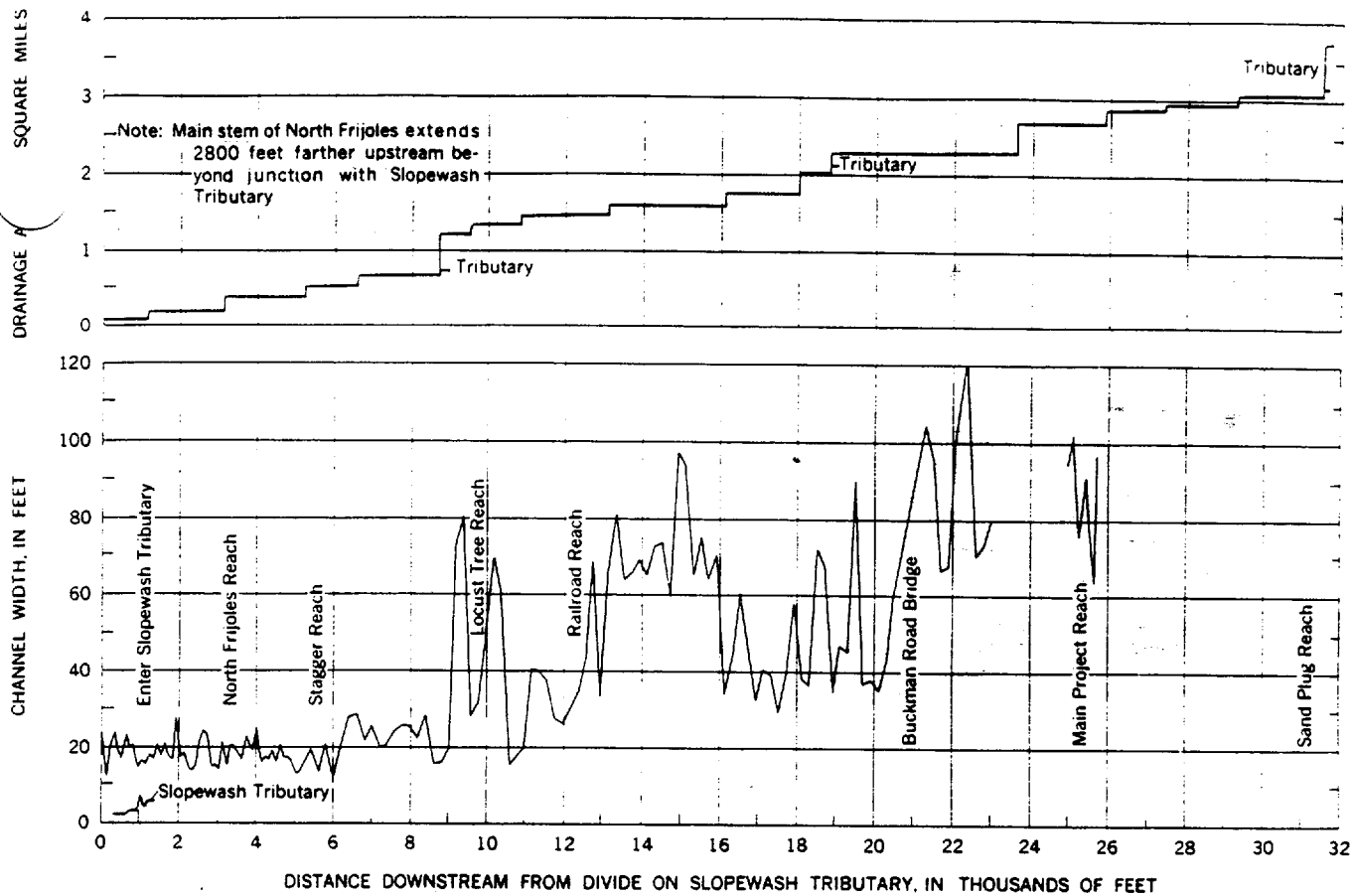


FIGURE 148.—Relation of channel width and drainage area to channel length, Arroyo de los Frijoles.

MOVEMENT OF COARSE PARTICLES

We had hypothesized that gravel bars owe their existence to the fact that particles in juxtaposition are less easily moved by flowing water than when widely separated. Marked cobbles arranged in groups of various spacings and collected after individual flows would provide a means of testing under field conditions whether this hypothesis would be sustained.

The following procedure was developed: Cobbles taken from the channel were completely painted. Each was given an identification number equal to its weight in grams, and this number was painted on the cobble. The rocks were placed in the channel in groups, each group contained a chosen particle-size distribution and comparable groups differed in spacing of the rocks. After each flow the entire length of the channel was searched for painted rocks. Those found were recorded, collected, and replaced to await the next flow. This procedure was carried out after each significant storm-flow during the summers of 1958-63, inclusive, and discontinued thereafter.

In these studies a group of particles consisted of 24 individual rocks arranged in a parallelogram. The distance or spacing between particles was one of three values, 2 feet, 1 foot, or 0.5 foot.

Except for the initial summer (1958) the individual groups included four particles in each of the following size (weight) classes:

Weight class (grams)	Intermediate size, approximate mean diameter (mm)
300-500	65
500-900	85
900-1,700	105
1,700-3,300	125
3,300-6,500	160
6,500-13,000	230

Individual particles in the grid were arranged in a Latin Square pattern, in which each line of six particles includes one and only one of each of the size classes, and in each cross-tier, no rocks of the same size are in juxtaposition.

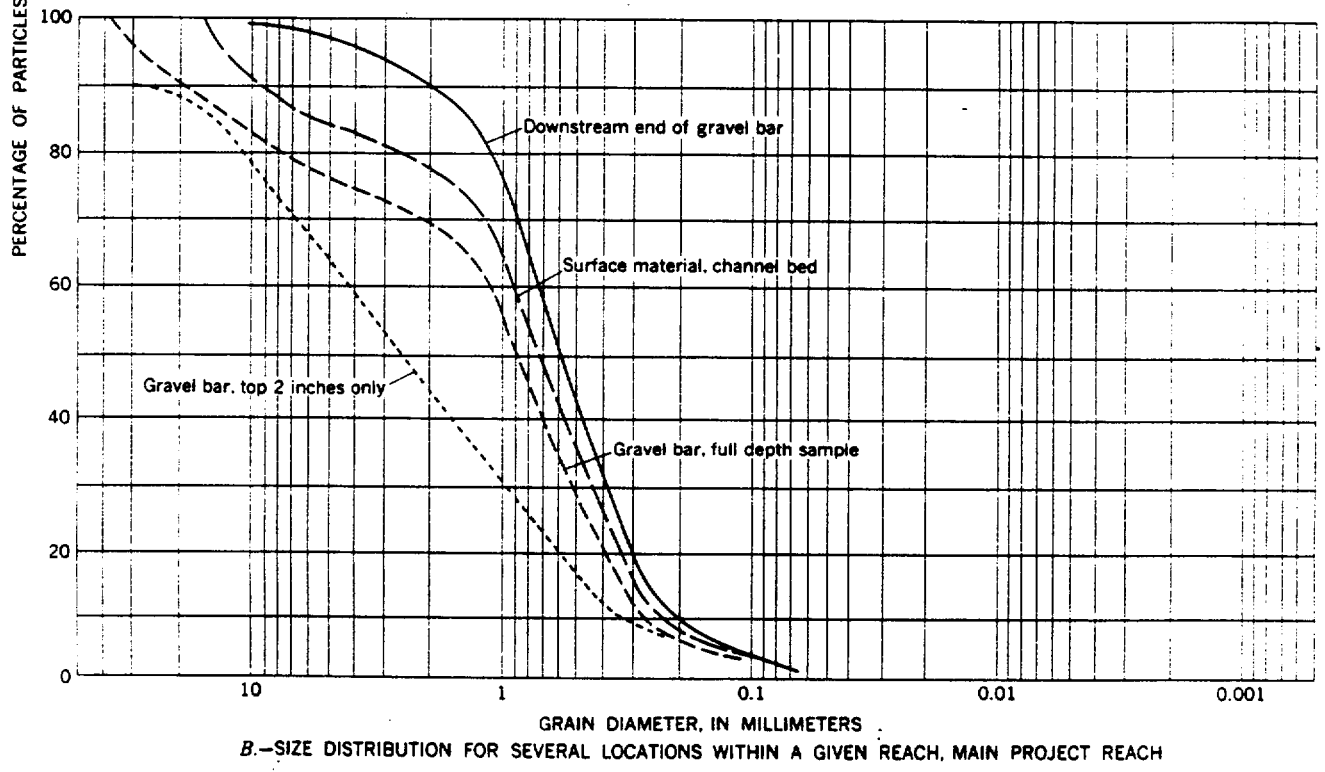
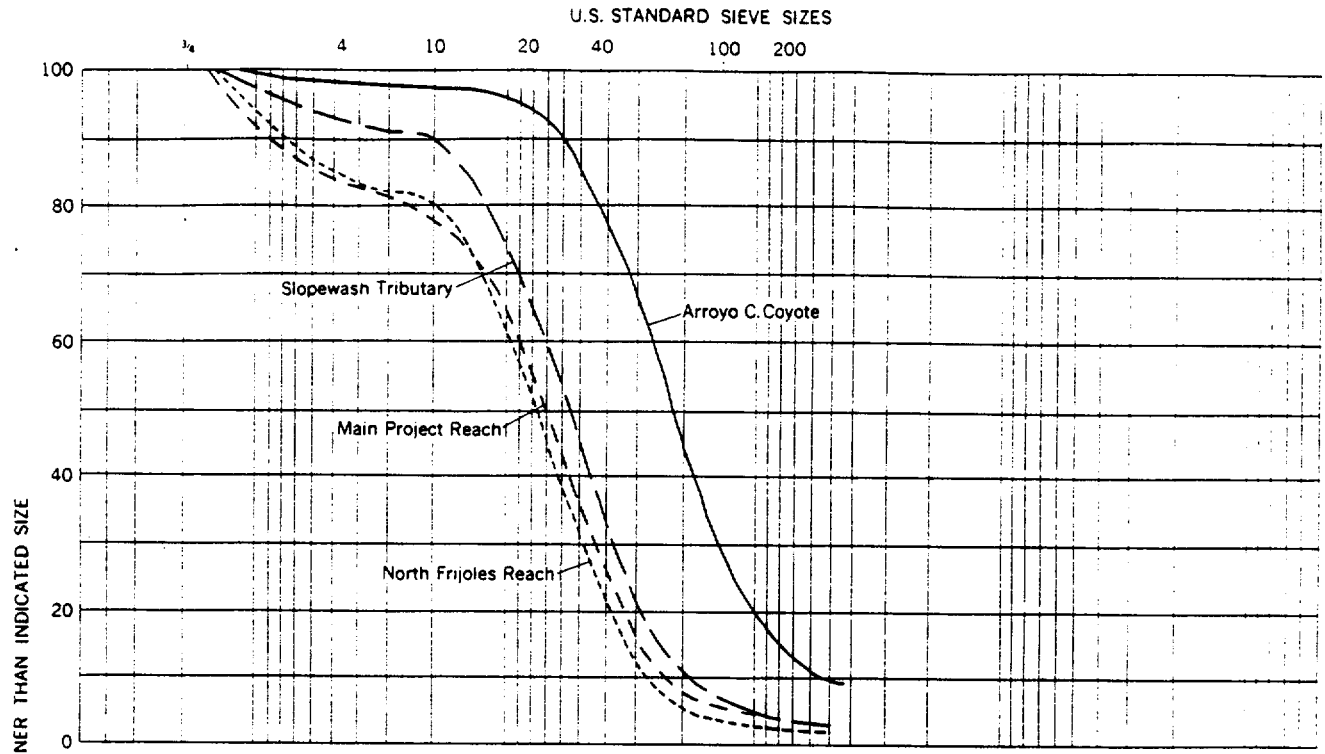


FIGURE 149.—Bed-material grain-size distribution, sieve analyses.

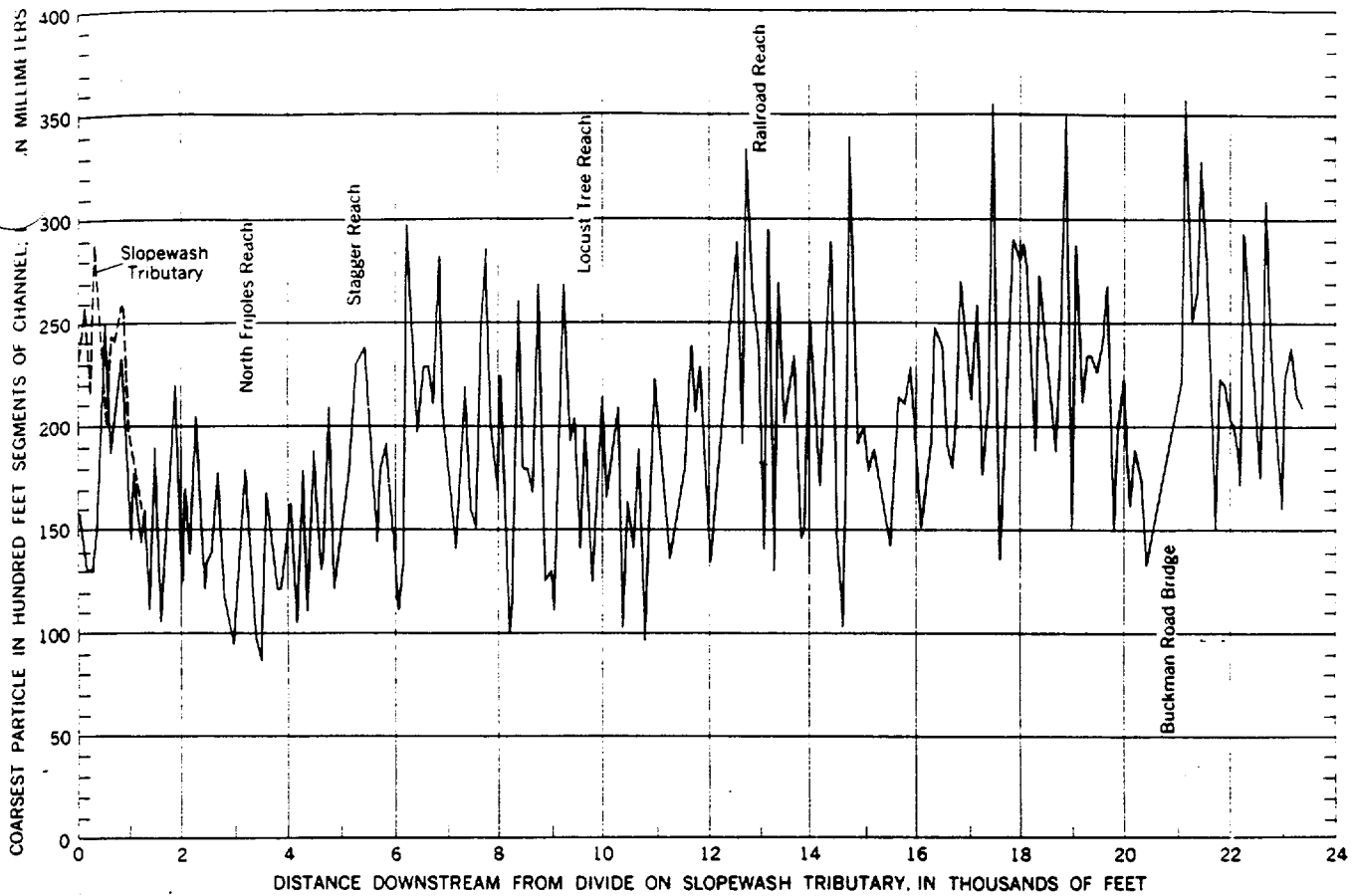


FIGURE 150.—Downstream distribution of coarsest particle in each 100-foot segment of channel.

Also, for several flows, the experiment included some rock groups composed of only one weight class. In this arrangement, rocks were spaced on 1, 2, or 3 diameters rather than by the absolute distances of 0.5, 1.0, or 2.0 feet.

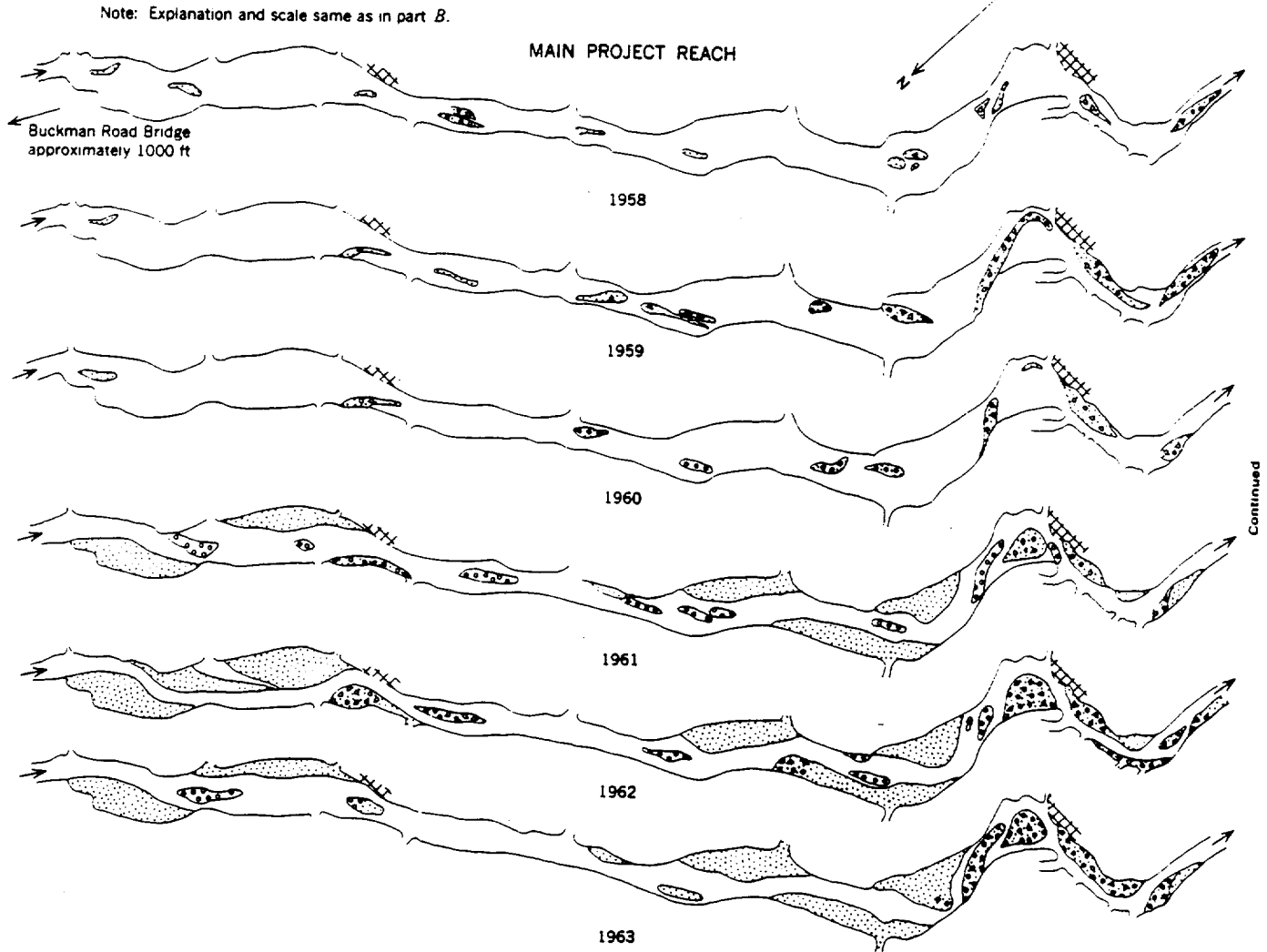
At the Main Project where the channel is straight, there were initially eight ranges of rock groups about 110 feet apart. The groups having 1-foot spacing lay along the centerline of the channel and the groups having $\frac{1}{2}$ -foot and 2-foot spacing on either side, alternating from one range to another. Arrangement of the four upstream ranges was the obverse of that for the four downstream ranges so as to eliminate bias in across-the-channel variation. The position of each particle was individually recorded together with its weight and dimensions of the long, intermediate, and short axes. In addition there were two lines of boulders (as much as 97,500 g) spaced 9 feet apart across the channel in this reach. At various times additional temporary ranges of particle groups have been installed at the Main Project Reach, but the eight ranges and two lines of large particles described above were maintained during the

entire investigation. After each flow we measured the distance that individual particles moved, and in preparation for the next flow, reconstructed each particle group in accordance with the specifications described.

Procedure at other reaches was basically the same as for the Main Project Reach. At the Locust Tree Reach there were originally two ranges, three since 1960, each including groups having two different spacings, and also a line of large rocks spaced 6 feet apart. The channel is so narrow at the North Frijoles Reach that the groups having different spacings were located along the length of the channel rather than along a line perpendicular to it.

At the Railroad Reach there was a single line of angular basalt boulders weighing as much as 111,000 grams and spaced 4 feet apart. The Stagger Reach had two lines of basalt boulders weighing as much as 47,500 grams, and spaced 3 feet apart. Basalt is a lithology foreign to the drainage basin and was derived from highway and railroad fills.

Tracing the downstream movement of painted gravel particles during a flow involved certain difficulties. An



A.—SAND AND GRAVEL BARS FROM BELOW BUCKMAN ROAD BRIDGE TO HALF-MILE SECTION

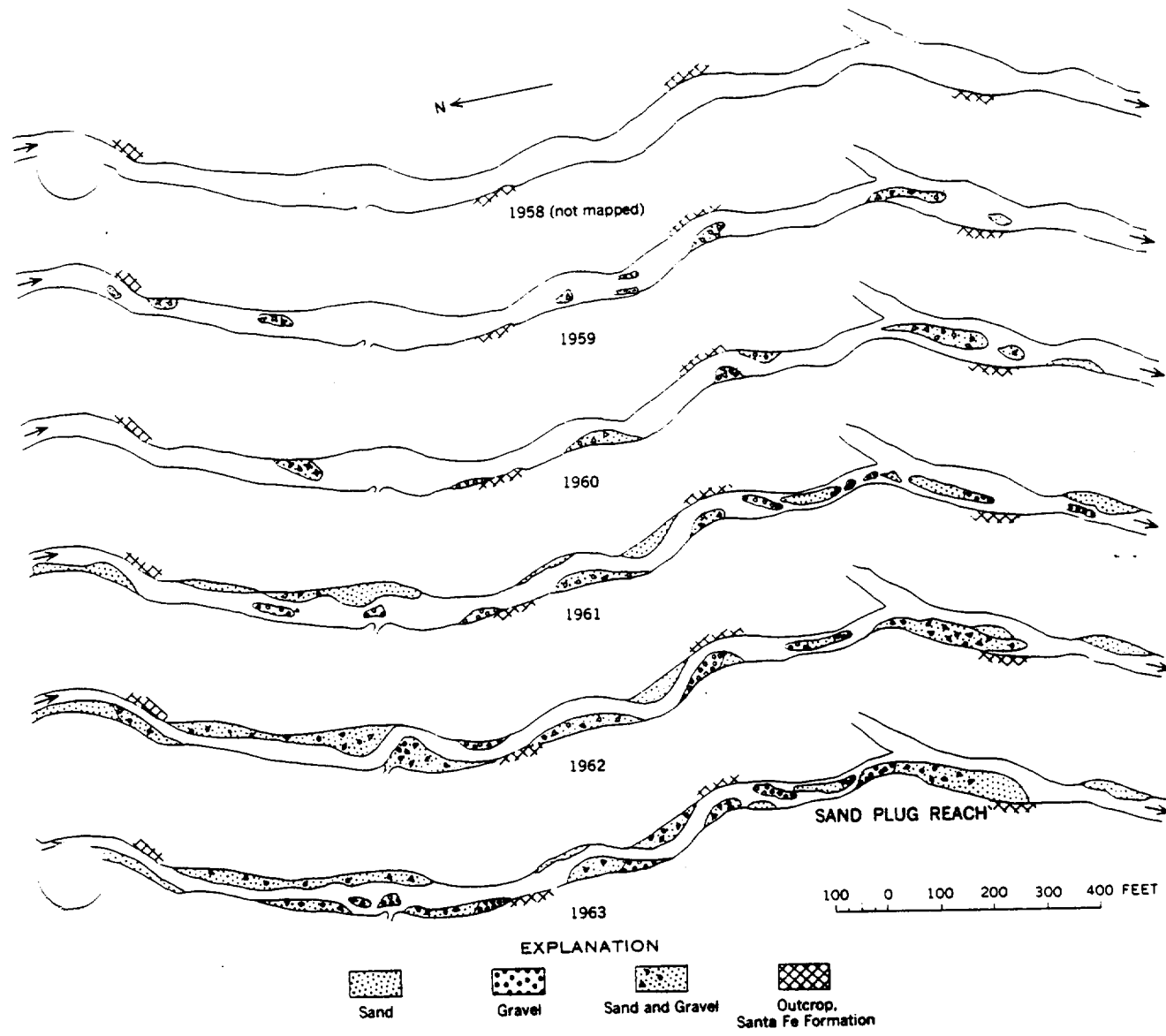
FIGURE 151.—Spacing and composition of

initial problem was to find a paint that is weather resistant during long periods of immobility and is abrasion-resistant during transport. Oil-base paints proved unsatisfactory because they peeled excessively. Except for the first year, water-base masonry paint was used with satisfactory results.

Even if the paint remains intact and every particle found is identifiable, there are still losses due to burial of particles in the sand, entrapment in brushy areas, or transport outside the search area. The rocks from a given group may move downstream distances ranging from a few feet to 3 miles, depending on the magnitude of the flow. Because of their bright color, painted rocks are plainly visible in the sandy channel unless

completely buried. Many particles are found partly buried (fig. 152) and the data on losses indicate that others become completely buried. Recoveries range from more than 90 percent in small flows to 2 percent for one exceptionally large flow. Apparently the losses have decreased since adoption of a water-base masonry paint, but even under optimum conditions losses of 10–30 percent during small flows and 30–50 percent during large flows are to be expected. The greatest losses occur in the smaller size classes.

Deep burial in the sandy channel seldom occurs in the area studied. Many holes 4 feet deep were drilled in the channel bed for installation of scour chains, and no coarse gravel was encountered. The composition of



B.—SAND AND GRAVEL BARS FROM HALF-MILE SECTION TO SAND PLUG REACH

avel bars. Arroyo de los Frijoles, 1958-63.

avel bars lends support to the conclusion that coarse particles occur only at or near the channel surface. A typical bar (fig. 152D) is strewn with coarse gravel, and in a typical cross section it is apparent that this is only a surface veneer extending at most a few grain-diameters deep.

Even when the bed scoured more than a foot in a high flow and subsequently filled to the original elevation, large gravel particles did not become deeply buried and, for the most part, projected slightly above the refilled surface.

The explanation of this phenomenon appears to be the Bagnold-dispersive-stress (1956) caused by grain-to-grain impact during motion. The stress increases

as the diameter squared and the large particles, subjected to highest stress, are forced to the bed surface where the dispersive stress is zero.

Subsequent to these observations, some streambeds in Maryland (annual precipitation 44 inches) were sampled to determine whether similar phenomena occur. It was found that gravel-bed streams in a sub-humid region also tend to have a concentration of the largest particles at the surface of the channel bed (Leopold and others, 1964, p. 211).

For the purpose of segregating the influence of size and spacing on particle movement it is not necessary to consider the distance a given rock moved during a flow; that is, whether it was actually found downstream or



A



B



C



D

FIGURE 152.—The painted rock experiments and a naturally occurring accumulation of large particles. A, Main Project Reach, showing Latin Square position of painted rock groups in the sandy channel. B, Rocks moved from Main Project Reach during flood of August 4, 1960; note scour pits around each boulder. C, Detail of rock weighing 7,100 grams at Main Project Reach, partially buried by sand and organic debris during flow of August 4, 1960. D, Gravel bar at Sand Plug Reach, Arroyo de los Frijoles, looking upstream.

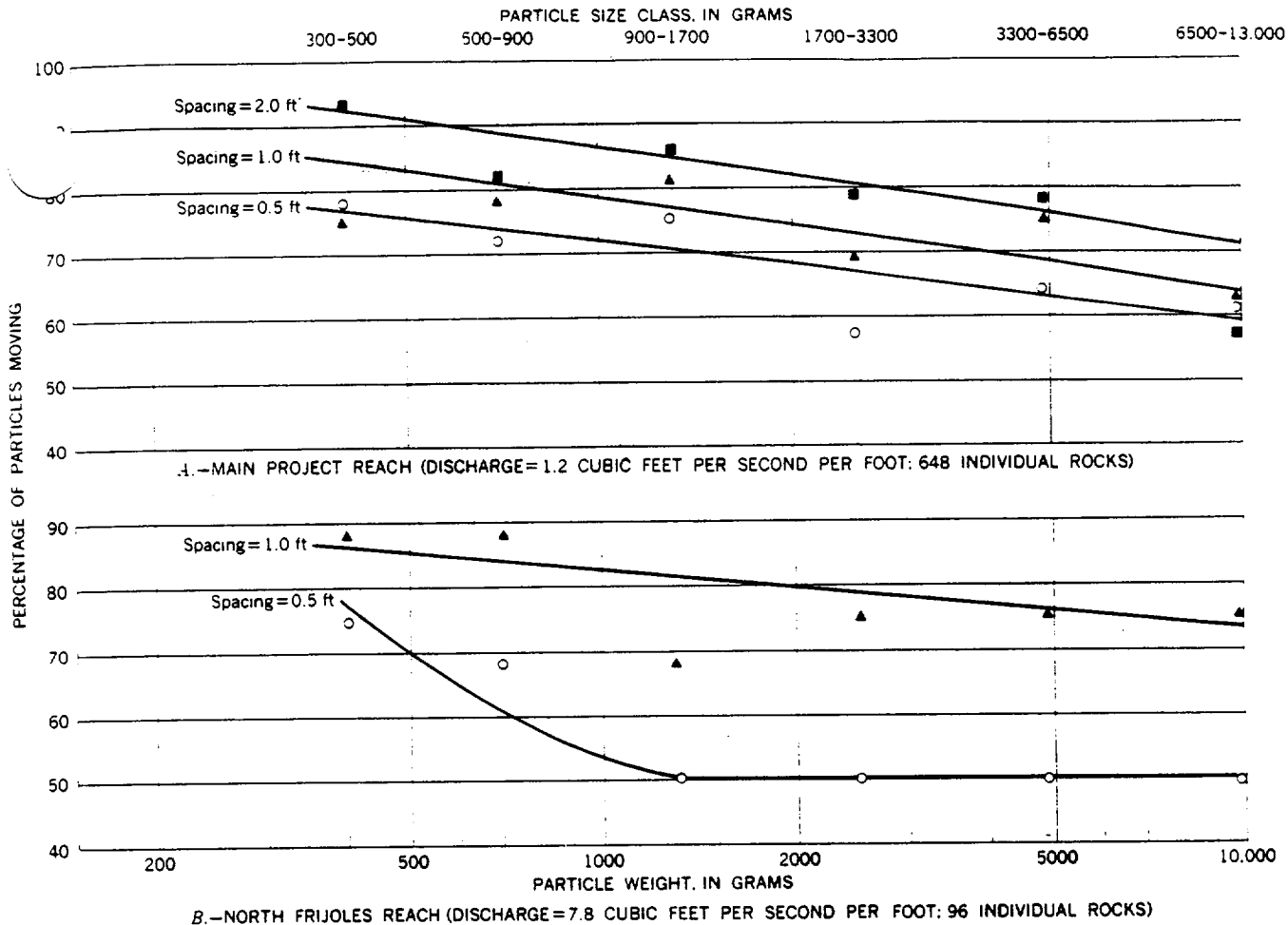


FIGURE 153.—The effect of spacing on percentage of rocks moving for a given discharge and particle size.

was simply missing. The particle had moved and how far it had moved was of no consequence. For each flow the percentage moved by size class and spacing was studied. In all, 14,000 observations were available for rock movements. The consistency of the data ranged from excellent to poor. A typical set of data are plotted on figure 153 to illustrate. From the set of graphs exemplified in this figure, further analysis was made in a manner explained in a separate paper by Langbein and Leopold. The pertinent results are presented in figure 154.

In summary, the results show that a larger flow is required to move particles which are close to one another than if they are spaced far apart. The influence of spacing decreases with increasing spacing and becomes negligible for spacings greater than about eight diameters. For example, a discharge of 11 cfs per ft would not move 500-gram particles if spaced at one diameter, but the same discharge would move 5,000-gram particles if spaced more than five diameters apart.

The effect of spacing on particle movement leads to

the concept that a gravel bar is a kinematic wave caused by particle interaction, and is comparable in theory to concentrations of cars on a highway.

Owing in part to the phenomenon just described, the distance a coarse particle moves during a given flow is only slightly related to its size (fig. 155 and table 3). Particles lost are assumed to have moved distances comparable to those found. For some flows, all the particles recovered, regardless of size, were transported distances roughly equal. This is probably related to downstream decrease in discharge due to percolation into the channel. The relation of distance moved to maximum discharge during the flow is shown in figure 156. In general, the small particles do not travel materially farther than the large ones, and nearly half the flows include examples of larger particles moving farther than small ones. There is thus no neat progression of transport distances inverse to particle size.

SCOUR AND FILL

Scour and fill data from the Arroyo de los Frijoles are being collected by means of scour chains buried ver-

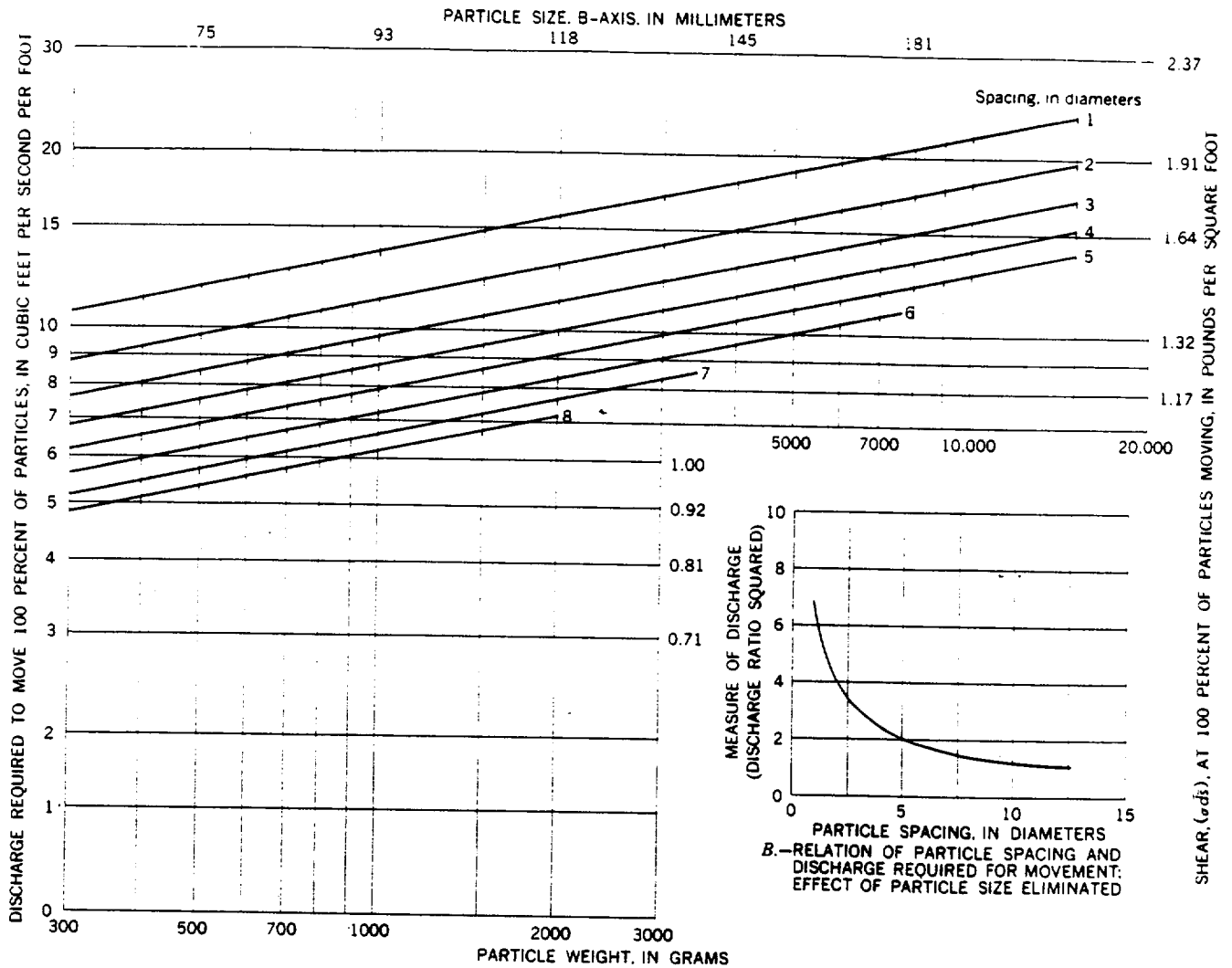


FIGURE 154.—Summary of data relating discharge, size, and spacing for painted rock experiments.

tically in the streambed with the top link at or slightly above the bed surface. After a flow the elevation of the streambed is resurveyed and the bed is dug until the chain is exposed. If scour has occurred, a part of the chain will be lying horizontally at some depth below the channel bed (fig. 157). The difference between the previous streambed elevation and the elevation of the horizontal chain is the depth of scour. The difference between the existing bed elevation and the elevation of the horizontal chain is the depth of fill. If no scour has occurred the depth of fill is the increase in bed elevation.

Scour chains, each 4 feet in length, were installed along a reach of nearly 6 miles, beginning in Slopewash Tributary and ending at Sand Plug Reach. The location of the chains usually followed the low-water channel. Over most of the study reach chains were placed at 1,000-foot intervals. In the Main Project Reach of

2,000 feet, chains were placed at 100-foot intervals. This spacing was believed sufficient to determine any downstream trend in the scour pattern in this arroyo. At seven of the chain sections, additional chains were installed across the width of the channel and provide an indication of any lateral variation in scour.

Scour-and-fill data are available for most of the 22 significant flows in the 7-year period, 1958-64. All data obtained during the scour-chain record are on file with the U.S. Geological Survey, Washington, D.C., 20242. However, since some chains were installed before others, an equal length of record does not exist for each chain location. In addition some chains, usually those in the uppermost or lowermost reaches, were not surveyed after each flow. These missing segments of data disallow a complete picture of scour and fill for individual storms,

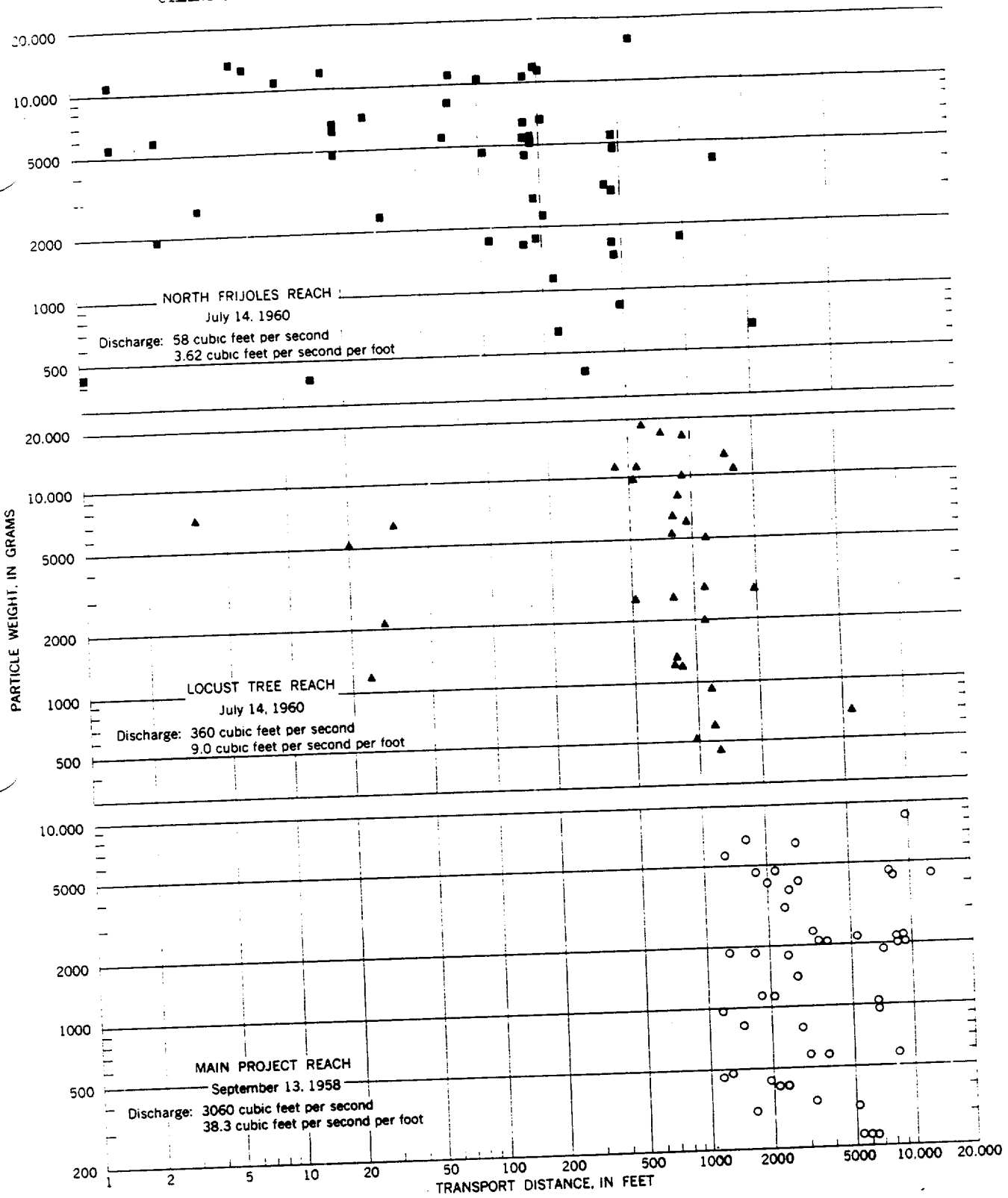


FIGURE 155.—Transport distance of coarse particles as a function of particle weight.

TABLE 3.—Relation of transport distance to flow discharge

[Leaders indicate that data are insufficient for an average or that category is inapplicable. Distance measurements centered in two columns represent data from adjacent size classes averaged together]

Location	Date	Discharge		Average transport distance, in feet, by size class of particle, in grams										Average for all sizes			
		Cfs	Cfs per ft	200-300	300-500	500-900	900-1,700	1,700-3,300	3,300-6,500	6,500-13,000	13,000-26,000	26,000-52,000	52,000-104,000				
Main Project	9-13-58	3,060	38.3	5,880	2,336	3,862	3,500	4,537	4,815								4,028
	7-25-62	1,300	16.3					1,771	1,783	1,811	1,087	363					1,775
	7-30-62	300	3.75														
	9-18-61	60	7.5					1,272	748		260						784
	9-19-61	250	3.13														
	8-04-60	152	1.90		495	630	605	172	136	99							456
	7-08-61	98	1.22		776	673	378	449	194	463	18						446
	8-12-61	90-90	1.06		489	380	130	51	83	141	2						186
	7-05-62	40	5.0														145
	7-14-60	35	4.4		126	103	76	121	38	24	0	0	0	0	0	0	93
	8-07-59	20-24	2.8		3	11				0	0	0	0	0	0	0	7
	7-23-59	10-15	1.6							0	0	0	0	0	0	0	11
Locust Tree	9-19-61	650	16.2		1,894			1,995	1,568								1,818
	7-08-61	498	12.5		925	1,952	471	841	1,592	496							1,123
	7-25-62	450	11.2						1,385								1,196
	7-30-62	450	11.2							1,120							
	7-14-60	360	9.0			2,198	796	1,116	720	806	757						1,051
	8-12-61	300-400	8.8		938			692	317								563
	7-05-62	150	3.75					266	84								234
	5-23-59	50-75	1.56		225	247	276	230	107								223
	8-17-59	20-25	2.5		397	299	126	29	34								151
	9-06-58	10	2.5					73	8								54
North Frijoles	9-19-61	230	14.4			789		674		547	972						670
	5-23-59	140	8.7				644		443	124	78						254
	8-12-61	85	5.32			550		316		142	170						332
	7-25-62	85	5.32			493		243		119							273
	7-14-60	67	4.18			108	659	336	242	269	78						216
	7-08-61	58	3.62			540	291	330	325	217	159	118					294
	8-24-59	50	3.12			117	229	218	110	79	48	71					125
	9-06-58	15-20	1.09		268	93		57									153
Stagger Reach	9-19-61										1,313	2,140					1,727
	7-14-60										458	304					400
	7-30-62										647	191					373
	8-12-61										49	199					109
	7-05-62										39	61					53
	7-25-62										45	35					38
Railroad Reach	7-08-61											14					14
	7-08-61										1,665	43	148				979
	7-14-60										381	260					340

but the net change in bed elevation since the time of the initial survey may still be obtained.

By 1959 the majority of the chains had been installed along the arroyo. Scour-and-fill data for a sample flow, for the year 1962, and for the period 1958-62 are shown in figure 158. The upper part of the figure shows the drainage area of Arroyo de los Frijoles and the general location of the chains by chain number. For the two individual flows, the lower dashed line represents the depth of scour. The upper dashed line represents the depth of fill. The heavy solid line represents the net change in bed elevation after scour and fill.

The nature of the flash flow is such that the entire length of the arroyo may not be flooded with each storm. The flow-producing rain may be so located that only lower reaches received runoff, or, for a smaller storm near the headwaters, a part or possibly the entire flow may be absorbed into the ground by percolation before it reaches a downstream section. A third possibility remains that a particular chain section may be left dry or has very little scour because it was not in the low-water path of flow. For a single storm, then there is a considerable variation in the recorded depth of scour from section to section. This variation is further exemplified in the Main Project Reach where the chains are

placed at 100-foot intervals. In spite of individual variations a general consistency prevails among the data, that is, at most sections along the channel there is a scour and subsequent fill. All flows produce this same pattern; the magnitude of scour is primarily dependent upon hydraulic factors of individual flows, and these factors are related to the intensity and total amount of rainfall.

North Frijoles, Locust Tree, and Main Project reaches of the channel are the objects of special study and are also the reaches where flow rates are measured. It is within these reaches that the chain sections are located to determine cross-channel patterns of scour. The mean depth of scour at a section may be determined by averaging the values from the several chains at each of the sections. Mean values of scour for each recorded flow are tabulated in table 4. The data are plotted in figure 159. Despite considerable scatter among the data, the mean scour depth appears to be proportional to the square root of discharge per unit width of channel.

An increasing depth of scour downstream is not observed in any single profile (fig. 158).

Probably for similar reasons, the depth of scour is apparently independent of channel width. Channel widths have been illustrated on figure 148. No sys-

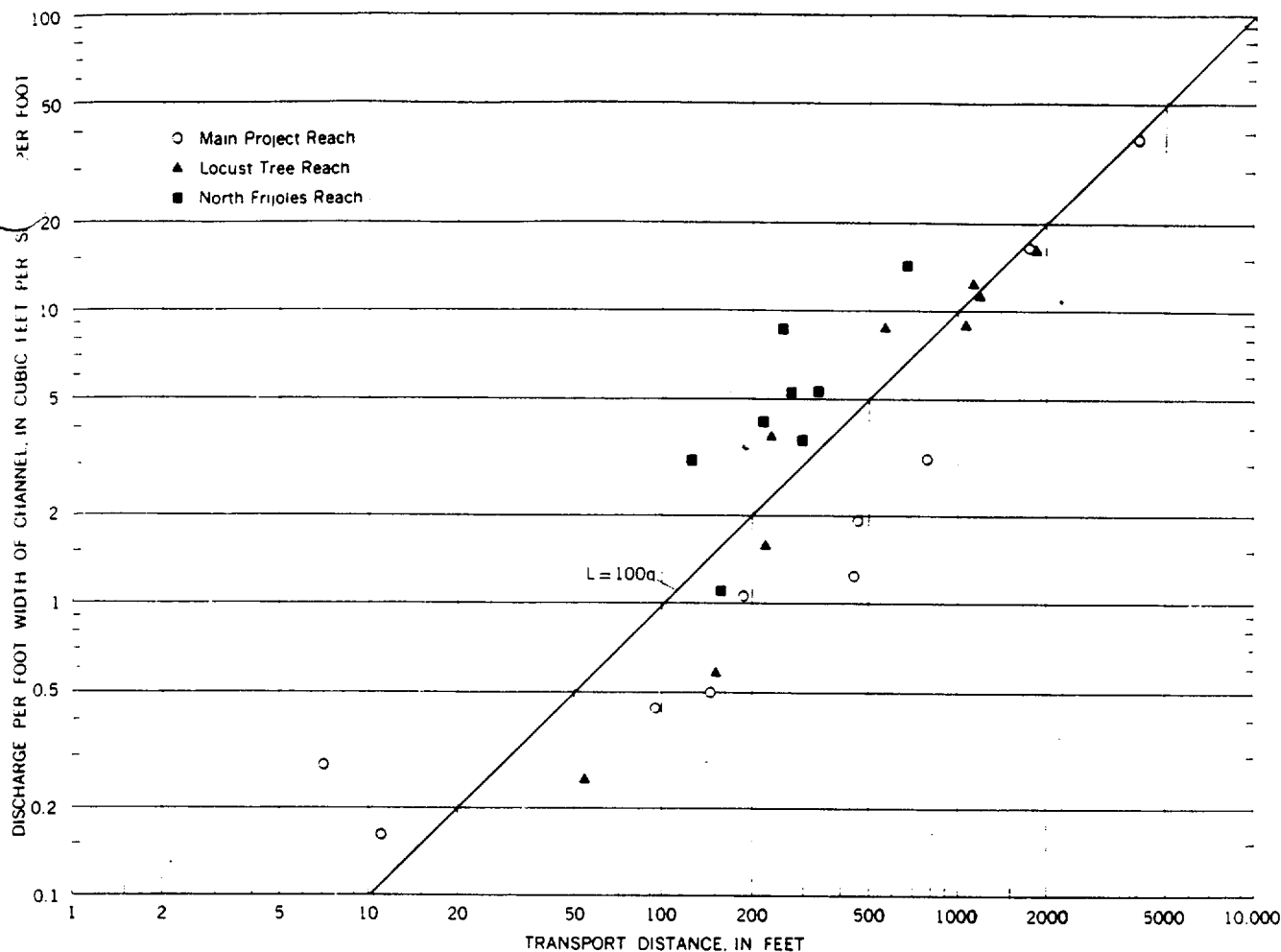


FIGURE 156.—Average transport distance of coarse particles as a function of discharge (sizes approximately 200–13,000 g).

tematic relation of local depth of scour to the corresponding channel width could be established.

The seven chain sections provided data to study lateral variations in scour across the width of the channel. One of these sections, chosen as representative of a typical reach, is illustrated on figure 160. This figure, illustrating a Main Project section near station 25,000 feet, indicates a net aggradation for the 6-year period. The whole width of the channel scours during nearly every flow, but the amount of scour and fill varies across the width.

The progressive effect of scour and fill over the length of the channel is illustrated in figure 161. Except for several isolated reaches, aggradation is occurring over the entire length of the channel. For the period of record, this aggradation amounts to an average of 0.04 ft per yr including those reaches which show a net scour.

Net scour in individual reaches can be partially explained either by natural or man-caused events. For

examples, at a stationing of 32,000 feet (fig. 161) the large flow of 1958 cut through a fan-type deposit (literally a sandplug and hence the name for this reach) at the chain location and indicated a large net scour. This fan had earlier been deposited at the mouth of an entering tributary. At this sand fan most of the channel width was accumulating a net fill and now, 1964, an islandlike deposit over a foot high occupies a large part of the channel width. Channel-wide, a net aggradation does exist at that location, but because of the placement of the chain a net scour shows on the graph of figure 161.

Also, in some of the upstream reaches of the channel, excavation of sand by local contractors is responsible, at least in part, for the apparent net degradation at these sections.

The downstream profiles of the channel bed showing progressive accretions of sediment during aggradation probably represent as detailed an historical record of this process as has been compiled.



FIGURE 157.—Horizontal part of chain lying at depth of maximum scour, here about half a foot. Vertical part of chain disappears below man's hand.

The record demonstrates some nonuniformity along a channel 6 miles long, some short reaches not following the general trend. The reaches not participating in the aggradation do so consistently, but as in the Sand Plug Reach at the lower end of the studied length, the reason for its deviation relates to special and understandable local circumstances. Interestingly, the random pattern of storm occurrence does not lead to a random location of reaches of sediment accretion, for the increment of deposition is rather uniform from year to year.

The exaggeration of scale in figure 161 must be kept in mind, and the variations in yearly increments are really very small considering the channel length involved. If one short reach aggraded a tenth of a foot more than another a thousand feet away, the channel slope in the reach would be changed by only 0.0001 foot per foot. The variability along the channel due to the irregularities of depositional increment are of this order. Thus, despite random character of storms and the local loss of flow to channel percolation the mean slope of the bed is maintained over long reaches.

A more complete discussion of the records of scour is given by Emmett and Leopold (1964). For the present purpose, suffice it to say that scour is associated with dilation of the grain bed through the scour depth, but that individual particles may move intermittently and at a speed much less than that of the water. The volume of material scoured and moved is large. Because of its low mean speed downstream, that whole volume does not move entirely out of a long reach but, in effect, is shifted downstream only a limited distance.

TABLE 4.—Mean depth of scour as a function of discharge

Date of flow	North Frijoles Reach				
	Discharge (cfs)	Upper section		Lower section	
		Discharge (cfs per ft)	Scour (ft)	Discharge (cfs per ft)	Scour (ft)
9-6-58	17.5	0.87	0.018	1.46	0.050
9-13-58	194	9.7	215	16.2	.977
5-23-59	140	7.0	103	11.7	.460
8-24-59	30	2.50	083	4.17	.000
7-14-60	67	3.50	068	5.59	.135
11-16-60	9	40	023	67	.315
7-08-61	58	2.90	130	4.84	.268
9-19-61	230	11.50	188	19.20	.598
7-05-62	7			58	.040
7-30-62	90	4.50	153	7.50	.175
7-20-63	10	50	180	83	.128
9-21-63	5	.25	293	.42	.448

Locust Tree Reach				
Discharge		Scour (ft)		
(cfs)	(cfs per ft)	Upper section	Middle section	Lower section
9-13-58	1320	34.0	0.820	
5-23-59	62.5	1.89	.132	0.076
8-07-59	22.5	.56	.196	0.060
7-14-60	360	9.0	.280	.212
7-08-61	498	12.47	.464	.406
8-12-61	350	8.75	.194	.368
9-19-61	650	16.25	.280	.138
7-05-62	150	3.75	.274	
7-30-62	450	11.2	.272	.334
7-20-63	15	.38	.134	.076
9-21-63	316	7.9	.314	.320

Main Project Reach						
Discharge (cfs)	Upper Reach		Lower Reach		Low-water chains	
	Discharge (cfs per ft)	Scour (ft)	Discharge (cfs per ft)	Scour (ft)	Discharge (cfs per ft)	Scour (ft)
8-18-58	20	0.235	0.053	0.286	0.023	
9-13-58	3060	36.0	.830	43.6	.557	
5-23-59	4	.047	.050	.057	.008	0.050
7-23-59	12.5	.147	.000	.178	.240	.156
8-07-59	22.5	.265	.033	.321	.022	.282
7-14-60	35	.412	.036	.500	.033	.439
8-04-60	152	1.79	.088	2.17	.425	1.90
7-08-61	98	1.15	.124	1.40	.118	1.23
9-19-61	250	2.94	.125			3.13
7-25-62	1300	15.3	.511	18.6	.810	16.3
7-20-63	5	.059	.024	.072	.010	.062
9-21-63	391	4.8	.236	5.59	.175	4.9

HILLSLOPE EROSION

EROSION PLOT ON SLOPEWASH TRIBUTARY

To measure the rate of hillslope erosion a grid system of erosion pins was installed in 1959 on one of the slopes in the drainage area of Slopewash Tributary. The general location of this grid system, or erosion plot, is shown in figure 144, and the locality is illustrated in figure 143. The erosion plot consists of 61 nails with washers spaced on 5-foot centers on an area 50x50 feet having a relief of 5 feet and furrowed by two shallow and narrow rills. These rills join midway through the grid system into a single larger rill.

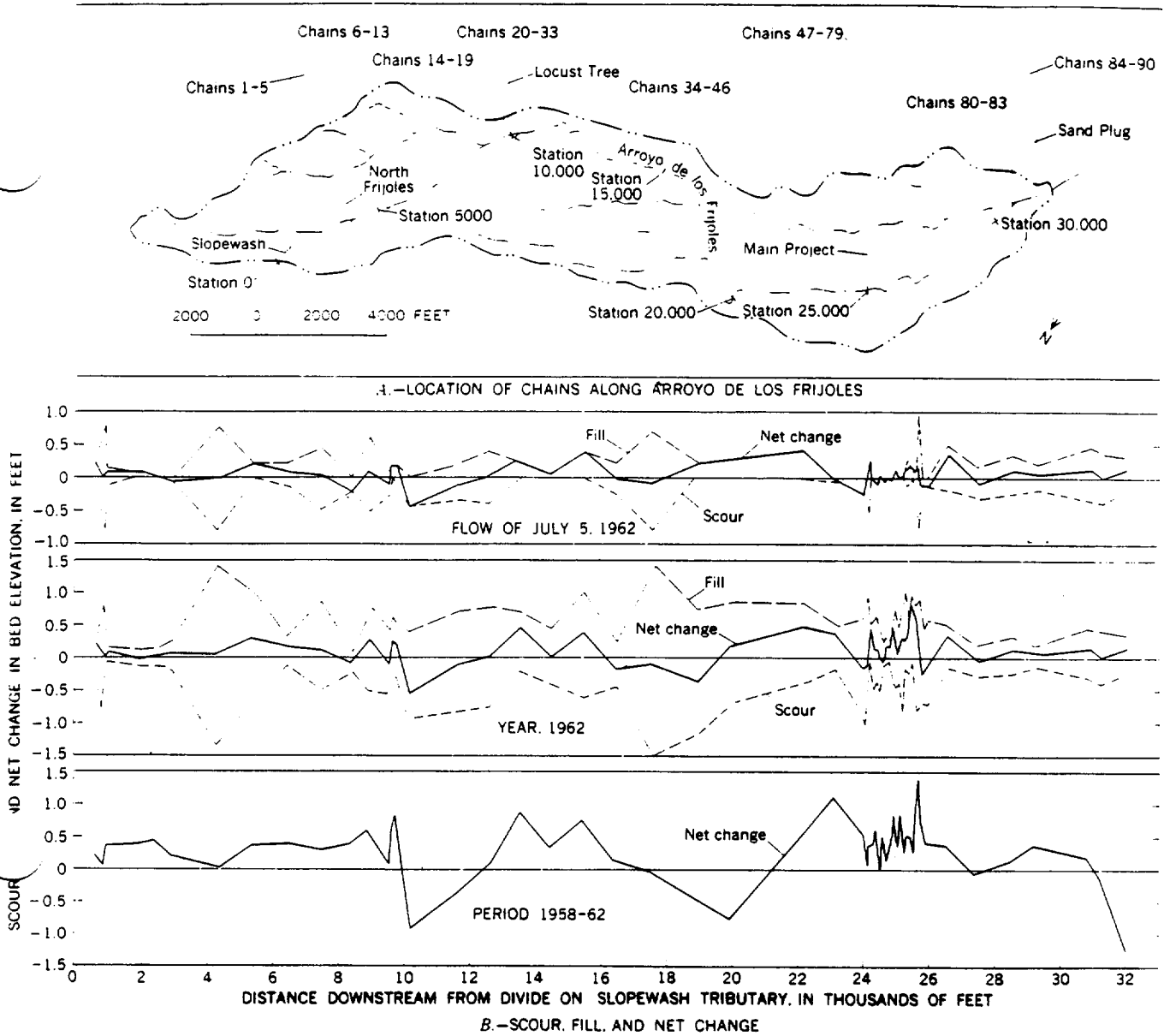


FIGURE 158.—Downstream pattern of scour, fill, and net change in bed elevation for a single-storm, a 1-year, and a 5-year period, 1958-62.

At the time of the installation, the nails (10-inch spikes) were slipped through a large washer and driven into the ground in a vertical position until the bottom of the washer was flush with the ground surface. Erosion undermines the washer, which then falls down a length of the pin. The pin protrudes above the washer at a distance equal to the erosion during the intervening period. While maximum erosion is marked by the washer, deposition may be recorded as the height of any material above the washer, a desirable feature in such places as a rill bottom where maximum and net erosion generally differ. Figure 162 shows typical erosion nails

on the erosion plot and on transects. Elevations of all nail heads were measured and resurveys show that the nails remain stable and are not being heaved by frost action.

An attempt was made to map erosion values as topographic contours of erosion quantity, but because of the short length of record no systematic trend is apparent among individual values. At this time it appears that the pins on the steeper slopes adjacent to the rills show a slightly higher rate of erosion.

Pins in or near rills tend to show some deposition on the washer following scour. Depth of overland runoff

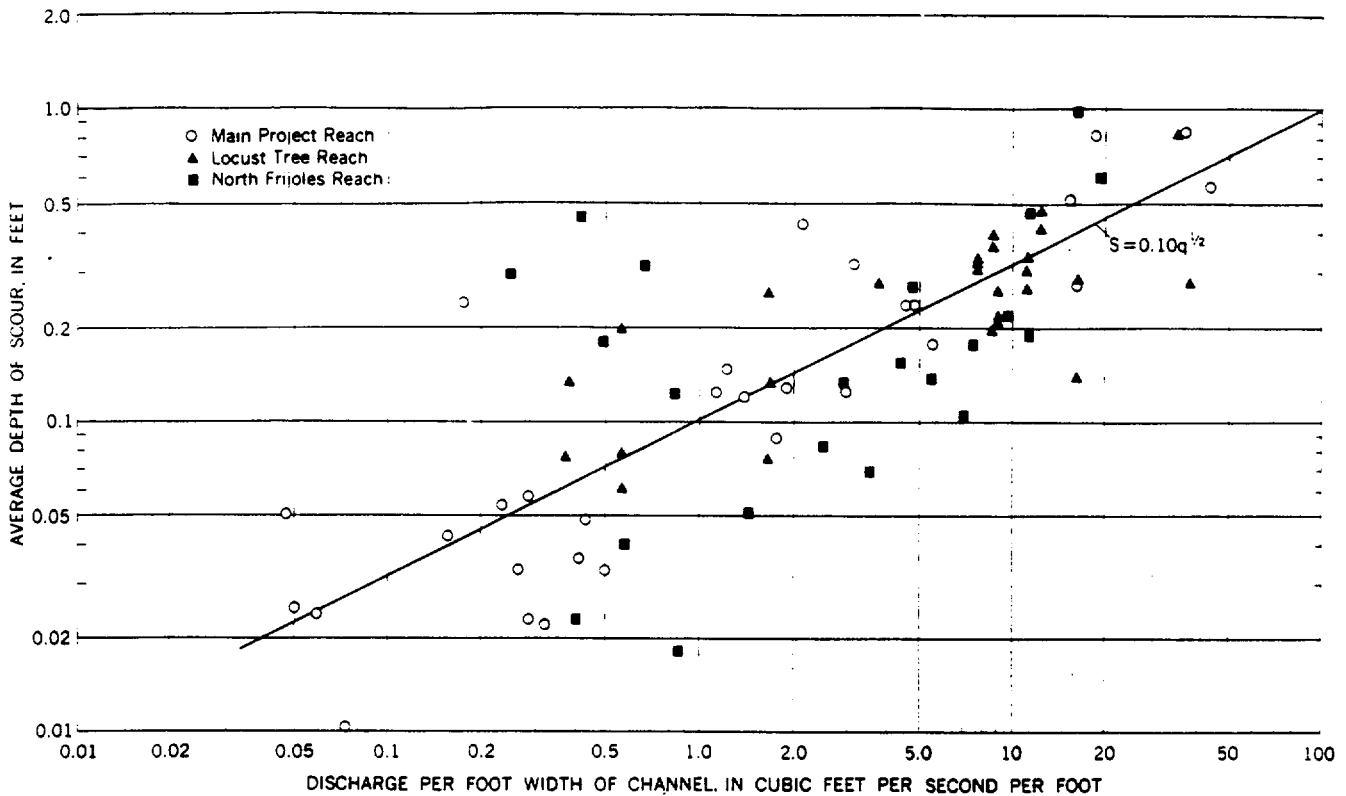


FIGURE 159.—Depth of scour as a function of discharge at chain sections: each point represents an average scour across the channel bed, based on 4–10 chains per cross-section.

is greater in such locations and it might be that erosion occurs during maximum overland flow depth and that deposition follows as the flow subsides. But deposition is the exception and not the general rule. The majority of the pins show very little or no filling on top of the washer.

Erosion data have been collected in the years 1961–64. Data in 1961 included only values of erosion and later, both erosion and deposition. The average erosion during the 5-year period, 1959–64, was 0.0117 ft per yr, and deposition on some of the pins averaged 0.0041 ft per yr—a net average rate of erosion of 0.0076 ft per yr.

Summary of data C contains data from the erosion-pin plot in Slopewash Tributary.

SLOPE-RETREAT PINS ON SLOPEWASH TRIBUTARY

Fifty-seven erosion pins are arranged on four lines transverse to the steep sides of Slopewash Tributary. These pins are the nail-with-washer just described, and are designated as “slope-retreat pins” on the location map of figure 144. An enlarged sketch elaborating details of these pins is shown in figure 163.

The pins are arranged in three groups, each group consisting of two lines spaced 2 feet apart. Each line, with pins spaced at 2-foot intervals, extends down the

steep slopes to the channel bed and, for one pair of lines, cuts across the channel and up the steep slopes on the opposite side of the tributary. The slopes range in steepness from 21 to 38 degrees, and these generalized slope angles are marked on figure 163 for identification.

The pins were installed in 1959 and erosion measurements were made once a year in the period 1961–64. Net values of erosion for the period are shown below the pin numbers on figure 163.

For the 57 pins, the average rate of net erosion is 0.0142 ft per yr. This figure consists of an average rate of maximum erosion of 0.0281 ft per yr and an average deposition of 0.0139 ft per yr. Individual measurements varied from a net deposition to an erosion of more than 0.08 ft per yr. A summary of all data from the slope-retreat lines is included in summary of data D.

Perhaps more meaningful rates of erosion could be obtained by dividing the 57 pins into 3 categories. Category 1 includes pins 1–29 of the upper line, category 2 includes pins 30–45 of the upper line, and category 3 includes the 12 pins, 46–57, in the lower line. Categories 1 and 3 are similar in their physiographic locations, but the pins in category 2 differ in that here apparent erosion is being disguised by channel deposits on some of the pins near the channel edge and by an accumulation of sloughed material on some of the lower

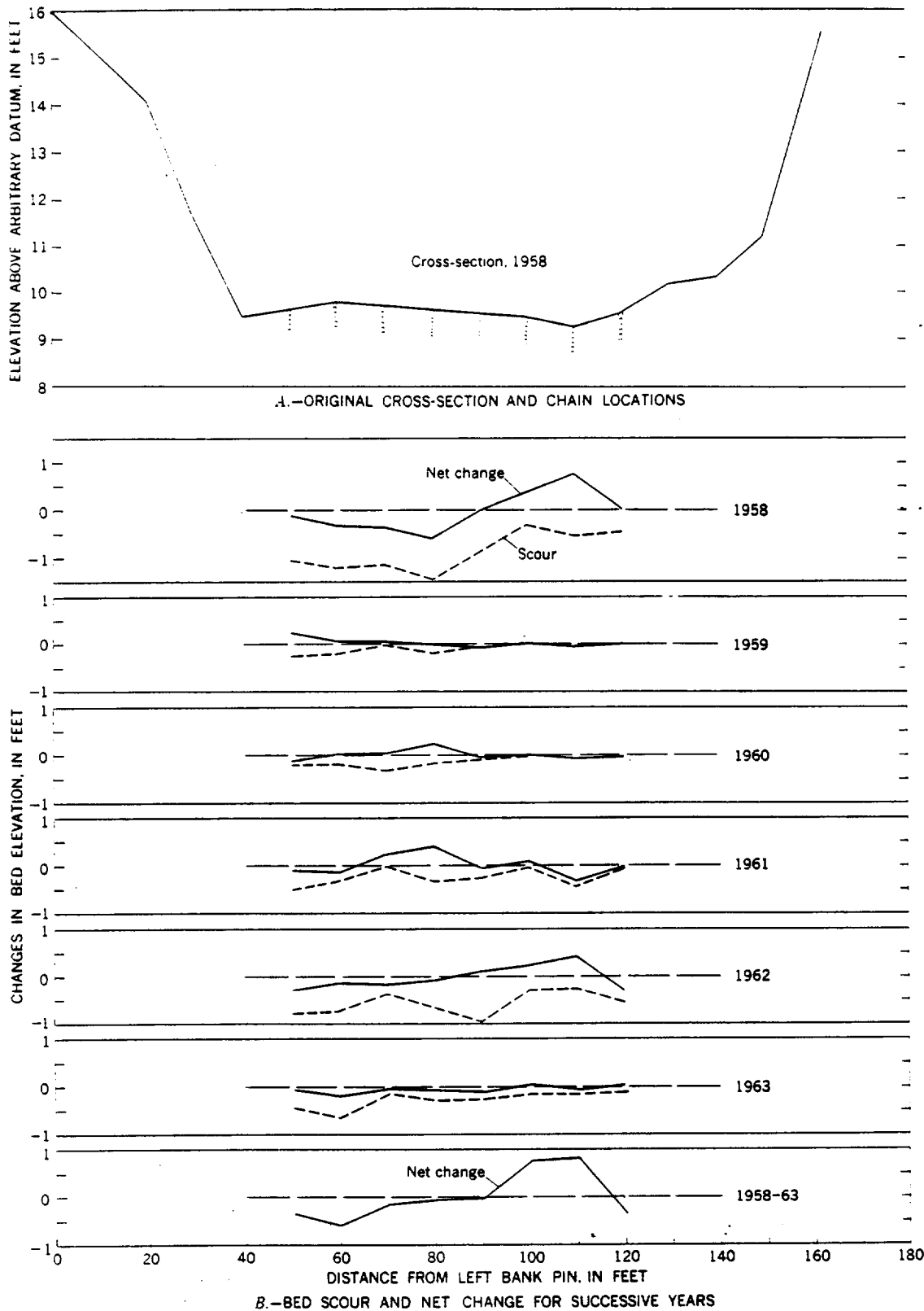


FIGURE 160.—Scour and net change in bed elevation, upper chain section, Main Project Reach.

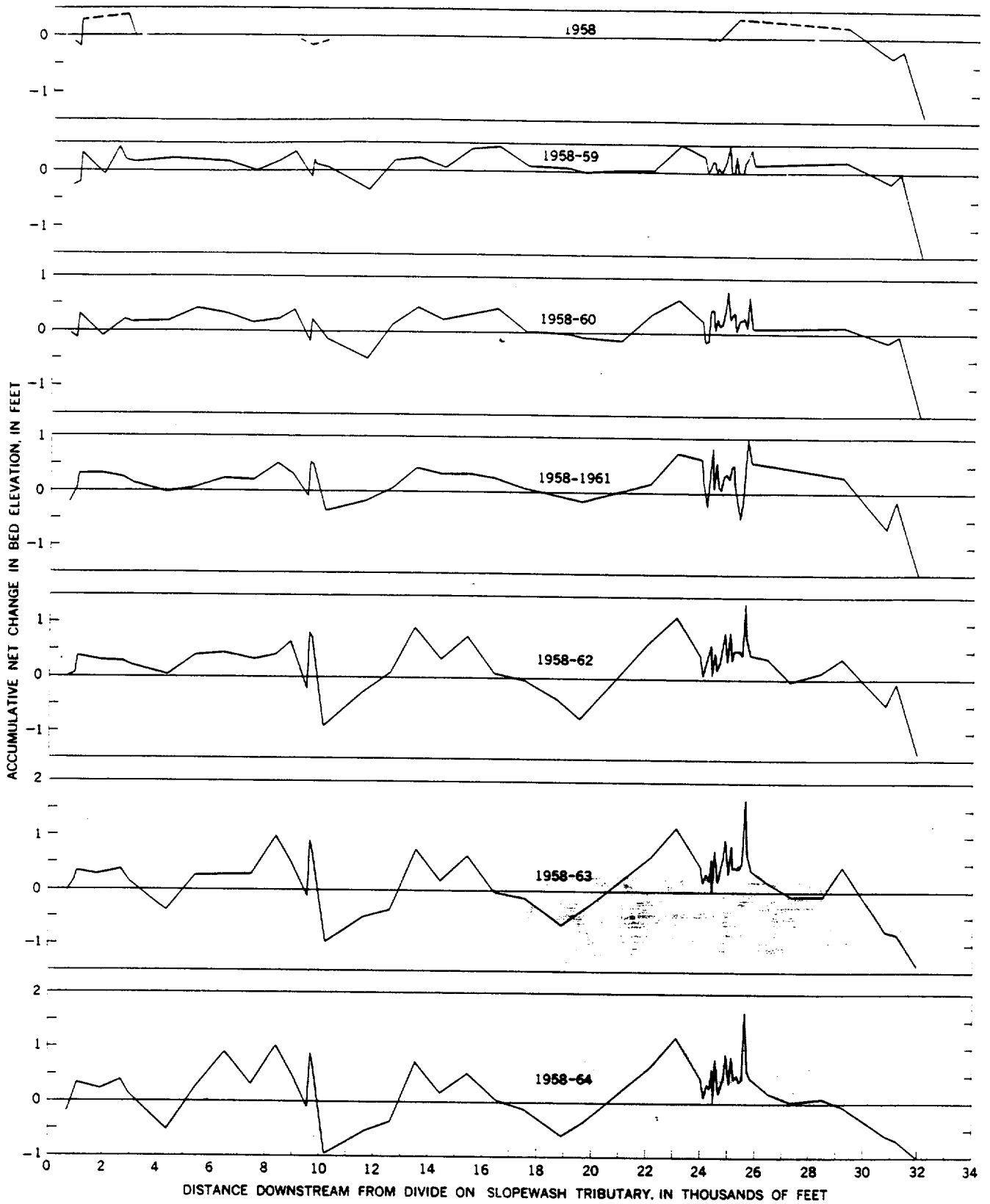
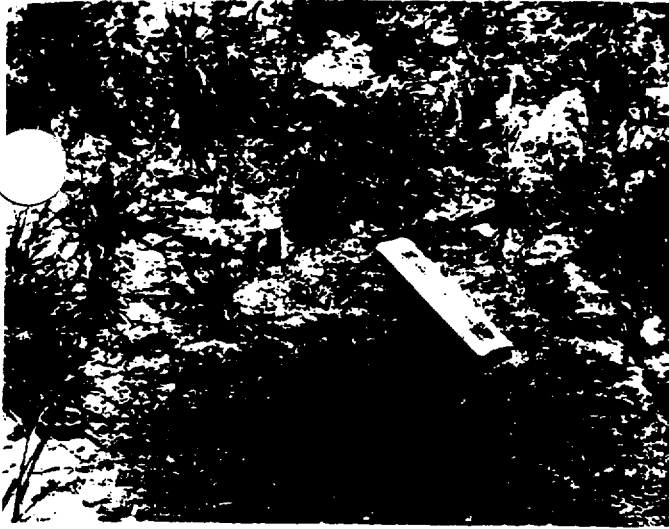
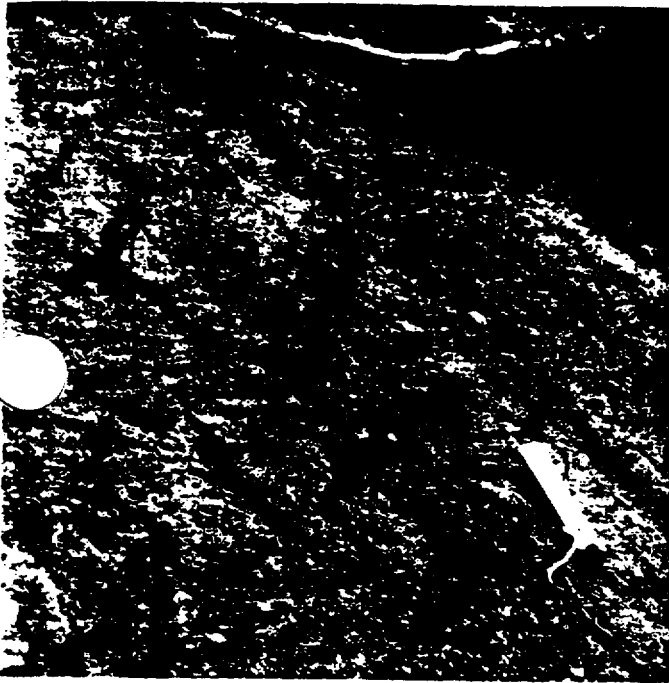


FIGURE 161.—Downstream pattern of accumulative net changes in bed elevation, Arroyo de los Frijoles.



A



B

FIGURE 162.—Erosion pins consisting of 10-inch spike and washer. A, Erosion pins in grid system, Slopewash Tributary (scale is a 6-inch ruler). B, Erosion pins on slope-retreat line, Slopewash Tributary.

pins on the sloping bank. Thus the 16 pins in this category actually show an average of a net deposition. Most likely this apparent deposition is only temporary, as a scour of the channel deposit will not only expose the lower nails again but will also allow the sloughed material to continue its downslope journey to the channel.

Rates of net erosion for pins in each of the three categories are: category 1, 0.0210 ft per yr; category 2,

-0.0034 ft per yr (the minus represents net deposition); and category 3, 0.0183 ft per yr. More complete computations are included at the end of summary of data D.

Excepting those pins just mentioned in category 2, generally only those pins on the channel bed showed consistent deposition above the washer, and the fact that in most places these pins were completely buried indicates an aggrading channel. Undoubtedly much of the aggraded material is derived from the erosion of the steep slopes adjacent to the channel. However, the erosion rate on these slopes more than compensates for the volume accumulation of sediment on the channel bed. Implicit, then, is that much of the eroded fine-grained sediment is being carried further downstream.

Oddly, in the pin lines here discussed, the greatest rates of erosion were on the less steep slopes (upper left group on fig. 163), but in considering all observations, steep slopes generally show a greater rate of erosion than less steep slopes. No attempt is made at this time to ascribe to either of these two sets of measurements the percentage of total sediment which each produces. While the gentler slopes have a smaller erosion rate, their land area within the watershed is greater. Consequently, in terms of total volume of sediment, the gentler slopes may yield the greater amount.

Location and elevation of pins along lines CB and BA as well as the net 6-year erosion at each are indicated on the profiles of figure 164. The profiles provide an insight to the occasional contradictory data among pins. It appears that the greater steepness in local surface slope (that slope within 1-2 ft of the pin) is accompanied by the greater erosion. The greatest erosion is indicated by those pins on the very steep slopes just adjacent to, but not in, the channel bed. The pins on a locally flat slope, especially those just downhill of a steeper slope (see pins 2CB and 3CB, fig. 164) actually show a deposition occurring. This deposited material was undoubtedly derived in part from the greater erosion on the steeper slopes just uphill, for example, from pin 1CB. Pins on relatively unbroken slopes are in general agreement with each other and usually indicate about the average rate of erosion. Thirteen of the 17 pins showed a net erosion and 4 a deposition. If only those pins showing a net erosion were considered, the average rate of erosion would increase from the reported 0.0072 ft per yr to 0.017 ft per yr. The former value is in agreement with the value from the erosion plot and the latter with the value from the slope-retreat lines. Generally, the topography along the iron-pin lines is intermediate between that of the erosion plot and that of the slope-retreat lines.

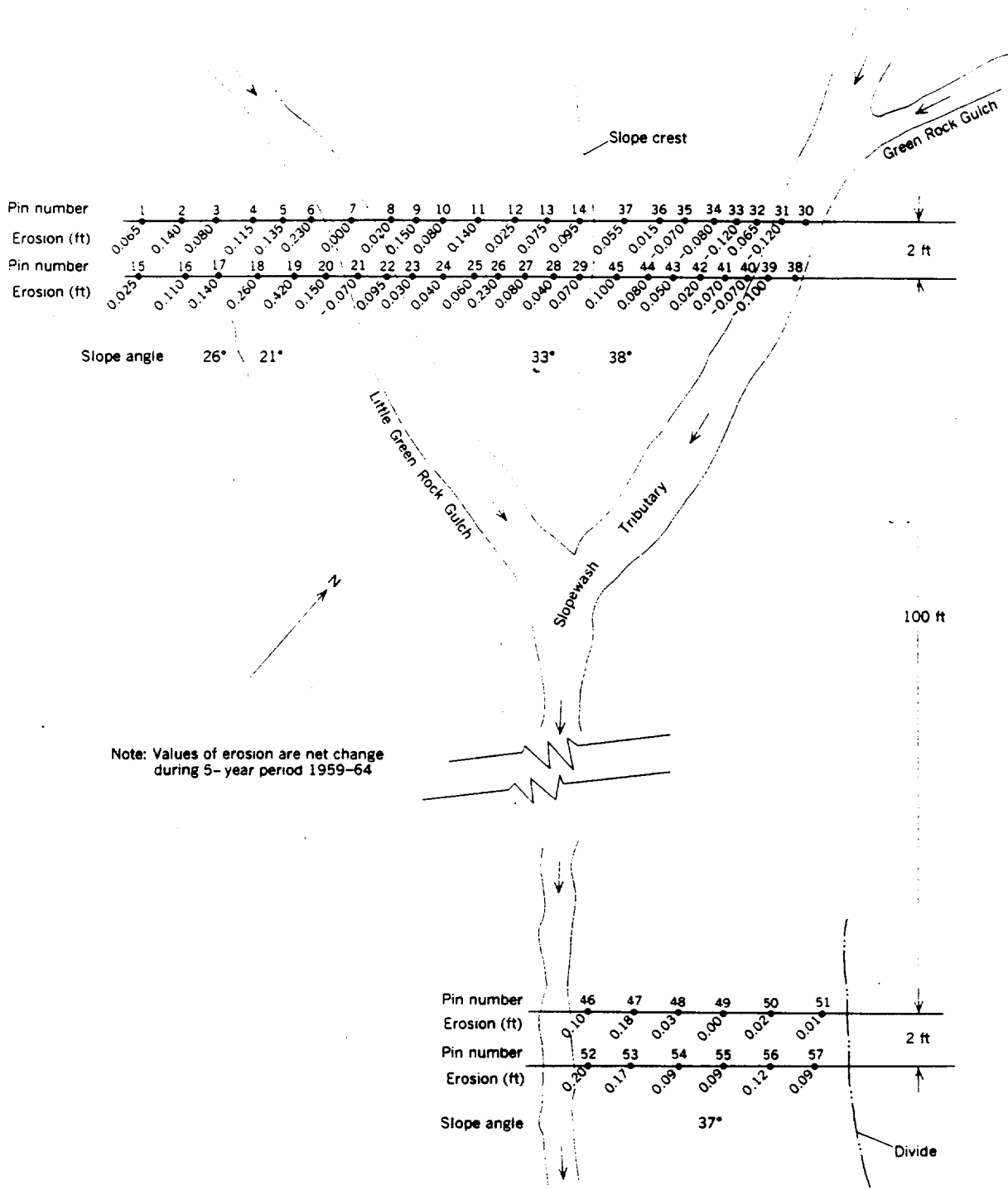


FIGURE 163.—Sketch map showing details of the slope-retreat pins, Slopewash Tributary.

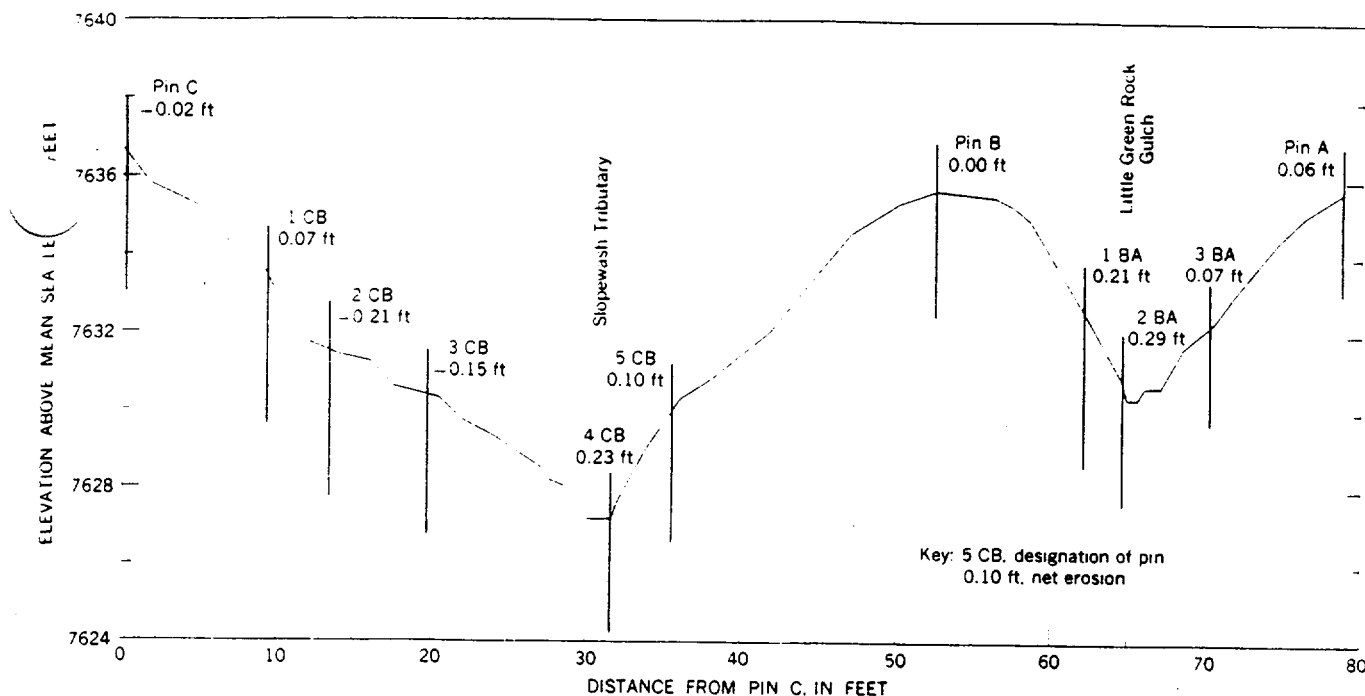


FIGURE 164.—Six-year (1958-64) net erosion on iron-pin line CBA, Slopewash Tributary drainage area.

OTHER MEASUREMENTS OF SLOPE EROSION ON SLOPEWASH TRIBUTARY

The second additional set of measurements for rates of erosion consists of eight iron pins located at the chain-sections below the junction on Slopewash Tributary (see fig. 144 for chain-section locations). These foot lengths of iron reinforcing rod, installed and moved as previously described. For each chain-section, a pin was located on each sloping bank and, for two of the sections, a pin was situated in the channel bed.

Installation was made in 1958 and data were collected in 1958-64, excepting 1961. The average rate of erosion for the bank pins is 0.0108 ft per yr and the bed pins indicate an average deposition of 0.0033 ft per yr. These rates are in agreement with the other observed rates for slope erosion and channel aggradation.

EROSION NAILS ON COYOTE C. ARROYO

On slopes leading into the headcut of Coyote C. Arroyo, a total of 65 erosion pins with washers are located on 3 lines, as shown in figure 145. The pins were installed in 1961 and have been remeasured yearly to 1964. Profiles were run on the pins to determine the slope, and also a resurvey of the pin elevations indicates no heaving due to either freeze-thaw or wet-dry actions. The average of the 65 pins indicates a yearly net erosion of 0.0237 foot. All the data for the pins are tabulated in summary of data F.

Rates of erosion for each of the three lines were consistent, ranging from 0.021 to 0.027 ft per yr. These values approximate the higher values for the slope-retreat pins in Slopewash Tributary, and it is believed that they exceed somewhat the average rate of erosion for the entire drainage of Coyote C. Arroyo, as is evidenced by a lower value for the grid system than for the slope-retreat lines in Slopewash Tributary.

Attempts to correlate individual rates of erosion with individual local ground slopes did not result in a neat regression of erosion rates with lessening slopes. To the observer on the ground, it appears rather instinctive that greater erosion is occurring on the steeper slopes; however, the disparity in the data is sufficient to mask attempts to illustrate graphically the relation of slope to rate of erosion.

TRACING OF FLUORESCENT SAND

A fluorescent sand (ASTM mesh size 40) was placed along three lines in two of the study areas to trace the movement of individual fine-grained sediment. One line was along the hillcrest of Morning Walk Wash (see fig. 139). The other two lines were in Coyote C. Arroyo, one along the nail line ED and the other along the mass-movement line (see fig. 145).

The sand was placed in 1961 and the initial position was marked. In 1962 the movement of this sand was determined by searching for grains at night with a black light. Despite a relatively large amount of erosion indicated by the erosion nails, the individual sand

grains appeared remarkably stable. For the short distance of 5-10 feet individual grains moved in quantity. However, for distances greater than this very few grains could be found. Maximum distance at which we found a grain was about 50 feet.

The original concentration of the grains was not recorded and it is not known how many of the grains had actually moved but could not be found. The concentration of grains in the initial position was still large in 1962. However, it is believed that many grains, either by moving completely out of the searched area or by being covered, were not found.

In 1964 a second attempt was made to trace the movements of the fluorescent sand. The concentration at the original placement area had considerably lessened over that observed in 1962. Many grains were found within 50 feet of the original line and a few were found between 50 and 100 feet. Below 100 feet, but within several hundred feet, a few grains were found which fluoresced with the same characteristics as the placed grains, but comparison of these with grains from other observations indicated that they probably were native fluorescent minerals.

If any conclusion may be drawn from these experiments it would be that grains on the flat of a watershed divide are moved very slowly but that, once they are on the steeper slopes and within an area capable of overland flow, they are moved much more rapidly. This conclusion is supported by a 1-year set of data for erosion pins on a transect across a divide near the houses of Las Dos. These pins are referred in the project files as Corral Flat nail and washer line, but because of the short period of record are not elsewhere presented in this report. The 1-year of data show no erosion or deposition exceeding 0.005 foot, and the average for the line indicates little or no systematic movement of individual grains.

CHANNEL ENLARGEMENT IN SLOPEWASH TRIBUTARY

Although the slope retreat pins give an indication for the rate of channel enlargement, another set of measurements was designed specifically to provide rates of bank recession and channel aggradation-degradation. This set of measurements, designated as nail sections A-J (location shown on fig. 144, consists of 10 observation sections spaced approximately at 50-foot intervals along Slopewash Tributary. At each section a nail with washer was located on each sloping bank and one at the center of the channel bed. Rates of erosion and deposition were observed as previously described.

The sections were installed in 1959. Data have been collected yearly to 1964, excepting 1960. These data

show that the average rate of bank erosion for the side pins is 0.0248 ft per yr. Deposition occurring at some of these pins averages 0.0058 ft per yr. The net bank recession is then equal to 0.0190 ft per yr. The channel bed pins indicate an eroded depth of 0.0694 ft per yr. This depth probably occurs as scour while surface runoff is flowing in the channel. Subsequent fill amounts to 0.1024 ft per yr. This leaves a net deposition of 0.0330 ft per yr, indicating an aggrading channel. This observation is consistent with other measurements indicating a channel aggradation. The channel aggradation is not confined to lower reaches of the channel but also extends upstream into the uppermost headwater rills. All nails in the channel on sections A-H show net deposition, and these vary in distance to watershed divide from 400 to 800 feet. Still, the amount of deposition in the small channels does not account for the volume eroded from upslope surfaces.

This excess of sediment is being supplied to the main streams and accounts for the aggradation observed there and reported in the section on scour and fill.

A summary of data for the nail sections are included in summary of data G.

SOIL CREEP OR MASS MOVEMENT

SLOPEWASH TRIBUTARY

To measure the magnitude of downslope soil movement occurring as soil creep, lines of mass-movement pins were installed in Slopewash Tributary and in Coyote C. basin (see figs. 144 and 145 for locations). The line in Slopewash Tributary is along the east fork some 100 feet above the junction of the tributaries. The line chosen crosses the meandering channel several times, and thus the pins are on the steep slopes (about 1:1) of the channel banks, alternately on one side and the other of the tributary. In figure 146 the photograph was taken with the camera at the north end of the line and the man is standing at the south end.

The two ends of the line are monumented and located in such a place that the monuments themselves are subject to no downhill movement. Iron rods, 4-foot long, were used to monument these end points. Generally at 5-foot spacings along the length of the line, 1/4 inch galvanized iron pipes, 10 inches long, were driven vertically into the ground. At the time of installation they generally protruded about 0.1 foot above the ground surface. A transit was set up over the center of the monument on the north end of the line, oriented to the center of the monument at the south end of the line, and the distance of each pin away from the line of sight was recorded. Similar measurements are made on a resurvey except that the angle of the pin from the ver-

tical and any increase in protrusion above the ground surface are also recorded.

Resurveys were made annually from 1961 to 1964. The average rate of downslope creep of the pin tops is 0.225 in. per yr. Considerable variations exist among annual measurements. However, all pins show net downhill movement for the 3-year period. Individual variations probably reflect local influences of the particular pin location: for examples, a twig, rock, local slope, or proximity to the channel.

All of the soil profile to the full depth of the pin is not moving as fast as the average rate reported. Most pins are rotating downhill, indicating that the top layers of soil creep at a faster rate than the lower layers. The average rotation of the pins is 1.4° per year. For seven of the pins the pin angles themselves explain all the observed downslope creep, the point of rotation being very nearly at, or slightly above, the bottom of the pin. For the other eight pins the center of rotation is a short distance below the bottom of the pin. For this latter set of pins it follows then that the entire soil profile, at least to the depth of these pins, must move downslope some distance. An average value of the downhill movement for the bottom of all pins is 0.003 in. per yr (a computed, not an observed value). This value, being so nearly equal to zero, indicates that only about the top 8 inches of soil are involved in mass-movement and that the soil nearest the surface has the greatest movement.

Since the pins are leaning downhill and some of the length protrudes above the ground surface, a more meaningful value of downhill creep would be that computed for the pin at the ground surface rather than at the pin top. These computations show the average rate of soil creep at the ground surface as 0.205 in. per yr, slightly less than the 0.225 in. per yr attributed to the tops.

Movement at the ground surface and at the pin base, along with the depth of inserted pin, allows computation of the volume of material moving. This value is 0.87 cu in. per in. of slope base per year, or 32 cu ft per mile of slope base per year.

The increasing protrusion above the ground surface observed at the mass-movement pins was also used to study erosion rates. The average rate of erosion for these pins is 0.025 ft per yr. Generally, these are the steepest slopes (approximately 45°) for which erosion values were obtained and they show the largest rate of erosion.

A summary of the downhill movement of the pin tops, rotation of the pins, and erosion at the pins are included in summary of data H.

COYOTE C. ARROYO

A mass-movement line of pins as just described was also installed along a tributary to Coyote C. Arroyo (location shown on fig. 145). The average downhill movement of the pin tops for the period 1961-64 was 0.267 in. per yr. During the period one pin showed an unexplained uphill movement.

The average downhill pin rotation during the period of observation was 1.7° per year. The relation of downhill movement to pin rotation is the same for these pins as for the pins in Slopewash Tributary.

The pins on this line showed greater erosion than those in Slopewash Tributary. Thus, computations for the rate of downhill movement at the ground surface used a value for the length of pin exposed equal to the original protrusion plus one-half of the erosion. Computations show the average rate of movement at the surface as 0.202 in. per yr, a figure remarkably close to that obtained in Slopewash Tributary. The volume rate is somewhat less than that in Slopewash owing to a smaller depth of soil movement, here 7.5 inches. The computed volume rate of mass-movement is 25.5 cu ft per mile of slope base per year.

A summary of data for the mass-movement line in Coyote C. Arroyo is included in summary of data I.

HEADCUT ENLARGEMENT

FENCE LINE HEADCUT

Fence Line Headcut is a tributary to the Arroyo de los Frijoles, entering on the left bank about 1,500 feet below the Main Project Reach. Figure 165 is a photograph of this headcut in 1964. In 1960 the headcut was staked with six iron pins, each 4 feet in length. The rate of enlargement of the headcut is determined by



FIGURE 165.—Fence Line Headcut.

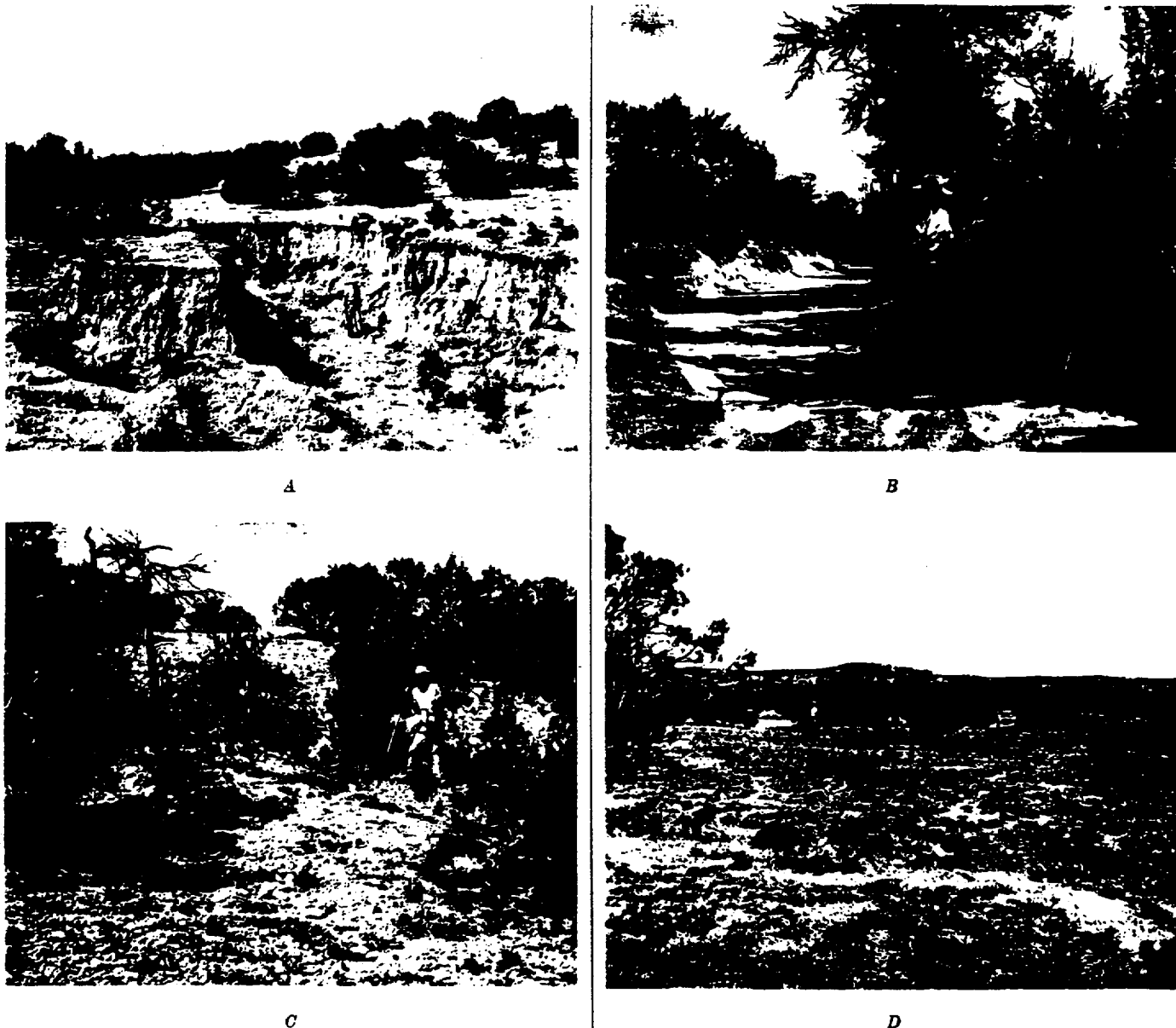


FIGURE 166.—Aspects of the drainage area of Coyote C. Arroyo. *A*, The largest headcut, cut in valley alluvium of Coyote C. Arroyo (also see map of fig. 167). *B*, Channel of Coyote C. Arroyo about 800 feet downstream from headcut pictured in *A*; man points with shovel to position where *C*¹ sample was obtained to date the Coyote terrace deposits. *C*, View near the watershed divide of Coyote C. Arroyo; note the lag gravel typical of headwater areas not covered by colluvium. *D*, Typical view of the valley alluvium; coarse particles are found here only in watercourses, as in that in foreground.

measuring the distance from the iron pins to the vertical walls of the cut. Resurveys indicate that the headcut is slowly enlarging at all points of measurements, but that the greatest rate of enlargement is at the upstream end where the headcut is advancing nearly 1.5 ft per yr. Height of the vertical walls of the cut averages 6 feet.

The average volume of sediment discharged by this one gully is estimated at over 500 cu ft per yr, mostly from headward advancing.

COYOTE C. ARROYO HEADCUT

Coyote C. Arroyo is a discontinuous gully involving four headcuts. About 2,000 feet below the headwater divide is the largest of the headcuts, below which the gully is continuous to the master stream. The area around this largest headcut has been studied in detail and figure 166 includes photographs of the vicinity. Rate of headcut enlargement is being recorded by yearly planetable mapping and by measurements from iron pins driven at known distances from the vertical walls.

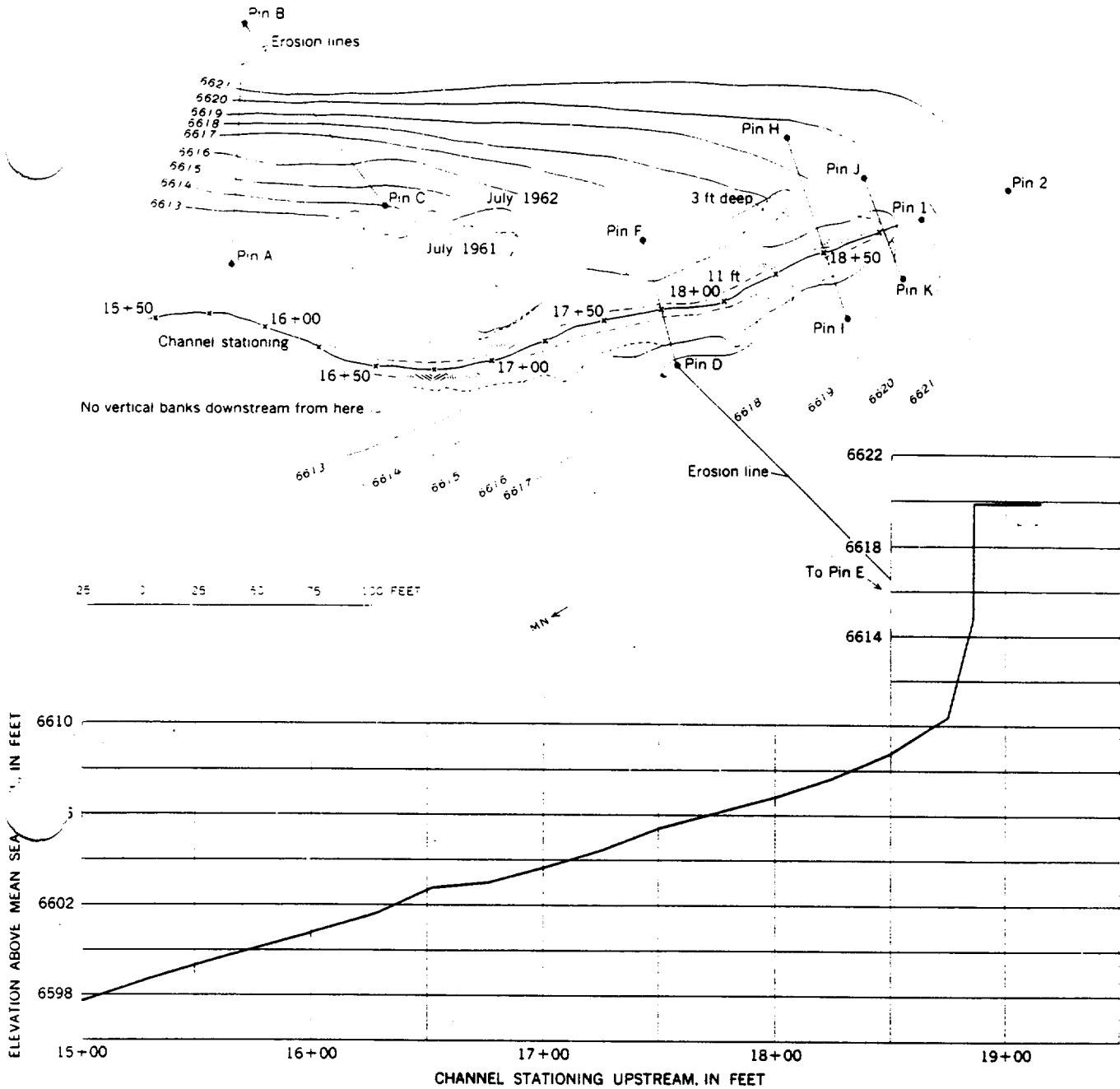


FIGURE 167.—Topographic map and profile of Coyote C. Arroyo headcut.

The planimetric map of 1962 is shown in figure 167 and, as a dashed line, the outline of the headcut as it appeared the previous year. Most of the headcut has retreated some and the greatest amount of retreat is recorded in extremities which extend either up the primary direction of the channel or in the direction of tributary swales. Measurements from the pins to the cut bank indicate a lateral retreat of 0.4 ft per yr and a retreat at the most headward extreme of 2.6 ft per yr. Thus, while the map of figure 167 provides some insights about

headcut retreat, mapping is not sufficiently accurate to delineate the relatively minute retreats which are occurring.

The initial 400 feet of channel profile is shown below the headcut map to provide an indication of channel slope and the sloughed material associated with the headcut. The average slope of the channel here is 0.03 ft per ft compared to 0.02 ft per ft in the channel 1,000 feet downstream. The volume of material contributed to the stream by the enlargement of this headcut has

been computed to be 1,650 cu ft per yr for the period 1961-64.

MOVEMENT OF LARGE PARTICLES IN HEADWATER RILLS SLOPEWASH TRIBUTARY

Two of the channels that have been studied in detail with respect to movement of individual rocks, Green Rock Gulch and Little Green Rock Gulch, are shown in figure 144. The former is also illustrated in figure 168. Starting at or near the mouth of these two channels individual rocks, each 3-6 inches in diameter, were completely painted. They were then replaced in the rills at measured distances from the mouth. This distance, in feet, was painted on each rock for identification and the total number of rocks at each distance was recorded. A total of 250 rocks was painted in Green Rock Gulch and placed at distances of 1-47 feet upstream of the mouth. Forty rocks were painted in Little Green Rock Gulch and placed from 21 to 36 feet upstream of the mouth.

The initial placement was in 1959 and resurveys were made annually. At the time of the resurveys the movements of the individual rocks were easily discernible because identification numbers on the painted rocks were no longer in consecutive order nor at the distance corresponding to their number.

Although the number of rocks moving has not been large, the recovery percentage is high. In 1964, 5 years after placement, 88 and 78 percent respectively of the rocks in the two gulches are still accounted for. Missing rocks are usually those that moved but later were obscured by either vegetation or a sand covering, that is, they were not buried in place. This is suggested by some of the rocks in the main study which were re-



FIGURE 168.—Green Rock Gulch, a tributary to Slopewash Tributary. Rocks wash into this minor rill from the lag gravel covering some of the hillslopes seen in the background.

ported as missing in a given flow but were found after a subsequent flow.

The data have not been sufficient to describe a trend in movement. Both the upper and the lower halves of the reach on Green Rock Gulch show about 25 percent of their rocks moving or missing. Because of the large number of rocks not moving and the large variability in distance of those moving, the data are perhaps not yet meaningful. However, the longest distances recorded to date are of rocks originally placed in the lower 10 feet of channel and these have moved as much as 540 feet.

GUNSHOT ARROYO

Gunshot Arroyo is the first tributary entering Arroyo de los Frijoles below the sweeping S-curve half-mile downstream of the Main Project Reach. Measurements in Gunshot Arroyo include the tracing of large particle movements in the channel bed and on a steep sloping bank of the channel, the retreat of a knickpoint formed in the channel by an outcropping of semiresistant Santa Fe formation, channel enlargement, and degradation-aggradation studies.

In 1960 the initial survey and installations included the selection, painting, and replacing of rocks in the channel. The rocks, ranging in diameter from about 3 to 10 inches, were completely painted and numbered with the distance in feet corresponding to the initial position upstream of the junction with Arroyo de los Frijoles. The largest number is 880 and the watershed divide is located at station 1,150 feet. The rocks were placed at 10-foot intervals.

In 1962 a complete resurvey was made of the existing measurements and a longitudinal-profile survey was run from 150 feet below the mouth of the arroyo to and over the watershed divide. This profile is shown on figure 169. No vertical or cut banks were observed above station 620 feet and the channel disappeared above station 1,050 feet.

Superposed on the profile of figure 169 is a schematic illustration of the rock movements as recorded in 1962. Each rock position is identified as to moving, missing, or stationary. For those rocks which were found, the distance moved in feet is indicated by the number above the original position of the rock.

Most rocks below station 750 feet moved. Downstream from station 750 feet to station 450 feet, most of the moving rocks were found. Below station 450 feet a large percentage of the rocks were reported missing. The upper of the two mentioned subreaches has a gravel bed and the lower a sand bed. In the lower reaches of the channel most rocks that had moved were found partly buried in sand and, with few exceptions, those which had traversed the length of the tributary

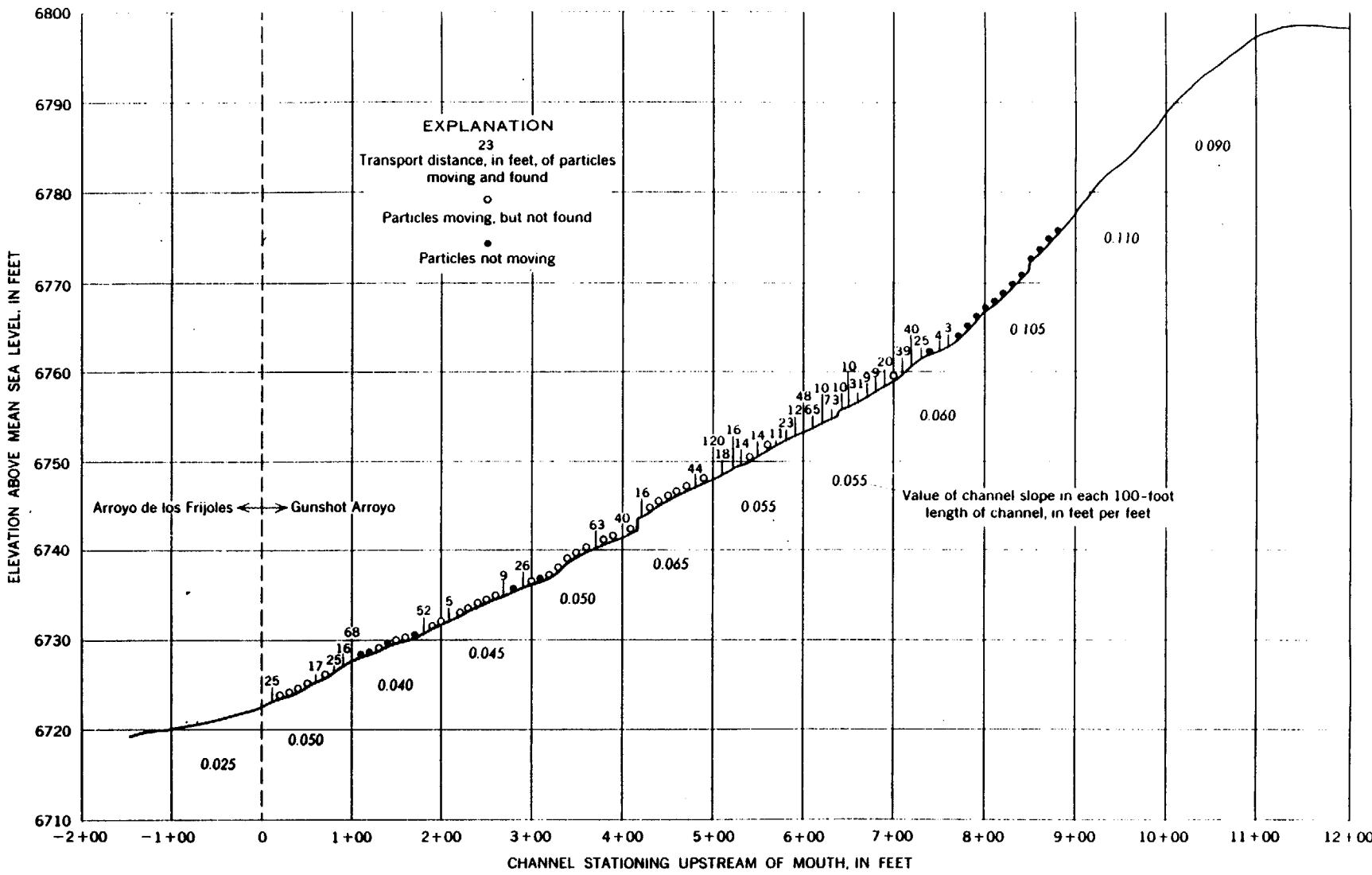


FIGURE 189.—Profile of Gunshot Arroyo illustrating movement of coarse particles, 1960-62. Average B- or intermediate-axis diameter of particles is 150 mm.

and into the channel of Arroyo de los Frijoles were not found. The rocks above station 750 feet were consistent in that none had moved despite the fact that these were on the steepest slopes.

At the time of the 1962 survey the rocks moving and found averaged a transport distance of 39 feet; the maximum distance recorded was 120 feet. If consideration were given to the missing rocks, which probably were transported entirely out of the tributary, these distances would be considerably increased. Of the rocks originally placed, 37 percent were missing and 22 percent had not moved.

After the 1962 survey the rocks found were returned to their original position, but the missing positions were not filled. Resurveys in 1963 and 1964 of these remaining rocks recovered only one rock reported missing in 1962. This adds credence to the probability that missing rocks were transported entirely out of the tributary.

In 1963 the number of total missing rocks increased to 82 percent, and all but 2 of the 55 rocks remaining after the 1962 survey had moved. Of these 14 were found and averaged a transport distance of 218 feet and a maximum distance of 930 feet. The large increase in percentage of missing rocks is probably attributable to the storm which caused a 1,300 cfs flow at Main Project and which occurred between the surveys of 1962 and 1963. Most rocks remaining for the latter survey were from upstream positions and had longer distances to travel before being exposed to the greater chance of loss in the main channel. By 1964 the number of missing rocks had increased to 85 percent.

Painted rocks on a typical steep slope (approximately 45°) at station 190 feet were resurveyed in 1962, 1963, and 1964. The rocks painted were native to the slope and generally ranged in intermediate-axis diameter from 1 to 3 inches. On an uncounted number of rocks painted in 1960, 175 remained in 1962 and 164 remained in 1964. Thus, in the last 2 years only 6 percent have

moved off the slope and have become lost in the channel. Between annual surveys an average of only 3 percent of the rocks (excluding those missing) moved over one foot, but a gradual slumping was noticeable. In 1964, 118 rocks (72 percent) had slumped downhill a measurable amount, and this slumping averaged 0.6 foot for the 4-year period. It appears that the effects of gravity, aided by such processes as freeze-thaw and wet-dry, have an appreciable influence on coarse particles on steep slopes.

The monumented knickpoint in the Santa Fe formation at station 417 feet averages about 1.3 feet in height, and between 1960 and 1964 no measurable amount of upstream retreat was recorded.

Scour chains placed in the arroyo bed at station 25 feet, 230 feet, and 468 feet indicate the channel is aggrading at a rate of 0.06 ft per yr for the 2-year period 1962-64. Although this is a short-term record, the value is in agreement with that of the main arroyo, 0.04 ft per yr.

MORNING WALK WASH

In 1961, painted rocks were placed at 10-foot intervals in the channel of Morning Walk Wash near Las Dos (fig. 139). The painted rocks ranged in diameter from 3 to 5 inches, the average rock size native to the gullies. A total of 166 such rocks were placed along the thalwegs of the two main channels and a smaller rill draining the hillslope.

A resurvey in 1962 indicated a very large percentage of the rocks had moved. Table 5 is a condensed presentation of the rock movements between 1961 and 1962. For example, in the north gully three times as many rocks had moved in the lower reaches than in the upper reaches and the rocks in the lower reaches tended to move greater distances. Many of the rocks were found in a fan deposit at the mouth of the channel.

As in Gunshot Arroyo the rocks found during the

TABLE 5.—Summary of particle movement Morning Walk Wash, 1961-62
(L, lower reach; U, upper reach)

Particles	South gully			South rill	North gully		
	L	U	Total or average		L	U	Total or average
Total originally placed.....	44	43	87	12	34	33	67
Percent moving, on basis of:							
Total found.....	41	40	40	25	77	12	45
Total found plus total missing.....	93	63	78	25	91	30	61
Percent not moving or not found.....	48	77	62	100			
Distance moved, in feet, on basis of total found:							
Average.....	177	339	258	211			
Maximum.....	473	723		613			

¹ Lower reach.

survey were returned to their original position to await movement during subsequent flows, but the missing positions were not filled with new rocks. Thus data after 1962 became less meaningful except to determine the erosion rate of the originally placed rocks. Data for the painted rock experiments in headwater channels are included in summary of data *J* for 1961-64.

The condition of the paint on the rocks found indicates that the rocks are transported with only little abrasive action, that is, they are not broken up in place and removed as smaller particles, this despite the rolling and tumbling over other rocks in their trip downstream.

Two monumented cross sections of the channels were installed in 1961 and resurveyed yearly to 1964. During this period the upper section, 170 feet above channel mouth, showed no significant changes, while the lower section at the mouth showed about 0.2 foot of deposition in each channel bed. This value is consistent with other observations for channel aggradation.

SEDIMENTATION IN CHANNELS AND RESERVOIRS

About 1937, at the lower end of Coyote C. Arroyo some 1,900 feet downstream of the present position of

the largest headcut, an earth dam was constructed across the arroyo. In 1961 the reservoir behind the dam was topographically mapped by planetable, and it was planned that resurveys would allow the determination of the amount of fill accumulating within the reservoir. Contours of equal deposition occurring during 1961-62, as well as original topography, are shown in figure 170.

Computations determining the volume amount of sediment collected in the reservoir during the period 1961-64 are shown in table 6. This amount totals 6,245 cu ft or 2,082 cu ft per yr. If the average rate of erosion shown by the erosion nails is assumed as a basin-wide average, the reservoir is shown to collect only about 5 percent of the total eroded sediment. However, the computation of this percentage may be of only academic interest because, as was remarked previously, values of the erosion rate computed from the pins installed in this basin are believed to be too large for the basin as a whole. Most of the sedimentation was in the year 1961-62.

The field-sketch map of figure 145 shows six channel cross sections at various distances up the arroyo. These cross sections were first surveyed in 1961; they have

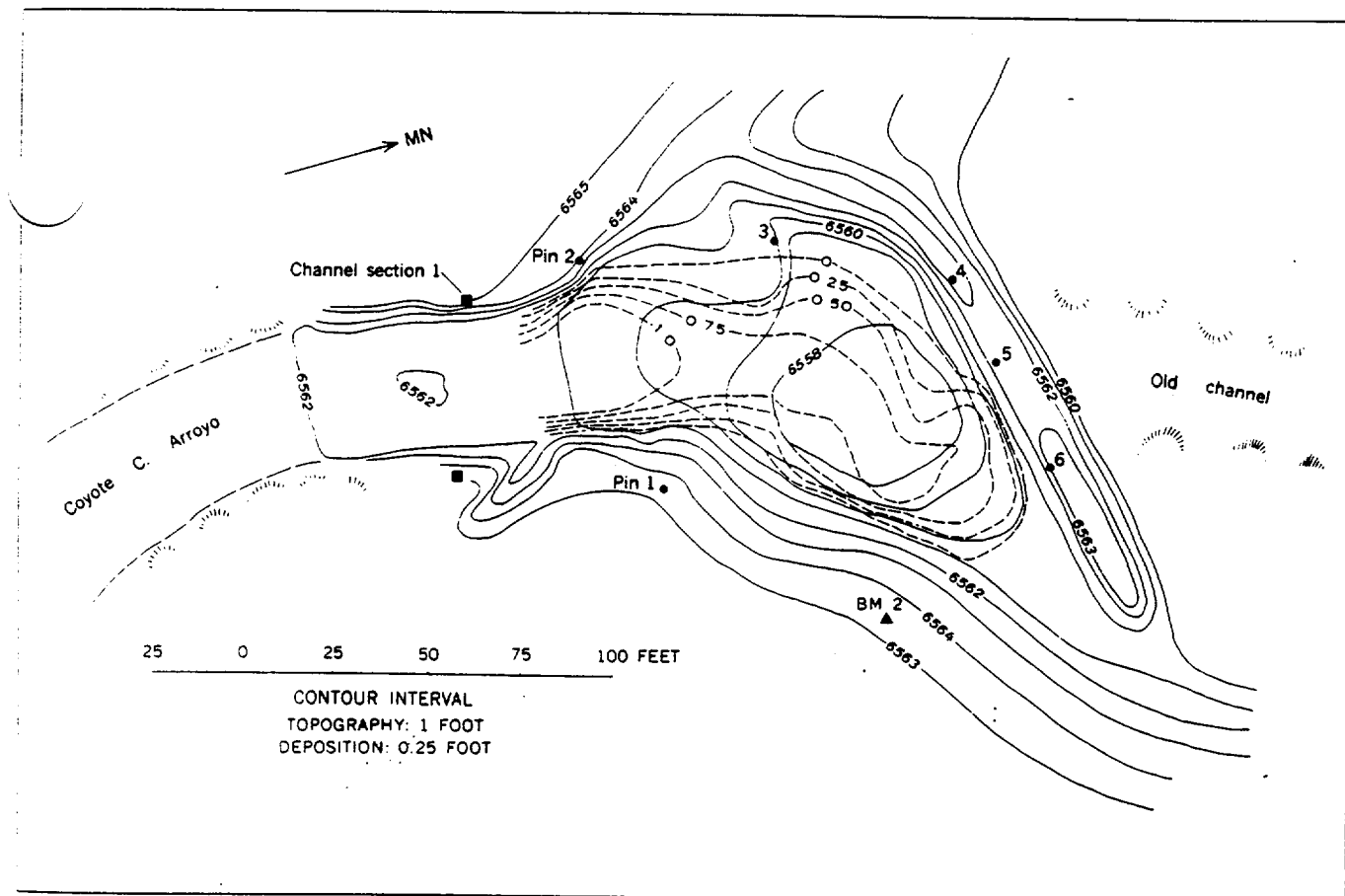


FIGURE 170.—Topography of dam and reservoir on Coyote C. Arroyo and contours of deposition, 1961-62.

TABLE 6.—Observed sedimentation in reservoir behind dam on Coyote C. Arroyo, 1961-64

Cross section	End pins	Decrease in area of cross section due to deposition (sq ft)			Effective width of section (ft)	Average depth of deposition (ft)			Effective area of reservoir (sq ft)	Amount of sedimentation ¹ (cu ft)		
		1961-62	1961-63	1961-64		1961-62	1961-63	1961-64		1961-62	1961-63	1961-64
1	BM 2-6	10.0	10.0	10.4	30	0.33	0.33	0.36	1,500	330	330	350
2	BM 2-6	28.3	26.2	24.3	43	.54	.61	.56	825	445	505	460
3	BM 2-4	29.0	38.0	39.0	53	.55	.72	.74	900	500	650	665
4	1-5	30.5	50.5	55.5	55	.55	.92	1.01	913	505	840	920
5	1-4	34.0	68.0	73.0	60	.57	1.13	1.22	1,436	920	1,620	1,750
6	1-3	15.5	8.5	14.5	35	.44	.24	.42	1,850	915	445	775
7	1-2	51.5	44.5	39.5	40	1.29	1.11	.99	1,336	1,725	1,485	1,325
Total										5,140	5,875	6,246
Rate—cu ft per yr										5,140	2,938	2,062

¹ Amount of sediment contributed from basin (40.8 acres):

$$\frac{2062}{40.8 \times 43,560} = 0.0012 \text{ ft per yr}$$

been resurveyed yearly to 1964 and allow computation of deposition in the channel. Stationing and channel changes are summarized in table 7. The volume accumulations of sediment in the 1,435-foot reach included by the sections are also shown in the table. These data indicate that 3,192 cu ft per yr of sediment is deposited in this reach, which corresponds to channel aggradation of about 0.10 ft per yr. This value represents about 8 percent of the total eroded sediment indicated by the erosion pins.

The percentages of total eroded sediment accounted for by the surveys in the reservoir and in the lower reach of channel are not total reservoir and channel storage of sediment for the entire basin. Our studies have indicated that even headwater rills are aggrading, thus there is much more channel length in the basin available for sedimentation processes. Although the surveyed reservoir is the only man-built barrier, other natural reservoirs are also available. The discontinuous nature of the channels provides many alluvial fans

and flats which may be considered as natural reservoirs: at least, sedimentation rather than erosion is occurring in these areas.

ANALYSIS OF SEDIMENT BUDGET

To account for sediment volumes contributed by erosion and to compile a balance sheet is not easy, because of the variance within the measurement data. With regard to what appears to be the main process contributing debris (sheet or surface erosion), the problem is how to average the rates observed by the nail and washer data at various localities and derive a figure applicable to the whole contributing area. To use the data on volumes contributed by headcuts presents little problem because there are only a few headcuts per square mile in the study area. Bank cutting and consequent channel enlargement is not an important source of sediment, as indicated by measured cross sections of channels. The data on mass-movement pins present a special problem because, lacking knowledge of certain details of the

TABLE 7.—Observed rates of channel changes in Coyote C. Arroyo

Section	Channel stationing (ft)	Change in channel shape (+, deposition; -, scour; (sq ft)			Length of reach (ft)	Volume of sediment ¹ (cu ft)		
		1961-62	1961-63	1961-64		1961-62	1961-63	1961-64
1	30	+30.75	+29.00	+28.25	120	3,690	3,480	3,390
2	210	+8.75	+10.00	+11.00	165	1,445	2,100	2,310
3	365	+16.75	+14.10	+14.75	225	3,770	3,180	3,320
4	650	-2.70	-.50	.00	290	-785	-145	0
5	955	+ .70	+ .80	+1.10	395	265	315	435
6	1,435	-1.30	-.25	+ .50	240	-310	-60	120
Total						8,075	8,870	9,575
Rate—cu ft per yr						8,075	4,435	3,192

¹ Amount of sediment contributed from basin (40.8 acres):

$$\frac{3192}{40.8 \times 43,560} = 0.0018 \text{ ft per yr}$$

process, the total area subject to effective sediment contribution from this source is difficult to estimate.

No great problem is presented by channel aggradation, for these measurements are far more complete than for other processes. Two important sources of possible error remain—the unmeasured volume of debris passing out of the basin as bedload or suspended load, and the trap efficiency of the reservoirs.

These difficulties face any investigator who is constructing a sediment budget. No perfect solution is available, but at least the assumptions made in the computations can be stated and the implications of the assumptions can be analysed. Although the quantities are only roughly approximate, a summary of debris inflow, outflow, and storage is attempted. Table 8 summarizes the average values of the measurement quantities. These values are arithmetic averages of individual readings taken over the period of measurement at the respective measurement points. Because comparison of mean and median values shows no great disparity, we used mean values exclusively in this report.

The main assumptions enter the computations in progressing from average-measurement data, table 8, to computations of average rates of erosion and deposition summarized in table 9.

The main source of data on sheet erosion is the pin-and-washer installations. More variance is noted between successive years than among the respective pins in the same year. Within a given group of nails the rate of erosion for the 3-year period was plotted against individual pins against the local ground surface slope at the pin, but no correlation was found. This lack of correlation is attributed to the fact that each group of nails applied to only a small range of slope values. Some influence of slope probably can be seen in the comparison of values of surface erosion in table 8. For example, the average land slope on the erosion plot of Slopewash Tributary is less than on the nail lines of Coyote C., and the corresponding net erosion rates are 0.008 and 0.024 ft per yr respectively.

But it appeared unjustifiable to correlate these net erosion values for different localities merely with slope because many other factors probably are also operative. The significance could not be tested statistically with only seven localities.

The average value of surface erosion for the whole basin (0.015 ft per yr; see table 9) represents our best judgment of the order of magnitude. This value is in agreement with the result obtained by equal weighting of number of pins and number of years of data, 0.0145.

Two values of volume eroded by headcut retreat are available. Approximately the average of these two was

TABLE 8.—Data on measured rates of erosion and deposition

[SWT, Slopewash Tributary]	
Erosion	
Surface erosion:	
Erosion plot, SWT:	
Pins.....	61
Years.....	5
Net erosion—ft per yr.....	0.008
Slope-retreat pins, SWT:	
Pins.....	57
Years.....	5
Net erosion—ft per yr.....	0.014
Nail lines, Coyote C. Arroyo:	
Pins.....	65
Years.....	3
Net erosion—ft per yr.....	0.024
Nail sections, bank, SWT:	
Pins.....	20
Years.....	5
Net erosion—ft per yr.....	0.019
Mass-movement pins, SWT:	
Pins.....	15
Years.....	5
Net erosion—ft per yr.....	0.025
Iron pins, SWT:	
Pins.....	19
Years.....	6
Net erosion—ft per yr.....	0.007
Chain section pins, on banks, SWT:	
Pins.....	8
Years.....	6
Net erosion—ft per yr.....	0.011
Gully erosion:	
Coyote headcut:	
Years.....	3
Retreat (ft per yr):	
Laterally.....	0.4
Headward.....	2.6
Volume of material eroded—cu ft per yr.....	1,650
Fence line headcut:	
Years.....	4
Retreat (ft per yr):	
Laterally.....	0.15
Headward.....	1.5
Volume of material eroded—cu ft per yr.....	500
Mass movement (soil creep):	
Slopewash Tributary:	
Pins.....	15
Years.....	5
Downhill movement at ground surface—in. per yr.....	0.205
Volume of material moved—cu ft per mile of slope base per yr.....	32
Coyote C. Basin:	
Pins.....	12
Years.....	3
Downhill movement at ground surface—in. per yr.....	0.202
Volume of material moved—cu ft per mile of slope base per yr.....	25
Movement of individual rocks:	
Morning Walk Tributary:	
South gully and rill:	
Rocks.....	99
Years.....	3
Rocks moved—percent.....	75
Average distance moved—ft per yr.....	180

TABLE 8.—Data on measured rates of erosion and deposition—Continued

Erosion—Continued	
Movement of individual rocks—Continued	
Morning Walk Tributary—Continued	
North Gully:	
Rocks.....	67
Years.....	3
Rocks moved—percent.....	67
Average distance moved—ft per yr.....	96
Gunshot Arroyo:	
Rocks.....	88
Years.....	4
Rocks moved—percent.....	100
Average distance moved—ft per yr.....	93
Green Rock Gulch:	
Rocks.....	250
Years.....	5
Rocks moved—percent.....	23
Average distance moved—ft per yr.....	59
Little Green Rock Gulch:	
Rocks.....	40
Years.....	5
Rocks moved—percent.....	32
Average distance moved—ft per yr.....	1
Deposition	
Aggradation of channels:	
Slopewash Tributary:	
Nail section:	
Number of chains, pins or sections.....	10
Years.....	5
Average net aggradation—ft per yr.....	0.033
Pins at chain section:	
Number of chains, pins, or sections.....	2
Years.....	6
Average net aggradation—ft per yr.....	0.003
Arroyo Frijoles, mainstem: including North Branch:	
Number of chains, pins, or sections.....	90
Years.....	6
Average net aggradation—ft per yr.....	0.040
Coyote C. Arroyo:	
Number of chains, pins, or sections.....	6
Years.....	3
Average net aggradation—ft per yr.....	0.100
Gunshot Arroyo:	
Number of chains, pins, or sections.....	3
Years.....	2
Average net aggradation—ft per yr.....	0.060
Filling of small reservoirs:	
Coyote C. Arroyo Dam:	
Drainage area—sq mile.....	0.064
Years.....	3
Volume deposition—cu ft.....	6.245
Sediment collected—ton per sq mile per yr.....	1.633
Big Sweat Dam:	
Drainage area—sq mile.....	0.0060
Years.....	1.2
Volume deposition—cu ft.....	95.3
Sediment collected—ton per sq mile per yr.....	660

applied to the number of headcuts per square mile estimated from detailed knowledge of the area.

Mass-movement pins are installed on sloping gully walls which are steeper than the hillslopes in general. Though when the measurements were begun we had not expected downhill creep to be of significance in a semi-arid climate, our observations and those of others (for

TABLE 9.—Average rates of erosion and deposition

Erosion	
Surface erosion:	
Average rate—ft. per yr.....	0.015
Percentage of total basin contributing.....	65
Erosion rate—tons per sq mi per yr.....	13.600
Gully erosion:	
Average volume per headcut—cu ft per yr.....	1.000
Headcuts per sq mi.....	4
Erosion rate—tons per sq mi per yr.....	200
Mass movement:	
Average downhill rate at ground surface—in. per yr.....	0.20
Length of channel affected—mi per sq mi.....	35.6
Average volume eroded—cu ft per sq mi per yr.....	1.960
Total volume—tons per sq mi per yr.....	98
Total erosion—tons per sq mi per yr.....	13,900
Deposition	
Aggradation of channels:	
Channel area—sq ft per sq mi.....	579×10 ⁴
Average rate of deposition—ft per yr.....	0.05
Deposition—tons per sq mi per yr.....	1.440
Collected in dams—tons per sq mi per yr.....	1.663
Total deposition—tons per sq mi per yr.....	3.073

summary see Leopold and others, 1964, p. 349–353) indicate that it is a process which cannot be disregarded. Mass wasting should deliver debris to the rills and channels in proportion to the rate of downhill creep and to the total length of channel in a given area. A drainage density was computed by using a Horton analysis of the number and lengths of channels. In a square mile the order of the largest channel including rills is seven. The number and lengths of various orders are as follows:

Order	Number	Length (miles)	Adjustment to channel segments		
			Length (mile)	Number	Number × length (miles)
7.....	1	1.2	0.50	1	0.5
6.....	3.5	.70	.48	4.5	2.2
5.....	11	.22	.11	14.5	1.6
4.....	45	.11	.06	56	3.3
3.....	140	.05	.027	185	5.0
2.....	400	.022	.013	540	7.0
1.....	1,200	.01	.01	1,600	16.0
Total.....					35.6

By this estimate there are about 35 miles of channel and rill in a square mile area, and because there are two banks of a channel, the length of channel boundary possibly subject to debris production by creep is some 70 miles. Using an average of 28 cu ft per mile of slope-base per year,

$$28 \times 70 = 1,960 \text{ cu ft per yr per sq mi,}$$

which at 100 lbs per cu ft is 98 tons per sq mi per yr.

Movement of individual rocks was not included as a separate item of contribution to sediment production.

Depositional data consisted of channel aggradation which was computed into tons per square mile as follows:

Order	Segment length (miles)	Width (ft)	Channel area (sq ft)
7	0.5	28	75,000
6	2.2	16	186,000
5	1.6	9	67,000
4	3.3	3.5	61,000
3	5.0	2.5	66,000
2	7.0	1.3	48,000
1	16.0	.9	76,000
Total			579,000

Then 579×10^3 sq ft of channel area aggrading at 0.05 ft per yr is 28,900 cu ft; at 100 pounds it equals 1,440 tons per sq mi per yr.

The collection of sediment behind the dam in Coyote C. Arroyo gave a figure of 1,633 tons per sq mi per yr. The production and trapping of sediment may be summarized as follows:

	Total sediment (tons per sq mi per yr)	Sediment production (percent)
Surface erosion	13,600	97.8
Gully erosion	200	1.4
Mass movement	98	.7
Total	13,900	100 ±
Deposition in channels	1,440	10
Trapped in reservoir	1,633	12
Total	3,073	22 ±

Far the largest contribution of sediment is by sheet erosion. Channel deposition is only about half of the total sediment trapped, the latter being only about one-quarter of that produced. It is recognized that if the budget were correct and the reservoir trap efficiency were 100 percent, the total of deposition in channels and trapped in the reservoir would equal sediment production. It is our opinion that the sediment moved as sheet erosion does not all get into the channel, but is temporarily stored in thin deposits widely dispersed over the colluvial area, and that furthermore, there is a very low trap efficiency to the reservoir.

Other measurements of sediment accumulation in western United States give values of 1,200 to 2,400 tons per sq mi per yr (Brown, 1945).

To our knowledge, of the published reports on sediment yield from semiarid drainage basins, by far the most excellent is that of Hadley and Schumm (1961), who measured, among other things, sediment accumulation in a large number of stock ponds and small reservoirs. These data were studied in relation to geo-

logic formation, runoff, and various geomorphic characteristics of basins. Their data are far more comprehensive than ours insofar as sediment accumulation in reservoirs is concerned. The only unique feature of the present data is that we attempt to assess the relative importance of different processes of sediment production.

Despite their deficiencies, our data bear comparison with the more extensive values published by Hadley and Schumm, as in the following:

Sediment accumulation:	Acre ft per sq mi per yr	Tons per sq mi per yr ¹
Coyote C. Arroyo (0.064 sq mi) accumulation in reservoir and channel	1.41	3.073
Average curve for all lithologies, for 0.06 sq mi area (Hadley and Schumm)	1.8	3.930

¹ Based on 100 lbs per cu ft.

For small basins the sediment accumulation observed by us in New Mexico is of the same order of magnitude as in basins of similar size in Wyoming underlain by shale or other lithologies high in silt content. Hadley and Schumm (fig. 30, p. 173) showed that for the Cheyenne Basin sediment accumulation was related to relief ratio (basin relief divided by basin length). The average relief ratio for our Coyote C. and Slopewash tributaries is 0.59. Entering this value in the Hadley-Schumm curve for all lithologies, the estimated value of sediment accumulation is 2.4 acre ft per sq mi per yr, and in the curve of those authors applicable to Fort Union formation only, the value is about 2.5. These values are slightly higher than the 1.41 observed in Coyote C. Arroyo but still of the right order of magnitude.

The finding of Hadley and Schumm (fig. 26, p. 163) that sediment accumulation per unit area of basin decreases rapidly with increasing drainage area is in keeping with our result that sheet erosion basin-wide estimated from erosion pins gives a value of sediment production about 4.5 times larger than can be accounted for in channel aggradation and reservoir accumulation. This feature is probably related in part to the same cause postulated by those authors: absorption of water in the dry channel beds below areas affected by local storms. But the fact remains that even in our detailed study of deposition, sediment spread thinly over colluvial areas does not show up in measurement data.

Another interesting comparison is with data on sediment production by dry sliding of debris on the steep

slopes of southern California. Krammes (1960) measured debris in metal troughs laid on contour in burned and unburned areas in San Dimas Experimental Forest near Glendora. He found a sediment yield of 24.7 tons per acre per year (15,800 tons per sq mi per yr) after a brush fire, which compared with 2.69 (1,720 tons per sq mi per yr) before the fire had denuded the slopes. Of the total annual yield 89 percent of the debris was contributed during nonrain periods by dry sliding. The figure for prefire condition is about half the sediment yield observed by us in New Mexico, but the postfire figure is five times larger than our value.

Returning to the question posed earlier in this report, it appears that in semiarid areas of the type studied sheet erosion not only predominates as a sediment source but also seems quite capable of providing the sediment making up the bulk of alluvial fills during periods of aggradation. Indeed, the present channels are aggrading, and at 0.05 ft per yr the observed rate would eventuate in a fill as deep as the Coyote alluvium under the high terrace in 100–200 years. No doubt such a rate would not be sustained as an average for so long a period because in a century there would be some years, no doubt, during which net degradation would occur.

Nonetheless, the present processes and their rates appear quite capable of resulting in deposition of alluvial fills comparable to those of past periods which filled major valleys. The present is, then, a reasonable picture of conditions during which valley aggradation occurred in post-Pleistocene time.

The importance of sheet erosion makes it quite possible that aggradation can occur in tributaries, even in small channels only a few hundred feet from the watershed divide. Gully or rill erosion was probably insignificant or absent during the deposition of the principal alluvial fills in these valleys. Gully erosion assumes its important role during periods of valley trenching or arroyo cutting as was observed in the post-1880 period.

CLIMATOLOGICAL OBSERVATIONS DURING AGGRADATION

From the archeologic materials and a C^{14} date, it is computed that the upper part of the Tesuque formation accumulated in the Tesuque Valley, a few miles from our study area, at an average rate of 104–156 yr per ft (Miller and Wendorf, 1958, p. 190). During the period 1958–64 we observed an average rate of channel bed change that would result in aggradation at the rate of about 25 yr per ft. The present landscape is similar to that under conditions which probably prevailed in the same area, let us say, in the first centuries of the Christian era. But the land at present has hardly begun to recover from widespread devastation of the overgrazing

in the late 19th century. The combination of a grazed range and the present climatic swing provides comparable rainfall-runoff conditions to those caused by a somewhat more unfavorable climate but uncomplicated by the effects of grazing animals.

What are the salient aspects of climate in relation to vegetation which create the difference between a period of aggradation and one of degradation in valleys? This question has merited the attention of many geomorphologists and has been answered tentatively in a variety of ways. Considerable evidence points to a coincidence of increasing aridity with degradation and increasing humidity with aggradation, but there are opposite views. Reaching a firm conclusion will have to await continuation of just the kinds of observations being here reported. Because we cannot hope to obtain a definitive answer to the question with 7 years of measurement, we are publishing our results principally to encourage others to join us in similar programs of simple measurement over a period of time in order that there will gradually become available concurrent data on rate of channel change, precipitation, and runoff.

The precipitation record for Santa Fe, N. Mex., is the longest in the United States. This record has been analysed in detail for its relation to the erosion problem (Leopold, 1951) and even then, 14 years ago, the difficulty of analysis lay not in the length of the precipitation record but in the lack of quantitative data on land erosion and channel changes. Our measurement data are not yet enough, but the nature of the problem can be more clearly seen than was possible without them, as will now be explained.

Leopold (1951) showed that the mean annual precipitation at Santa Fe did not significantly change between the first and second half of the century of record, but the frequency of daily rainfall amounts did change. In the present discussion we will review briefly that argument and bring the analysis up to date of the present writing, 1964.

Three graphs are presented in figure 171. Graph *A*, the annual march of yearly precipitation totals, is plotted without any averaging. Graphs *B* and *C* show that part of the annual amounts contributed in summer (July–Sept. incl.) months. The mean summer total of 6.06 inches consists mostly of thunderstorm rainfall which each season begins about July 15 after a relatively dry late spring and early summer. Thunderstorms are nearly daily occurrences in the nearby mountains from mid-July to early September. Graph *C* shows that part of the summer rainfall made up by rains totalling one inch or more in a day.

In the three parts of figure 171, trends in the 114 years are not easily discernible without the use of mov-

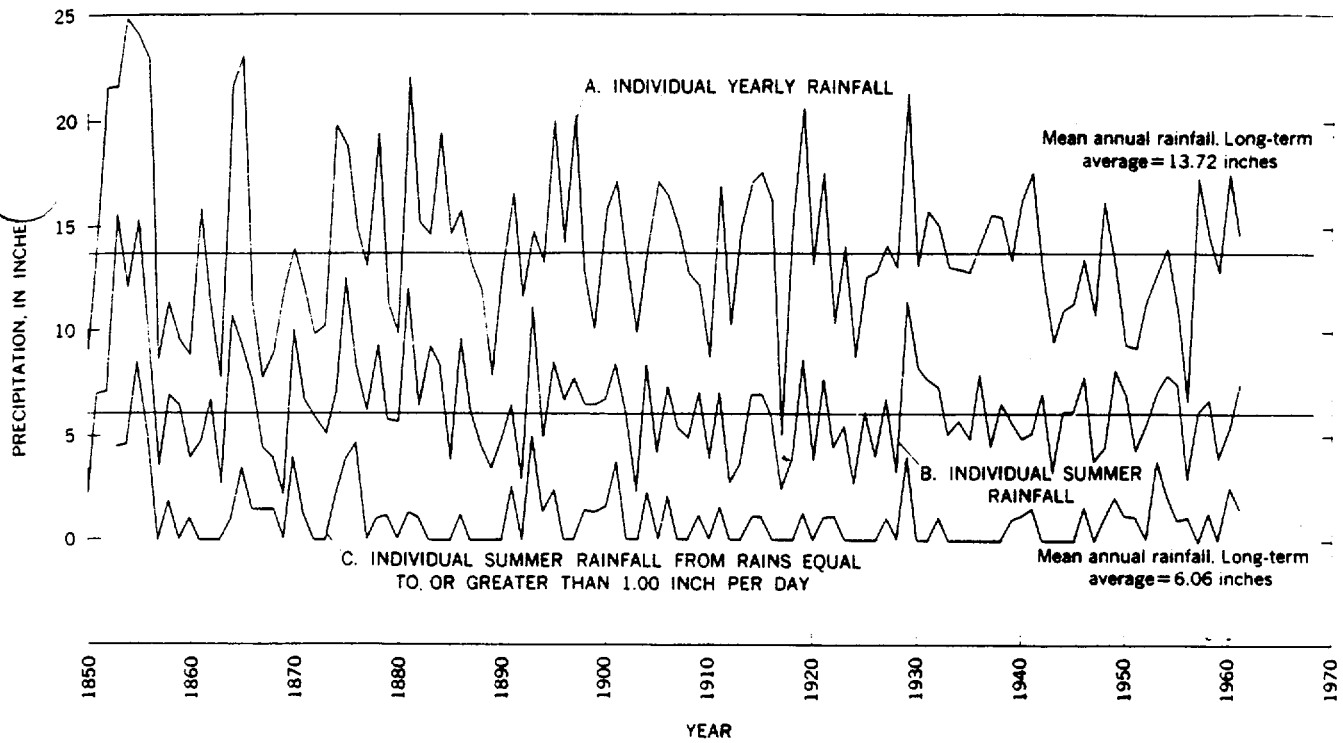


FIGURE 171.—Precipitation, Santa Fe, N. Mex.

ing averages. Inspection of the graphs reveals the dry period of the 1940's and early 1950's and the heavy summer rainfalls of the early 1850's.

Figures 172 and 173 break the precipitation record into its summer and nonsummer components, and then

again into the number of rains of different categories of size of daily rainfalls. The secular change in number of nonsummer rains of less than 0.5 inch in a day so prominent in Leopold's analysis is obvious here, figure 173B. A more subdued but parallel trend is seen also

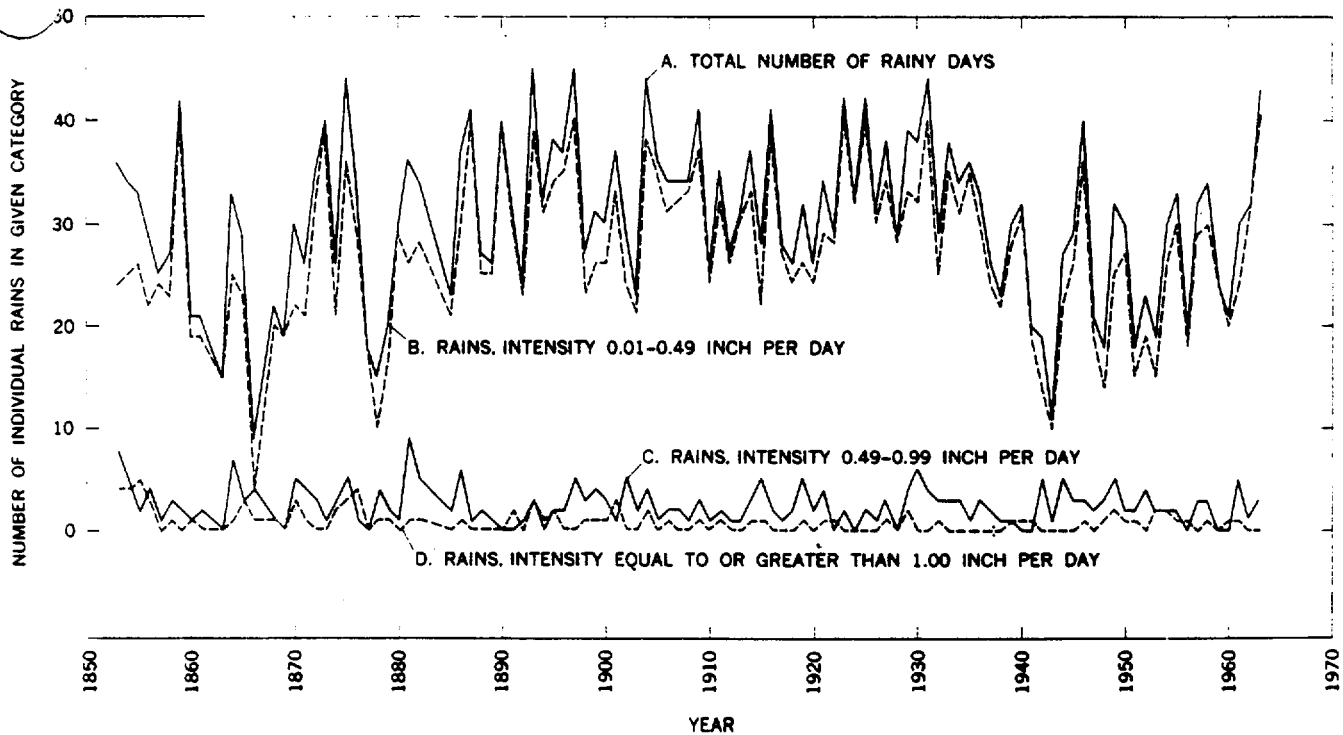


FIGURE 172.—Number of individual summer rains (July-Sept. incl.), Santa Fe, N. Mex.

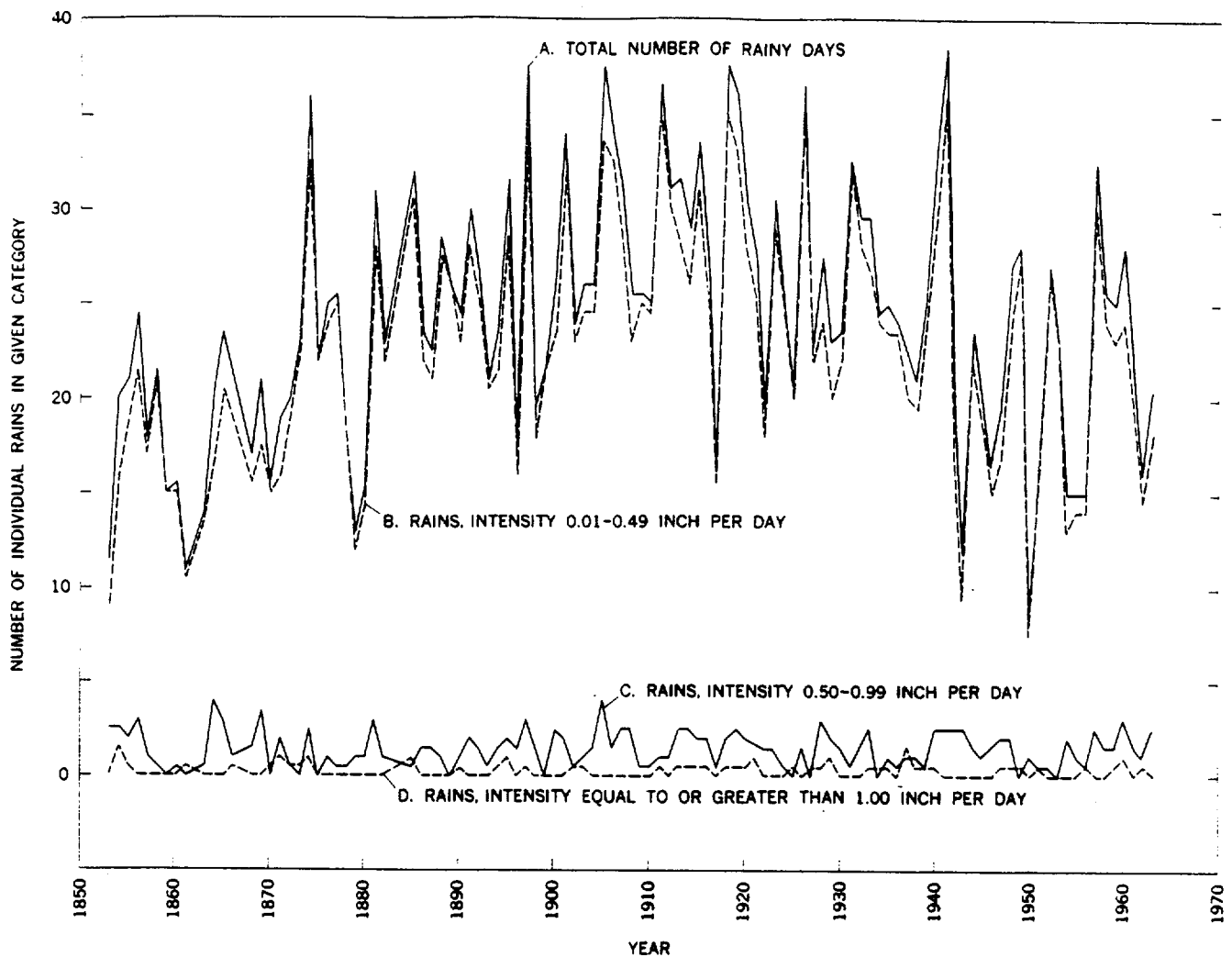


FIGURE 173.—Number of individual nonsummer rains, Santa Fe, N. Mex.

in the number of summer rains less than 0.5 inch per day. These secular changes leave the general impression that the last 25 years were more similar to the first 25 years of record than to the middle of the record period; that is, 1942-57 seems to resemble 1853-72.

This impression is strengthened by examination of figure 174 which shows the annual march of the average intensity of rain expressed as inches per day per rainy day, that is, the number of inches of rain in a year divided by the number of rainy days that year. The rains of the early and final part of the record were more intense than during the middle of the record.

Similar analysis led Leopold (1951) to argue that the period coincident with the advent of heaviest grazing, 1850-80, was characterized by a deficiency of the low-intensity rains which succor vegetation and by more than the average number of heavy rains which could act upon a weakened vegetal cover and promote erosion. This argument is a reasonable one, but to demonstrate

its validity one needs concurrent and detailed data on erosion rates. Such concurrent data are now available for the 7-year period 1958-64, but this period includes years of both high and low intensity rainfall. The precipitation data are not clearly of the character that one could say unequivocally that erosion should be large or should be small. In short, the 7-year record is not long enough.

But the nature of the question ought to be clear from the data presented. Geomorphologists must make quantitative observations of erosion rates and channel changes over a long enough period to be clearly related to the concurrent precipitation record.

It is our hope that the presentation even of the short record now available will spur our colleagues to establish similar areas and continue simple measurements over a period of time so that those who follow us will have more to work with in analysis of this hydrologic and geomorphic problem.

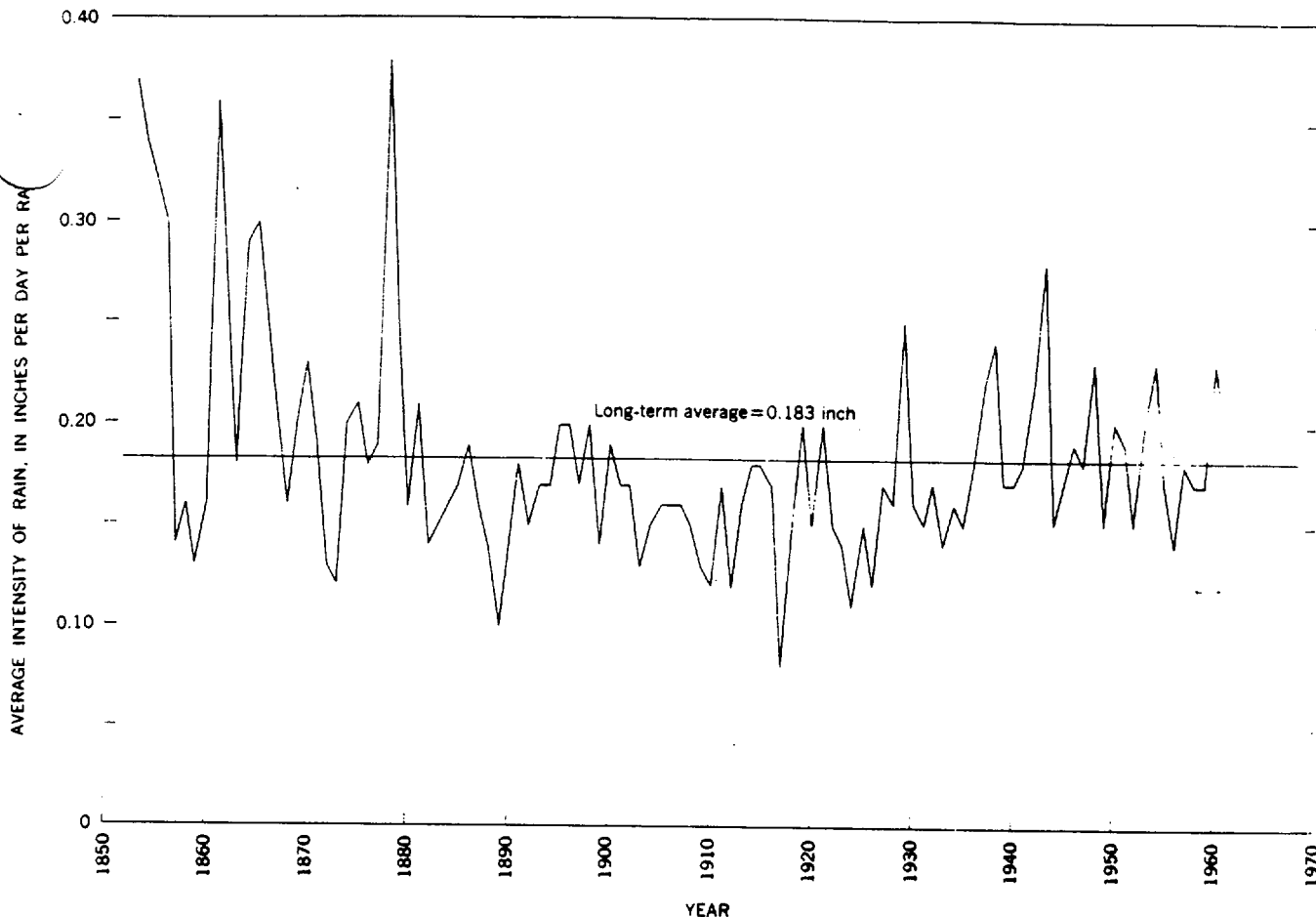


FIGURE 174.—Average annual intensity of rainfall, Santa Fe, N. Mex.

REFERENCES

- Bagnold, R. A., 1956. The flow of cohesionless grains in fluids: Royal Soc. [London] Philos. Trans., ser. A no. 964, v. 249, p. 235-297.
- Brown, C. B., 1945. Rates of sediment production in Southwestern United States: U.S. Soil Conserv. Service, SCS-TP-65, 40 p.
- Emmett, W. W., and Leopold, L. B., 1964. Downstream Pattern of River-Bed Scour and Fill: Proc., Federal Inter-Agency Conf. on Sedimentation, Jackson, Miss.
- Hadley, R. F., and Schumm, S. A., 1961. Hydrology of the upper Cheyenne River Basin: U.S. Geol. Survey Water-Supply Paper 1531-B, 198 p.
- Krammes, J. S., 1960. Erosion from mountain side slopes after fire in southern California: U.S. Forest Service, Pacific S. W. Forest and Range Expt. Sta., Research Note 171.
- Leopold, L. B., 1951. Rainfall frequency, an aspect of climatic variation: Am. Geophys. Union Trans., v. 32, no. 3, p. 347-357.
- Leopold, L. B., and Miller, J. P., 1954. A post-glacial chronology for some alluvial valleys in Wyoming: U.S. Geol. Survey Water-Supply Paper 1261 89 p.
- 1956. Ephemeral streams—hydraulic factors and their relation to the drainage net: U.S. Geol. Survey Prof. Paper 282-A, 37 p.
- Leopold, L. B., Wolman, M. G., and Miller, J. P., 1964. Fluvial processes in geomorphology: San Francisco, W. H. Freeman Co., 522 p.
- Miller, J. P., and Wendorf, F., 1958. Alluvial chronology of the Tesuque Valley, New Mexico: Jour. Geol., v. 66, no. 2, p. 177-194.
- Miller, J. P., Montgomery A., and Sutherland, P. K., 1963. Geology of part of the Southern Sangre de Cristo Mountains, New Mexico: New Mex. Inst. of Mining and Tech. Mem. 11, 106 p.
- Wolman, M. G., 1955. The natural channel of Brandywine Creek, Pennsylvania: U.S. Geol. Survey Prof. Paper 271, 56 p.

SUMMARY OF DATA

A.—Summary of nonrecorded rain-gage data, Arroyo de los Frijoles, 1959-63

[Date of observation may be several days after storm date. Record should not be considered as annual precipitation. Tr., trace amount. Gage locations shown on fig. 143]

Date of observation	Precipitation, in inches, at rain-gage-											
	1	2	3	4	5	6	7	8	9	10	11	12
8-07-59	0.80	1.13	0.80	0.90	0.88	1.05	0.80	1.20	1.20	0.80	1.00	1.06
8-19-59	.25	.25							.20			.30
8-24-59	.50	.58	.50	.35	.32	.36			.30		.48	.65
10-30-59	1.00		1.45	1.40		1.40	1.38			1.32	1.20	1.26
9-10-60	.76	.70	.85	.80	.85	.90	.90	.90	1.05	.94	1.10	1.10
7-15-60	.50	.00	.80	.65	.35	Tr.	Tr.	Tr.	.00	.00	.00	1.02
8-05-60	.20	1.00	.90		.75	.50	.65	.45	.25	1.10	.35	.91
10-17-60	1.30	2.70	2.40	1.90	2.20	2.30	2.20	2.30	2.40	2.50	2.50	1.89
5-23-61	.00	.00	.00	.00	.00	.00	Tr.	.10	.30	.10	.20	
6-16-61	.20	.20	.40	.30	.20	.20	.20	.20	.20	.30	.20	
6-19-61	.00	.40	.00	.00	.00	.20	Tr.	.20	.10	.20	.20	.51
6-29-61	.10	.20	.40	.30	.50	.40	.50	.50	.30	.10	Tr.	.16
7-10-61	.60	.10	.80	.90	.40	.60	.60	.80	.90	.60	.60	.87
8-14-61	1.00	1.20	1.30	1.00	1.10	1.00	1.30	1.20	1.30	1.40	1.20	1.33
9-23-61	1.10	1.10	1.15	1.10	.90	1.00	.80	.80	.96	1.10	.85	1.13
9-19-61	1.20	.88	1.40	.95	.87	1.00	.82	1.00	.79	.89	.75	1.35
7-02-62		.20	.70									.90
7-09-62	.20	.50	.35	1.30	1.20	.20	.20	.30	.20		.40	1.09
7-27-62		2.00	.50	.50	.30	.80	.60	.70	1.00	1.10	.90	1.50
9-01-62	.40	.90	1.10		.60	.00	.60	.60	.20	.00	.00	.00
9-13-63	.79		1.20	.90	.20	.75	.80	.72	.71	.55	.50	.57
9-17-63	.20	.35		.40	.40	.60	.75	.75	.60	.55	.55	.35
7-10-63	Tr.		.02	Tr.	Tr.	.00	Tr.	Tr.	Tr.	.60	.35	.20
7-22-63	1.00	.00	.75	.50	.30	.35	.20	.10	.00	.00	Tr.	.07
9-27-63	.15	.20	.20	.40	.30	.30	.35	.40	.20	.25	.20	.40
9-23-63	1.30	1.30	1.40	1.10	1.00	1.10	1.30	1.30	1.20	1.30	1.10	1.67

B.—Summary of recording rain-gage data, Arroyo de los Frijoles, 1959-62

[Date of observation is within several days of major precipitation, but total precipitation includes also that between observations. Records should not be considered complete for use as annual precipitation. Gage located at Main Project Reach; see fig. 143]

Date of observation	Precipitation (inches)	Date of observation	Precipitation (inches)
8-07-59	1.06	7-08-61	.60
8-20-59	.26	7-28-61	.31
8-24-59	.80	8-13-61	1.33
8-26-59	.23	8-15-61	.10
10-02-59	.08	8-23-61	1.13
10-30-59	1.50	9-12-61	.70
11-13-59	.50	9-19-61	.80
12-17-59	.01	9-20-61	.10
		10-27-61	.70
1-21-60	.50	12-06-61	.10
2-29-60	.50		
5-18-60	.00	1-16-62	.30
6-10-60	1.10	3-09-62	.20
7-15-60	1.20	3-26-62	.20
8-05-60	.81	5-01-62	.10
8-23-60	.25	6-11-62	.10
10-07-60	.70	6-30-62	1.10
10-17-60	1.89	7-02-62	.00
12-12-60	.60	7-09-62	1.09
		7-23-62	.70
1-12-61	.10	7-26-62	1.50
4-03-61	1.30	7-30-62	.00
4-18-61	.38	8-02-62	.00
6-16-61	.20	8-28-62	.20
6-19-61	.60	9-17-62	.50
6-29-61	.30	11-26-62	.30

EROSION AND SEDIMENTATION IN A SEMIARID ENVIRONMENT

C.—Summary of data, erosion-pin plot in Slopewash Tributary, 1959-64

[Minus values in the net change columns represent deposition rather than erosion]

Pin	1959-61		1959-62		1959-63		1959-64		Net change 1959-64 (ft per yr)
	Erosion (ft)	Erosion (ft)	Deposition (ft)	Erosion (ft)	Deposition (ft)	Erosion (ft)	Deposition (ft)		
1	0.02	0.00	0.01	0.04	0.04	0.04	0.20	-0.005	
2	0.01	0.00	0.01	0.03	0.02	0.02	0.05	0.04	
3	0.01	0.00	0.01	0.01	0.02	0.02	0.05	0.04	
4	0.04	0.06	0.01	0.05	0.01	0.00	0.00	0.08	
5	0.03	0.03	0.00	0.05	0.00	0.00	0.00	0.09	
6	0.02	0.04	0.03	0.04	0.04	0.01	0.05	0.07	
7	0.02	0.03	0.02	0.04	0.04	0.01	0.05	0.07	
8	0.02	0.03	0.02	0.03	0.04	0.01	0.05	0.07	
9	0.02	0.03	0.03	0.03	0.04	0.01	0.05	0.07	
10	0.02	0.03	0.00	0.03	0.04	0.00	0.05	0.07	
11	0.04	0.13	0.11	0.11	0.04	0.00	0.05	0.04	
12	0.01	0.05	0.00	0.05	0.02	0.03	0.05	0.04	
13	0.03	0.05	0.02	0.05	0.02	0.03	0.05	0.04	
14	0.02	0.05	0.00	0.05	0.02	0.03	0.05	0.04	
15	0.03	0.05	0.00	0.05	0.02	0.03	0.05	0.04	
16	0.01	0.04	0.00	0.05	0.02	0.03	0.05	0.04	
17	0.02	0.03	0.00	0.05	0.02	0.03	0.05	0.04	
18	0.02	0.03	0.00	0.05	0.02	0.03	0.05	0.04	
19	0.02	0.03	0.00	0.05	0.02	0.03	0.05	0.04	
20	0.02	0.03	0.00	0.05	0.02	0.03	0.05	0.04	
21	0.03	0.05	0.00	0.05	0.02	0.03	0.05	0.04	
22	0.03	0.05	0.00	0.05	0.02	0.03	0.05	0.04	
23	0.02	0.03	0.00	0.05	0.02	0.03	0.05	0.04	
24	0.02	0.03	0.00	0.05	0.02	0.03	0.05	0.04	
25	0.03	0.05	0.00	0.05	0.02	0.03	0.05	0.04	
26	0.05	0.06	0.00	0.05	0.02	0.03	0.05	0.04	
27	0.01	0.02	0.00	0.05	0.02	0.03	0.05	0.04	
28	0.01	0.02	0.00	0.05	0.02	0.03	0.05	0.04	
29	0.01	0.02	0.00	0.05	0.02	0.03	0.05	0.04	
30	0.02	0.03	0.00	0.05	0.02	0.03	0.05	0.04	
31	0.01	0.02	0.00	0.05	0.02	0.03	0.05	0.04	
32	0.02	0.03	0.00	0.05	0.02	0.03	0.05	0.04	
33	0.01	0.02	0.00	0.05	0.02	0.03	0.05	0.04	
34	0.02	0.03	0.00	0.05	0.02	0.03	0.05	0.04	
35	0.02	0.03	0.00	0.05	0.02	0.03	0.05	0.04	
36	0.01	0.02	0.00	0.05	0.02	0.03	0.05	0.04	
37	0.01	0.02	0.00	0.05	0.02	0.03	0.05	0.04	
38	0.01	0.02	0.00	0.05	0.02	0.03	0.05	0.04	
39	0.02	0.03	0.00	0.05	0.02	0.03	0.05	0.04	
40	0.03	0.05	0.00	0.05	0.02	0.03	0.05	0.04	
41	0.02	0.03	0.00	0.05	0.02	0.03	0.05	0.04	
42	0.02	0.03	0.00	0.05	0.02	0.03	0.05	0.04	
43	0.03	0.05	0.00	0.05	0.02	0.03	0.05	0.04	
44	0.04	0.06	0.00	0.05	0.02	0.03	0.05	0.04	
45	0.04	0.06	0.00	0.05	0.02	0.03	0.05	0.04	
46	0.01	0.02	0.00	0.05	0.02	0.03	0.05	0.04	
47	0.01	0.02	0.00	0.05	0.02	0.03	0.05	0.04	
48	0.01	0.02	0.00	0.05	0.02	0.03	0.05	0.04	
49	0.03	0.05	0.00	0.05	0.02	0.03	0.05	0.04	
50	0.03	0.05	0.00	0.05	0.02	0.03	0.05	0.04	
51	0.03	0.05	0.00	0.05	0.02	0.03	0.05	0.04	
52	0.03	0.05	0.00	0.05	0.02	0.03	0.05	0.04	
53	0.03	0.05	0.00	0.05	0.02	0.03	0.05	0.04	
54	0.02	0.03	0.00	0.05	0.02	0.03	0.05	0.04	
55	0.01	0.02	0.00	0.05	0.02	0.03	0.05	0.04	
56	0.02	0.03	0.00	0.05	0.02	0.03	0.05	0.04	
57	0.04	0.06	0.00	0.05	0.02	0.03	0.05	0.04	
58	0.02	0.03	0.00	0.05	0.02	0.03	0.05	0.04	
59	0.01	0.02	0.00	0.05	0.02	0.03	0.05	0.04	
60	0.01	0.02	0.00	0.05	0.02	0.03	0.05	0.04	
61	0.02	0.03	0.00	0.05	0.02	0.03	0.05	0.04	

Summary

Average erosion, 0.0117 ft per yr.
Average deposition, 0.0041 ft per yr.
Net average erosion, 0.0076 ft per yr.

D.—Summary of data, slope-retreat pins in Slopetwash Tributary, 1959-64

[Minus values in the net change columns represent deposition rather than erosion]

Pin	1959-61		1961-62		1962-63		1963-64		1964-65		Net change 1959-64	Total	Yearly Average (ft per yr)
	Erosion (ft)	Deposition (ft)											
1	0.01	0.00	0.03	0.00	0.01	0.01	0.025	0.000	0.075	0.010	0.065	0.013	
2	0.06	0.00	0.04	0.00	0.01	0.01	0.02	0.000	0.030	0.030	0.030	0.028	
3	0.05	0.00	0.03	0.00	0.03	0.03	0.02	0.015	0.130	0.010	0.140	0.028	
4	0.04	0.00	0.05	0.00	0.01	0.01	0.12	0.000	0.045	0.045	0.090	0.016	
5	0.07	0.00	0.04	0.00	0.02	0.01	0.13	0.000	0.125	0.010	0.115	0.023	
6	0.17	0.00	0.03	0.00	0.02	0.02	0.030	0.000	0.145	0.010	0.135	0.027	
7	0.01	0.16	0.03	0.17	0.02	0.06	0.040	0.000	0.350	0.020	0.230	0.046	
8	0.01	0.00	0.03	0.00	0.00	0.06	0.070	0.000	0.330	0.000	0.000	0.000	
9	0.02	0.00	0.02	0.00	0.09	0.01	0.080	0.000	0.110	0.090	0.020	0.004	
10	0.03	0.00	0.01	0.00	0.04	0.01	0.030	0.000	0.060	0.010	0.050	0.030	
11	0.02	0.00	0.01	0.09	0.06	0.02	0.040	0.000	0.080	0.000	0.080	0.016	
12	0.08	0.03	0.02	0.07	0.03	0.02	0.015	0.000	0.140	0.000	0.140	0.028	
13	0.01	0.00	0.02	0.00	0.06	0.02	0.005	0.000	0.085	0.020	0.075	0.015	
14	0.04	0.00	0.02	0.00	0.025	0.025	0.005	0.015	0.065	0.000	0.065	0.019	
15	0.00	0.00	0.02	0.00	0.015	0.025	0.020	0.015	0.065	0.040	0.025	0.035	
16	0.04	0.00	0.02	0.00	0.015	0.035	0.035	0.000	0.110	0.000	0.110	0.022	
17	0.04	0.00	0.00	0.00	0.035	0.03	0.035	0.000	0.140	0.000	0.140	0.028	
18	0.15	0.00	0.11	0.00	0.03	0.03	0.040	0.000	0.330	0.070	0.260	0.052	
19	0.09	0.00	0.13	0.00	0.02	0.04	0.020	0.025	0.400	0.040	0.420	0.084	
20	0.08	0.00	0.07	0.00	0.04	0.04	0.025	0.025	0.215	0.065	0.150	0.030	
21	0.00	0.13	0.22	0.10	0.03	0.03	0.030	0.040	0.290	0.330	0.070	0.014	
22	0.03	0.00	0.03	0.00	0.04	0.04	0.050	0.005	0.140	0.045	0.095	0.019	
23	0.02	0.04	0.06	0.02	0.04	0.04	0.030	0.020	0.150	0.120	0.030	0.006	
24	0.01	0.03	0.04	0.00	0.04	0.05	0.070	0.000	0.120	0.080	0.040	0.008	
25	0.02	0.00	0.02	0.00	0.05	0.03	0.020	0.050	0.110	0.050	0.060	0.012	
26	0.04	0.00	0.01	0.03	0.15	0.05	0.035	0.000	0.290	0.030	0.260	0.046	
27	0.02	0.00	0.02	0.00	0.04	0.04	0.035	0.005	0.135	0.035	0.090	0.016	
28	0.02	0.00	0.02	0.00	0.04	0.04	0.000	0.040	0.080	0.040	0.040	0.008	
29	0.03	0.00	0.01	0.01	0.02	0.02	0.020	0.000	0.080	0.010	0.070	0.014	
30	0.00	0.00	0.00	0.00	0.00	0.00	0.000	0.000	0.000	0.000	0.000	0.000	
31	0.02	0.00	0.00	0.00	0.01	0.07	0.055	0.000	0.085	0.035	0.120	0.024	
32	0.02	0.00	0.01	0.00	0.01	0.09	0.060	0.000	0.110	0.075	0.065	0.013	
33	0.03	0.00	0.01	0.00	0.02	0.07	0.075	0.000	0.135	0.015	0.120	0.024	
34	0.04	0.00	0.00	0.00	0.02	0.02	0.025	0.045	0.075	0.015	0.060	0.016	
35	0.01	0.00	0.00	0.01	0.00	0.02	0.030	0.080	0.040	0.110	0.070	0.014	
36	0.02	0.00	0.00	0.00	0.03	0.03	0.030	0.005	0.070	0.035	0.035	0.003	
37	0.02	0.00	0.01	0.00	0.02	0.02	0.015	0.000	0.075	0.020	0.055	0.011	
38	0.03	0.00	0.00	0.00	0.04	0.13	0.050	0.110	0.140	0.240	0.100	0.020	
39	0.03	0.00	0.00	0.00	0.04	0.11	0.050	0.080	0.120	0.190	0.070	0.014	
40	0.03	0.00	0.00	0.00	0.00	0.00	0.000	0.000	0.000	0.000	0.000	0.000	
41	0.02	0.00	0.00	0.01	0.03	0.00	0.030	0.000	0.080	0.010	0.070	0.014	
42	0.01	0.00	0.02	0.05	0.02	0.03	0.030	0.000	0.100	0.080	0.020	0.004	
43	0.00	0.00	0.03	0.06	0.01	0.01	0.030	0.000	0.120	0.070	0.050	0.010	
44	0.00	0.00	0.04	0.04	0.01	0.00	0.000	0.000	0.130	0.040	0.090	0.016	
45	0.01	0.00	0.05	0.00	0.02	0.01	0.030	0.000	0.110	0.010	0.100	0.020	
46	0.00	0.00	0.00	0.00	0.19	0.04	0.030	0.000	0.140	0.040	0.100	0.020	
47	0.00	0.11	0.00	0.00	0.00	0.04	0.110	0.000	0.220	0.040	0.180	0.036	
48	0.05	0.00	0.03	0.00	0.00	0.03	0.010	0.000	0.080	0.030	0.050	0.006	
49	0.03	0.03	0.00	0.00	0.01	0.00	0.000	0.040	0.060	0.040	0.020	0.000	
50	0.00	0.04	0.00	0.00	0.02	0.02	0.020	0.020	0.060	0.040	0.020	0.004	
51	0.00	0.02	0.00	0.00	0.02	0.02	0.010	0.010	0.040	0.030	0.010	0.002	
52	0.03	0.03	0.00	0.00	0.08	0.00	0.090	0.000	0.200	0.000	0.200	0.040	
53	0.03	0.00	0.07	0.00	0.07	0.00	0.070	0.000	0.170	0.000	0.170	0.034	
54	0.04	0.05	0.10	0.05	0.01	0.00	0.030	0.000	0.140	0.030	0.110	0.018	
55	0.02	0.02	0.01	0.01	0.01	0.00	0.070	0.000	0.100	0.010	0.090	0.018	
56	0.00	0.10	0.00	0.04	0.00	0.15	0.210	0.000	0.310	0.190	0.120	0.024	
57	0.00	0.09	0.04	0.04	0.00	0.02	0.060	0.000	0.150	0.060	0.090	0.018	

Summary of erosion rates, in foot per year

Pins	Erosion	Deposition	Net erosion	Pins	Erosion	Deposition	Net erosion
1-29	0.0829	0.0116	0.0210	46-57	0.0272	0.0099	0.0183
30-45	0.0197	0.0231	0.0034	1-57	0.0281	0.0139	0.0142

E.—Summary of data, iron-pin lines in Slopewash Tributary, 1958-64

[Minus values in net-change column represent deposition rather than erosion]

Pin	Protrusion, in feet						Net change, 1958-64	
	1958		1960		1962			1964
	1958	1959	1960	1962	1962	1963		1964
C.....	0.12	0.08	0.10	0.12	0.10	0.10	-0.02	
1-cb.....	0.12	0.10	0.16	0.20	0.21	0.19	0.07	
2-cb.....	0.11	0.04	0.00	0.00	0.00	0.00	-0.21	
3-cb.....	0.26	0.12	0.16	0.08	0.07	0.11	-0.15	
4-cb.....	0.30	0.23	0.25	0.30	0.35	0.33	-0.23	
5-cb.....	0.06	0.13	0.13	0.15	0.16	0.16	0.00	
B.....	0.12	0.13	0.11	0.12	0.13	0.12	0.00	
1-ba.....	0.09	0.15	0.12	0.21	0.32	0.30	-0.21	
2-ba.....	0.21	0.27	0.35	0.35	0.38	0.38	-0.29	
3-ba.....	0.11	0.11	0.12	0.18	0.17	0.18	0.07	
A.....	0.14	0.16	0.19	0.15	0.20	0.20	0.06	
C.....	0.15	0.15	0.16	0.21	0.21	0.22	-0.07	
1-cd.....	0.04	0.02	-0.05	-0.10	-0.20	-0.17	-0.21	
2-cd.....	0.11	0.12	0.15	0.15	0.15	0.13	-0.02	
3-cd.....	0.11	0.12	0.11	0.16	0.20	0.17	0.06	
D.....	0.24	0.10	0.20	0.15	0.15	0.36	0.12	
1-db.....	0.11	0.11	0.12	0.13	0.16	0.13	-0.02	
B.....	0.11	0.11	0.12	0.13	0.16	0.13	-0.02	
E.....	0.11	0.11	0.12	0.13	0.16	0.13	-0.02	
Average net erosion.....						0.0072	

F.—Summary of data, erosion-nail lines in Coyote C. Arroyo, 1961-64

[Minus values in rate column represent deposition rather than erosion. Values in erosion columns do not include that erosion necessary to remove any deposition reported in previous years. Values in deposition columns represent data only for year of observation]

Pin	1961-62		1961-63		1961-64		Rate
	Erosion (ft)	Deposition (ft)	Erosion (ft)	Deposition (ft)	Erosion (ft)	Deposition (ft)	
Line BA	0.065	0.000	0.090	0.000	0.095	0.000	0.032
1.....	0.055	0.010	0.070	0.000	0.070	0.000	0.023
2.....	0.070	0.000	0.070	0.000	0.070	0.000	0.020
3.....	0.065	0.000	0.060	0.000	0.065	0.000	0.023
4.....	0.050	0.000	0.050	0.000	0.060	0.000	0.017
5.....	0.060	0.015	0.050	0.020	0.045	0.000	0.027
6.....	0.060	0.000	0.065	0.000	0.060	0.000	0.023
7.....	0.055	0.000	0.050	0.030	0.050	0.000	0.018
8.....	0.060	0.000	0.060	0.000	0.060	0.000	0.035
9.....	0.055	0.000	0.070	0.000	0.070	0.000	0.043
10.....	0.060	0.000	0.060	0.000	0.060	0.000	0.020
11.....	0.050	0.015	0.045	0.000	0.055	0.000	0.040
12.....	0.035	0.000	0.040	0.000	0.040	0.000	0.020
13.....	0.050	0.000	0.060	0.000	0.070	0.000	0.020
14.....	0.060	0.010	0.060	0.000	0.060	0.000	0.025
15.....	0.060	0.000	0.060	0.000	0.060	0.000	0.025
16.....	0.060	0.000	0.060	0.000	0.060	0.000	0.037
17.....	0.060	0.000	0.060	0.000	0.060	0.000	0.025
18.....	0.055	0.025	0.060	0.015	0.050	0.000	0.017
19.....	0.060	0.000	0.065	0.000	0.060	0.000	0.030
Average net erosion.....						0.0072

F.—Summary of data, erosion-nail lines in Coyote C. Arroyo, 1961-64—Continued

Pin	1961-62		1961-63		1961-64		Rate
	Erosion (ft)	Deposition (ft)	Erosion (ft)	Deposition (ft)	Erosion (ft)	Deposition (ft)	
20.....	0.070	0.000	0.075	0.000	0.100	0.000	0.033
21.....	0.060	0.000	0.060	0.000	0.070	0.000	0.023
Average net erosion.....						0.027
Line BC	0.065	0.000	0.100	0.000	0.120	0.000	0.040
1.....	0.060	0.000	0.060	0.000	0.065	0.000	0.038
2.....	0.055	0.000	0.060	0.000	0.060	0.000	0.028
3.....	0.065	0.000	0.060	0.000	0.060	0.000	0.030
4.....	0.065	0.000	0.075	0.000	0.060	0.000	0.023
5.....	0.050	0.000	0.060	0.020	0.070	0.000	0.033
6.....	0.065	0.000	0.060	0.000	0.060	0.000	0.011
7.....	0.050	0.060	0.055	0.055	0.050	0.000	0.021
8.....	0.110	0.000	0.060	0.000	0.070	0.000	0.020
9.....	0.040	0.000	0.055	0.010	0.060	0.000	0.020
10.....	0.020	0.000	0.030	0.010	0.030	0.000	0.020
11.....	0.040	0.000	0.060	0.000	0.060	0.000	0.022
12.....	0.040	0.000	0.070	0.000	0.065	0.000	0.023
13.....	0.045	0.000	0.055	0.000	0.070	0.000	0.022
14.....	0.060	0.030	0.070	0.000	0.060	0.000	0.027
15.....	0.050	0.000	0.060	0.000	0.065	0.000	0.022
16.....	0.040	0.000	0.055	0.000	0.060	0.000	0.027
17.....	0.060	0.000	0.060	0.000	0.060	0.000	0.027
18.....	0.045	0.030	0.070	0.000	0.060	0.000	0.023
19.....	0.045	0.000	0.070	0.000	0.075	0.000	0.025
Average net erosion.....						0.023

Pin	1961-62		1961-63		1961-64		Rate
	Erosion (ft)	Deposition (ft)	Erosion (ft)	Deposition (ft)	Erosion (ft)	Deposition (ft)	
1.....	0.055	0.000	0.055	0.000	0.070	0.000	0.023
2.....	0.060	0.000	0.060	0.000	0.060	0.000	0.020
3.....	0.040	0.000	0.040	0.000	0.070	0.000	0.017
4.....	0.040	0.000	0.050	0.000	0.050	0.000	0.027
5.....	0.030	0.000	0.050	0.000	0.050	0.000	0.023
6.....	0.050	0.000	0.050	0.000	0.070	0.000	0.018
7.....	0.070	0.015	0.060	0.000	0.070	0.000	0.035
8.....	0.065	0.000	0.075	0.010	0.075	0.000	0.043
9.....	0.070	0.050	0.070	0.030	0.060	0.000	0.020
10.....	0.060	0.000	0.060	0.000	0.060	0.000	0.040
11.....	0.040	0.000	0.040	0.010	0.060	0.000	0.020
12.....	0.040	0.050	0.065	0.000	0.065	0.000	0.025
13.....	0.060	0.000	0.060	0.000	0.075	0.000	0.025
14.....	0.075	0.000	0.060	0.000	0.060	0.000	0.037
15.....	0.045	0.000	0.035	0.000	0.045	0.000	0.017
16.....	0.060	0.000	0.060	0.000	0.065	0.000	0.020
17.....	0.070	0.000	0.070	0.000	0.075	0.015	0.020
18.....	0.070	0.000	0.075	0.000	0.075	0.000	0.012
19.....	0.060	0.000	0.060	0.000	0.060	0.000	0.023
20.....	0.060	0.030	0.065	0.050	0.070	0.000	0.015
21.....	0.060	0.000	0.060	0.000	0.060	0.000	0.020
22.....	0.060	0.000	0.060	0.000	0.060	0.000	0.020
23.....	0.060	0.000	0.060	0.000	0.060	0.000	0.020
24.....	0.060	0.000	0.060	0.000	0.060	0.000	0.020
25.....	0.060	0.000	0.060	0.000	0.060	0.000	0.020
Average net erosion.....						0.021
Average net erosion for all 65 pins.....						0.027

G.—Summary of data, nail sections A-J in Slopewash Tributary, 1959-64

[Pin: L.B. left bank; C.L. centerline; R.B. right bank]

Section	Pin	1959-61		1961-62		1962-63		1963-64		1964-64		Rate
		Erosion (ft)	Deposition (ft)									
A.....	L.B.	0.040	0.000	0.020	0.000	0.000	0.000	0.050	0.000	0.065	0.000	0.013
	C.L.	0.120	0.010	0.060	0.270	0.000	0.000	0.185	0.285	0.365	0.151	-0.078
	R.B.	0.040	0.000	0.000	0.000	0.030	0.000	0.035	0.000	0.050	0.000	0.021
B.....	L.B.	0.020	0.000	0.030	0.000	0.000	0.000	0.070	0.000	0.120	0.000	0.024
	C.L.	0.000	0.020	0.020	0.000	0.040	0.000	0.060	0.060	0.060	0.036	-0.024
	R.B.	0.030	0.000	0.010	0.000	0.000	0.000	0.150	0.000	0.190	0.038	0.000
C.....	L.B.	0.100	0.000	0.030	0.060	0.000	0.000	0.085	0.075	0.110	0.043	0.000
	C.L.	0.040	0.030	0.040	0.040	0.040	0.040	0.030	0.100	0.140	0.129	0.000
	R.B.	0.050	0.000	0.030	0.000	0.000	0.000	0.150	0.000	0.190	0.038	0.012
D.....	L.B.	0.100	0.000	0.000	0.000	0.000	0.000	0.060	0.000	0.060	0.000	0.004
	C.L.	0.100	0.020	0.000	0.000	0.020	0.030	0.050	0.050	0.070	0.034	-0.004
	R.B.	0.010	0.000	0.000	0.000	0.000	0.000	0.060	0.000	0.100	0.000	0.020
Average net erosion.....											0.027

G.—Summary of data, nail sections A-J in Slopewash Tributary, 1959-64—Continued

Section	Pin	1959-61		1961-62		1962-63		1963-64		1959-64		Rate	
		Erosion (ft)	Deposition (ft)	Erosion (ft per yr)	Deposition (ft per yr)		Net change (ft per yr)						
E	LB	0.020	0.000	0.010	0.040	0.050	0.000	0.100	0.000	0.180	0.040	0.036	0.028
	CL	0.040	0.030	0.010	0.210	0.000	0.130	0.000	0.170	0.280	0.540	0.056	0.108
	RB	0.000	0.000	0.050	0.060	0.060	0.050	0.020	0.000	0.130	0.110	0.024	0.004
F	LB	0.010	0.000	0.010	0.000	0.000	0.000	0.100	0.000	0.020	0.000	0.004	0.004
	CL	0.060	0.230	0.140	0.000	0.000	0.140	0.100	0.000	0.160	0.470	0.032	0.004
	RB	0.060	0.050	0.040	0.030	0.000	0.000	0.020	0.000	0.100	0.080	0.020	0.016
G	LB	0.000	0.000	0.030	0.000	0.000	0.000	0.070	0.000	0.160	0.000	0.032	0.000
	CL	0.030	0.130	0.160	0.140	0.140	0.155	0.190	0.101	0.505	0.540	0.101	0.108
	RB	0.020	0.000	0.000	0.000	0.000	0.000	0.000	0.030	0.050	0.000	0.010	0.000
H	LB	0.000	0.000	0.060	0.060	0.050	0.050	0.000	0.000	0.110	0.140	0.022	0.028
	CL	0.000	0.210	0.230	0.350	0.350	0.140	0.030	0.030	0.610	0.730	0.122	0.145
	RB	0.040	0.000	0.020	0.000	0.010	0.000	0.010	0.000	0.040	0.000	0.018	0.000
I	LB	0.020	0.000	0.090	0.000	0.000	0.000	0.140	0.000	0.150	0.455	0.028	0.028
	CL	0.010	0.010	0.230	0.230	0.150	0.120	0.140	0.135	0.530	0.000	0.030	0.007
	RB	0.030	0.000	0.020	0.000	0.000	0.000	0.120	0.000	0.190	0.000	0.006	0.008
J	LB	0.010	0.000	0.030	0.000	0.000	0.000	0.000	0.000	0.040	0.000	0.006	0.000
	CL	0.120	0.080	0.230	0.230	0.110	0.120	0.190	0.160	0.650	0.580	0.130	0.118
	RB	0.010	0.000	0.020	0.000	0.000	0.000	0.060	0.000	0.080	0.000	0.018	0.018

Summary of average erosion rates, in foot per year

Bank.....	Erosion	Deposition	Net erosion
Channel.....	0.0248	0.0058	0.0190
	0.0644	0.1024	0.0380

H.—Summary of data, mass-movement line in Slopewash Tributary, 1959-64

[Erosion for 1959-61 not measured]

Pin	1959-61			1959-62			1959-63			1959-64				
	Downhill movement (in.)	Pin rotation (degrees)	Downhill movement (in.)	Erosion at pin (ft)	Pin rotation (degrees)	Downhill movement (in.)	Erosion at pin (ft)	Pin rotation (degrees)	Downhill movement (in.)	Erosion at pin (ft)	Pin rotation (degrees)	Downhill movement (in.)	Erosion at pin (ft)	Pin rotation (degrees)
1	0.38	0	0.83	0.01	4	1.24	0.10	4	1.50	7	0.09	0.300	1.4	0.018
2	0.02	0	0.07	-0.05	4	1.13	-0.02	4	1.27	0	0.01	0.054	0	0.002
3	1.00	5	1.27	0.09	10	1.20	0.17	8	1.09	10	0.17	0.300	2.0	0.034
4	1.01	3	1.03	0.09	5	1.69	0.11	7	2.09	11	0.18	0.418	2.2	0.032
5	1.82	0	1.43	0.09	3	1.42	0.10	6	1.48	5	0.13	0.296	1.0	0.028
6	1.04	0	1.43	0.10	3	1.91	0.08	6	2.07	9	0.14	0.414	1.8	0.022
7	1.07	4	1.31	0.07	3	2.01	0.08	6	1.15	7	0.11	0.230	1.4	0.022
8	1.02	4	1.31	0.08	5	2.01	0.11	11	2.90	18	0.18	0.520	3.6	0.036
9	0.30	0	0.09	0.05	0	0.07	0.05	0	0.24	1	0.07	0.048	0.6	0.014
10	0.30	0	0.01	0.01	1	0.09	0.01	1	0.18	3	0.06	0.036	0.6	0.016
11	0.68	0	0.37	0.15	3	1.55	0.12	7	1.56	10	0.17	0.312	2.0	0.034
12	0.20	0	0.09	0.07	0	0.21	0.03	3	0.01	6	0.18	0.002	1.2	0.036
13	1.11	0	1.22	0.03	0	0.50	0.02	6	0.42	8	0.04	0.094	1.6	0.008
14	1.39	4	1.78	0.13	5	1.33	0.06	6	1.38	8	0.10	0.276	1.2	0.020
15	0.62	1.3	0.63	0.10	2	0.83	0.14	4	0.44	4	0.25	0.068	0.8	0.050
Average.....	0.62	1.3	0.76	0.08	1.03	1.03	0.09	5.1	1.13	7.0	0.13	0.225	1.40	0.025

I.—Summary of data, mass-movement line in Coyote Arroyo, 1961-64

Pin	Local ground slope (degrees)	1961-62		1961-63		1961-64		Yearly average 1961-64		
		Downhill movement (in.)	Pin rotation (degrees)	Downhill movement (in.)	Pin rotation (degrees)	Downhill movement (in.)	Pin rotation (degrees)	Downhill movement (in. per yr)	Pin rotation (degrees per yr)	
1	31	-0.10	0	-0.01	0	0.07	1	0.32	0.023	0.3
2	30	-0.08	0	-0.19	0	-0.19	10	0.30	0.063	3.3
3	24	-0.08	0	-0.15	0	-0.28	2	0.27	0.083	7
4	4	-0.13	0	-0.23	0	-0.26	1	0.20	0.057	3
5	31	-0.27	0	-0.71	0	-0.75	3	0.25	0.080	1.0
6	30	-0.27	0	-0.40	0	-0.45	0	0.25	0.080	1.0
7	30	-0.58	0	1.46	0	1.80	9	0.53	0.150	9
8	28	-0.28	7	1.56	10	1.86	12	0.56	0.160	9
9	37	0.28	-7	1.14	3	1.54	4	0.49	0.132	4.3
10	21	1.00	11	2.03	11	2.03	16	0.27	0.077	3.3
11	18	0.00	0	-0.19	0	-0.28	0	0.83	0.263	0
12	22	0.03	0	-0.39	0	-0.49	3	0.32	0.083	1.0
Average.....	25	0.33	1	0.67	3	0.80	5	0.27	0.067	1.7

CHANNEL AND HILLSLOPE PROCESSES, SEMIARID AREA, NEW MEXICO

J.—Summary of data, movement of coarse particles in Morning Walk Wash, 1961-64—Continued

Rock	Distance moved (feet)		
	1962	1963	1964

North gully—Continued			
Rock	1962	1963	1964
220	45	M	200
230	241	6	0
240	M	355	14
250	M	M	M
260	0	0	0
270	0	0	0
280	291	11	3
290	291	76	10
300	168	5	0
310	321	M	M
320	5	0	8
330	0	0	0
340	M	M	M
350	M	M	M
360	0	M	M
370	M	M	M
380	M	M	M
390	0	M	0
400	M	M	M
410	M	M	M
420	0	0	0
430	0	0	0
440	0	0	0
450	36	0	0
460	0	0	M
470	8	0	0
480	66	0	0
490	0	0	0
500	0	0	0
510	0	0	0
520	20	0	0
530	0	0	0
540	0	0	0
550	0	0	0
560	0	0	0
570	0	0	0
580	0	0	0
590	0	0	0
600	0	0	0
610	0	0	0
620	0	0	0
630	0	0	0
640	0	0	0
650	0	0	0
660	0	0	0

- Oxburgh, E. R., and Turcotte, D. L., 1968, Problem of high heat flow and volcanism associated with zones of descending mantle convective flow [abs.]: *Am. Geophys. Union Trans.*, v. 49, p. 318.
- , 1970, Thermal structure of island arcs: *Geol. Soc. America Bull.*, v. 81, p. 1665-1668.
- Page, B. M., 1970, Sur-Nacimiento fault zone of California: continental margin tectonics: *Geol. Soc. America Bull.*, v. 81, p. 667-690.
- Papike, J. J., and Clark, J. R., 1968, The crystal structure and cation distribution of glaucophane: *Am. Mineralogist*, v. 53, p. 1156-1173.
- Peterman, Z. E., Hedge, C. E., Coleman, R. G., and Snively, P. D., 1967: $^{87}\text{Sr}/^{86}\text{Sr}$ ratios in some eugeosynclinal sedimentary rocks and their bearing on the origin of granitic magma in orogenic belts: *Earth and Planetary Sci. Letters*, v. 2, p. 433-439.
- Plas, L. van der, 1959: Petrology of the northern Adula region, Switzerland (with particular reference to glaucophane-bearing rocks): *Leidse Geol. Meded.*, v. 24, p. 415-602.
- Ransome, F. L., 1894, The geology of Angel Island: California Univ. Pub., Geol. Sci., v. 1, p. 193-240.
- Raymond, L. A., 1970, Relationships between blueschists facies metamorphism, folding, and faulting in Franciscan rocks, Seegers Ranch area, northeastern Diablo range, California [abs.]: *Geol. Soc. America Abs. with Programs*, v. 2, no. 2, p. 133-134.
- Ringwood, A. E., and Green, D. H., 1966, An experimental investigation of the gabbro-eclogite transformation and some geophysical implications: *Tectonophysics*, v. 3, p. 383-427.
- Robertson, E. C., Birch, Francis, and MacDonald, G. J. F., 1957, Experimental determination of jadeite stability relations to 25,000 bars: *Am. Jour. Sci.*, v. 255, p. 115-137.
- Roeber, W. P. de, and Nijhuis, H. J., 1963, Plurifacial alpine metamorphism in the eastern Betic Cordilleras (SE Spain), with special reference to the genesis of the glaucophane: *Geol. Rundschau*, v. 53, p. 324-336.
- Saad, A. H., 1969, Paleomagnetism of Franciscan ultramafic rocks from Red Mountain, California: *Jour. Geophys. Research*, v. 74, p. 6567-6578.
- Safonov, A., 1962, The challenge of the Sacramento Valley, California, in O. E. Brown, Jr., ed., *Geologic guide to the gas and oil fields of Northern California: California Div. Mines and Geology Bull.* 181, p. 77-98.
- Saito, M., Hasimoto, K., Sawata, H., and Shimazaki, Y., 1960, Geology and mineral resources of Japan, 2d ed.: Tokyo, Japan, Geol. Survey, 304 p.
- Seki, Y., Ernst, W. G., and Onuki, H., 1969, Phase proportions and physical properties of minerals and rocks from the Franciscan and Sanbagawa metamorphic terranes, a supplement to *Geol. Soc. America Mem.* 124: Tokyo, Japan, Japan Soc. Promotion Sci., 85 p.
- Smith, J. P., 1907, The paragenesis of the minerals in the glaucophane-bearing rocks of California: *Am. Philos. Soc. Proc.*, v. 45, p. 183-242.
- Suppe, John, 1969a, Franciscan geology of the Leech Lake Mountain-Anthony Peak region, northern Coast Ranges, California [abs.]: *Geol. Soc. America Abs. with Programs*, 1969 (v. 1), pt. 2, p. 65-66.
- , 1969b, Times of metamorphism in the Franciscan terrain of the northern Coast Ranges, California: *Geol. Soc. America Bull.*, v. 80, p. 135-142.
- Taliaferro, N. L., 1945, Franciscan-Knoxville problem: *Am. Assoc. Petroleum Geologists Bull.*, v. 27, p. 109-219.
- Taylor, H. P., and Coleman, R. G., 1968, $\text{O}^{18}/\text{O}^{16}$ ratios of coexisting minerals in glaucophane-bearing metamorphic rocks: *Geol. Soc. America Bull.*, v. 79, p. 1727-1756.
- Turner, F. J., 1968, *Metamorphic petrology*: New York, McGraw-Hill, 403 p.
- Washington, H. S., 1901, A chemical study of the glaucophane schists: *Am. Jour. Sci.*, 4th ser., v. 11, p. 35-59.
- Wray, J. L., and Daniels, F., 1957, Precipitation of calcite and aragonite: *Am. Chem. Soc. Bull.*, v. 79, p. 2031-2034.

[AMERICAN JOURNAL OF SCIENCE, VOL. 270, FEBRUARY 1971, P. 109-135]

RATES AND MODES OF DENUDATION, WHITE MOUNTAINS, EASTERN CALIFORNIA*

DENIS E. MARCHAND

Department of Geology and Geography, Bucknell University,
Lewisburg, Pennsylvania 17837, and U.S. Geological Survey

ABSTRACT. Long-term total erosion rates in the White Mountains, estimated from depths of removal beneath a 10.8-m.y.-old basalt, range from 1 to 3 cm per 1000 years. Present rates of chemical denudation, corrected for contributions from the atmosphere and biosphere, are 0.14 to 0.19 cm per 1000 years in dominantly adamellite terrain and 1.7 to 2.1 cm per 1000 years in areas underlain by Reed Dolomite. These figures are much lower than Reed Dolomite denudation rates estimated from botanical evidence in the same area (LaMarche, 1968) but are consistent with erosion rates in the nearby Sierra Nevada. Chemical denudation by plant uptake and litter erosion was evaluated and compared with removal in solution. Although total amounts of biogeochemical erosion do not appear to be significant, this process may account for some part of the extraction of P and K and is apparently responsible for appreciable portions of Al, Fe, and Mn denudation.

In stream waters draining dolomite, partial pressures of CO_2 exceed values for air and adamellite-derived waters by over an order of magnitude. These differences are ascribed to biological factors rather than to solution of carbonate minerals.

INTRODUCTION

The upland surface of the southern White Mountains is underlain by diverse lithologies, has been little affected by human activities, and is drained by a number of small streams, many of which can be related to single rock types. The region thus provides an opportunity to study modern denudation rates of contrasting materials under a reasonably consistent semiarid, subalpine climate. Current chemical erosion by streams was estimated by standard methods of gaging and water analysis. Plant litter collections, organic matter traps on the streams, and wet chemical analyses of plants allowed estimates of the biological component of chemical denudation, a potentially important aspect of the geochemical cycle. The presence of a radiometrically dated Tertiary basalt in the area permitted calculation of long-term erosion rates for comparison with modern values.

Location and physiography.—Situated east of the Sierra Nevada close to the Nevada border, the White Mountains extend northward from Westgard Pass to Montgomery Peak (north of fig. 1) with elevations along the mountain divide ranging from 2290 m at the pass to 4345 m at White Mountain Peak (fig. 1). The area investigated (fig. 2) spans approximately 80 sq km along the crest of the southern part of the range, east of Bishop, California. A gently undulating topographic surface slopes eastward and southward from Sheep Mountain, interrupted by peaks such as Blanco Mountain, County Line Hill, and Campito Mountain rising 150 m or more above the rolling terrain. The steep western escarpment of the range descends 2000 to 3000 m to the floor of Owens Valley at a gradient of 190 m per km. The eastern flank slopes much more gradually but is incised by a series of canyons as much

* Publication authorized by the Director, U.S. Geological Survey

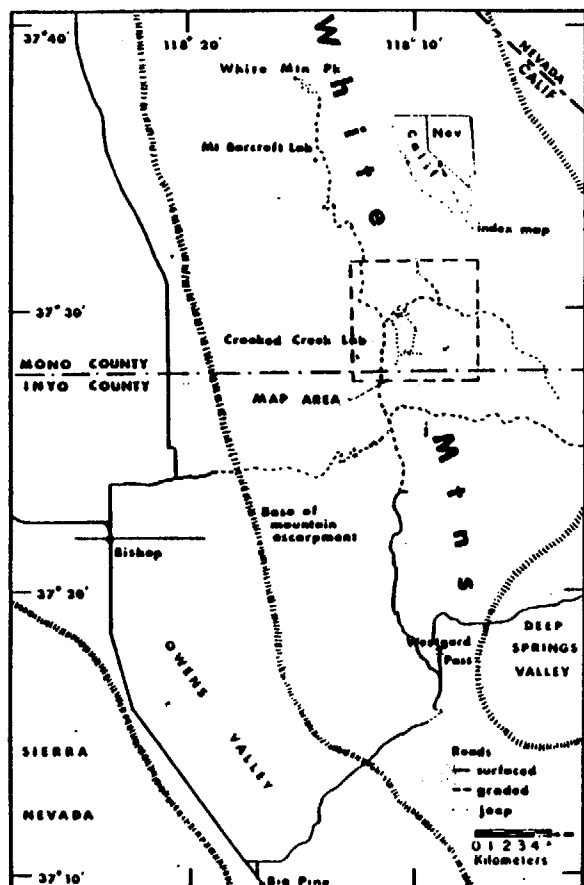


Fig. 1. Map of east-central California, showing location of the study area.

as 310 m deep which drain southeastward to Deep Springs Valley and eastward to Fish Lake Valley.

Climate.—The White Mountains lie in the rain shadow of the Sierra Nevada and are generally characterized by a cold, dry climate (BWk to BSk of Köppen notation). Climatic data for the Crooked Creek (3096 m) and Mt. Barcroft (3803 m) Laboratories of the White Mountain Research Station are given in table 1. Precipitation occurs largely in the form of snow and as intense summer storms, which are often quite localized. Powell (ms) reports 20 cm of rainfall in slightly more than 2 hours on Chiatovitch Creek north of White Mountain Peak, during a July storm. Data from five auxiliary weather stations maintained in the study area from June, 1966 to August, 1967 indicate that temperatures are about 3° to 6°C higher on the upland surface than at the Crooked Creek Laboratory, situated in a small valley. This information (see Marchand, ms, p. 16-25, for more complete discussion) also shows

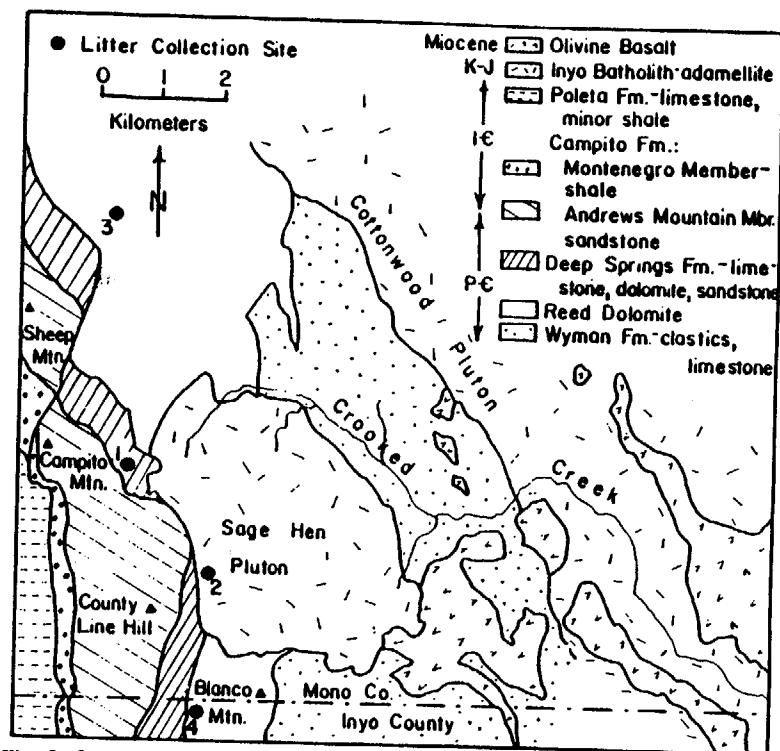


Fig. 2. Generalized geologic map of a portion of the study area, showing location of litter collection sites. Topographic relief is approximately 1000 m.

that although precipitation and relative humidity are slightly higher in the northern part and temperatures somewhat lower, present climatic gradients in the area investigated are not pronounced.

Vegetation.—The flora of the study area includes the Sagebrush Scrub and Bristlecone Pine Forest plant community types of Munz and Keck (1959, p. 11-18). Toward lower elevations the vegetation passes into Pinyon Juniper Woodland and at higher elevations into Alpine Fell Fields. Stands of bristlecone pine (*Pinus aristata*), limber pine (*Pinus flexilis*), and aspen (*Populus tremuloides*) make up a discontinuous tree canopy along the crest of the range below about 3800 m. A nearly continuous understory of shrubs is dominated by sagebrush (*Artemisia tridentata* and *A. arbuscula*) and to a lesser extent by rabbitbrush (*Chrysothamnus viscidiflorus*), mountain mahogany (*Cercocarpus ledifolius* and *C. intricatus*), creambush (*Holodiscus microphyllus*), mountain misery (*Chamaebatiaria millefolium*), and currant (*Ribes velutinum*). Beneath this two-story canopy of trees and sagebrush scrub is a nearly ubiquitous but sparse cover of grasses and herbaceous perennials, mostly low to the ground and often inconspicuous.

The distribution of plant species in the area is strongly controlled by geologic substrate (Mooney, St. Andre, and Wright, 1962). Edaphic

TABLE 1

Summary of climatic means and extremes from Crooked Creek (3096 m) and Mt. Barcroft (3803 m) Laboratories for the indicated periods

	Crooked Creek Lab*	Mt. Barcroft Lab**
Highest maximum temperature (°C)	24.4	22.2
Mean maximum temperature (°C)	7.8	1.9
Mean temperature (°C)	1.5	-2.6
Mean minimum temperature (°C)	-4.8	-6.8
Lowest minimum temperature (°C)	-29.4	-37.2
Mean diurnal difference (°C)	12.6	8.9
Largest diurnal difference (°C)	32.4	24.4
Smallest diurnal difference (°C)	0.6	1.1
Days 0°C or above per year	291.6	204.5
Mean 8 a.m. relative humidity (%)	50.7	55.1
Mean 8 a.m. barometer (mm Hg)	523.8	481.3†
Mean snowfall (cm/yr)	290.6	419.6†
Mean snow depth (cm)	11.9	18.3†
Highest snow depth (cm)	238.8	185.4
Mean snow water (cm/yr)	25.8	37.77
Mean rainfall (cm/yr)	6.9	5.36
Mean total precipitation (cm/yr)	32.7	43.13
Mean maximum wind (km/hr)	28.4	40.4
Maximum wind direction (%)		
north	5.8	12.7
northeast	11.0	5.6
east	3.5	5.4
southeast	7.5	5.0
south	6.5	7.9
southwest	26.2	17.0
west	29.6	39.9
northwest	10.3	9.8

* 1949-1965

** 1953-1965

† 1953-1962

restriction is evident in all stories of vegetational strata, from bristlecone and limber pine to the smallest perennials and grasses. The principal botanical discontinuities occur across boundaries between carbonate and noncarbonate rocks; dolomites and limestones support similar vegetation, as do, with a few notable exceptions, noncarbonate lithologies.

Geologic history.—Complex mixtures of sedimentary, igneous, and metamorphic rocks comprise the bedrock of the southern White Mountains (fig. 2). The oldest strata in the region are a slightly metamorphosed late Precambrian-early Cambrian succession of miogeosynclinal sandstone, shales, limestones, and dolomites (Nelson, 1962, 1966). The Precambrian Wyman Formation, consisting primarily of sandstone and shale with minor but conspicuous lenses of white limestone, is the oldest of this group. Overlying the Wyman is the Reed Dolomite, a massive and very pure carbonate rock. The Deep Springs Formation, comprised of alternating members of limestone or dolomite and clastic rocks (quartzitic sandstone and shale) overlies the Reed. The next younger formation

is the Campito, consisting of a lower quartzitic sandstone member, the Andrews Mountain, and an upper shale member, the Montenegro. The youngest stratigraphic unit of the group is the Poleta limestone, which also contains some shale.

This succession was tilted toward the west and then intruded by the Sage Hen Flat and Cottonwood adamellites during Jurassic and Cretaceous time (compare Krauskopf, 1968, for a summary of the involved plutonic history of the area). Early to middle Tertiary erosion resulted in the beveling of a regional surface of low relief, although monadnocks of Reed Dolomite and Andrews Mountain sandstone stood well above the erosion surface during its development. Parts of this surface were subsequently covered by extensive basaltic flows, K/Ar dated by Dalrymple (1963) at 10.8 m.y.

In terms of late Cenozoic structure, the White Mountains represent a tilted horst, with relative uplift on the west greatly predominating over the east. The range is bounded on the west by a steeply dipping fault zone having up to 3050 m of normal displacement. The eastern margin is faulted along the northwest side of Deep Springs Valley, but individual displacements here are in the order of 300 m or less. The basalts and underlying erosion surface are tilted and faulted from 1830 m at the northeast end of Deep Springs Valley to 3290 m at Bucks Peak, showing that uplift of the range occurred later than 10.8 m.y. ago. Bateman and Wahrhaftig (1966) have presented convincing evidence for regional uplift of east-central California and westernmost Nevada between about 9 and 3.5 m.y. and formation of Owens Valley and other collapse structures along the axis of upwarping during a period of downfaulting beginning about 2.5 m.y. ago. The major part of the Waucoba Lakebeds, exposed on the upthrown side of the frontal fault east of Big Pine, possess an exclusively Sierran mineralogy and apparently represent deposition in an early Pleistocene pluvial lake prior to the downfaulting of Owens Valley. The uppermost of several rhyolitic tuffs in the lakebeds has yielded a K/Ar age of 2.3 m.y. (Hay, 1966, p. 20). Coarse clastic debris from the White Mountains intertongues with and overlies the upper part of the lakebeds, which now dip westward at 5° to 7°. Bateman (1965) reports remnants of the Bishop Tuff, K/Ar dated at 700,000 yrs (Dalrymple, and others, 1965), locally preserved along the west flank of the range at altitudes about 600 m above its level in the Owens Valley. Displacements along the boundary fault, probably down-dropping the Owens Valley rather than uplifting the White Mountains, apparently were concentrated in the period between 2.3 and 0.7 m.y. ago but have continued in significant amounts to the present. Regional arching and uplift appears to have preceded faulting by at least 1 m.y. in this region.

Pleistocene glaciation along the eastern slope of the White Mountains incised cirques and U-shaped valleys into the upland surface and left morainal and outwash deposits along the valley walls and floors. According to D. R. Powell (1967, oral commun.), recognizable glacial advances

in the White Mountains appear to correlate with those of the eastern Sierra Nevada. The study area, however, bears no evidence of glaciation.

Present geomorphic processes.—Surficial processes in the White Mountains have been discussed in some detail by Kesseli and Beaty (1959), Beaty (ms), Powell (ms), and LaMarche (1968). Frost heaving, solifluction, altiplanation, nivation, and other periglacial phenomena become increasingly important toward higher elevations. Rillwash channels as much as 5 cm deep and debris accumulations behind trees, fallen limbs, bushes, and large boulders are especially common on the relatively bare slopes beneath pine forests. Talus slopes and stone stripes are frequent, particularly in the Campito and other sandstones or shales. Although eastward-draining canyons are gradually eroding headward into degraded remnants of the White Mountains erosion surface, fairly extensive parts of the surface are still undissected and often serve as local or temporary base levels for periglacial processes and slopewash. The net effect of this situation is the accumulation of colluvium (consisting of weathered and unweathered rock, mineral, and organic material) on gentle slopes and in topographic lows on these surfaces.

Loose particulate material and plant litter are removed largely during the major summer storms. Kesseli and Beaty (1959, p. 27-31) report that 60 percent of White Mountains floods occur in July or August. Winter floods, resulting from warm rain on snow cover, and spring floods, due to rapid snowmelt, are much less common and usually of lesser magnitude, according to these authors. In checking weather records back to 1872, they find an average of about one major flood per year for the range as a whole. Flood frequency at any given locality is about once in every 5 to 10 years. Episodes of high runoff result in the clearing of rock and plant debris that has accumulated temporarily on the slopes, especially if the storm follows a period of rainfall sufficient to saturate the surface soil. Consequently erosional processes in semiarid ranges such as this are extremely sporadic.

LONG-TERM RATES OF DENUDATION

Methods.—Most of the topographic surface in the area lies 50 m or more below the level of the Tertiary erosion surface. Approximate long-term rates of erosion can be estimated for the Cottonwood and Sage Hen Flat plutons using the average depths of erosion beneath the projected base of the radiometrically dated basalt. This method assumes that the erosion surface beneath the basalt had relatively low relief over the areas measured, that the basalts were never covered by younger deposits, and that erosion began immediately after their extrusion. Presently available evidence supports these assumptions, but assumptive errors would tend to increase the rates reported here. Four topographic profiles were constructed across parts of the Cottonwood adamellite and two across the Sage Hen Flat adamellite (fig. 3). For each profile, the base of the basalt was projected across the intervening distance, eroded cross-sectional area determined by planimetry, and the area divided by d.

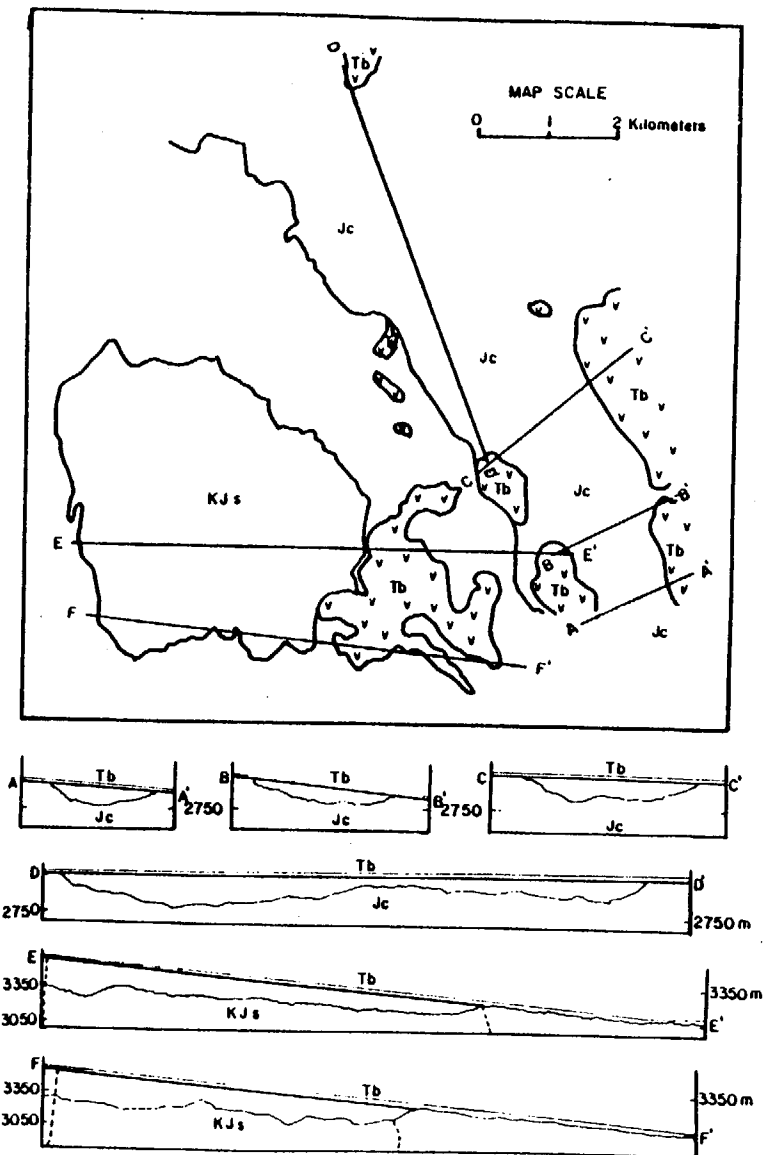


Fig. 3. Map and profile views showing location and characteristics of topographic profiles used in long-term denudation calculations. Horizontal and vertical scale of profiles is 1 cm = 442 m. KJs = Sage Hen Flat adamellite; Jc = Cottonwood adamellite; Tb = Tertiary basalt.

tance measured along the base of the basalt to determine an average lowering of the subvolcanic terrain. The values from each cross section were weighted according to length of profile to obtain overall mean depths of erosion for each pluton. The average thickness of basalt, taken

TABLE 2

Comparison of total and chemical erosion rates and aeolian deposition rates (cm/1000 yrs) for varying lithologies and areas. Chemical and aeolian rates are present-day values; total rates are averages for the last 10.8 m.y.

	Probable minimum	Most probable	Probable maximum
Total, Sage Hen Flat adamellite + basalt	1.7	2.0	2.4
Total, Cottonwood adamellite + basalt	1.1	1.6	2.0
Chemical, Cottonwood Basin (largely dolomite)	1.7	—	2.1
Chemical, Sage Hen Creek Basin (largely adamellite)	0.14	—	0.19
Aeolian deposition, study area average (see p. 127)	0.05	—	—

as 37 m, was then added to the amounts of lowering for the adamellite to obtain total erosional depths.

Results.—Total rates of erosion, calculated using means and extremes of both radiogenic age and depths of degradation to compute maximum, minimum, and most probable values, are listed at the top of table 2. Since there is a possibility that the basalt-stripped areas were topographic highs at the time of eruption, the "most probable" values may be somewhat low. Differences in rates between the two intrusives are not necessarily significant, because there is less control on the projected base of the basalt across the Sage Hen Flat pluton than across parts of the Cottonwood pluton, but the higher rates for the Sage Hen adamellite plus basalt may reflect absence of resistant basalt capping over part of Sage Hen Flat. From local topographic relationships (pl. 1), it is evident that the dolomite and basalt are more resistant to erosion than the adamellites. Consequently the long-term erosion rates for adamellite plus basalt are undoubtedly lower than those for adamellite alone, which may fall in the range of 3 to 4 cm per 1000 yrs. The total long-term Reed erosion rates cannot have exceeded those of the adamellite for any appreciable period of time; otherwise relief between the dolomite and the plutons would have diminished with time, a trend that is contradicted by geologic and topographic evidence.

Discussion.—Denudation rates presented here are lower by an order of magnitude than the average rates of LaMarche (ms), who measured the lowering of local areas in Reed Dolomite terrain with respect to the axes of bristlecone pine roots. LaMarche's mean rate of about 30 cm per 1000 years is consistent with some published data (Corbel, 1959; Schumm, 1963), but high denudation rates in many areas can be related to accelerated erosion caused by construction, lumbering, overgrazing, cultivation, pollution, and other human activities (Meade, 1969). At 30 cm per 1000 years the basalt-covered topography would have been stripped to its present level in less than 900,000 years, yet the basalt has been exposed to erosion for 10.8 m.y. Degradation was undoubtedly increased by regional arching and lowering of base level due to downfault-

PLATE 1



A. View south across Sage Hen Flat, showing Blanco Mountain, underlain by Reed Dolomite, extending above the Sage Hen Flat adamellite.



B. View east from Sage Hen Flat, showing resistant basalt capping less resistant metasediment and granitic intrusive rock.

ing along the range flanks, but these structural events were largely completed before 0.7 m.y. It appears unlikely that greatly accelerated erosion has occurred in this area during the past few thousand years, while the measured bristlecones were growing. Studies in the Sierra Nevada by

Helley (ms) and in the San Joaquin Valley by Janda and Croft (1967) suggest that major alluviations (and hence erosional events) occur during glacial rather than interglacial periods, even in unglaciated drainage basins. By analogy the past several thousand years, under postglacial conditions, should be characterized by comparatively moderate or low denudation rates. It should be noted, however, that LaMarche recorded values in the order of 9 cm per 1000 years on gently sloping interfluvies. Perhaps these lower rates are better equated with regional long-term figures than are the average bristlecone rates, which are strongly influenced by the preponderance of steep slopes in the present-day Reed Dolomite terrain. The long-term average denudation rates given here (1 to 3 cm per 1000 yrs) are probably less than those at present in the region, and because of basic assumptions the values of this paper should probably be regarded as somewhat low. Thus the discrepancy between the long-term rates and values based on the bristlecones could in fact be reconcilable. A clearer answer may emerge from core drilling in Deep Springs Valley sediments, where depth to potentially datable ash deposits (Marchand, 1970) would permit determination of sediment volumes deposited over a known period of time.

The erosion rates of this paper agree well with those of a number of local and regional studies. In compiling suspended load and reservoir siltation data for much of the Sierra Nevada, Janda (1969, oral commun.) finds maximum rates of 3.0 cm per 1000 years for the entire range. He reports highest values at intermediate elevations (1500-2500 m), progressively decreasing toward higher altitudes, although this relationship may hold only for ranges with similar distribution of precipitation, vegetation, and soils. Helley (ms) estimated present denudation in the Sierra Nevada foothills at 4.3 cm per 1000 years, based on complete suspended load, bedload, and dissolved load data, and showed that this figure was consistent with alluvial fan deposition during the past several hundred thousand years. Wahrhaftig and Curry (1966) reported extremely high erosion rates in the North Coast Ranges of California, but Brown and Ritter (1969) showed that the measured rates of 15 to 75 cm per 1000 years are anomalously high and restricted to this region.

PRESENT RATES OF CHEMICAL DENUDATION BY DISSOLVED LOAD

The drainage basins of Sage Hen Creek and of the South Fork of Cottonwood Creek above the Poison Creek confluence (fig. 4) were selected for studies of present chemical denudation because their streams have nearly continuous flow, were relatively accessible for sampling, and drain predominantly monolithologic terrain—Sage Hen Flat adamellite in the case of Sage Hen Creek and Reed Dolomite in the case of Cottonwood Creek. Pertinent information concerning the two basins is summarized in figure 4. Rates of removal by solution were calculated from discharge and water quality data obtained at temporary gaging stations (pls. 2 and 3) on each of the two streams.

BASIN OF COTTONWOOD CREEK, SOUTH FORK, ABOVE THE POISON CREEK CONFLUENCE

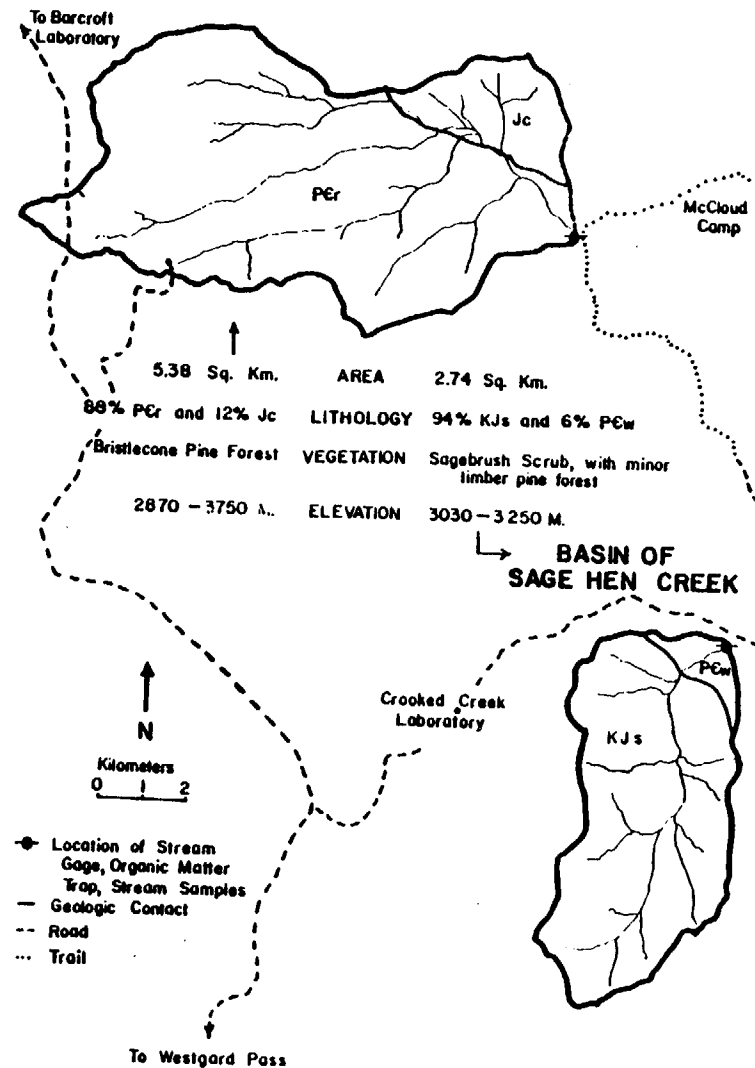
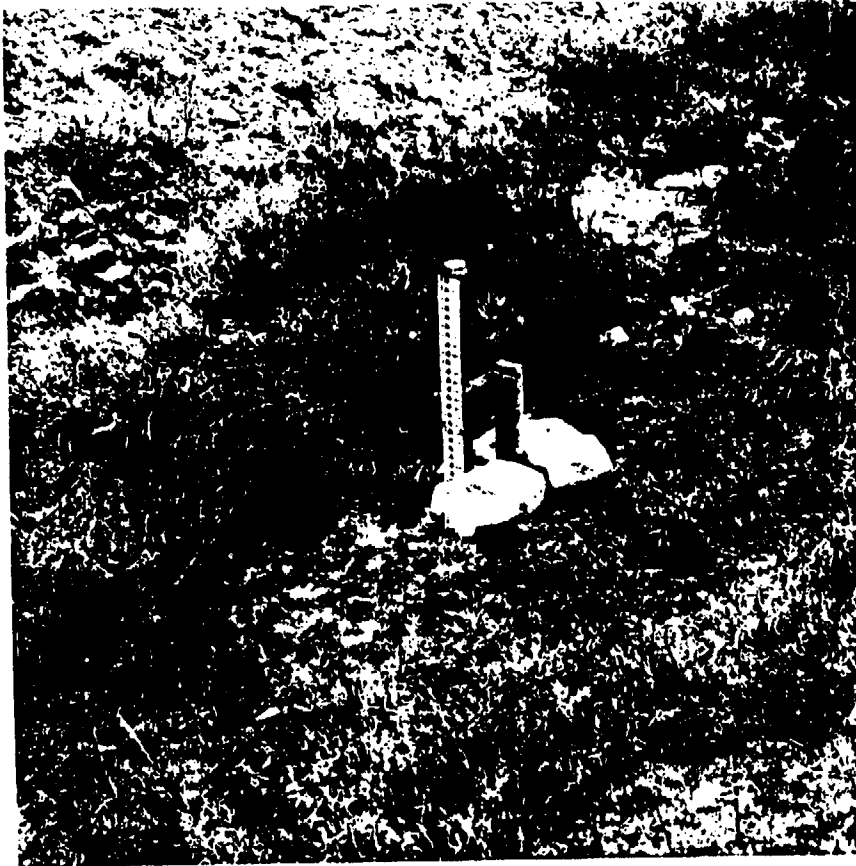


Fig. 4. Location and relevant data concerning two drainage basins where current chemical denudation was estimated. PCw = Wyman Formation; PCr = Reed Dolomite; Jc = Cottonwood adamellite; KJs = Sage Hen Flat adamellite.

Stream discharge.—For discharge estimates, a staff gage and flood crest gage were installed on Sage Hen Creek and a staff gage and water-level recorder were placed on Cottonwood Creek on August 15, 1966. Cross-sectional profiles of both channels were mapped. A Pygmy current meter was used to obtain discharge measurements throughout the

PLATE 2



Staff gage and flood crest gage at Sage Hen Creek gaging site.

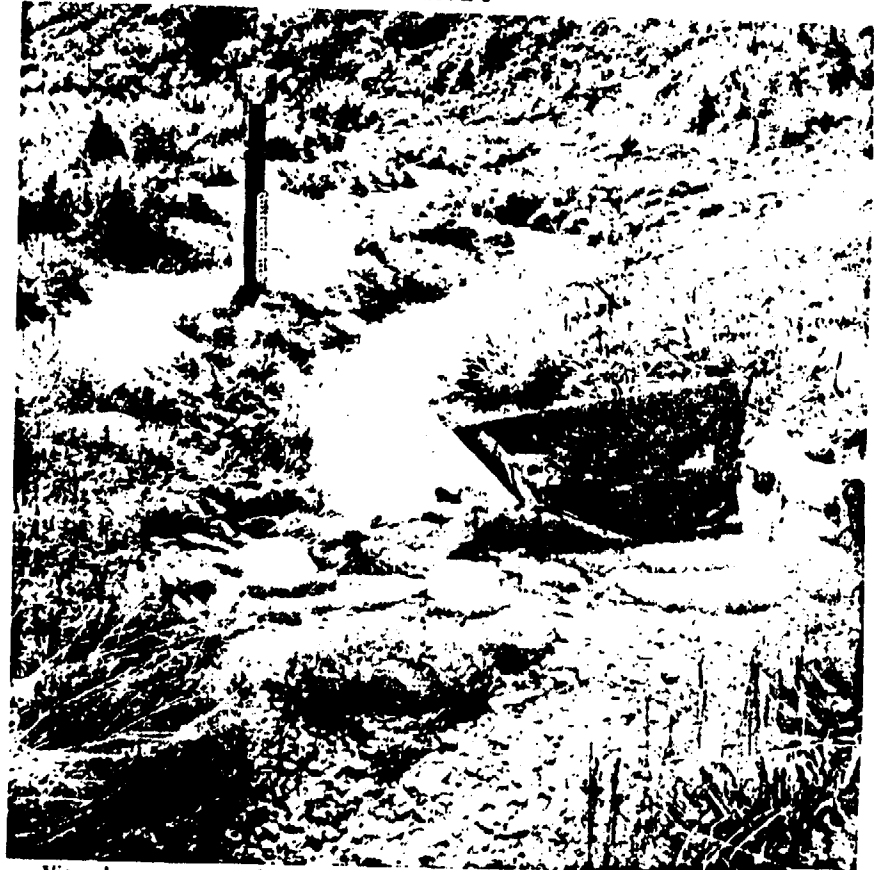
summer and fall of 1966 and at several intervals during the summer of 1967 until August 15. To determine discharge during floods, debris levels were projected to the staff gage (or read from the flood crest gage, in the case of the 1967 flood on Sage Hen Creek), flood slope was determined by plane table and alidade mapping of the debris line, and flood velocities were calculated from the Chezy-Manning equation,

$$v = \frac{1.49}{n} R^{2/3} s^{1/2}$$

where n is Manning roughness,¹ R is the hydraulic radius, and s the slope of the water surface. Flood channel areas were obtained by planimetry and flood discharge was then calculated from the area-velocity product,

¹John T. Limerinos of the Water Resources Division, U.S. Geological Survey, Menlo Park, Calif., estimated roughness coefficients for the equation from photographs of the channels.

PLATE 3



View downstream at Cottonwood Creek gaging site, showing organic matter trap (foreground) and staff gage and water-level recorder (left rear).

$$\begin{aligned} Q &= A_{\text{flood}} \times V_{\text{flood}} \\ &= 39.1 \text{ cfs for Sage Hen Creek, August 2, 1966} \\ &\quad \text{(used in establishing the rating curve)} \\ &= 30.6 \text{ cfs for Sage Hen Creek, July 13, 1967} \\ &= 134 \text{ cfs for Cottonwood Creek, July 13, 1967} \end{aligned}$$

Cottonwood Creek was found to have a steady flow of approximately 2.0 cfs throughout the year, the single major exception being the July 13, 1967 flood. Total yearly discharge was obtained by extrapolating the mean discharge throughout the period and adding the flood value to the total:

$$\begin{aligned} Q_{\text{total}} &= (2.0 \text{ cfs}) (364 \text{ days}) + (134 \text{ cfs}) (1 \text{ day}) \\ &= 862 \text{ cfs-days} \\ &= 2.11 \times 10^{12} \text{ gs/yr.} \end{aligned}$$

Since Sage Hen Creek showed considerable fluctuation in runoff, a stage-discharge curve (fig. 5) was utilized to estimate discharge from gage

SAGE HEN CREEK RATING CURVE

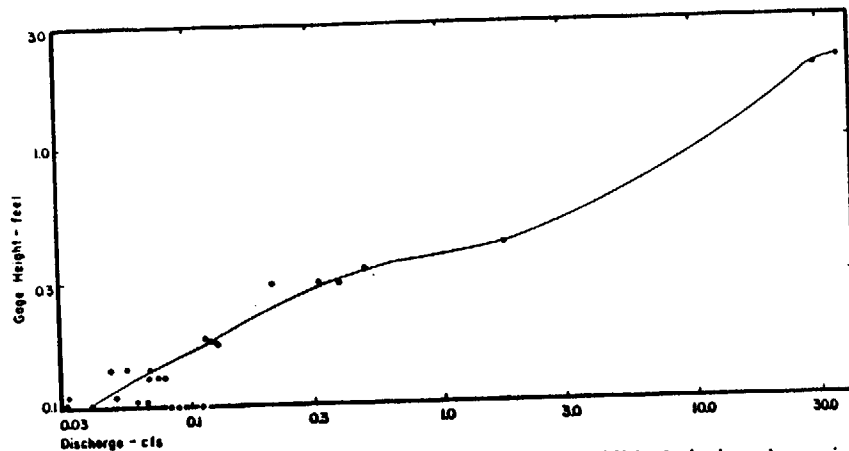


Fig. 5. Stage-discharge curve for Sage Hen Creek, established during the period August 1, 1966, to August 15, 1967.

height readings. A hydrograph (fig. 6), plotted from available gage height data for the year, was integrated to obtain total yearly discharge:

$$Q_{\text{total}} = 159 \text{ cfs-day} = 3.89 \times 10^{11} \text{ gs/yr}$$

Chemical composition of stream waters.—Water samples were collected during the summer and fall of 1966 and during the summer of

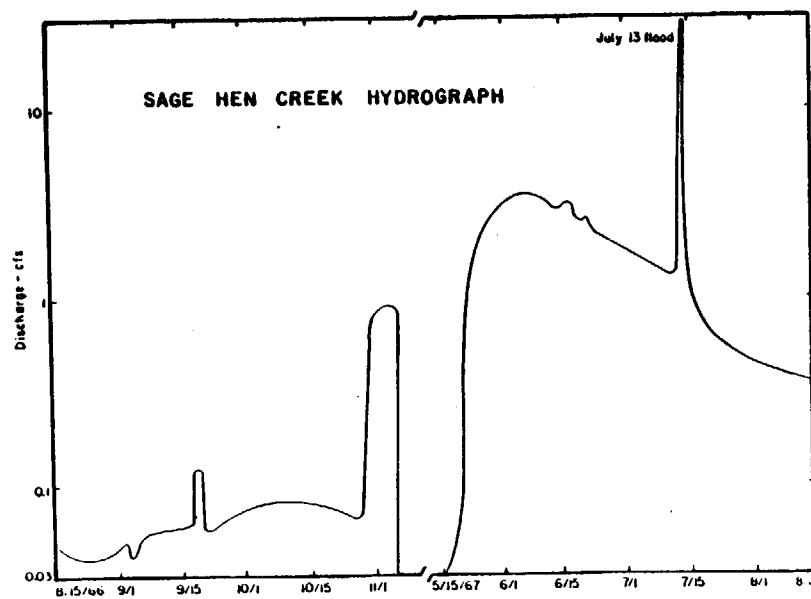


Fig. 6. Hydrograph for Sage Hen Creek for period August 15, 1966, to August 1, 1967.

1967. Samples cover all parts of the flow regimes except flood stage, which occurred only once during the sampling period. The procedures of Barnes (1964) were followed for field determination and calculation of pH and alkalinity. Water samples were filtered through 0.45-micron paper into air-tight polyethylene containers. A portion of each sample collected during the summer of 1967 was acidified to pH 2 to prevent precipitation of metals and was used for analysis of Al, Fe, and Mn. All analyses were conducted by the Menlo Park, California, laboratories of the Water Resources Division, U.S. Geological Survey. Aluminum values are markedly higher for the 1967 samples, reflecting either precipitation of Al in previous samples or solution of particles less than 0.45 microns in the acidified portions. There is relatively good agreement of Fe and Al values in the 1967 Sage Hen Creek samples with those reported for granitic waters in the Sierra Nevada, by Feth, Roberson, and Polzer (1964). pH, alkalinity, and temperature varied considerably, and Sage Hen Creek, a very shallow stream, displayed diurnal fluctuation in cation concentrations as well.

Chemical data for the two streams are given in table 3. Cottonwood Creek samples at the gaging site are characterized by higher concentrations of Ca, Mg, and $\text{HCO}_3 + \text{CO}_3$, and by lower Na, Cl, and SO_4 than

TABLE 3
Field and laboratory analytical data for Cottonwood and Sage Hen Creeks (all concentrations in ppm)

	Sage Hen Creek		Cottonwood Creek	
	Mean	Standard deviation	Mean	Standard deviation
Field pH	8.46	0.49	8.05	0.21
Spec. cond. (μmhos)	97**		256*	
K ⁺	1.03	0.09	0.78	0.02
Na ⁺	6.58	0.34	1.48	0.04
Ca ^{**}	14	2	26	1
Mg ^{**}	1.58	0.16	15.9	0.4
Ba ^{**}	0.5*		0.5	
Mn	0.009**		0.004*	
Fe	0.040**		0.031*	
Al	0.029**		0.044*	
SiO ₂	17		9.9	
B	0.015**	1	0.01*	1.9
Field HCO ₃ ⁻	58	9	162	3
NO ₃ ⁻	0.34**		0.3*	
SO ₄ ⁻	8.7	0.9	2.7	0.4
PO ₄	0.16**		0.08*	
Water temp (°C)	15.5	5.1	7.6	0.5
Cation epm	1.14		2.69	
Anion epm	1.18		2.73	
No. of analyses	8		11	

* based on 1 analysis

** based on 2 analyses

epm = equivalents per million

TABLE 4

Most probable and extreme values for partial pressures of carbon dioxide in stream waters and comparison with atmospheric $p\text{CO}_2$, taken as 2.3×10^{-4} atm.

		Sage Hen Creek	Cottonwood Creek
$p\text{CO}_{2(w)}$	Maximum	2.51×10^{-4}	2.14×10^{-3}
	Most probable	1.87×10^{-4}	1.24×10^{-3}
	Minimum	4.03×10^{-5}	7.29×10^{-4}
$p\text{CO}_{2(w)}$	Maximum	3.7	9.3
$p\text{CO}_{2(a)}$	Most probable	0.81	5.4
	Minimum	0.18	3.2

Sage Hen Creek, also sampled at the gaging site. The chemistry of natural waters in this area will be considered in some detail in a future publication. Barnes (1965) has investigated the geochemistry of Birch Creek, located just south of the area.

Partial pressures of carbon dioxide in the stream waters (table 4) were computed using the relationship:

$$p\text{CO}_2(\text{aq}) = \frac{(\text{H}^+)(\text{HCO}_3^-)}{K_1 K_{\text{CO}_2}}$$

where

$$K_1 = \frac{(\text{H}^+)(\text{HCO}_3^-)}{(\text{H}_2\text{CO}_3)}$$

and

$$K_{\text{CO}_2} = \frac{(\text{H}_2\text{CO}_3)}{p\text{CO}_2}$$

The values of Harned and Davis (1954, p. 2030) were used for K_1 , and a graphical solution was employed for determination of K_{CO_2} , using the data of Markam and Kobe (1941, p. 449). Calculated values for Sage Hen Creek are close to atmospheric CO_2 pressure, but Cottonwood Creek shows a most probable CO_2 partial pressure 5.4 times greater than the air, and similar computations for the headwater spring about a quarter of a mile upstream (not shown in table 4) range up to 22 times higher than the air. Waters related to the dolomite terrain thus have much higher carbon dioxide concentrations than the air or the adamellite-derived fluids. Solution of dolomite would tend to increase pH, yet the pH of Cottonwood Creek is actually lower than that of Sage Hen Creek. The explanation for the striking CO_2 contrast between the two groups of analyses must partially lie in the marked vegetational differences between the two lithologies: the adamellites are dominated by limber pine, sagebrush, and grasses, whereas bristlecone pine and a sparse coverage of certain perennial herbs are found on the dolomite terrain. Perhaps photosynthetic and metabolic rates differ

the two groups of plants. In any event it is apparent that local vegetational changes may play an important role in controlling the pH of ground water, even overriding the effects of pronounced lithologic contrasts, and hence in regulating rates of chemical degradation.

Adjustments for chemical denudation calculations.—The data above serve to emphasize the contention of Janda (1969) that large amounts of many of the chemical species usually included in computing rates of chemical denudation have in fact been contributed from the biosphere and atmosphere and do not reflect net chemical losses from the rock and soil. Following Janda, the values of table 3 were corrected in table 5 as follows: (1) concentrations in precipitation (average values for four rain and three snow samples collected between June 30, 1966, and June 30, 1967) were subtracted from concentrations in stream waters, (2) no mineral phases that could supply any appreciable amount of nitrogen occur in either the adamellite or dolomite, so NO_3 was eliminated from the chemical denudation totals, (3) no known phases that could supply Cl, S, or P occur in the dolomite, so their concentrations in Cottonwood Creek waters were assumed to represent the approximate levels of nonlithospheric contributions in the area and were therefore subtracted from the corresponding values for Sage Hen Creek, (4) no carbonate phases exist in the Sage Hen Flat pluton, so the alkalinity figures for Sage Hen Creek were also assumed to be nonlithospheric and were subtracted from those of Cottonwood Creek. Nonlithospheric anions cannot reach the stream waters without a corresponding input of cations, but due to the absence of any information regarding cation additions from the biosphere, this correction was omitted. For this reason the values reported here might be somewhat high, but since losses in solution via deep percolation to springs at lower elevations were also un-evaluated, the two effects should tend to cancel one another. Comparison of B and NO_3 between precipitation and stream water indicates that precipitation has not been greatly concentrated by evaporation.

Since water-quality figures during flood discharge were not known for either stream, two sets of rates were computed for each: values assuming constant dissolved load (probable maximum) and values assuming flood concentration equal to that of precipitation (probable minimum).

Results and discussion.—Denudation rates for individual species and total dissolved solids in each basin are summarized in the right-hand columns of both sides of table 5. When converted to numbers indicating average lowering of the land surface, calculations for Cottonwood Creek Basin (primarily underlain by dolomite) yield values of 1.7 to 2.1 cm per 1000 years and Sage Hen Creek Basin (almost entirely in adamellite) shows rates of 0.14 to 0.19 cm per 1000 years (table 2). These figures indicate that, in terms of chemical denudation by dissolved load, the dolomite terrain is presently being lowered more than ten times as rapidly as the adjacent adamellites. Since the Reed stands in positive relief against the adamellites (pl. 1), total rates of denudation for the dolomite must be

TABLE 5
Rates of chemical denudation by dissolved load transport

	Cottonwood Basin			Sage Hen Basin			
	Precipitation (ppm)	Chemical Denudation Rates (g/yr)		Sage Hen Creek (ppm)	Sage Hen Creek, corrected (ppm)	Chemical Denudation Rates (g/yr)	
		Cottonwood Creek (ppm)	Cottonwood Creek, corrected (ppm)			Conc = K	Conc = K
K	0.14	0.78	0.64	1.03	0.89	3.5×10^6	3.0×10^6
Na	0.34	1.48	1.14	6.58	6.24	2.4×10^6	2.1×10^6
Ca	0.36	26	25.6	14	13.6	5.3×10^6	4.6×10^6
Mg	0.9	15.9	15.8	1.58	1.49	5.8×10^6	5.0×10^6
Mn	0.003	0.004	0.001	0.009	0.006	2.3×10^6	2.0×10^6
Fe	0.014	0.031	0.017	0.040	0.026	1.0×10^6	8.8×10^5
Al	0.012	0.044	0.032	0.029	0.017	6.6×10^6	5.7×10^6
Si	0.051	4.6	4.55	7.95	7.9	3.1×10^6	2.7×10^6
B	0.01	0.01	—	0.015	0.005	1.9×10^6	1.7×10^6
Cl	0.4	0.5	—	1.25	0.75	2.9×10^6	2.5×10^6
HCO ₃ CO ₂	2.7	159	102	57	—	—	—
N ₂ O ₅	0.2	0.3	—	0.34	—	7.8×10^6	6.8×10^6
SO ₄ as S	0.02	0.90	—	2.9	2.00	3.1×10^6	2.7×10^6
PO ₄	0.00	0.08	—	0.16	0.08	1.93×10^6	1.11×10^6
TOTALS							
						3.15×10^6	2.69×10^6

the same as or less than those for the granitic terrain, and therefore mechanical erosion must be much greater for the latter. Observations by the author and by Kesseli and Beaty (1959) indicate that virtually all the detrital erosion in the White Mountains is accomplished by runoff and floods accompanying intense summer storms. Because of the extremely sporadic nature and variable intensities of such storms, reliable present values of the mechanical component of erosion would be difficult to evaluate by suspended load and bedload measurements. Present minimum rates of aeolian deposition in the White Mountains, based on dust trap and snow residue data from Marchand (1970), are in the order of 0.05 cm per 1000 years (table 2). Presumably aeolian erosion from the range crest occurs at a comparable or higher rate. Perhaps the best means of determining overall physical erosion rates in the region would lie in studying rates of detrital accumulation on alluvial fans and bajadas along the base of the range.

CHEMICAL DENUDATION BY UPTAKE AND LITTER EROSION

Lovering (1958, 1959) first raised the possibility that plants may remove significant amounts of some elements released by weathering, basing his arguments on ash analyses of certain accumulator plants and postulations as to possible amounts of removal. The following discussion presents a semiquantitative assessment of chemical degradation in the above two drainage basins by plant uptake and litter erosion and comparison with values for dissolved load transport. The results indicate that although plant extraction is apparently of little importance in terms of total amounts of chemical removal, it may be significant for certain elements, especially metals.

Methods.—To obtain data for removal rates by plants, chemical analyses were made of typical plant species, and organic matter carried by each stream was collected in traps over a 1-year period. Attempts to analyze the plant material in the traps proved unsuccessful due to appreciable contamination by silt and clay particles. As a check on litter erosion rates, amounts of litter fall were measured at each of three collection sites.

Chemical concentrations in vegetation.—For practical reasons, only a few of the hundreds of White Mountains plant species could be analyzed. Above-ground portions of sagebrush (*Artemisia arbuscula*), junegrass (*koeleria cristata*), and sandwort (*Arenaria kingii*), and twigs, needles, and cones of bristlecone pine (*Pinus aristata*) and limber pine (*Pinus flexilis*) were collected on both dolomite and adamellite. Above-ground portions of flax (*Linum perenne*) were obtained from dolomite terrain. These six species were chosen to represent vegetational groups as follows: *Pinus aristata* and *Pinus flexilis*—trees; *Artemisia arbuscula*—sagebrush and shrubs; *Koeleria cristata*—grasses; *Arenaria kingii*—noncarbonate-associated herbs; and *Linum perenne*—carbonate-associated herbs.

Collected organic matter was washed as free of sediment as possible, oven dried, and weighed. Additional weight caused by sediment particles was believed to be more than compensated for by losses of organic matter during accumulation and collection (around, under, or through the trap). Amounts of removal in the form of finely divided organic materials were not evaluated but could be important.

At Cottonwood Creek, an average rate of 47 g per day was calculated from daily collections during August, 1966. Discharge here remained essentially constant throughout the year, litter transport did not change appreciably, and the creek did not freeze during the winter. The daily rate of litter transport was therefore extrapolated for the year, with the exception of the July 13, 1967, flood. Unfortunately the Cottonwood Creek trap was washed out by this flood, so no direct measurement of organic matter transport was possible. The amount was estimated by multiplying the normal rate of accumulation by the ratio of flood discharge to normal discharge. The total yearly amount of organic matter transport was then calculated as follows:

$$\begin{aligned} \text{Litter/year} &= (\text{daily rate}) (364 \text{ days}) + \\ &\quad (\text{daily rate}) (Q_{\text{flood}}/Q_{\text{normal}}) (1 \text{ day}) \\ &= (47) (364) + (47) (134/2.0) (1) \\ &= 20,300 \text{ g.} \end{aligned}$$

At Sage Hen Creek the litter transport data are somewhat more complete. The trap held during the July, 1967, flood, and collections obtained throughout the year totalled 2,990 g. It was obvious, however, that part of the flood debris had escaped the trap, both over the top and around the sides, and so the total figure is a minimal value.

Rates of litter fall and potential litter erosion.—The amounts of litter fall at three relatively level sites of up to 230 sq m were measured over a 1-year period. Four sites (fig. 2), two in Sagebrush Scrub and two in Bristlecone Pine Forest community types, were originally selected, but heavy winter snows and uncleared roads made June collections impossible at site 3. Each site was cleared of debris on June 26, 1966, and plant litter from the same area, as marked by metal stakes, was hand picked on June 26, 1967, oven dried, and weighed. Litter fall data for sites 1, 2, and 4 and calculated values of yearly litter rates for each basin are given in table 7.

The rates based on total litter fall, 8.9×10^7 g per year and 2.0×10^7 g per year for Cottonwood Basin and Sage Hen Creek Basin, respectively, presume that all plant debris is eventually removed. That at least some litter remains and eventually decomposes is evidenced by the accumulation of plant debris and humus beneath trees and shrubs and the presence of from 0.5 to 2.3 percent organic carbon in ten analyzed soils from as many different lithologies. Decomposition rates are certainly not high in this dry, cool climate though, and it does not seem unreasonable to assume that at least 1 percent of the yearly litter fall is stripped from the slopes, especially in such steep terrain as occurs within the K Dolomite. Such an assumption would give minimum yearly

TABLE 7
Litter fall data, June 26, 1966 to June 26, 1967 and calculation of litter fall rates

Community type	Area of site (m ²)	Litter fall g/yr	Litter fall (g/yr) (g/m ² /yr)	Cottonwood Creek South Fork			Sage Hen Creek		
				Area of basin above gage (m ²)	% of community type in basin	Litter fall in basin (g/yr)	Area of basin above gage (m ²)	% of community type in basin	Litter fall in basin (g/yr)
Site 1 Sagebrush scrub	232	850	3.7	5.38 × 10 ⁶	11.7	3.87 × 10 ⁷	2.74 × 10 ⁶	9.8	4.83 × 10 ⁶
Site 2 Sagebrush scrub	37.2	320	mean = 6.15						2.0 × 10 ⁶
Site 4 Bristlecone pine forest	163	2931	8.6	5.38 × 10 ⁶	88.3	85.5 × 10 ⁷	2.74 × 10 ⁶	90.2	15.2 × 10 ⁶
Totals				5.38 × 10 ⁶	88.3	85.5 × 10 ⁷	2.74 × 10 ⁶	90.2	15.2 × 10 ⁶

litter erosion rates of 890,000 g for Cottonwood Basin and 200,000 g for Sage Hen Creek Basin, figures one to two orders of magnitude greater than those obtained by direct collection along the streams. The large discrepancy between the two sets of rates may lie in (1) inability of the organic matter traps to collect all transported plant material, (2) errors in assumptions used to obtain total organic matter transport (that is, flood transport not proportional to flood discharge or yearly extrapolations of daily rates not valid), (3) difficulty of obtaining representative yearly erosion rates from an area where sporadic flooding comprises a large proportion of the total discharge, and (4) erosion of yearly litter fall below the postulated 1 percent minimum or significant errors in litter collection.

Rates of biogeochemical removal.—The product of plant concentration and litter erosion rates gives an estimate of chemical denudation by this biogeochemical process for any given element. The figures of table 6 and measured litter fall and litter erosion values were used to compute maximum and minimum denudation rates (table 8). The maximum rates assume total removal of litter and are at least an order of magnitude too high; the minima are definitely too low, due to trap losses. No "most probable" values can be assigned from the present data.

Summary and comparison.—Total chemical denudation by dissolved load exceeds the maximum possible litter erosion component and is about four orders of magnitude greater than the minimum contribution of litter erosion. The relative importance of dissolved load is greater in Cottonwood Basin as would be expected from its dominantly carbonate lithology.

Denudation rates of nine elements are compared for both mechanisms in figure 7. The huge spread between maximum and minimum litter denudation values creates considerable problems in interpretation, but several trends are apparent. The effect of litter erosion in accomplishing chemical removal increases relative to dissolved load according to

TABLE 8
Rates of chemical denudation by plant uptake and litter erosion in gs/yr for total area of each basin

	Sage Hen Basin		Cottonwood Basin	
	Max*	Min**	Max*	Min**
Si	3,600	0.85	28,000	6.6
Al	240,000	36	450,000	104
Fe	7,200	1.1	66,000	15
Mn	980	0.15	5,300	1.2
Mg	42,000	6.3	190,000	42
Ca	176,000	26	810,000	180
Na	1,410	0.22	7,500	1.4
K	66,000	10	330,000	74
P	10,780	1.6	49,000	11
Total	5.48×10^7	82.2	1.94×10^8	4.35×10^7

* based on rate of litter fall
** based on measured rate of litter transport

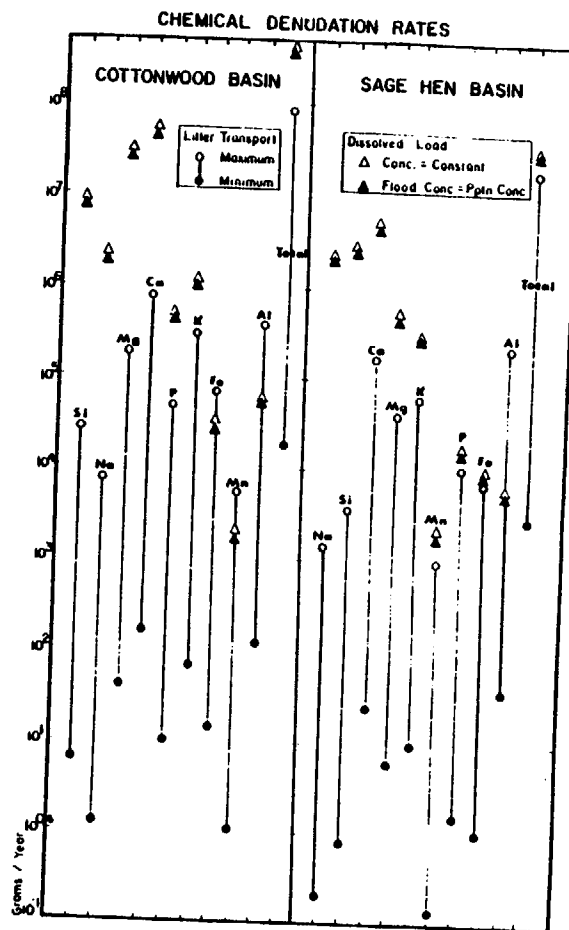


Fig. 7. Comparison of present chemical denudation rates by litter transport and dissolved load for the two stream basins studied.

the general sequence: $Na < Si < Mg \approx Ca < K \approx P < Mn < Fe < Al$. For Na, Si, Mg, and Ca, the effects of litter erosion are insignificant. Potassium and P are largely removed in solution, but litter erosion may have some importance. Plant uptake is evidently fairly important in the case of Mn and Fe, and litter erosion may even exceed dissolved load in removing Al from the bedrock and soil. The high Al content of some plants, however, may be due to external contamination from adhering dust, so comparisons of Al removal should be viewed with some caution.

The ratio of dissolved load to litter erosion for any given element will probably vary considerably from one region to another. Steep slopes promote heavy runoff and litter erosion, whereas gentle slopes favor water percolation through the soil and resultant increases in dissolved load. Humid climates produce greater biomasses, which would tend to

give lower ratios, but they also accelerate chemical solution of bedrock. Woody plants and evergreens generally contain less inorganic solids than do annuals, perennials, grasses, and deciduous plants. Dissolved load would be of greatest importance in areas of highly or moderately soluble lithologies. High soil pH would tend to favor losses of metals by plant extraction rather than leaching. Plant uptake and litter erosion should, therefore, be most important in steep, rugged terrain underlain by relatively insoluble materials, having a moderate to high soil pH, and supporting dense herbaceous or deciduous vegetation. It is doubtful if this biogeochemical process would ever be significant for Na, Ca, Mg, or Si, except in areas dominated by plants that accumulate these elements in extraordinarily large quantities. Appreciable amounts of K, P, and especially metals, however, may be removed from rock by organic processes coupled with litter erosion. Improved organic matter traps, gaging records, and analytical data should lead to much more accurate estimates of vegetational extraction as a chemical denudation component.

ACKNOWLEDGMENTS

The cooperation of Dr. Nello Pace and the Staff of the White Mountain Research Station in providing lodging, field vehicles, and logistical assistance is gratefully acknowledged. Jack Major and Richard S. Mitchell aided in plant identification; the White Mountains herbarium, established at Crooked Creek Laboratory by Mitchell and Robert S. Lloyd, was of considerable help in this regard. Edward J. Helley aided in installing stream gages and in measuring discharge. Ashing and chemical analysis of plant residues were performed by Barbara Lewis and James L. Clayton. The manuscript has benefited in its various stages of preparation from the critical reading of E. J. Helley, R. J. Janda, Clyde Wahrhaftig, R. L. Hay, Peter W. Birkeland, John D. Hem, and F. J. Kleinhampl. Financial support was provided by the U.S. Geological Survey, a Penrose bequest of the Geological Society of America, and by the Department of Geology and Geophysics, University of California at Berkeley, at which institution the research took place.

REFERENCES

- Barnes, Ivan, 1964, Field measurement of alkalinity and pH: U.S. Geol. Survey Water-Supply Paper 1535-H, 17 p.
 Bateman, P. C., 1965, Geology and tungsten mineralization of the Bishop District, California: U.S. Geol. Survey Prof. Paper 470, 208 p.
 Bateman, P. C., and Wahrhaftig, Clyde, 1966, Geology of the Sierra Nevada, in Bailey, E. H., ed., Geology of northern California: California Div. Mines and Geology Bull. 190, p. 107-172.
 Beaty, C. B., ms, 1960, Gradational processes in the White Mountains of California and Nevada: Ph. D. dissert. geography, Univ. of California, Berkeley.
 Brown, W. M., and Ritter, J. R., 1969, Phenomenal erosion rates in the Eel River Basin, California [abs.]: Geol. Soc. America Abs. 1969, Pt. 7, p. 21-22.
 Corbel, Jean, 1959, Vitesse de l'érosion: Zeitschr. Geomorphologie, v. 3, p. 1-28.
 Dalrymple, C. B., 1963, Potassium-argon dates of some Cenozoic volcanic rocks of the Sierra Nevada, California: Geol. Soc. America Bull., v. 74, p. 379-390.
 Dalrymple, C. B., Cox, Allan, and Doell, R. R., 1965, Potassium-argon age and paleomagnetism of the Bishop Tuff, California: Geol. Soc. America Bull., v. 76, p. 667-674.

- Feth, J. H., Roberson, C. E., and Polzer, W. L., 1964, Sources of mineral constituents in water from granitic rocks, Sierra Nevada, California and Nevada: U.S. Geol. Survey Water-Supply Paper 1535-I, 70 p.
 Harned, H. S., and Davis, Raymond, Jr., 1943, The ionization constant of carbonic acid in water and the solubility of carbon dioxide in water and aqueous salt solutions from 0°C to 50°C: Am. Chem. Soc. Jour., v. 65, p. 2030-2037.
 Hay, R. L., 1966, Zeolites and zeolitic reactions in sedimentary rocks: Geol. Soc. America Spec. Paper 85, 130 p.
 Helley, ms, 1966, Sediment transport in the Chowchilla River basin: Mariposa, Madera, and Merced Counties, California: Ph. D. dissert. geology, Univ. of California, Berkeley, 153 p.
 Janda, R. J., 1969, Significance of chemical denudation and chemical weathering in the erosion of crystalline silicate rocks in temperate regions [abs.]: Geol. Soc. America Abs. 1969, Pt. 7, p. 115.
 Janda, R. J., and Croft, M. G., 1967, The stratigraphic significance of a sequence of noncalic brown soils formed on the Quaternary alluvium of the northeastern San Joaquin Valley, California in Morrison, R. B., and Wright, H. E., eds., Quaternary Soils: Internat. Assoc. Quaternary Research Cong., 7th, Reno, Nevada, Proc., v. 9, p. 158-190.
 Johnson, C. M., and Ulrich, Albert, 1959, Analytical methods for use in plant analyses: Calif. Agr. Expt. Sta. Bull. 766, Pt. 2, p. 26-77.
 Jones, L. H., and Thurman, D. A., 1957, The determination of aluminum in soil, ash, and plant materials using Eriochrome Cyanine R. A.: Plant and Soil, v. 9, no. 2, p. 131-142.
 Kesseli, J. E., and Beaty, C. B., 1959, Desert flood conditions in the White Mountains of California and Nevada: U.S. Army Quartermaster Corps Tech. Rept. EP-108, 107 p.
 Krauskopf, K. B., 1968, A tale of ten plutons: Geol. Soc. America Bull., v. 79, p. 1-18.
 LaMarche, V. C., Jr., 1968, Rates of slope degradation as determined from botanical evidence, White Mountains, California: U.S. Geol. Survey Prof. Paper 352-I, p. 341-377.
 Lovering, T. S., 1958, Accumulator plants and rock weathering: Science, v. 128, no. 3321, p. 416-417.
 ——— 1959, Significance of accumulator plants in rock weathering: Geol. Soc. America Bull., v. 70, p. 781-800.
 Marchand, D. E., ms, 1968, Chemical weathering, soil formation, and geobotanical correlations in a portion of the White Mountains, Mono and Inyo Counties, California: Ph. D. dissert. geology, Univ. of California, Berkeley, 376 p.
 ——— 1970, Soil contamination in the White Mountains, eastern California: Geol. Soc. America Bull., v. 81, p. 2497-2506.
 Markam, A. A., and Kobe, K. A., 1941, The solubility of carbon dioxide and nitrous oxide in aqueous salt solutions: Am. Chem. Soc. Jour., v. 63, p. 449.
 Meade, R. H., 1969, Errors in using modern stream-load data to estimate natural rates of denudation: Geol. Soc. America Bull., v. 80, p. 1265-1274.
 Mooney, H. A., St. Andre, G. and Wright R. D., 1962, Alpine and subalpine vegetation patterns in the White Mountains of California: Am. Midland Naturalist, v. 68, p. 257-273.
 Munz, P. A., and Keck, D. D., 1959, A California flora: Berkeley, Univ. of California Press, 1681 p.
 Nelson, C. A., 1962, Lower Cambrian-Precambrian succession, White-Inyo Mountains, California: Geol. Soc. America Bull., v. 73, p. 139-144.
 ——— 1966, Geologic map of the Blanco Mountain quadrangle, Inyo and Mono Counties, California: U.S. Geol. Survey Map GQ-529.
 Powell, D. R., ms, 1963, The physical geography of the White Mountains, California-Nevada: M.A. thesis geography, Univ. of California, Berkeley.
 Schumm, S. A., 1963, Disparity between present rates of orogeny and denudation: U.S. Geol. Survey Prof. Paper 454-H, 13 p.
 Wahrhaftig, Clyde, and Curry, R. R., 1966, Geologic implications of sediment discharge records from the North Coast Ranges, California: California Univ., Berkeley, Assembly Comm. Nat. Resources, Planning and Public Works (Subcomm. on Forest Practices and Watershed Management), Transcripts of Proc.
 Woolley, J. T., and Johnson, C. M., 1957, Silicon determination in ashed plant material: Agr. and Food Chemicals, v. 5, no. 11, p. 872.

LANDSCAPE INHERITANCE AND THE PEDIMENT PROBLEM IN THE MOJAVE DESERT OF SOUTHERN CALIFORNIA

THEODORE M. OBERLANDER

Department of Geography, University of California,
Berkeley, California 94720

ABSTRACT. Currently there appears to be no expansion of granitic pediments in the Mojave Desert due to stabilization of rock slopes under the existing climate. The presence of early Pliocene volcanics on the higher portions of both major and minor pediments graded to existing base levels indicates those erosional surfaces to be inherited features, formed in their entirety prior to the establishment of full desert conditions in the Mojave region. During the late Pliocene and Quaternary the Mojave pediments have been altered primarily by the stripping of a weathered mantle inherited from the preceding semiarid morphogenetic system. Fragments of this mantle are preserved under Tertiary volcanics widely distributed throughout the region. Active pedimentation in the Tertiary landscape seems to have been predicated upon "denudational equilibrium" in which hillslope erosion was in balance with regolith renewal by rapid chemical breakdown of granitic rock along the subsurface weathering front. Relationships at piedmont angles in the present stripped landscape require parallel rectilinear back-wearing (rather than downwearing) of soil-covered slopes during most active landscape morphogenesis. Tertiary weathering profiles and landscape evolution in the Mojave region appear similar to those of non-desert areas in which pediments appear to be expanding at present. Pedimentation by slope retreat in a soil-covered landscape can be explained in terms of a combination of findings previously contributed by Schumm (1956, 1962, 1966), Ruxton and Berry (1961), and Emmett (1970).

INTRODUCTION

The results of recent morphometric analyses of Mojave Desert pediment landscapes (Cooke, 1970; Cooke and Reeves, 1972) are illustrative of the degree to which the most fundamental questions related to desert pediments remain unresolved. Cooke has advanced several good reasons for the unproductiveness of past research on pediments. To these I venture to add one more of a quite different nature, which this paper will attempt to substantiate: namely, that in the Mojave Desert region, at least, it is futile to attack the pediment problem through analysis of contemporary process/form associations because the classic pediment landscapes in this region developed under an altogether different morphogenetic regime than that dominant in the area at present. It appears that pediments are still expanding in crystalline rock in the southwestern United States but not in true desert landscapes and not in the manner suggested by the majority of American writers on the subject.

THE PEDIMENT PROBLEM

The "pediment problem" that has occupied the attention of so many distinguished American geomorphologists proceeds from the difficulty of accounting for the conspicuous ramp-like erosion surfaces that truncate resistant rock in the arid regions of the southwestern United States and that terminate so abruptly against steep mountain walls and relief forms of the "inselberg" type. The fact that bold relief forms are developed in bedrock that differs in no apparent way from that exposed on adjacent erosionally subdued pediments is the crux of the pediment problem. The

origin of geometrically similar erosion surfaces that bevel relatively erodible materials adjacent to resistant relief-forming outcrops has seldom been regarded as an enigma. However, surfaces of the latter type, which were discussed by Gilbert in 1877 (p. 120-126) in his discussion of "planation," have also come to be known as "pediments" (for example, Denny, 1967; Twidale, 1967; Cooke and Warren, 1973) despite warnings against the tendency (Howard, 1942; Tator, 1952; Birot and Dresch, 1966). Planation surfaces bordering uplands composed of more resistant rock (*peripeditment* of Howard, *glacis* of Birot and Dresch) are commonly capped by gravels derived from rocks other than those truncated, are clearly localized by outcrop pattern, and (except where peripheral to a horizontal cap rock) have never been imagined as expanding headward through time. These characteristics are all in marked contradistinction to peripheral erosion surfaces that are cut *into* the rocks of the upland itself. In the following, the term *pediment* is used exclusively in reference to the more problematical form—the ramp-like erosion surface cutting the same resistant rock that forms the adjacent upland.

THE PEDIMENT LANDSCAPE

Erosional pediments abutting on rocky inselbergs, escarpments, and mountain walls are particularly characteristic of the granitic terranes of southern Arizona and the Mojave Desert of southern California, extending also into the Sonoran Desert in Mexico. According to the most recent summary of the literature on pediments in the southwestern United States (Hadley, 1967), the preponderant opinion is that pediments truncating hard rock have originated as a concomitant of the backwearing of escarpments and serve as slopes of transportation for the fine products of weathering derived from the positive forms rising above them. Where granitic rock is involved, there is an abrupt change of slope, the "pediment angle" (Ruxton, 1958), between the pediment, which rarely attains a slope in excess of 5 degrees, and the steeper forms rising above it at angles generally exceeding 20 degrees. The steep slopes are in most cases mantled with boulders, whereas the pediment surface is veneered with coarse sand occasionally interrupted by exposures of bedrock. Frequently granitic pediment surfaces are studded with rocky tors or are dissected by washes cut into decomposed bedrock or opened along joints in sounder material.

It has been noted by many investigators that the reduction of granitic boulders to a certain minimum size (approx 30 cm, or 1 ft, diam) is followed by their direct breakdown into grus. The conspicuous slope break between pediments and surmounting residual masses has been attributed to the resulting bimodal size distribution of granitic debris: the steep boulder slopes above pediments being regarded as the repose slopes for blocks loosened by weathering into joints (for example, Gilluly, 1937), and the pediment being the minimum slope permitting evacuation of the grus resulting from weathering in the boulder zone. Bryan (1923) and Davis (1938) pointed out that weathering of most non-granitic rocks pro-

duces fragments having a continuous gradation of sizes; as a consequence pediments developed on such rocks commonly merge with mountain front slopes by way of a smooth concavity, with no abrupt slope break evident. The association of pediments with granitic rocks has generally been stressed (Davis, 1938; Gilluly, 1937; Tuan, 1959; Birot and Dresch, 1966) and attributed to the distinctive bimodal size grading of granitic weathering products. This suggests that the presence of a well-defined piedmont angle is critical to identification of the pediment landform. A recent analytical treatment of pediment systems (Cooke and Warren, 1973, p. 188-215) contains no suggestion that existing pediment forms may not be the product of processes presently observable in desert regions.

THE PEDIMENT PROBLEM TODAY

Recent quantitative studies have cast doubt upon certain of the above assumptions. Melton (1965) established that the angles of boulder slopes are not clearly related to boulder size, refuting Bryan's concept of the "boulder controlled" slope, and morphometric analyses by Mamerickx (1964), Cooke (1970), and Cooke and Reeves (1972) have indicated that pediment slope cannot be correlated with pediment length, tributary area, rock type, or particle size, which suggests that the function of existing pediments as slopes graded for transportation is not as straightforward as some have supposed. On the basis of denudation rates, the evidence of paleosols, and current weathering tendencies the present author has attempted to show that the backwearing of slopes required to produce pediments is not occurring at present in granitic terranes in the Mojave Desert, where the major landscape features appear to be relict from pre-Quaternary non-desert morphogenetic regimes (Oberlander, 1972).

THE PROBLEM IN ITS GEOGRAPHICAL SETTING

The following interpretation of Mojave Desert pediments presents further evidence suggesting that the origin of these erosional forms is not to be sought in studies of the existing morphogenetic regime but through reconstruction of the Tertiary history of the region. The evidence is derived not only from examination of the pediments themselves but from associated landforms and surficial deposits suggestive of the environment in which the pediments were developed.

The conclusions offered here are an application of previous findings related to Tertiary weathering profiles in the Mojave Desert (Oberlander, 1972). The reader is referred to the latter for the details summarized with little substantiation in the first portion of the present paper. The work as a whole is based upon examination of granitic landforms in various portions of the Mojave Desert over a period of several years, with particular concentration upon the area extending from Victorville to Dale Lake (in the maximum rain shadow of the San Bernardino Mountains) and between Baker and Amboy in the central portion of the desert (fig. 1). The annual precipitation in these areas is generally less than 100 mm (4 in.), the majority occurring between November and April as a result

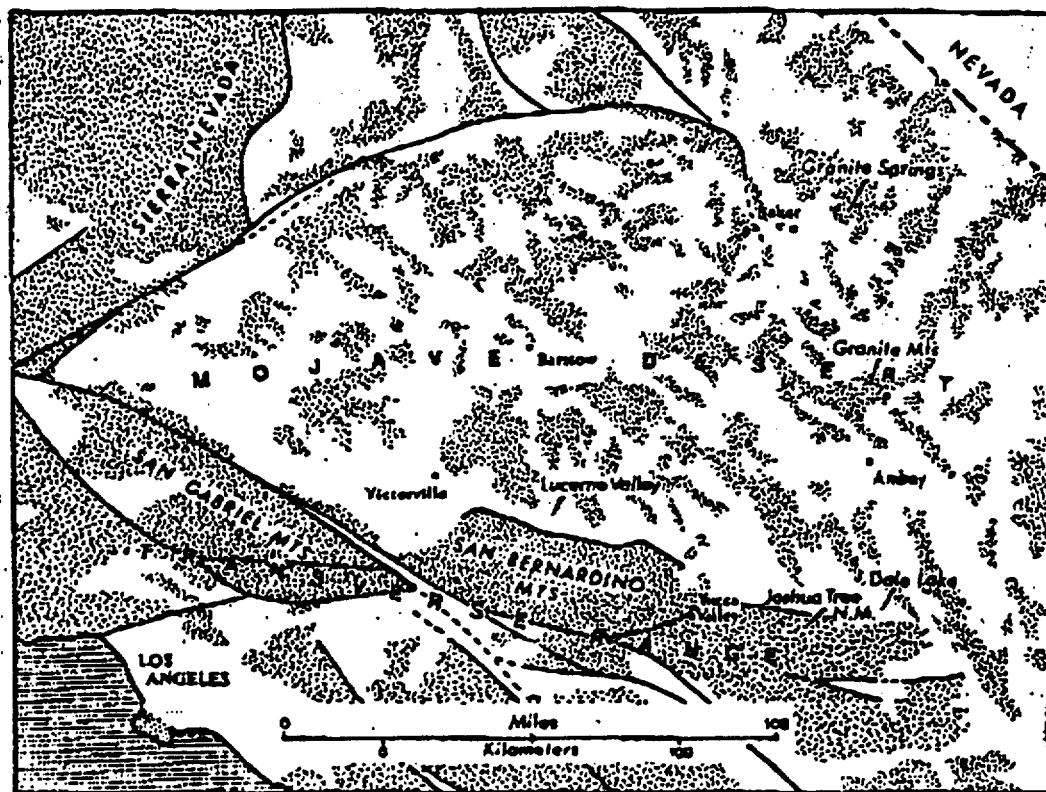


Fig. 1. Mojave Desert area and adjacent locations referenced in text. Lines indicate major faults. Patterned areas represent eroding uplands and peripheral pediments. Unpatterned areas represent Quaternary alluvium.

of frontal activity. The characteristic vegetation is creosote bush (*Larrea divaricata*) and *Yucca schidigera*, joined at higher elevations by *Yucca brevifolia*, with isolated pinyon pine and juniper encountered above 1100 m (3500 ft) at points of runoff concentration from bare rock slopes. The scenery within the areas studied is diverse, the southern region being dominated by extensive pediments peripheral to large and small granitic masses, while the central desert area includes several broad, almost featureless granitic domes (such as Cima Dome) having diameters of 3 to 8 km, as well as significant granitic highland masses bordered by pediments exposing bedrock a kilometer or more beyond the mountain front. The dominant granitic rock is medium-grained equigranular quartz monzonite containing 2 to 7 percent biotite and equal proportions of plagioclase and potassic feldspar. Granite, granodiorite, gneiss, and meta-volcanic rocks are local constituents of the pediment-inselberg landscapes of the region.

GENERAL CONSIDERATIONS

Before considering the specific evidence bearing upon the origin of the Mojave pediments two facts should be noted:

1. Botanical indications (Axelrod, 1958) and stratigraphic evidence related to the time of uplift of the Transverse Ranges (Richmond, 1960) both suggest that the rain shadow accounting for the Mojave Desert was not fully developed until late Pleistocene time. Axelrod's interpretation

of the palynological record has been disputed insofar as it ignores the possible-existence of local pockets of aridity prior to this time — a point of great importance in the evolution of the Mojave Desert flora — but his conclusion that aridity became general over the region this recently has not been argued (Johnson, 1968). Assuming (generously) that the present arid conditions became prevalent about 6 m.y. ago and that pedimentation by slope backwearing ensued, the minimum rate of slope retreat in bedrock necessary to produce pediments as little as 1500 m (5000 ft) in length would be 254 mm (10 in.)/1000 yrs. ★

2. The presence of patination ("desert varnish") and case hardening over boulders and massive rock outcrops on residuals rising above pediments suggests that retreat of such surfaces is exceedingly slow at present. Relations at the sites of indurated radiometrically-dated wood rat (*Neotoma*) middens in the Lucerne Valley area and Joshua Tree National Monument indicate no obvious retreat of the quartz monzonite faces that have enclosed them over the past 10,000 yrs. Beyond the Mojave Desert proper, there has been no measurable wearing back of the granitic outcrops in the climatically and morphologically similar Alabama Hills of the Owens Valley region in approximately 50,000 yrs, since the Tahoe-age glacial outwash of Lone Pine Creek accumulated against them. North of the San Bernardino Mountains basalts having radiometric ages exceeding 8 m.y. lie within 40 m of existing low elevation piedmont angles (Oberlander, 1972). Depths of removal of quartz monzonite beneath radiometrically dated basalt in the adjacent White Mountains indicate rates of erosion ranging between 10 and 30 mm/1000 yrs over the past 10.8 m.y. (Marchand, 1971). Removal of well-decayed quartz monzonite and granodiorite from beneath basalt dated at 8.9 ± 0.9 m.y. in the Lucerne Valley area of the western Mojave Desert (Oberlander, 1972) provides a maximum erosion rate of approximately 8 mm/1000 yrs. 47
5 mm/1000 yr
71 m / 8.9 m

Adherence to the belief that the Mojave pediments are a product of backwearing of boulder-clad slopes under the existing morphogenetic regime (for example, Warnke, 1969) requires one to find some means of reconciling the denudation rate thereby required with the preceding evidence of slow contemporary modification of exposed bedrock surfaces. Unless the length of the arid period has been underestimated by an order of magnitude, it must be admitted that the Mojave pediments are not primarily a product of arid morphogenesis. ★

THE TERTIARY LANDSCAPE

Although Quaternary erosion clearly has produced the existing topography in terranes composed of less consolidated materials, both direct and indirect evidence suggests that the granitic pediments of the Mojave region are indeed relict forms inherited from prior non-desert landscapes. Such landscapes were still in existence in the present desert region some 8 to 10 m.y. ago. Their remnants, locally affected by both vertical and horizontal tectonic displacements, are widely distributed in the Mojave Desert and can be recognized through their distinctive

weathering profiles, which are preserved under basaltic lavas having radiometric ages in excess of 8 m.y. Details relating to key sites, the nature of the ancient weathering profiles, and their significance in the development of existing boulder slopes, have been published previously (Oberlander, 1972). The picture that can be assembled from investigation of all accessible sub-volcanic exposures in the Mojave Desert west of Baker and south of Barstow is one of a strongly weathered landscape blanketed by an occasionally brick-red (5YR 4/4 to 2.5YR 3/6-4/6) argillaceous soil locally containing either dense clay pans or massive calcrete crusts (these also rubified and thus easily distinguished from Pleistocene developments).

This ancient landscape included both cut and fill surfaces of considerable extent, surmounted by steep-sided hills that appear to have maintained a soil cover. The steep phase of the soil is preserved in a few sub-volcanic exposures, and its former existence is suggested indirectly by the convexo-concave nature of certain existing boulder slopes, as well as by projection of truncated soil remnants preserved on pediments (Oberlander, 1972). Stone layers in the basal soil and local discontinuities between the soil mantle and subjacent friable rock suggest that movement of a colluvial mantle was characteristic of some hillslopes. Maintenance of a soil cover on moderate to steep slopes implies a complete cover of vegetation of non-desert composition and type and tends to support Axelrod's conclusions regarding the Miocene and Pliocene flora of the region. Parallel rectilinear slope recession appears to have been characteristic, predicated upon the existence of a mantle of saprolite overlying an active subsurface weathering front along which chemical alteration of the subsurface rock kept pace with surface erosion. Preserved sub-volcanic exposures indicate that exposed bedrock was friable and easily planed by surface wash. There are no exposures of Tertiary basalt in contact with sound granitic rock.

In the Mojave region early Pliocene hillslope weathering profiles in quartz monzonite and granodiorite varied in depth between 6 and 14 m (20 to 40 ft), with rock decay occasionally extending to depths in excess of 30 m (100 ft) in piedmont areas. The subsurface weathering front in granitic rock varied greatly in position and character as a consequence of local structural and petrographic characteristics. In many localities there is clear stratigraphic continuity between the boulders littering present day hillslopes and corestone horizons in the basal portions of weathering profiles covered by volcanics having K-Ar ages exceeding 8 m.y. Wherever datable materials and *in situ* boulders have been seen together the boulders can be shown to have been derived from an early Pliocene regolith (Oberlander, 1972, figs. 11, 12, 13). The associated landscapes are often close to existing base levels and are unusual only by the presence of a few thin basaltic remnants. Thus I believe that the existing boulder mantles characteristic of granitic hillslopes in the Mojave Desert may consist, in general, of former corestones originating within pre-Quaternary weathering profiles. These have been exposed by Quaternary strip-

Proven?

ping of the Tertiary weathered mantle. Cessation of subsurface decay and acceleration of surface erosion during the late Pliocene and Quaternary is presumed to be the consequence of the establishment of negative moisture balances and deterioration of the vegetative cover during Pliocene and Pleistocene time. These changes have been documented by Axelrod's analysis of the pollen record since Miocene time (Axelrod, 1958). The general climatic desiccation of this period seems largely attributable to tectonism producing rain shadow conditions east of the rising Western Cordillera, particularly the Sierra Nevada, and the Transverse and Peninsular ranges of southern California.

TERTIARY PEDIMENTS

Saprolite-covered pediments were an integral part of the Tertiary landscape. Certain existing pediments still carry remnants of Tertiary weathering profiles preserved under remnants of lava flows that have survived the general denudation of the past few million years. Such examples clearly indicate that existing pediments in the Mojave region were already fully developed at least 8 m.y. ago and have been modified subsequently only by removal of soil and decayed rock inherited from the Tertiary morphogenetic regime.

In this regard the nature of the somewhat misleading parallel to the well-investigated history of Australian arid landscapes should be made clear. In both the Australian and southern Californian deserts stripping of an inherited Tertiary weathered mantle followed late Quaternary climatic desiccation. The absence of strong tectonism in interior Australia indicates that the stripping process there was primarily a consequence of climatic change and its effect on the vegetative cover (Mabbutt, 1965). In the Mojave region pediments have downslope profiles exposing bedrock to a distance of a kilometer or more beyond hillfronts, with Tertiary volcanics preserved on the pediments themselves. On the contrary, the Australian pediments seem to be secondary features formed subsequent to the onset of aridity, being a consequence of Quaternary subsoil notching of structurally determined hill bases inherited from the Tertiary landscape (Mabbutt, 1965, 1966). Similar notching has likewise affected the bases of bedrock eminences in the Mojave Desert but is a very superficial feature, amounting to a few meters at most. Pedological and stratigraphic evidence suggests that the Mojave climate has been more arid than that of interior Australia since early Tertiary time. There was no laterite or silcrete formation in the Mojave region prior to the onset of full desert conditions, and the existing climate and vegetation continue to be of a somewhat more xeric nature than their counterparts in the Australian deserts. Thus complete parallelism in the development of the two regions should not be anticipated. However, Mabbutt's clear demonstration that the Australian interior has been stripped of an inherited mantle as a consequence of climatic change, without assistance from tectonism, is of the utmost importance to an understanding of the existing Mojave Desert landscape.

*folded
grah!*

*subsoil
notch*

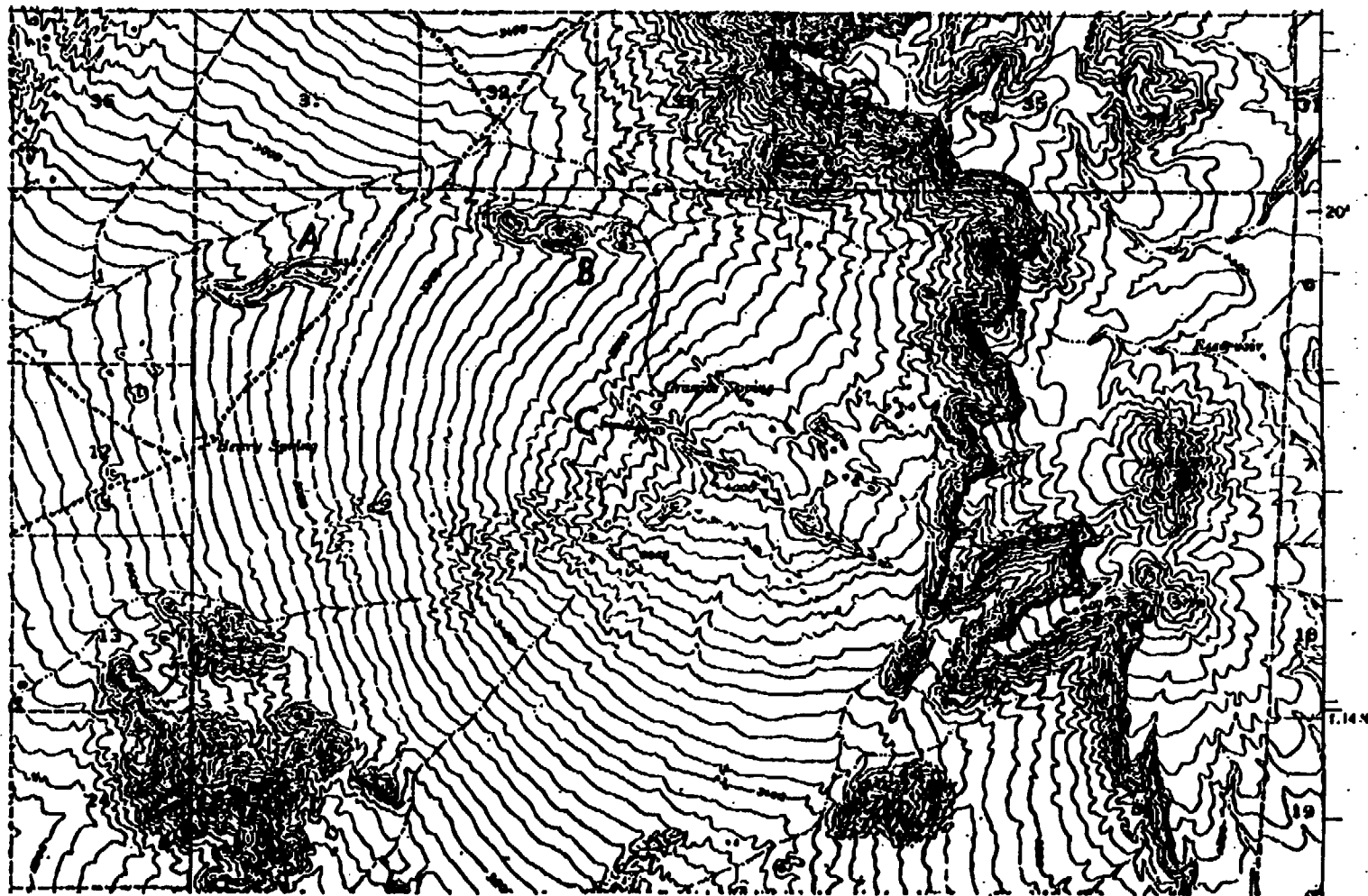


Fig. 2. Granite Springs pediment, east of Baker, Calif. (Halloran Spring 15-min quadrangle). Numbered sections cover 256 km² (1 sq mile). Escarpment to east is composed of flood basalts of probably Pliocene age, covering decayed quartz monzonite. At locations A, B, and C, Tertiary quartz monzonite weathering profiles are preserved under remnants of basalt dated at 9.2 m.y. Bedrock is exposed west of the pediment apex to approximately the 792 m (2600 ft) contour, a distance of some 5.6 km (3.5 miles).

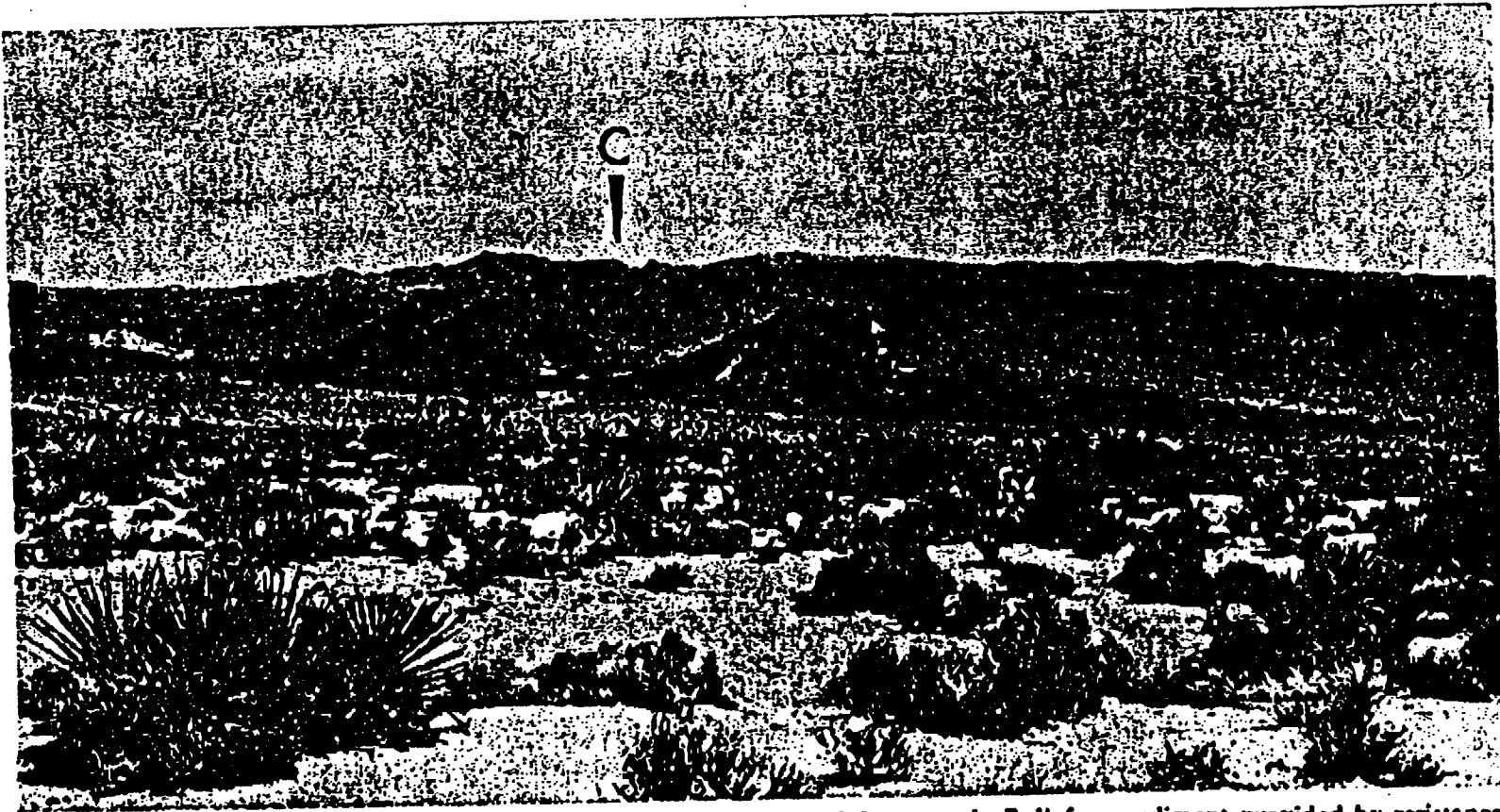
An instructive example of Mojave pediment characteristics may be seen 24 km (15 miles) east of Baker at Granite Spring (Halloran Spring 15-min quadrangle). At this locality remnants of basalt having a K-Ar age of 9.2 ± 0.6 m.y. indicate that Pliocene lavas flooded westward across the higher portion of a classically-formed pediment and onto its lower slopes (fig. 2, pl. 1). Radiometric ages of basalts from the summit and base of the bedrock pediment, spanning a distance of 3.2 km (2 miles), vary by only 1 percent, suggesting that the samples were taken from remnants of a formerly continuous single sheet, as would be concluded from the field relations. Even if the remnants are from different flows, they define one subvolcanic surface. Thus the Granite Spring pediment is more than 8 m.y. old and has been modified during late Pliocene and Quaternary time only by the stripping of the Tertiary weathering profile seen beneath the remaining basaltic fragments. As could be anticipated in the case of an erosion surface produced by backwearing, weathering below the sub-volcanic Tertiary surface was significantly deeper toward the distal portions of the pediment. Subsequent erosion, stripping off the lava and underlying Tertiary saprolite, has left basalt-capped mesas standing 70 m (200 ft) above the denuded pediment at the 1040 m (3400 ft) level, whereas those near the summit, 120 to 180 m (400 to 600 ft) higher, rise much less conspicuously 30 m (100 ft) or less above the surrounding topography. The height of such mesas, excluding the thickness of the lava, approximates the local depth of weathering in the Tertiary landscape, reflecting the fact that arid Quaternary denudation has selectively affected previously decayed rock and has been ineffective in the sound rock exposed at the ancient weathering front. It is tempting to suppose that the steepening of pediment gradient resulting from erosional stripping in this instance may have been a general tendency during the transition to desert conditions at the close of the Tertiary. Such an interpretation would be based on the normal inverse relationship between surface slope and surface water discharge. In actuality, any such steepening more probably is diagnostic of the depth profile of the erodible weathered mantle inherited from the prior morphogenetic system — the latest phase of removal terminating against the more resistant surface of the former weathering front.

As the bases of 8 to 10 m.y. old lava caps in various widely separated localities in the Mojave region repeatedly stand 20 to 45 m (70 to 150 ft) above adjacent solid and continuous granitic outcrops, the average depth of pre-Quaternary weathering on the larger granitic pediments appears to have fallen within this range.

STRIPPING OF PEDIMENTS VERSUS PEDIMENT "EXHUMATION"

During the late Pliocene and Quaternary, pediments and residuals alike have been largely denuded of their former regolith mantle. The consequence in the case of hillslopes has been to leave them clad with boulders: some let down as a lag of corestones, others delineating the joint-controlled pre-Quaternary basal surface of weathering (Oberlander,

PLATE 1



Summit of Granite Springs pediment and basalt remnants viewed from north. Relief on pediment provided by resistance of northwest-trending dikes. Small intrusive neck of basalt centered in gap between basalt caps in middle distance. Behind this is the highest remnant of flow basalt (C in fig. 2).

1972). In the case of pediments, stripping, presumably as a consequence of deteriorating vegetative cover associated with climatic desiccation, has led to wholesale exposure of the Tertiary weathering front, which has been interpreted by several prior observers as "exhumation" of a rock-cut suballuvial bench (for example, Tuan, 1959; Cooke, 1970, p. 36-37). Examination of relict weathering profiles indicates that the granitic pediments of the Mojave were not cut in rock but were extended by erosion of regolith that was constantly being renewed at the weathering front, as proposed by Ruxton and Berry (1961) in their model of slope retreat based on observation of Sudanese landscapes. According to this reconstruction, the Mojave pediments were not formed as suballuvial benches in a desert environment in the manner first proposed by Lawson (1915) but developed as either wash-graded or maturely-dissected foot-slopes fronting escarpments retreating under semiarid conditions. Export of detritus to a few distant tectonic depressions appears to have been characteristic during pedimentation. These depressions originated by subsidence during post-Eocene tectonic dislocations, trapping fluvial and lacustrine sediments that formerly had been carried to the sea (Dibblee, 1967). The present local endoreic hydrography with rising base levels and the encroachment of alluvial embankments onto the pediments themselves seems to be a subsequent development resulting from late Pliocene and Quaternary desiccation.

The Quaternary alluvium presently veneering pediments in the Mojave Desert may consist predominantly of translocated weathering products inherited from the pre-Quaternary landscape. After the strongly oxidized and occasionally duricrusted surface horizons of the Tertiary soil were removed from pediments and associated uplands, a much greater thickness of erodible decomposed quartz monzonite was bared. Seen without the distinctive surface soil this material would not be (and has not been) recognized as the C-horizon of a formerly more extensive weathering profile. This inherited preweathered material is continuing to be eroded today, both on pediments and residual relief, and is the source of modern alluvial accumulations.

The present alluvial veneer over pediments is in contact with the bases of most sizable mountainous masses due to continuing sediment arrivals from large catchments or long slopes above, where large quantities of preweathered material persist. However, where pediments are crowned by very small residuals, the alluvial edge is well separated from the summit relief forms, which uniformly consist of naked rock which supplies far less detritus than existing transportational processes are competent to remove from the slope foot (pl. 3, p. 863). Bedrock exposures below the piedmont angle in such instances are expanding, but after a complex evolution apparently involving (1) the general stripping of the upper portion of the former weathering profile; (2) transport of debris continuing to issue from the higher residual relief, in which erosion has exploited deeply decayed partitions to vastly increase the mesorelief; and (3) stripping to solid rock at the former weathering front as a consequence

of diminution of sediment deliveries from increasingly denuded tributary slopes. The processes that have resulted in the present degree of bedrock exposure cannot be envisaged as simple and uni-directional in time, as such a landscape would be a delicate indicator of the many climatic fluctuations that have affected the southwestern United States over the past several million years.

Trimming of projecting bedrock irregularities on bedrock pediment surfaces continues to occur subaerially, but such projections have themselves been exposed by stripping of preweathered material, and the total amount of backwearing produced by surficial exsudation and flushing (mostly in the form of basal undercutting) seems nowhere more than 4 or 5 m — half this amount being more characteristic. This seems essentially the full extent of erosional modification of solid granitic outcrops under the present morphogenetic system. Even this doubtless includes removal of some material preweathered along the Tertiary basal surface of rock decay.

As existing "stripped" pediments vary in configuration from planar expanses of massive rock to bouldery chaoses, it is not clear whether the Tertiary pediments were smooth surfaces — "graded" for transport of sediment arriving from the steeper relief above them — or were "born dissected" as proposed by Gilluly (1937) and Sharp (1940). If the first is true, pediment stripping may have been accelerated by erosional stagnation in the higher standing relief as a consequence of near-complete loss of its own much thinner regolith. Even if pediments are "born dissected", as seems likely, decrease in sediment arrivals from divide regions as a consequence of either diminishing relief or regolith stripping on steep slopes would trigger incision of washes, leading to eventual exposure of solid rock at the former weathering front. In either case the change would be very gradual, involving slow adjustment of pediment wash profiles to existing sediment-discharge relationships and modes of water and sediment transport.

THE PIEDMONT ANGLE

Where the slopes of pediments and inselbergs are regarded as a consequence of the bimodal size distribution of granitic weathering products, the sharpness of the piedmont angle between the pediment and surmounting residual relief is generally emphasized. The reality of this sharp slope break cannot be disputed where boulder slopes terminate downward against surfaces of sandy alluvium, as is commonly the case; it is also well defined at the base of domed inselbergs that rise abruptly above well planed crystalline rock. In the Tertiary landscape, however, sharply defined piedmont angles appear not to have been present, for all surfaces seem to have been mantled by saprolite, with no contrast in the size of particles on retreating hillslopes and expanding peripheral surfaces.

Where bedrock is exposed continuously from hillslope to piedmont in the present landscape, a sharp piedmont angle may or may not be present. Where the pediment is itself free of detritus at the piedmont angle the nature of the latter varies according to the character of the as-

sociated hillslope, which may be composed of solid rock or loose boulders. The best developed piedmont angles appear where the smaller detached boulders first exposed on hillslopes in the stripping process have disintegrated, exposing smooth dome-like forms or well-jointed steep-sided masses rising from exposed solid bedrock pediments. The associated pediments have likewise been severely denuded, as seen in the absence of boulders and tors and the continuous flat expanses of sound rock in which only the master joint sets are open (usually in one dominant direction), with the subsidiary joints being tightly compressed. The sharp piedmont angles defining granitic domes are frequently situated on open joints, but they also cut across joints perpendicularly. In such instances complete disintegration of former boulder mantles has been followed by basal weathering at the ground surface, a true desert phenomenon that girdles the inselberg, creating an abrupt piedmont angle unrelated to joint configuration. Basal undercutting amounting to 3 to 4 m in some cases creates a very sharp piedmont angle by a process having nothing to do with the original backwearing that produced the pediment itself.

Where the Tertiary weathering profiles were unusually deep as a consequence of high macro-porosity due to dense jointing, the stripping process has left slopes mantled with a residuum of loose boulders (former corestones) of relatively small size (0.5 to 1 m diam). The hills north of Yucca Valley are an accessible example. Beneath this rubble the subjacent rock is decayed to a depth of several meters. The profiles of such slopes reflect the original surface slope, which in the Tertiary landscape appears to have been smoothly concave from hillslope to pediment. The piedmont angle remains poorly developed in such settings, as the boulder slope is transitional into the pediment over a broad concavity. There is no possibility of basal weathering in such circumstances as there are no solid outcrops to be notched.

LOCALIZATION OF THE PIEDMONT ANGLE

All the foregoing is predicated upon evidence that backwearing has indeed occurred, and that the plan and position of the positive relief forms — hill fronts, escarpments, domes, and tors — are not fully predetermined by structural characteristics. Whereas backwearing of slopes in semiarid and arid regions has been accepted by most American geomorphologists (Hadley, 1967), observers of arid landscapes in some other parts of the world have stressed almost total structural control of the morphology and position of both major and minor relief elements, including the piedmont angle (for example, Twidale, 1967). According to the latter view, parallel rectilinear slope recession occurs only where a relatively resistant caprock is being undercut by the more rapid erosion of its substrate.

Well-known quantitative investigations by Schumm (1956, 1962) seem to refute this hypothesis. However, Schumm's analyses have concentrated upon manageable small scale landforms in essentially soil-free landscapes, from which extrapolation to larger forms and longer time

scales may be hazardous. Likewise, Emmett's overland flow experiments (1970) seem to explain the mechanism of parallel retreat of soil-covered convexo-concave hillslopes, but his conclusions rest upon an extremely likely but as yet unproved deduction regarding the most probable balance of the hydrologic factors in overland flow. Ruxton and Berry (1961) have outlined a mechanism of slope backwearing that appears to be in complete harmony with the Mojave evidence; however, caution is advisable in any extrapolation from present Sudanese landscapes to those of the Tertiary in southern California. Thus, it does not appear that one can disregard the possibility of downwearing (as opposed to backwearing) of major relief forms, even under arid conditions.

In a landscape that is dominated by downward erosion, all piedmont angles separate areas of either unlike lithology or unlike joint density; both the position and the plan of relief forms are structurally predetermined; and existing pediments do not enlarge significantly through time.

Opposing any such interpretation of the Mojave landforms are several facts that seem much more compatible with horizontally migrating piedmont angles between backwearing hillslopes and expanding pediments:

1. The landscape existing during the period of pediment formation in the Mojave region was veneered with a soil developed on granitic saprolite that appears to have blanketed hillslopes and pediments alike. This soil and its parent saprolite are preserved under basaltic remnants in a variety of locations and on slopes as steep as present boulder slopes in the region. Thus the eroding land surface and the joint controlled weathering front were well separated and independent of one another during the period of most active morphogenesis. Variations in effective joint density appear to have been insufficient to permit the agencies of transportation to be more effective quantitatively than those of downward rock decay even where abrupt positive relief forms are present today. Hillfronts seem to have retreated under conditions of denudational equilibrium (Ruxton and Berry, 1961; Ahnert, 1967) in which creation of erodible material by weathering below the surface is quantitatively equivalent to erosion of the surface. The Tertiary geomorphic system appears to have been "transport-limited", whereas the presently-existing system is "weathering-limited". How parallel rectilinear slope retreat can occur in a transport-limited system is considered at the conclusion of this paper.

2. A downslope transect through the weathering profile preserved under Tertiary basaltic remnants on the Granite Spring pediment (fig. 2; pl. 1) indicates that the depth of weathering was proportionate to distance from the pediment apex. This single instance is compatible with the backwearing hypothesis, since the time available for rock decay should increase outward from the apical region as the pediment extends headward at the base of a shrinking residual mass. Unfortunately, no other pediments in the Mojave region have been sufficiently engulfed by

lavas to allow preservation of ancient weathering profiles over a significant distance along the pediment radius.

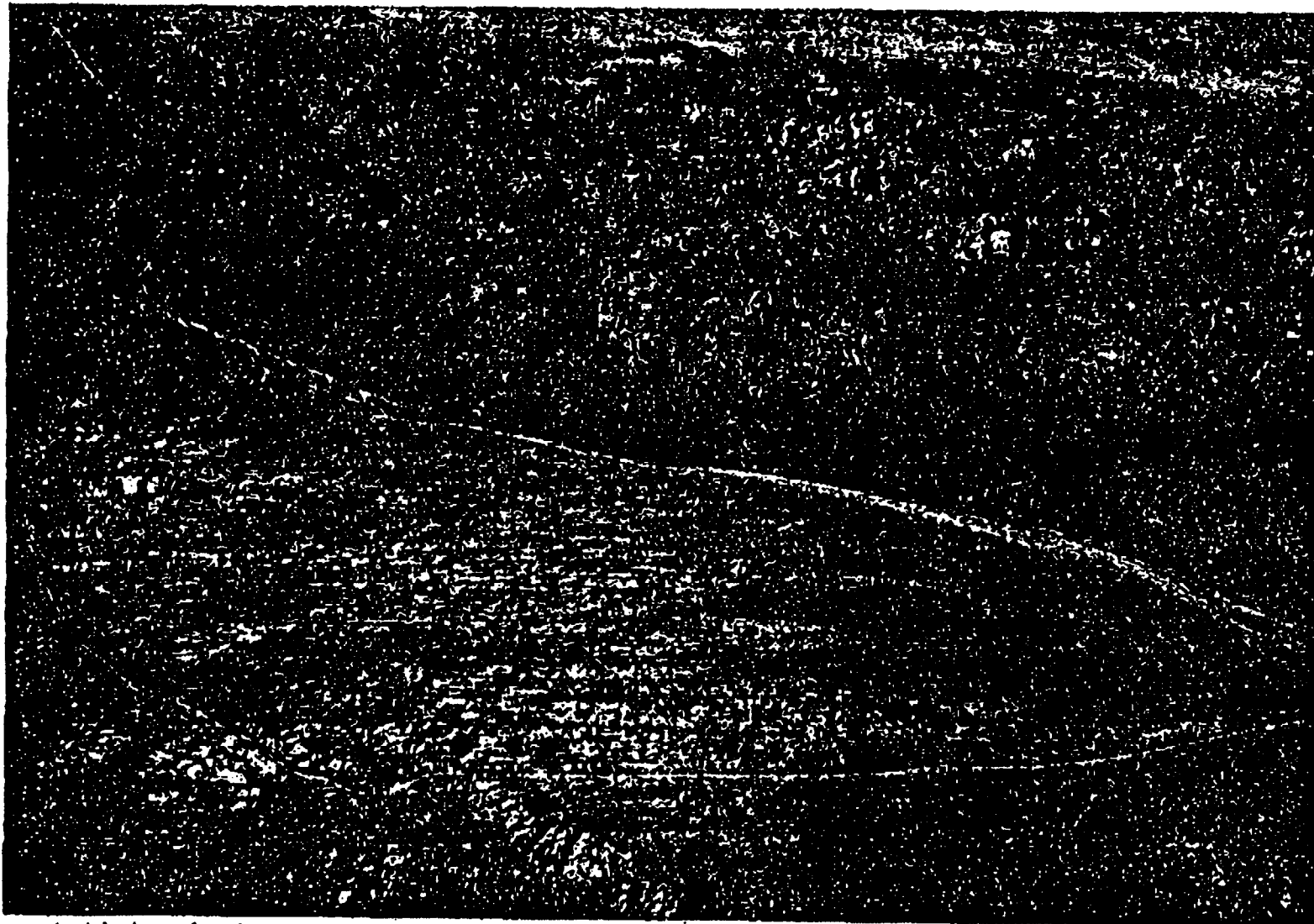
3. If downwearing under the control of joint density is altogether responsible for the epigene profiles of the desert, the ramp-like pediment form is difficult to explain. No one would suggest that the distance between joints increases regularly as the pediment rises. Thus one must assume that the pediment profile was, initially at least, a slope of transportation and not totally the consequence of structure. The downwearing hypothesis would require an enormous contrast in bedrock characteristics to allow steep-sided structurally controlled relief forms to abut against smooth slopes across which bedrock resistance has been entirely subjugated by decay and hydraulic erosion.

It is clear that in the granitic terranes of the Mojave Desert no such contrast in resistance exists between the pediment and surmounting residual masses. Indeed, this has been the essence of the pediment problem in the southwestern United States. Pediments in the Lucerne Valley district of the Mojave Desert expose sound quartz monzonite over expanses of tens to hundreds of hectares, often remaining free of either residuum or alluvium a km beyond the hillfront. Joint spacing above the pediment angle and outward from it for hundreds of meters may be measured to the centimeter with a steel tape on the ground, and the overall pattern is clear and unambiguous in aerial view (pls. 2 and 3). In such a naked landscape one is often perplexed by the surprising absence of correspondence between structure and surface form. Where open vertical joints dominate the mesorelief, as in the Granite Mountains, narrow fins of rock in areas of close jointing may stand as high as thick monolithic slabs; likewise, the jointing seen on smooth pediments may extend into rough hill masses without discernible change in density or character (pl. 3). While the residual relief is compartmentalized by jointing, the pediment angle not uncommonly runs transverse or oblique to the dominant joint set and may be localized on minor fractures whose adjacent counterparts produce little or no surface effect. Indeed, it was the anomalous relationship between visible jointing characteristics and slope plans and profiles that first suggested to the writer — independently of the direct evidence discovered later — that a blanket of residuum must have been present in some depth over the entirety of this landscape while its present relief was being established.

PEDIMENT MORPHOMETRY

Morphometric analyses of the characteristics of pediments and associated landscape elements have failed to produce evidence of the mode of origin or geomorphic function of the pediment landform (Mammerickx, 1964; Cooke, 1970; Cooke and Reeves, 1972). Cooke has adduced evidence for pediment exhumation, but the exhumation hypothesis fails to explain the origin of the erosion surface so revealed. Both Cooke and Mammerickx found that, among other enigmas, so fundamental a prop-

PLATE 2



Aerial view of pediments east of Lucerne Valley, showing degree of bedrock exposure (light areas). Residual shown in plate 3 is near center of left margin of photograph.

PLATE 3



View of residual on quartz monzonite pediment in Lucerne Valley north of San Bernardino range, showing nature of jointing on pediment and residual. Rather than localization of the residual by less dense jointing, there seems to be a higher density of visible joints in the residual, probably due to relaxation associated with off-loading.

erty as pediment slope correlates only weakly with "pediment length" (as usually defined) and shows little relation to rock type or particle size.

While agreeing with Cooke's criticism of past research on pediments, I feel that for two reasons morphometric analysis of the pediment landform — as it appears in the Mojave Desert — will not be able to provide more positive results than more traditional investigative approaches to the pediment problem. These reasons have to do with the nature of the information used in the morphometric analyses that have been carried out and the inapplicability of the technique to relict landscapes.

First, the fundamental property of "pediment length" has been defined as the exposure of bedrock between the upper edge of the alluvial apron and the mountain front (Tuan, 1959; Cooke, 1970); this is easily measured both in the field and on geological maps and aerial photographs but treats only the emerged portion of an iceberg-like phenomenon. The bulk of the erosion surface whose length and slope might be expected to be correlated inversely is presently hidden from view beneath the ubiquitous alluvial veneer and receives no consideration in the analysis. The stripping and/or exhumation that has exposed the pediment is a recent superficial development unrelated to the formation of the erosion surface itself. It has resulted from local imbalances between weathering and erosion perhaps contingent upon tectonism or the erosional condition of the sediment source (the upland). Recent migrations of the alluvial edge, characterized as "exhumation", bare an erosion surface produced at a different time by different processes. Thus "pediment length", defined as the recently exposed portion of a partially buried erosion surface, should have little bearing upon the pediment slope established much earlier by an altogether different mechanism.

The second disability of morphometric analysis in the Mojave Desert context proceeds from the facts presented in the present paper: the pediments of the Mojave region are relict from a prior morphogenetic system. Morphometric analysis of a landscape undergoing active pedimentation would doubtless yield positive results. But conventional morphometric analysis of a relict landscape that has been stripped to a fossil weathering front can at best reveal anomalies that indicate lack of adjustment between form and process in the landscape.

Existing bedrock pediment slopes appear to express the surface slopes in the Tertiary landscape minus the thickness of the former weathered mantle. Thus the longer pediment slopes might be significantly steepened by arid stripping owing to downslope increase in the depth of pre-Quaternary weathering, as in the Granite Spring example. As this effect would not be so marked on shorter pediments, whose mean gradients have been presumed to be relatively steep (Lawson, 1915; Cooke, 1970), pediment gradients might not differ significantly after stripping regardless of pediment length. Absence of good correlation between pediment length and pediment slope in the stripped landscape produces a geomorphic quandry and a tendency to introduce the possibility of tectonic disturbance. However, restoration of the pre-Quaternary

PLATE 4



Exposure of pedimented quartz monzonite east of Wilhoit, Ariz., showing nature of bedrock susceptible to pedimentation. Weathering to this degree prior to pedimentation is shown by boulder content of correlated alluvium.

slope gradients might well show that prior to stripping the relationship between pediment slope and pediment length actually was of the expected nature.

What morphometric analysis can do, and apparently has done in the case of pediment studies, is to indicate a lack of consistent relationships between elements of the existing landscape hitherto regarded as closely associated. Other types of evidence are then required to produce explanations for the unexpected discrepancies. In the present case we have the obverse of the nice morphometric relationships described by Denny (1967) in reference to alluvial fans and fluvial planation surfaces in several regions of the western United States, which could be interpreted as expressing steady-state development. In Denny's investigations the study of paleosols was intentionally disregarded. This seemed valid because the forms described truly appear to be products of the morphogenetic system in which they are presently seen, quite unlike the granitic pediments of the Mojave Desert.

EXISTING ANALOGUES TO TERTIARY PEDIMENTATION

The classic pediments cutting crystalline rocks in the desert Southwest of the United States continue to be treated by many geomorphologists as products of arid morphogenesis (for example, Hadley, 1967; Warnke, 1969; Cooke and Warren, 1973). However, investigators working elsewhere have identified pediments in a wide variety of climatic settings. Beyond the United States the pediment landform is widely recognized as an indicator of semiaridity rather than true desert conditions. This view appears to take cognizance of the efficiency of surface wash resulting from torrential rainfall that occurs seasonally on surfaces lacking a dense vegetative cover. So widely experienced an observer as Birot has suggested that the development of pediments on crystalline rock is most rapid in the warm and seasonally wet low-latitude thorn forests, with pediment formation in the less humid mid-latitude semiarid environment being much less effective (Birot, 1960).

Analogues to the conditions under which pedimentation seems to have occurred in the Mojave region in pre-Pliocene time appear to exist today in the southwestern United States. On the lee side of the San Gabriel and San Bernardino ranges, less than 1000 m above the nearby pediments of the western Mojave Desert, shrubland dominated by pinyon pine, oak, juniper, and chaparral species form a cover over steep slopes that maintain a veneer of granitic saprolite only occasionally interrupted by exposed corestones and tor-like outcrops. As these ranges have been elevated by Plio-Pleistocene movements, which continue today, they are bordered by alluvial fans rather than pediments, although the fans appear to cover range-front pediments in some cases. However, the upland topography includes numbers of surfaces of low relief that can easily be construed as pediments that are continuing to expand by the slow erosion of fine regolith on adjacent slopes. Similar surfaces veneered by reddish soils under a dense brush cover are conspicuous in Riverside County west of the San Jacinto Range and south of Hemet.

A clearer parallel to the Tertiary landscape of the Mojave region exists in the uplands of central Arizona. Weathering profiles and surface forms in granitic areas such as the Sierra Prieta, west of Prescott, seem to present a modern counterpart to the ancient Mojave landscape.

Throughout the Sierra Prieta, red weathering profiles derived from quartz monzonite abound with corestones in various stages of disengagement from surrounding rotted bedrock. Although these occasionally appear at the surface, the steeper slopes overlooking the western piedmont of the range, and rising from valleys within it, are essentially smooth, being cut across friable decomposed rock. A pediment borders the low western escarpment of the Sierra Prieta, exposing thoroughly decomposed quartz monzonite in a 2.5 km-wide band along the mountain front (fig. 3). Beyond this, rubified bouldery alluvium laps onto the pediment, thickening westward. A thin layer of colluvium similar in appearance to the bouldery alluvium is conspicuous on the lower slopes of several residuals that rise from the pediment just at the upper margin of the alluvial apron. Granitic boulders in both the colluvium and alluvium are strongly decayed and friable.

The western pediment of the Sierra Prieta emerges from beneath the overlapping older alluvium at an elevation of about 1500 m (5000 ft) near Wilhoit (Kirkland 15-min quadrangle), where it is easily accessible from Highway 89 (fig. 3). The transition from pediment to older alluvium is clearly evident in the texture of the surface material — coarse grus characterizing eroding pediment surfaces, in contrast to the argillaceous surface soil on the older alluvium. Exposed corestones are thinly scattered over the rolling surface of the pediment, but most slopes are smooth, being developed in saprolite veneered by a lag of coarse granules and vein fragments. The proportion of bare ground exposed on the pediment is no more than 30 to 35 percent, the present cover consisting of bunch grass, scrub oak, mountain mahogany (*Cercocarpus*), catclaw acacia (*A. gregii*), manzanita (*Arctostaphylos*), prickly pear (*Opuntia*), and other shrubby species. Appropriately, both the flora and the climatic regime of the Sierra Prieta, which receives year-around precipitation averaging well in excess of 500 mm (20 in.), closely corresponds to Axelrod's reconstruction of conditions in the western Mojave during Miocene time, when the Mojave pediments appear to have been expanding. The vegetation of the Sierra Prieta pediment and hillfront is sufficiently dense that paths must be consciously searched out, and backtracking is frequently necessary (pl. 5). Cattle trails and washes provide the best access. The composition and density of the vegetation has been affected to an unknown extent by grazing, and shrubby growth may be more characteristic at present than under former natural conditions. Open areas of bunch grass, in which no bare ground is exposed, are present on the older alluvium and may approximate the natural cover in the piedmont zone.

The overall slope of the bedrock pediment is about 4 degrees, but it is far from a plane surface. If pedimentation is indeed active here, as it seems to be, there can be no doubt that pediments in this area are "born

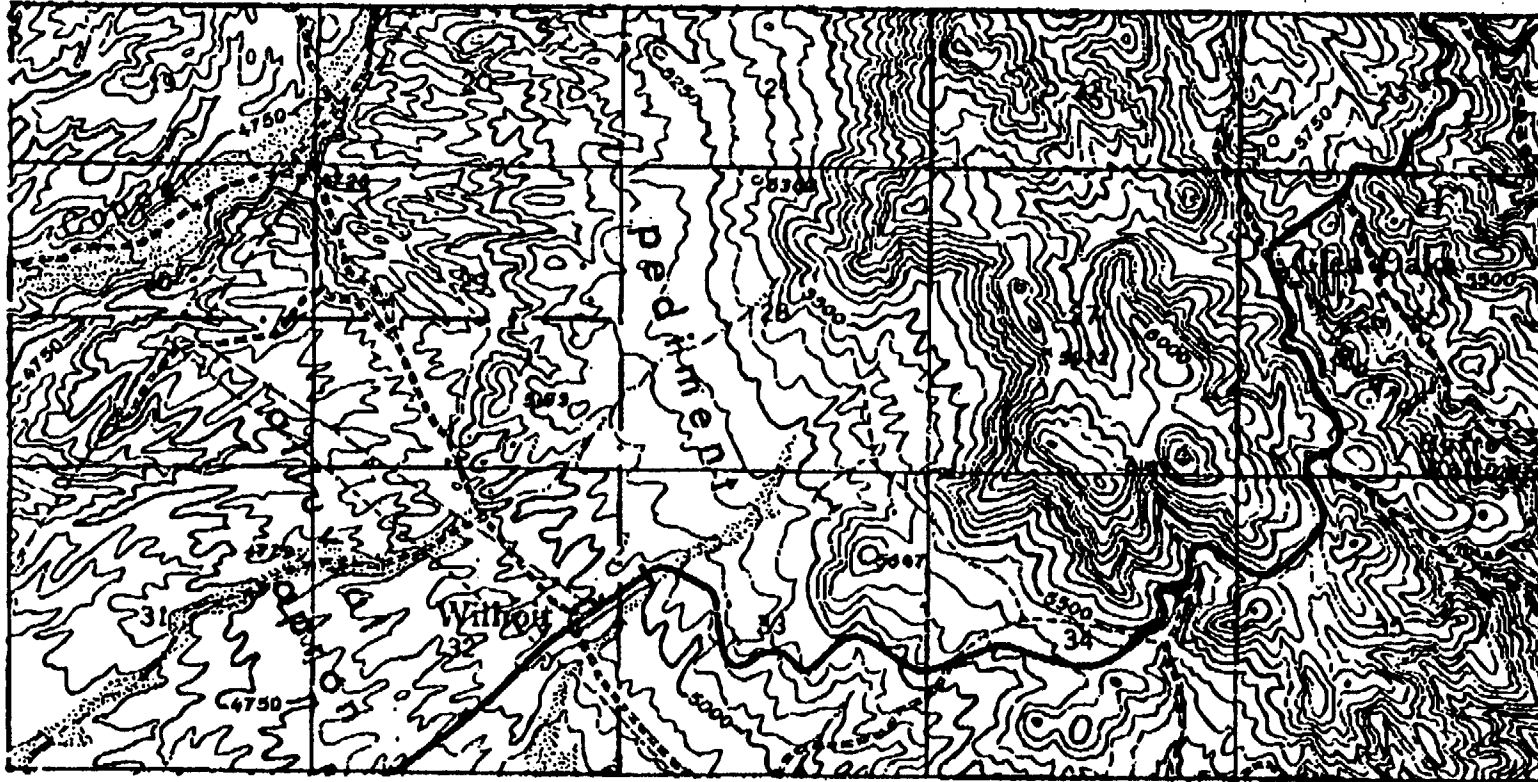


Fig. 3. Pediment along western front of Sierra Prieta, west of Prescott, Ariz. (Kirkland 15-min quadrangle). Numbered sections cover 2.56 km² (1 sq mile). Decomposed granite of the pediment is exposed continuously from the upland to Willhoit, the upper edge of the alluvial apron to the west more or less coinciding with the 1524 m (5000 ft) contour.

PLATE 5



Sierra Prieta pediment, showing nature of relief and density of vegetative cover. Light areas on distant hillslopes are grass.

dissected" and exemplify Ruxton and Berry's "dissected plinth", which borders actively retreating hillfronts in the dry savanna and wet semi-arid regions of the Sudan (Ruxton and Berry, 1961). The Wilhoit pediment merges with the low frontal escarpment of the Sierra Prieta by a sweeping concavity that is accurately portrayed by 50-ft (15.24 m) contours on the Kirkland 15-min quadrangle (fig. 3). As the contours indicate, dissection of the upper pediment is more severe than gulying on the frontal escarpment; nevertheless, the lines of erosion on the pediment do indent the slope of the mountain front. Here we apparently have an excellent example of a mountain front retreating, without change in declivity, in consequence of erosion of fine weathering products that are continually renewed by subsurface rock decomposition. The products of slope erosion are evacuated through a network of washes that dissect the pediment, which is a multi-convex surface that is itself lowered uniformly as the mountain front recedes. While it is tempting to imagine the eroding scarp/dissected pediment/alluvial apron association migrating relentlessly eastward without change in either form or elevation, the cross-cutting relationships between the older (rubified and dissected) and younger alluvial deposits signify breaks in the continuity of erosion and deposition in the piedmont zone. It could be expected that in an area currently receiving 500 mm of precipitation, pre-Quaternary and Pleistocene climatic fluctuations—and resultant periodic changes in vegetative cover and runoff—would have marked effects on sediment deliveries and hydraulic gradients. Detailed investigation of this locality, as of most others, would almost certainly indicate complexities in Quaternary erosional history. What the Sierra Prieta piedmont does seem to illustrate, however, is an observable case of parallel rectilinear backwearing of soil-covered slopes developed on saprolite containing detached corestones. The presence of thoroughly decayed spheroidal boulders (originally corestones) in the older alluvium of the piedmont zone clearly indicates that the deep weathering noted on eroding surfaces did not post-date pedimentation but was, in fact, critical to it.

This instance reinforces the evidence from Tertiary weathering profiles in the Mojave Desert indicating that pediment development in crystalline rock is predicated upon the existence of a saprolite that can be eroded by surface wash but at no greater rate than its renewal by subsurface weathering.

SLOPE RETREAT IN THE TERTIARY LANDSCAPE

The problem of how parallel rectilinear slope retreat can proceed in a convex-concave soil covered landscape may not be as difficult as once supposed (for example, King, 1967, p. 157). Schumm (1962, 1966) has demonstrated that backwearing at a constant angle requires only that there be no accumulation of debris at the slope foot. His quantitative investigations in the Badlands of South Dakota indicate how this condition is achieved in the case of the miniature pediments of that area, where decrease in roughness from hillslope to pediment result in water

not necessary
- for this (the
showing?

inference

flows on the pediment having velocities as high or higher than those on the hillslope. Schumm (1956) had previously established that the process of creep tends to anchor the slope foot, causing the slope angle to diminish with time. Schumm's field measurements thus indicated that where surface wash was the principal mode of sediment transport, slopes retreated parallel to themselves, whereas removal by gravitational transfer caused slope flattening. More recently, controlled experiments on slope development by Emmett (1970) have suggested that the normal transition from laminar to mixed to turbulent overland flow on hillslopes produces parallel retreat of soil-covered slopes that are convex at the summit, straight in the middle portion, and concave at the base. It seems significant that convexo-concave slopes are characteristic in the Sierra Prieta and in those localities within the Mojave Desert where the boulder cover is best preserved and slope profiles are least altered from their Tertiary configuration.

For continuous slope retreat in this manner, "denudational equilibrium" must prevail; that is, subsurface weathering penetration must provide erodible materials at a rate at least equal to removal by surface wash. Ruxton and Berry (1961) have presented evidence suggesting how this requirement is met in Sudanese landscapes. They place emphasis on the particularly aggressive nature of subsurface moisture on soil-covered hillslopes. As subsurface water migrates downslope it is replenished more rapidly than on level surfaces, making it more reactive with the bedrock at the weathering front. A parallel with the well-known effects of solvent motion on limestone solution seems obvious. Thus decay of subsurface rock on hillslopes is rapid — providing a continuous supply of erodible material — but is not intense (mature weathering products not having time to form prior to erosional removal). Ruxton and Berry's conclusions are based upon tangible evidence of the presence of strong subsurface flow and removal of both solid and dissolved material on both hillslopes and pediments (Ruxton, 1958; Ruxton and Berry, 1961). The same evidence, mainly in the form of lateral eluviation of fines, can be seen in many parts of the Mojave Desert where alluvium is present or a weathered mantle persists.

The possibility of parallel retreat of soil-covered slopes having been demonstrated by several types of evidence, it remains a question whether those of the Tertiary Mojave region would lend themselves to this mode of development. On the basis of facts presently available the crucial factor appears to be the relative importance of creep versus overland flow in the erosional process. This would appear to be controlled by both the surface and mass permeability of the quartz monzonite weathering profile. High surface permeability discourages overland flow and favors the creep process (Schumm, 1956). However, creep may be less active on materials of high mass permeability than on materials with a shallow permeable layer, where a sharp weathering front or discrete lubricated zone is present, or where volume changes are localized, producing a well defined horizon or zone of shear. It is an obvious temptation at this point

What does this mean?

to emphasize the high mass permeability of quartz monzonite residuum. Obvious colluvial movement in the Tertiary Mojave weathering profiles has, in fact, been discovered only in instances in which there *was* an abrupt transition to altered but coherent rock less than a meter below the surface. The vast majority of exposures of Tertiary surfaces investigated closely resemble those of the Sierra Prieta, which has almost everywhere been eroded by surface wash. In both instances, weathering profiles characteristically are gradational into solid rock through a zone of corestones in a saprolite or grus matrix overlying a highly irregular joint controlled weathering front.

CONCLUSION

The contemporary landscape in such areas as the Sierra Prieta, as well as observations by Ruxton and Berry, Schumm, and Emmett, seem to demonstrate that parallel rectilinear slope recession can and does proceed in saprolite-mantled terranes like those that characterized the Mojave region during the Tertiary. This type of development accounts for the pediment landscape of the present, which we see stripped of a former weathered mantle. This stripping presumably occurred as a consequence of Pliocene climatic change that produced greater surface exposure due to impoverishment of the vegetative cover. Stripping of hillslopes to solid rock at the former weathering front has terminated pediment expansion by arresting the retreat of slopes, which are essentially stagnant under present conditions. It seems ironic that the problem of pediment formation in the North American deserts may be, in the last analysis, the problem of slope retreat in a soil-covered landscape.

ACKNOWLEDGMENTS

I wish to thank William Bull and Robert P. Sharp for their valuable comments on the original manuscript. Radiometric age determinations were made by the Geochron Division of Krueger Enterprises, Cambridge, Mass., and were funded by the National Science Foundation through the Committee on Research, University of California, Berkeley.

REFERENCES

- Ahnert, Frank, 1967, The role of the equilibrium concept in the interpretation of landforms of fluvial erosion and deposition, in Macar, P., ed., *L'évolution des versants* v. 1: Internat. Geog. Union Internat. Symposium de Geomorphologie, Univ. Liege, Belgium, p. 23-41.
- Axelrod, D. I., 1958, Evolution of the Madre-Tertiary Geoflora: *Bot. Rev.*, v. 24, p. 433-509.
- Biró, P., 1960, Le cycle d'érosion sous les différents climats: Rio de Janeiro, Centro de Pesquisas de Geog. Brasil, 135 p.
- Biró, P., and Dresch, J., 1966, Pediments et glaciais dans l'Ouest des États-Unis: *Annales de Géographie*, v. 411, LXXV^e année, p. 513-552.
- Bryan, Kirk, 1923, Erosion and sedimentation in the Papago Country: *U.S. Geol. Survey Bull.* 730, p. 19-90.
- Cooke, R. U., 1970, Morphometric analysis of pediments and associated landforms in the western Mojave Desert, California: *Am. Jour. Sci.*, v. 269, p. 26-38.
- Cooke, R. U., and Reeves, R. W., 1972, Relations between debris size and slope of mountain fronts and pediments in the Mojave Desert, California: *Zeitschr. Geomorphologie*, v. 16, p. 76-82.

pediment problem in the Mojave Desert of Southern California 875

- Cooke, R. U., and Warren, A., 1973, *Geomorphology in Deserts*: Berkeley, Univ. Calif. Press, 394 p.
- Davis, W. M., 1938, Sheetfloods and streamfloods: *Geol. Soc. America Bull.*, v. 49, p. 1337-1416.
- Denny, C. S., 1967, Fans and pediments: *Am. Jour. Sci.*, v. 265, p. 81-105.
- Dibblee, T. W., Jr., 1967, Areal geology of the western Mojave Desert, California: *U.S. Geol. Survey Prof. Paper* 522, 153 p.
- Emmett, W. W., 1970, The hydraulics of overland flow on hillslopes: *U.S. Geol. Survey Prof. Paper* 662-A, 68 p.
- Gilbert, G. K., 1877, Report on the geology of the Henry Mountains: *U.S. Geog. Geol. Survey of the Rocky Mountain Region*, p. 99-150.
- Gilluly, James, 1937, Physiography of the Ajo Region, Arizona: *Geol. Soc. America Bull.*, v. 48, p. 323-348.
- Hadley, R. F., 1967, Pediments and pediment forming processes: *Jour. Geol. Education*, v. 15, p. 83-89.
- Howard, A. D., 1942, Pediment passes and the pediment problem: *Jour. Geomorphology*, v. 5, p. 3-31, 95-136.
- Johnson, A. W., 1968, The evolution of desert vegetation in western North America, in Brown, G. W., Jr., ed., *Desert Biology*, v. 1: New York, Acad. Press, p. 101-140.
- King, L. C., 1967, *The Morphology of the Earth*: New York, Hafner, 726 p.
- Lawson, A. C., 1915, The epigene profiles of the desert: *Univ. Calif. Dept. Geology Bull.* 9, p. 23-48.
- Mabbutt, J. A., 1965, The weathered land surface in Central Australia: *Zeitschr. Geomorphologie*, v. 9, p. 82-114.
- 1966, Mantle-controlled planation of pediments: *Am. Jour. Sci.*, v. 264, p. 79-91.
- Maunderickx, Jacqueline, 1964, Quantitative observations on pediments in the Mojave and Sonoran deserts: *Am. Jour. Sci.*, v. 262, p. 417-435.
- Marchand, D. E., 1971, Rates and modes of denudation, White Mountains, Eastern California: *Am. Jour. Sci.*, v. 270, p. 109-134.
- Melton, M. A., 1965, Debris-covered hillslopes of the Southern Arizona desert: *Jour. Geology*, v. 73, p. 715-729.
- Oberlander, T. M., 1972, Morphogenesis of granitic boulder slopes in the Mojave Desert, California: *Jour. Geology*, v. 80, p. 1-20.
- Richmond, J. F., 1960, Geology of the San Bernardino Mountains north of Big Bear Lake, California: *San Francisco, California Div. Mines Spec. Rept.* 65, p. 1-58.
- Ruxton, B. P., 1958, Weathering and subsurface erosion in granite at the piedmont angle, Balos, Sudan: *Geol. Mag.*, v. 95, p. 353-377.
- Ruxton, B. P., and Berry, L., 1961, Weathering profiles and geomorphic position on granite in two tropical regions: *Rev. Geomorphologie Dynamique*, v. 12, p. 16-31.
- Schumm, S. A., 1956, The role of creep and rainwash on the retreat of badland slopes: *Am. Jour. Sci.*, v. 254, p. 693-706.
- 1962, Erosion on miniature pediments in Badlands National Monument, South Dakota: *Geol. Soc. America Bull.*, v. 73, p. 719-724.
- 1966, The development and evolution of hillslopes: *Jour. Geol. Education*, v. 14, p. 98-104.
- Sharp, R. P., 1940, Geomorphology of the Ruby-East Humboldt Range, Nevada: *Geol. Soc. America Bull.*, v. 51, p. 337-371.
- Tator, B. A., 1952, Pediment characteristics and terminology: *Am. Geographers Assoc. Annals*, v. 42, p. 293-317.
- Tuan, Yi-Fu, 1959, Pediments in southeastern Arizona: *Univ. California Pub. Geography*, v. 13, 163 p.
- Twidale, C. R., 1967, Origin of the piedmont angle as evidenced in South Australia: *Jour. Geology*, v. 75, p. 393-411.
- Warneke, D. A., 1969, Pediment evolution in the Halloran Hills, Central Mojave Desert: *Zeitschr. Geomorphologie*, v. 13, p. 357-389.

Stream capture followed deposition of Q₁, eliminating upvalley sediment contributions to the Yucca Wash alluvial fan. As a result, sufficiently old strain gauges (Q₁ and Q₂) are preserved across northern Midway Valley to assess possible north-trending faults. Surficial units near prospective surface facilities include Q₁ to Q₄. Stratigraphic relationships suggest that younger units (Q₁ to Q₂) are thin (1 to 2 m) and overlie older units more suitable for assessment of low slip rate faults.

To assist the identification of possible Quaternary faults, photolineaments were mapped in Midway Valley. Photolineaments of possible tectonic origin were identified in colluvial/alluvial map units along the Paintbrush Canyon and Bow Ridge faults, however, no displacement of alluvial surfaces has been recognized across lineaments in other parts of the valley. Photolineaments near potential surface facilities have been identified as possible "targets" for future site-specific trenching activities.

This work was performed for the U.S. Department of Energy, Yucca Mountain Site Characterization Office, under contract DE-AC04-76DP0078V

NNA.920320.0149

GS.91.M.000143

03:30 p.m. O'Neill, J. M.

No 1384

STRIKE-SLIP FAULTING AND OROCLINAL BENDING AT YUCCA MOUNTAIN, NEVADA: EVIDENCE FROM PROTOGEOLOGIC AND KINEMATIC ANALYSES

O'NEILL, J. M., WHITNEY, J. W., and HUDSON, M. R., U.S. Geological Survey, M.S. 913, Federal Center, Denver, CO 80225

The main structural grain at Yucca Mountain, as seen from low-sun angle aerial photographs, is a pronounced north-trending linear fabric defined by parallel, east-dip-sloping fault blocks. Fault-block ridges are bounded on the west by normal faults that appear as isolated, colinear scarps in alluvium and as offset bedrock units. All ridge-bounding faults in this area are structurally connected to adjacent subparallel faults, most commonly by short north-west-trending fault splays. The generally north-trending high-angle faults primarily display down-to-the-west normal offset but also have a minor, auxiliary component of left-lateral slip. Left-lateral slip is indicated by (1) en echelon fault splays that are structurally linked, commonly by north-west-trending pull-apart zones, (2) slickenlines, and (3) apparent offset of stream channels. These pull-apart zones range from tens of meters to more than 3 kilometers wide. The smallest pull-apart zones are well developed along the Windy Wash and Solitario Canyon faults on the west side of Yucca Mountain. The largest of these features is interpreted to structurally link the Bow Ridge and Solitario Canyon faults in the north-central part of Yucca Mountain, directly south of Yucca Wash; the pronounced north-west-trending drainage system in this northern part of Yucca Mountain appears to be controlled by tension fractures related to the left-lateral component of movement on these north-trending faults. Midway Valley, directly east of the large pull-apart zone, may also owe its origin, in part, to a pull-apart mechanism.

Paleomagnetic data collected from Miocene ash-flow sheets indicate that Yucca Mountain has undergone clockwise vertical-axis rotation as large as 30°. This rotation increases to the south and began about 15 Ma. The left-lateral component of slip along Yucca Mountain faults is interpreted to reflect displacements between rigid fault blocks within a structural domain undergoing clockwise, "domino style" rotation. Evidence of left-lateral slip in Quaternary deposits suggests that clockwise rotation is an ongoing process.

03:45 p.m. Whitney, John W.

No 1399

QUATERNARY MOVEMENT ON THE PAINTBRUSH CANYON-STAGECOACH ROAD FAULT SYSTEM, YUCCA MOUNTAIN, NEVADA

WHITNEY, John W. and MUHS, Daniel R., U.S. Geological Survey, Box 25046, M/S 913, Denver, CO 80225

The north- to northeast-trending Paintbrush Canyon-Stagecoach Road fault system is a primary fault system for which maximum vibratory ground motion and surface displacement will be calculated for the design of the potential underground repository at Yucca Mountain and adjacent surface facilities in Midway Valley. The fault system is 33 km long, near the east edge of Yucca Mountain, and well exposed along five segments. The three southern segments show Quaternary fault activity over distances of 3-4 km on each segment, and Quaternary movement is suspected, but not proven, on the northern segments. Slickenlines exposed on Tertiary-age fault blocks on the three southern segments demonstrate a component of left-lateral slip with strikes as great as 47°. Deflected and offset stream channels that cross the Fran Ridge and Stagecoach Road fault segments suggest that left-lateral oblique movement has continued during the Quaternary.

Faults and fractures are exposed to a depth of about 20 m in deep arroyos cut into sand ramps on the west flanks of Busted Butte and Fran Ridge. At least four, probably five, soils are present in the sand ramps; all are offset, but not all soils are exposed in each arroyo. An apparent maximum dip-slip displacement of 4.1 m was measured on the deepest soil exposed at Busted Butte. This soil has a maximum age of about 700,000 yr, but it overlies an eolian sand unit that contains the 738,000-yr-



ABSTRACTS WITH PROGRAMS



Jack Keume

1991 ANNUAL MEETING

SAN DIEGO, CALIFORNIA • OCTOBER 21-24, 1991
SAN DIEGO CONVENTION CENTER

ASSOCIATED SOCIETIES

Association of Geoscientists for International Development
Association for Women Geoscientists
Cushman Foundation*
Geochemical Society*
Geoscience Information Society*
Mineralogical Society of America*
National Association of Geology Teachers*
National Earth Science Teachers Association
Paleontological Society*
Sigma Gamma Epsilon
Society of Economic Geologists*
Society of Vertebrate Paleontologists

*Representatives serve on the 1991 Joint Technical Program Committee

NOTICE
THIS MATERIAL MAY BE PROTECTED BY
COPYRIGHT LAW (TITLE 17 U.S. CODE)

PIXE BEAM ANALYSIS FOR THE DETERMINATION OF CATION RATIOS AS A MEANS OF DATING SOUTHERN AFRICAN ROCK VARNISHES

C.A. PINEDA and M. PEISACH

National Accelerator Center, PO Box 72, Faure, 7131 Republic of South Africa

L. JACOBSON

State Museum, Windhoek, 9000 South West Africa

Stone artefacts found on the surface over much of the arid areas of Southern Africa are often covered with a rock varnish, the trace element composition of which has been analyzed by particle-induced X-ray emission (PIXE) and particle-induced gamma-ray emission (PIGME). Because Ti deposited in the varnish is less soluble and mobile, substitution of alkali metals by Ti served as a basis for dating. An experimental relationship was established between the "cation ratio" and the age of artefacts dated by more conventional means. This relationship provides a cation leaching curve from which undated samples can be dated by their cation ratios.

1. Introduction

The determination of the age of archaeological artefacts from surface sites is often impossible using conventional methods such as radiocarbon dating, because they lack direct association with dateable organic material. For about a century [1] interest has been directed to the coating observed on rocks and artefacts from arid regions. This coating has been referred to as "rock varnish" [2], but the term "patina" has been used in South Africa [3,4] for this phenomenon although the former term will be used here.

Varnish or patina had long been considered by South African archaeologists as a means of dating [3] stone artefacts but the result of varnish thickness measurements on Middle Stone Age artefacts from the Erongo Mountains of Namibia were not found to be meaningful [4]. In both instances, varnishes were confused with the weathering of rock surfaces. Rock varnishes are relatively thin surface layers formed from dust particulates, silicate clays and small amounts of organic material. Their rate of formation depends on climatic factors and biological processes [2]. Elemental analyses of the varnish have shown that this is not necessarily derived from the matrix on which it was formed and usually consists of clay minerals containing, inter alia, Mn and Fe; the minor elements include Na, P, S, K, Ca and Ti [5].

Because Ti deposited in the varnish layers is less soluble and mobile [8,9], substitution of alkali metals by Ti can serve as a basis for dating by using ratios of alkali metals (K, Ca) to Ti, here called the cation ratio.

In this study these cation ratios gave an indication of how long the artefact had been exposed to the leaching process and could thus be used to date the artefact.

2. Experimental

2.1. Description of the samples

To test this technique, a suite of artefacts with rock varnishes of different thicknesses and colours and from a number of surface sites were selected. Samples originated from the region of the Orange river in the Northern Cape, South Africa. Details of these samples are given in table 1.

2.2. Irradiation and measurement

All the analysed artefacts were small enough to be irradiated inside a multipurpose scattering chamber [6]. Varnish spots were selected at random for analysis. These spots were irradiated with a collimated beam, 300 μm in diameter, of 5 MeV $^4\text{He}^+$ ions, obtained from the Faure Van de Graaff accelerator. Average beam currents were about 1 nA. The X-rays generated by the bombarding beam were measured with a Si(Li) detector placed at 90° to the beam about 11 cm from the point of incidence of the beam on the artefact. Two absorbers of photographic film, each about 135 μm thick, were placed in front of the detector to prevent the passage of scattered ions and of low energy X-rays. Collected data were recorded on magnetic tape for off-line processing.

Table 1
Description of analysed samples

Sample nity	Excavation site	Typological classification	Approximate age/ 10^3 yr
J/1 8460/2 8460/3	Site 3, Joubertsgif. (see sample 8459)	Smith-field B	1
8459/1A 8459/1B 8459/1C	Site 2, Joubertsgif. 7.2 km ENE of Norval's Pont on edge of HF Verwoerd Dam	Smith-field A (Late Stone Age)	10
8462/1 8462/2 8462/3	Site 1, Dagbreek. 9.6 km SSW of Bethulie	MSA ^a II	80
8461/1A 8461/2A 8461/1B 8461/2B	Grootverlang on the Van der Kloof Dam, 27 km ENE of Petrusville	MSA ^a I	120

^a MSA = Middle Stone Age.

Analysis by PIGME with a beam of $^4\text{He}^+$ at the bombarding energy of 5 MeV was carried out simultaneously with PIXE to determine the content of N, O, Na, Mg and Al through the measurement of the intensities of the following prompt gamma-rays: 871 keV ^{14}N p(1, 0); 351 keV ^{18}O n(1, 0); 417 keV ^{23}Na n(2, 0) and 440 keV ^{23}Na (1, 0); 585 keV ^{25}Mg (1, 0); and 709 keV ^{27}Al n(2, 0). The gamma-rays are named according to the chemists' convention [7].

In order to obtain analysis of increasing thicknesses of varnish, selected samples were bevelled at an angle of about 5° with a new silicon oxide wheel running at variable speeds up to 1500 rpm. The bevelled surface formed a wedge of varnish in which the various layers of formation were revealed. Thus the exposed length of about 6 mm could be analysed stepwise to provide a scan across the entire varnish thickness.

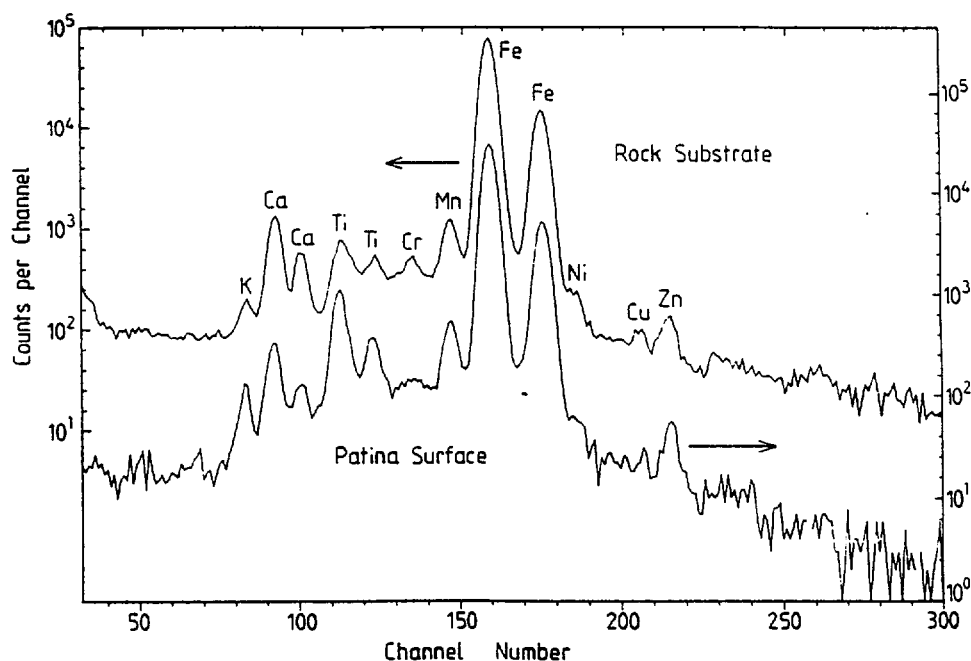


Fig. 1. X-ray energy spectra of varnish surface (lower curve) and the rock substrate, obtained from bombardment with 5 MeV $^4\text{He}^+$ ions.

3. Results and discussion

3.1. X-ray spectrometry

A typical X-ray energy spectrum obtained from a varnish sample bombarded with 5 MeV $^4\text{He}^-$ ions is shown in fig. 1. The spectrum is compared with that obtained from the rock substrate. The varnish shows an increased concentration of Ti, but decreased concentrations of K and Ca, reflecting the changes of the cation ratio $(\text{K} + \text{Ca}) : \text{Ti}$. The concentrations of Cr, Mn, Fe, Cu and Zn in the varnish and the rock substrate are very similar. It may be noted that under these conditions of analysis the sensitivity of PIXE is poor for heavier elements, but is useful for determining elements with $Z \leq 30$.

3.2. Rock varnish scan

When comparing a series of spectra obtained from a scan across a wedge-shaped layer of varnish, it was necessary to determine the relative yields from the elemental components. A plot of the summed relative yield from K and Ca is shown in fig. 2 as a function of the relative Ti yield. Included in the figure are plotted points from replicate analyses of the stone matrix. The most recent portion of the varnish (outer layer) and the oldest layer (interface substrate-varnish) are marked in the figure. Deviation from linearity occurred in the direction of increasing Ti content and corresponded to increasing age, as was expected from the postulate that varnish growth is accompanied by leaching of alkali earths [2]. The composition of the basalt stone matrix of the artefact showed a very high relative concentration of K and Ca, different from that in the varnish. Because the replicate analyses agreed reasonably well with each

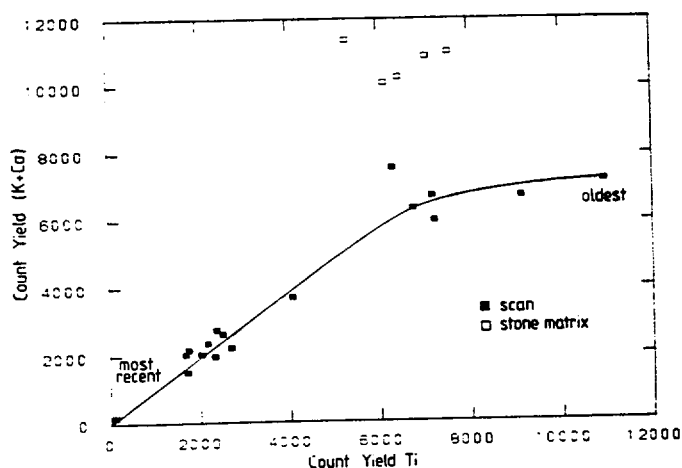


Fig. 2. The summed relative yield from K and Ca as a function of the relative Ti yield obtained from a scan across a wedge-shaped varnish layer. Replicate analyses from the stone matrix are plotted for comparison.

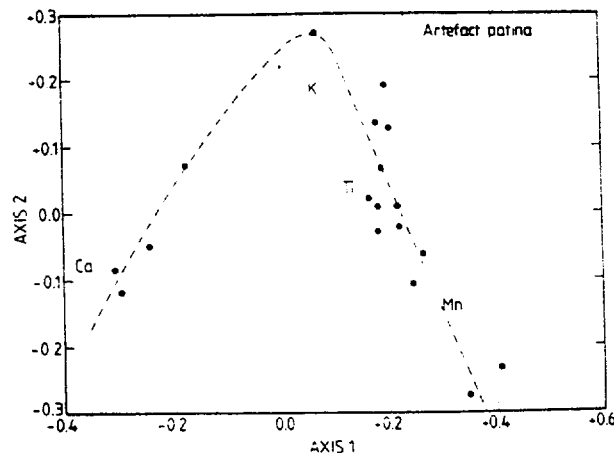


Fig. 3. Plot of the first two axes of a correspondence analysis of the data on the content of K, Ca, Ti, Mn and Fe in measured spots of a scan across the varnish thickness. The dotted line is inserted for the eye to distinguish the "horseshoe effect" as a result of graded variation of elemental concentrations.

other, it was accepted that its composition was homogeneous in the scanned area.

Nitrogen could be considered as a marker for organic material. Since the leaching of organic material was thought to run parallel to the leaching of varnish components that are relatively immobile [8,9], the relative yield of $(\text{K} + \text{Ca}) : \text{N}$ was compared to that of $(\text{K} + \text{Ca}) : \text{Ti}$. No correlation was found between these two sets of ratios. It was therefore deduced that the rates of deposition and removal of organic material were different from those of the inorganic elements.

Preliminary comparison of elemental ratios of Na, Mg and Al relative to Ti have, as yet, proved inconclusive.

3.3. Correspondence analysis of the data

Elemental concentrations of K, Ca, Ti and Mn relative to Fe obtained from a scan across the varnish layer of sample 8459/1B were used to calculate correspondence analysis plots [10,11] to visualise the multielemental composition data from the various scan spots. A plot of the first two axes is shown in fig. 3. The dotted line was added to the figure to allow the eye to distinguish the "horseshoe effect" resulting from graded concentration changes. The order in which the points appear in the plot of the horseshoe was found to correspond to different depths of varnish, and hence different ages. During the scan, the beam had a diameter of 0.3 mm and the step size between scan spots was also 0.3 mm. Accordingly, overlapping of beam spot halos could have affected the precision of analysis detrimentally.

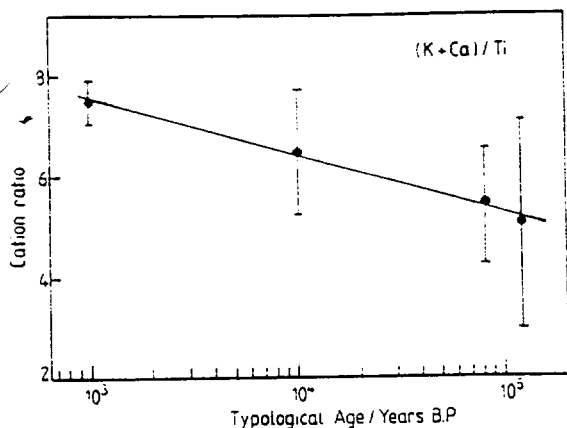


Fig. 4. The correlation between the cation ratio and the typological age.

3.4. Cation ratio-age correlation

The approximate age of the analysed samples was first estimated on typological grounds. This information is included in table 1. The analytical data for all the samples were used to calculate the mean and standard deviation for the cation ratios K:Ti, Ca:Ti and (K+Ca):Ti. These values were plotted as a function of the typological age and the resulting values obtained for the (K+Ca):Ti ratio are shown in fig. 4. The error bars in the figure refer to the standard deviation. It will be noticed that the standard deviation increases with time, reflecting a higher variability of the cation ratio if it is accepted that all specimens from one site have the same age. Alternatively, the wide spread of cation ratios for older specimens could indicate that not all of the specimens have the same age, although found on the same site. Another interesting point is the similarity of the curve in fig. 4 to those published from other areas [2]. Even making due allowance for local environmental differences, the curve has the same apparent "kink" at approximately 10^5 years as well as the same overall fit.

This is most encouraging and confirms the validity of the cation ratio curve established in our experiment, although much work still remains to be done to extend and refine our initial results particularly, for different areas within southern Africa.

Thanks are due to Mr. M. Wilson of the South African Museum, Cape Town, Republic of South Africa, who kindly supplied a number of samples for analysis and the details of the archaeological sites and Dr. J. Deacon of the Archaeology Department, Stellenbosch University, for commenting on patinas and the typological dating. Final responsibility for any interpretations remains ours, however. The staff of the Faure Van de Graaff accelerator are thanked for their helpful cooperation. This work may form part of a thesis to be submitted to the University of Cape Town (by C.A.P.) and is published with permission.

References

- [1] J. Walther, *Akad. Wissensch. Math.-Phys. Klasse, Abhand.* 16 (1891) 435.
- [2] R.I. Dorn, *Quaternary Res.* 20 (1983) 49.
- [3] A.J.H. Goodwin, *S. Afr. Archaeol. Bull.* 15 (1960) 67.
- [4] A. Viereck, *S. Afr. Archaeol. Bull.* 19 (1964) 36.
- [5] P. Duerden, D.D. Cohen, D. Dragovich and E. Clayton, *Nucl. Instr. and Meth.* B15 (1986) 643.
- [6] I.S. Giles and M. Peisach, *J. Radioanal. Chem.* 32 (1976) 105.
- [7] M. Peisach, *J. Radioanal. Chem.* 12 (1972) 251.
- [8] R.M. Potter and G.R. Rossman, *Science* 196 (1977) 1446.
- [9] R.I. Dorn and D.S. Whitley, *Ann. Assoc. Am. Geogr.* 74 (1984) 308.
- [10] M.J. Greenacre, *Theory and Applications of Correspondence Analysis* (Academic Press, London, 1984).
- [11] L.G. Underhill and M. Peisach, *J. Trace Microprobe Tech.* 3 (1985) 41.

Effect of height and orientation (microclimate) on geomorphic degradation rates and processes, late-glacial terrace scarps in central Idaho

KENNETH L. PIERCE *U.S. Geological Survey, Box 25046, M.S. 913, Federal Center, Denver, Colorado 80225*
 STEVEN M. COLMAN *U.S. Geological Survey, Woods Hole, Massachusetts 02543*

ABSTRACT

Terrace scarps can serve as a nearly ideal natural laboratory for the study of the evolution of slopes. This paper examines the effects of scarp size (height) and orientation (microclimate) by keeping constant variables such as age, lithology, and regional climate.

If a scarp degrades as a closed system, and downslope movement is *directly proportional to surface gradient*, the evolution of the scarp is modeled by the diffusion equation. For a group of scarps of same age and known starting angle, the diffusion-equation model predicts the relation between maximum scarp angle (θ) and scarp height (h). Late Pleistocene terrace scarps now as steep as 33.25° , as well as measured angles of repose for sand and gravel, require a starting angle as steep as 33.5° . For latest Pleistocene Idaho and Utah scarps, as h increases, θ is gentler (more degraded) than modeled by the diffusion equation with a constant rate coefficient. The degradation-rate coefficient (c) increases tenfold with scarp height; it should not change with height if downslope movement is solely determined by surface gradient (to the first power). Soil wash appears to be responsible for this departure from the diffusion-equation model, for transport rate by soil wash is a function of scarp size (height).

South-facing scarps are less vegetated and more degraded than north-facing scarps. For scarps 2 m high, the degradation rate (c^*) on

S-facing scarps is 2 times that on N-facing scarps; for 10-m scarps, it is 5 times.

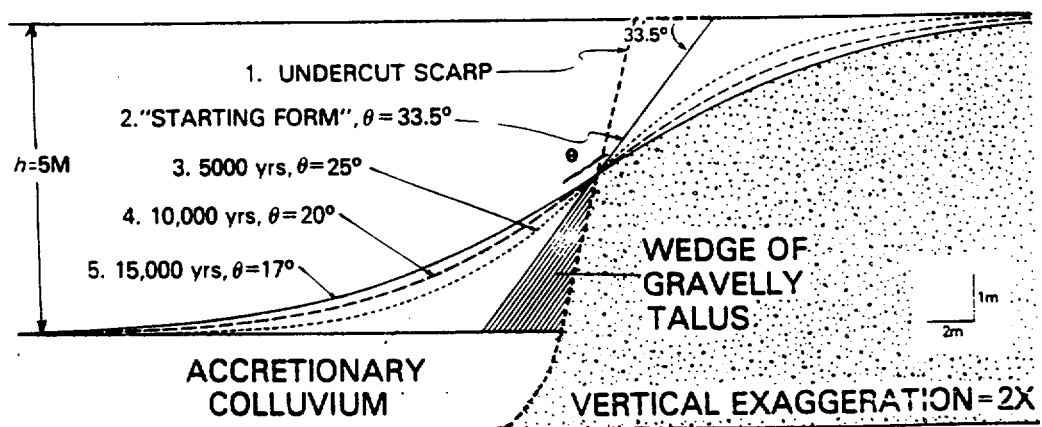
The observed dependence of the rate coefficient c^* on scarp height can be removed by normalizing c^* to values for west-facing scarps of the same height. The residual c^* values calculated by this method correlate well with differences in incident solar radiation resulting from the different scarp orientations and maximum gradients. This correlation demonstrates the importance of orientation on slope processes and their rates through the differences in freeze-thaw cycles, soil moisture, and vegetative cover.

Scarp morphology may be used to estimate age, if one accounts for the effects of climate and for scarp height, orientation, and lithology. For example, using the dated Bonneville shoreline scarps for calibration and comparing only scarps of equal height, we estimate the Drum Mountains fault scarps to be 9,000 yr old. This age is about twice that produced by previous diffusion-equation calculations that have not accounted for the height as we have here, but it is the same as independent geologic estimates of their age.

INTRODUCTION

Understanding slope processes is fundamental to geomorphology, because most of the landscape is in slope. Measurement of slope processes is difficult, however, and, for most slopes, neither their original form nor

Figure 1. Stages in the evolution of a terrace scarp. 1. Lateral undercutting of terrace gravels by stream to form a scarp steeper than the angle of repose. 2. This oversteepened slope rapidly ravel to form a rectilinear scarp at the angle of repose, here inferred to be 33.5° (see text), which is our starting form for diffusion-equation modeling. 3, 4, 5. Scarp profiles predicted by diffusion-equation model at stated time intervals (degradation rate coefficient, c , of $12 \times 10^{-4} \text{ m}^2/\text{yr}$).



An appendix of scarp measurements and derived values and a text with supplementary description of the scarps and measurement procedures can be obtained free of charge from the Data Repository of the Geological Society of America. Request Supplementary Data 86-17 from the GSA Documents Secretary.

their age is known. Rates of degradation may vary greatly among natural slopes because of differences in local climate, surficial materials, and slope processes.

Terrace scarps, narrow ramps between alluvial surfaces, provide an ideal natural laboratory for studying geomorphic processes. Their original form and age commonly can be inferred. Material eroded from the upper part of the scarp is deposited on the lower part in an essentially closed system. Terrace scarps integrate the long-term effects of slope processes, and, because they are formed in unconsolidated materials, the system is "transport-limited" rather than "loosening-limited" (Gilbert, 1877; Carson and Kirkby, 1972; Nash, 1980a). Figure 1 shows stages in the idealized evolution of a terrace scarp.

For ~100 terrace scarps formed in late glacial time on alluvial fans in semiarid central Idaho, this study examines scarp degradation following two themes: (1) the effect of size (height) of scarps on rates and kinds of slope processes and (2) the climatic effect of differences in scarp orientation on slope processes and rates.

Along a single-age scarp, Bucknam and Anderson (1979) first documented that θ (maximum scarp angle) increases approximately linearly with $\log h$ (scarp height) and that, for a given height, θ diminishes with scarp age. Subsequent studies, drawing on slope models using the diffusion equation (Culling, 1960, 1963, 1965), studied the relation between θ , h , and age for fault, terrace, and wave-cut scarps (Nash, 1980a, 1984; Colman and Watson, 1983; Hanks and others, 1984; Mayer, 1984). This

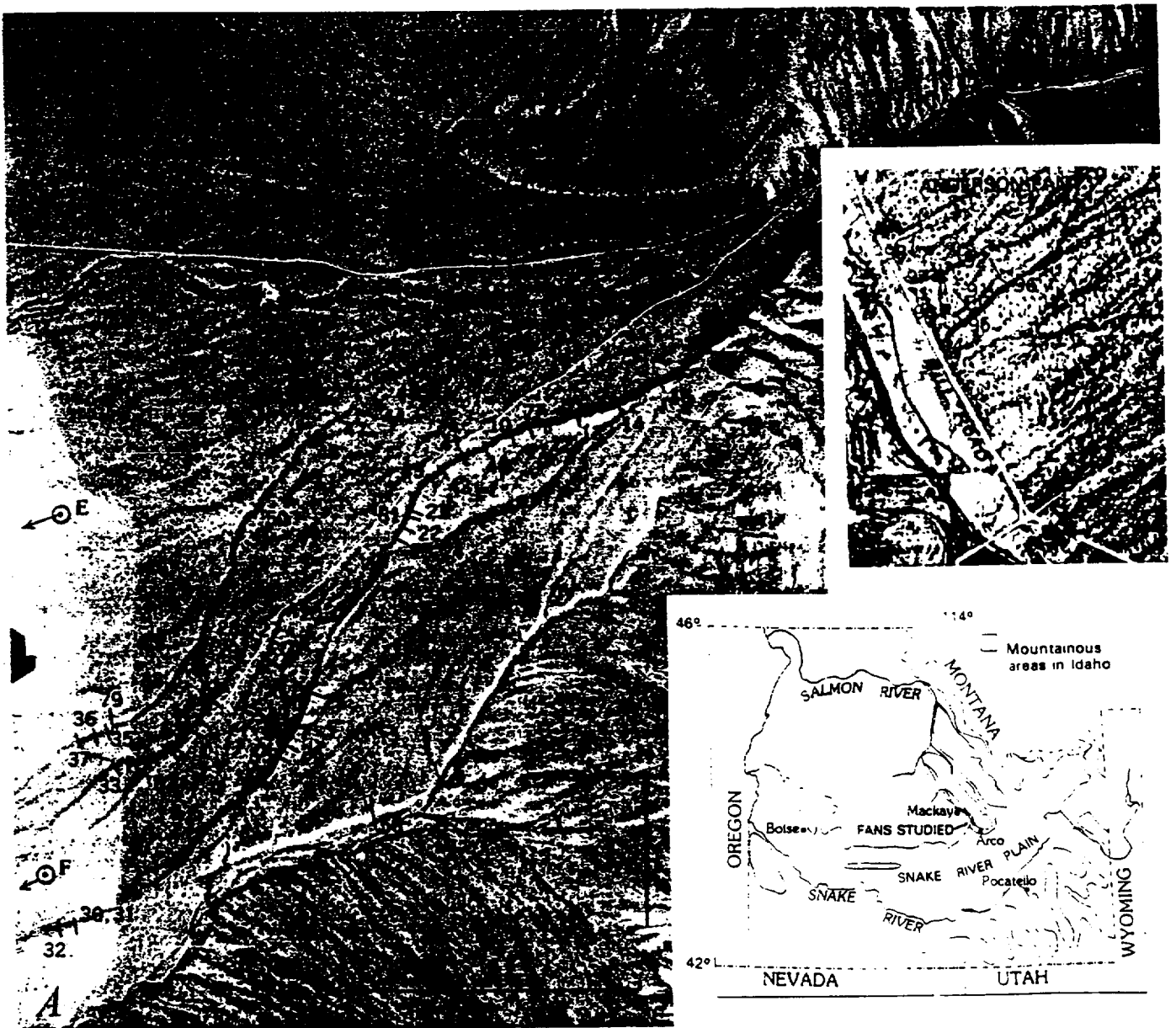


Figure 2. Aerial photographs of alluvial fans in the Big Lost River Valley, Idaho, showing locations of terrace-scarp profiles studied (short lines, numbered as in Appendix). Carbonate-coat measurement sites (letters and circled dot) on surface estimated to be ~15,000 yr old. A. Ramshorn Canyon fan; inset maps show locations of study area in central Idaho and locations of scarps studied on Anderson Canyon fan, which is 2 km south of the southwest corner of the area of the photograph.

diffusion-equation model simply assumes that continuity exists and that downslope movement is directly proportional to surface gradient. Along a scarp with different heights, the relation between θ and h is predicted by the diffusion-equation model. Our analysis of scarps in Idaho and Utah shows that, compared to lower scarps, higher scarps are more degraded than modeled by the diffusion equation. The greater degradation of these high scarps probably results from increased soil wash, which is not modeled by the diffusion equation. This height effect can be incorporated into age estimates of fault scarps based on the diffusion-equation model.

Slopes of varying orientation have climatic differences. This influence of microclimate commonly is manifested by asymmetry of valleys, although the processes involved are poorly understood (Carson and Kirkby, 1972; see Dohrenwend, 1978, Table 1, for outline of problem). Stream activity at the base of valley slopes introduces complications (Melton, 1960; Dohrenwend, 1978), whereas terrace scarps form a closed system and permit isolation of microclimatic effects on slope processes.

Microclimate varies greatly among the central Idaho scarps, as shown by vegetative cover of desert-shrub appearance on steep south-facing (S-facing) scarps, contrasted with that of prairie-grassland appearance on the steep, north-facing (N-facing) scarps. Other factors being equal, S-facing scarps have lower slopes, larger volumes of transported material, and higher transport rates than do N-facing scarps. The disparity between N-facing and S-facing scarps increases with slope and height. For all scarp orientations, the degradation rates correlate with the incident solar radiation. Solar radiation affects the rates and relative importance of slope processes through its interrelated effects on soil moisture, vegetation, and freeze-thaw and wet-dry cycles.

GEOMORPHOLOGY AND MEASUREMENT OF TERRACE SCARPS

Setting

The terrace scarps studied are on three adjoining alluvial fans along the east side of the Big Lost River Valley of central Idaho (Fig. 2; see Scott, 1982, for regional surficial geologic map). We studied scarps on the Ramshorn, Anderson, and King Canyon alluvial fans at altitudes between

1,800 and 1,900 m. These canyons head 1,000–1,500 m higher, commonly in cirques. The fans slope 3° to 4.5° and consist of gravel and sand derived from upper Paleozoic carbonate rocks. The terrace scarps were formed by lateral-stream planation of fan gravels and are distinct from Basin Range fault scarps, which also cut across the heads of some of the alluvial fans (Scott and others, 1985).

The climate is cold and semiarid: MAT is 5.5 °C and MAP is 23 cm (U.S. Weather Bureau, 1959, Arco and Mackay stations). Solar radiation and global cloudiness index at Pocatello are 415 Langley and 63% and at Boise are 406 Langley and 62% (Knapp and others, 1980). Generalized maps by Visher (1954, p. 135–136) show that the area has >130 freeze-thaw cycles a year, with frost penetration to 50–100 cm. Soil moisture builds up during winter and early spring and is consumed by evapotranspiration during spring and early summer. Although the climate during the last two-thirds of the scarps' history (Holocene time) probably was similar to the present, colder climates and consequent greater soil moisture of late glacial time prevailed during their earlier history (Pierce and Scott, 1982).

Scarp Measurement and Orientation

About 100 terrace scarps having various orientations and heights were profiled using an Abney level, measuring tape, and rod (Appendix: Fig. 1).¹ We estimate that scarp heights are accurate within a few percent for scarps higher than 5 m and are accurate within 5% to 10% for scarps 1–2 m high. The maximum scarp angle (θ) commonly subtends about one-half of the scarp height. We estimate θ to be accurate to within about a degree. Profiles were measured perpendicular to the trend of the scarp, proceeding from slopes in the plane of the profile of 0° to 2° on the lower surface to equally low slopes on the upper surface. Some S-facing scarps had upper surface slopes 3° to 4° in loess (Fig. 3B). The scarp height excluded any thickness of the loess greater than 0.5 m (Fig. 3), because that loess partly postdates the scarp, and it is readily eroded by deflation and by soil wash. Errors in the measurement of h and θ would produce only minor effects on our analysis.

¹The appendix is available free of charge by requesting Supplementary Data 86-17 from the GSA Documents Secretary.



Figure 2B. King Canyon fan.

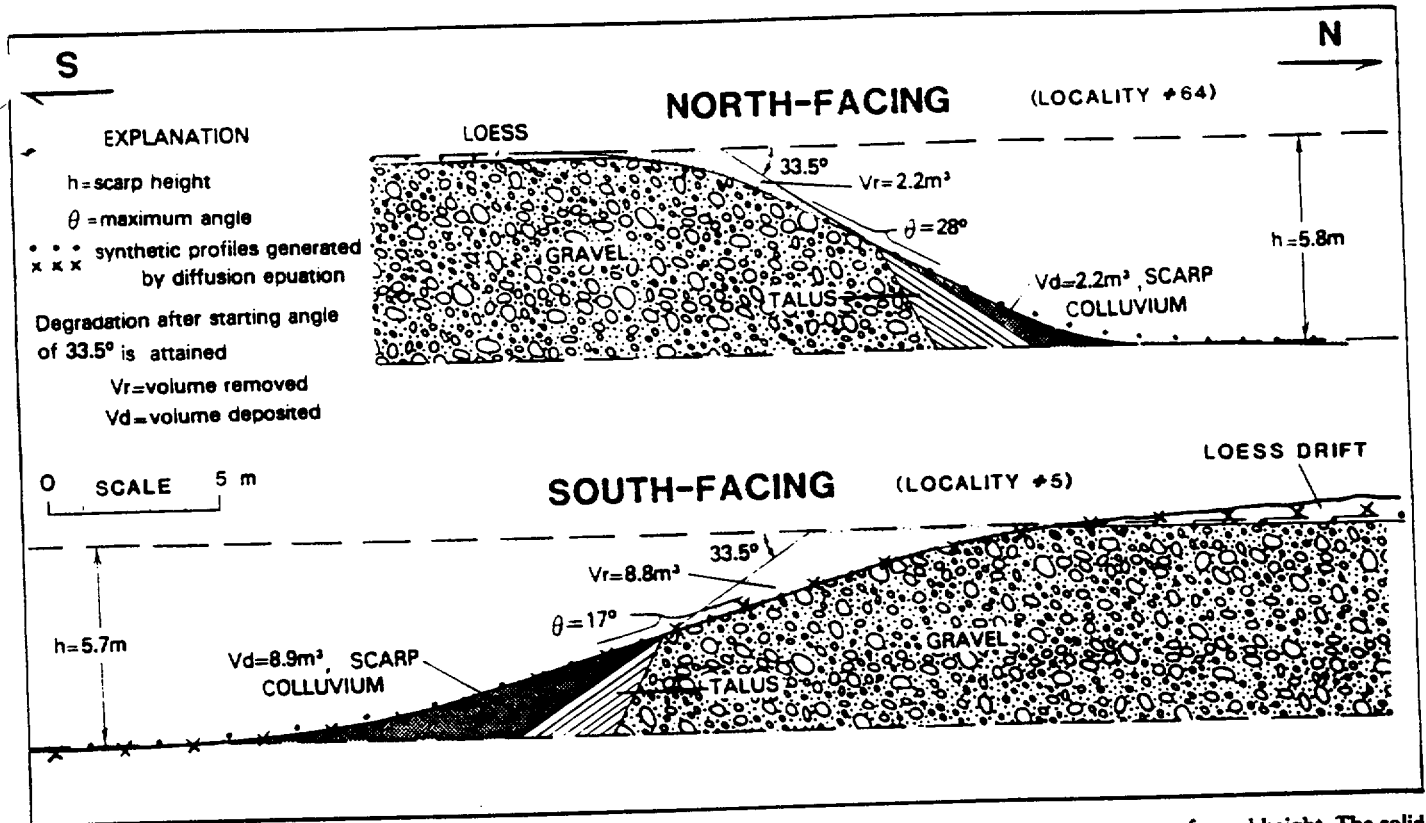


Figure 3. Cross sections across scarps showing greater degradation of S-facing than of N-facing terrace scarps of equal height. The solid inclined line represents an assumed starting angle of 33.5°. See text for discussion of diffusion-equation simulated profiles.

The scarps were divided into four groups based on orientation (Fig. 4). The stronger drying effect of the afternoon sun and the prevailing southwest winds make scarps that are oriented somewhat west of south the warmest and driest and those that are slightly east of north the coolest and wettest. The boundaries between orientation groups consequently are arbitrarily shifted 17° clockwise, so that the warmest and coolest slopes are inferred to center in their respective groups (Fig. 4). Analysis for the east-facing group is not presented, because only six suitable profiles were found.

Origin and Evolution of Scarps

The terrace scarps were formed in unconsolidated gravel during lateral planation by late-glacial streams. They show concave re-entrants separated by cusps similar in curvature to the channelways on the late-glacial alluvial surface (Fig. 2). At the time of uncutting, the scarps are inferred to have been steeper than the angle of repose (Fig. 1). Shortly thereafter, piecemeal gravitational collapse (raveling) from the free face reduced the scarps to the angle of repose (Wallace, 1977), the "starting form" of this study (Fig. 1). At the "starting time," the scarps were stable enough to be vegetated, as currently are some scarps as steep as 33° to 35°, and scarp degradation thereafter proceeded by much slower processes (Fig. 1).

The scarps probably attained the angle of repose in a short time, compared to their estimated 15,000-yr age. In Nevada, 2-m fault scarps in gravelly sand have raveled to an angle of repose of ~33° in 70 yr (K. L.

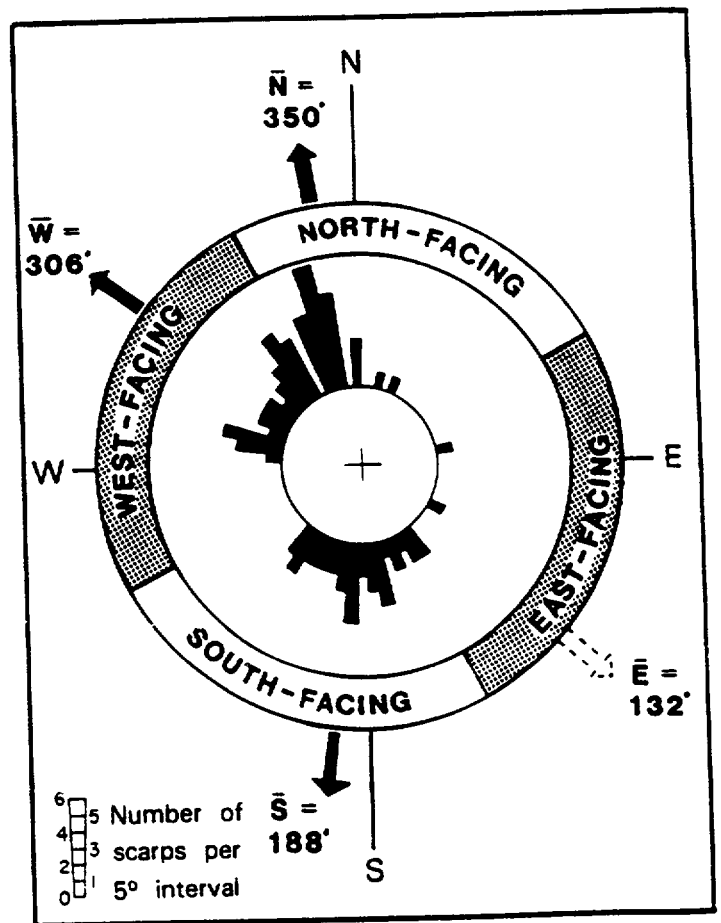


Figure 4. Rose diagram showing compass orientation and grouping of measured scarps, as well as average orientation of scarps in each group. Boundaries between orientation classes are shifted 17° clockwise (see text).

Pierce, unpub. data). Within 2 wk of the 1983 Borah Peak, Idaho, earthquake, scarps in gravel had raveled to slopes of $37 \pm 1^\circ$, which spanned three-fourths of the 2-m-high scarps along Arentson Creek (K. L. Pierce, unpub. data), and scarps along Rock Creek had raveled to $30 \pm 1^\circ$ (R. C. Bucknam, 1983, oral commun.). A year after the earthquake, scarps on Rock Creek had local angle-of-repose "graded" surfaces of $\sim 35^\circ$ (K. L. Pierce, unpub. data).

We use a starting angle of 33.5° , because some scarps in the data set are as steep as 33.25° (Appendix), and other vegetated scarps in gravel in the area are as steep as 35° . Angles of repose in sand and gravel pits average 33° (Rahn, 1969). Angles of repose in well-sorted sand having a porosity of 40% are 30° , but in mixtures of sand and gravel-sized spheres (porosity = 20%), the angle of repose increases to 35° – 36° (Statham, 1974, Table 2). Although a starting angle of 35° or steeper may be appropriate, for our diffusion-equation analysis we use the more conservative value of 33.5° , because a key finding of this study is the dependence of the rate coefficient on the height of the scarp, and choosing a steeper starting angle would accentuate this dependence.

The starting angle is considered to be independent of orientation or height. Rahn (1969) found that angles of repose in gravel pits and in stream banks show no relation to orientation. Furthermore, a positive correlation between starting angle and scarp height, such as might be caused by deep-seated slumps, was not observed and is unlikely for the heights of low-cohesion, sandy gravel forming the scarps.

Age

For eastern Idaho, Pierce and Scott (1982) presented evidence that the last interval of major fluvial activity on alluvial fans was in late-glacial time and that alluvial activity since then has been minor and generally confined to the mountain areas and fan heads. The scarps in this study were formed by lateral planation during this last episode of Pleistocene alluvial activity. Near the fan heads, small side-stream fans bury the main channel and show that the main streams have been relatively inactive since late-glacial time. On the basis of regional climatic history, the scarps were cut before the late-glacial to modern climatic shift that occurred 11,000–12,000 yr ago and do not predate full-glacial time, dated as $\sim 18,000$ – $20,000$ yr ago (Pierce and Scott, 1982; Porter and others, 1983; Heusser, 1983). Major, but not final, deglaciation of the Rocky Mountains occurred $\sim 14,000$ to $15,000$ yr ago (Porter and others, 1983, p. 99; Carrara and others, 1984). The scarps are inferred to date from the last time of extensive fluvial activity on the fans $\sim 15,000$ yr ago and are probably not more than 4,000 yr younger or older than 15,000 yr.

The late-glacial fan surfaces and associated terrace scarps show no significant differences in age. Braided channels are clearly displayed on aerial photographs (Fig. 2), as they also are on other late-glacial, but not older, fans in the region. Pierce and Scott (1982) showed that the thickness of carbonate coats on clasts from calcic soil horizons is a useful correlation and relative-age method. Ten different sites where ~ 20 individual carbonate coats were measured averaged 1.07 ± 0.16 mm as follows: Ramshorn fan, 1.0 ± 0.2 , 1.0 ± 0.3 , 1.3 ± 0.4 , 1.1 ± 0.4 , 1.3 ± 0.5 , 1.2 ± 0.4 ; King fan, 1.0 ± 0.2 , 1.1 ± 0.4 , 0.9 ± 0.3 ; Anderson fan, 0.8 ± 0.3 . These carbonate coats are of the same thickness as those on nearby till and outwash deposits of later Pinedale age (Pierce and Scott, 1982). Dating of carbonate coats by the $^{230}\text{Th}/^{234}\text{U}$ isochron method indicates the rate of build-up of these coats is ~ 1 mm/15,000 yr (Szabo and Rosholt, 1982; Pierce and Scott, 1982; Pierce, 1985).

Soils associated with the late-glacial fan surfaces are weakly developed, having cambic B-horizons ~ 15 cm thick and calcic horizons ~ 30 cm thick. The calcic horizons contain stages I and II carbonate morphology (Gile and others, 1966), consistent with soils on late glacial deposits in the region. The soils at the tops of the scarps are not cemented and consequently have not inhibited scarp degradation.

Two 25- to 30-m scarps at the head of the King Canyon fan may have been undercut after late-glacial time, although their form and the relation between material eroded and material deposited on them do not suggest younger undercutting (Appendix, Part 3, sites 86 and 87). These S-facing scarps are not used in the analysis, but they are shown on plots because their large degradation requires degradation rates at least equal to those based on lower scarps.

In conclusion, the scarps used in this analysis are all about the same age and are relict from large stream flows and associated lateral planation during late-glacial time. These scarps are estimated to be $\sim 15,000$ yr old, on the basis of (1) the similar thicknesses of carbonate coats in soils at 10 sites on alluvial surfaces, the depositing streams of which also undercut the scarps; (2) the carbonate-coat thicknesses similar to those on outwash surfaces of the last glaciation; (3) carbonate coats 1 mm thick, indicating an age of 15,000 yr based on $^{230}\text{Th}/^{234}\text{U}$ isochron calibrated rates of deposition; (4) only local modification of the fans by the main streams since late-glacial time; (5) dating of major (but not final) deglaciation in the Rocky Mountains $\sim 14,000$ to $15,000$ yr ago (Porter and others, 1983, p. 99); and (6) similarity with the Lake Bonneville area in Utah, where deposition of fan gravels had largely ceased when the Bonneville shoreline was abandoned $\sim 14,000$ yr ago (W. E. Scott, 1983, written commun.; Scott and others, 1983). An uncertainty of $\pm 4,000$ yr is based on end of glacial conditions $\sim 11,000$ yr ago and full glacial conditions 20,000–18,000 yr ago, with fluvial activity and extensive regrading of fan surfaces from full-glacial time to 14,000–15,000 yr ago.

Present Character of Scarps

The scarps are cut into deposits of sandy gravel. Gravelly colluvium on the scarps now has a silty matrix derived from loess (Pierce and others, 1982) deposited on or at the top of the scarps. The scarps have a rounded, convex upper part and a concave lower part. N-facing scarps are steeper than S-facing scarps (Fig. 3). The midsections are steepest and have a nearly constant surface gradient for about one-half of the scarp height. Excavations show that erosion has occurred above the scarp mid-point and deposition below it. Nearly all of the material eroded from the upper half has been deposited on the lower half, and, with the exception of a minor volume of silt, no detritus has been carried beyond the base of the scarp.

N-facing scarps are better vegetated than are S-facing ones (Fig. 5). Bare ground is exposed over $\sim 70\%$ of the surface on the highest S-facing scarps, compared with only $\sim 10\%$ for the highest N-facing scarps. N-facing scarps have a silty, root-bound sod ~ 5 – 10 cm thick that is resistant to penetration by a shovel, whereas the surface materials on S-facing scarps are nearly cohesionless, with widely scattered roots.

On the scarps, a surface layer one stone thick mantles nearly stone-free silt ~ 5 – 15 cm thick. This segregation of stones from silt is best developed on S-facing scarps. Frost heaving most likely moves stones to the surface and leaves silty material behind (Washburn, 1980, p. 80–90). This segregation process appears to be strong enough to maintain the stone-poor layer, despite mixing due to other slope processes.

Near the mid-points of S-facing, W-facing, and N-facing scarps, pits were dug through the scarp colluvium to in-place gravel to determine the geometry of materials on the scarp. Above the scarp mid-point, colluvium is generally about one-half metre thick and contains 20% to 60% (by volume) loessial silt. On some S-facing scarps, colluvium near the mid-point appears thicker; at one site it is 1 m thick just above the scarp mid-point. Below the mid-point, the colluvium thickens in a manner consistent with an inclination of 30° to 35° on the contact between colluvium and the underlying sandy gravel (see Figs. 1 and 3). Pits near the scarp mid-point exposed soils with cambic B-horizons developed above weak calcic horizons with stage I to stage II carbonate development.



$h = 2.9\text{m}, \theta = 20^\circ$, Loc. 76 (N 20° W)



$h = 1.7\text{m}, \theta = 12^\circ$, near Loc. 35 (S 40° E)



$h = 16.5\text{m}, \theta = 33^\circ$, Loc. 84 (N 15° W)
North-facing



$h = 28.2\text{m}, \theta = 27.5^\circ$, Loc. 87 (S 20° W)
South-facing

Figure 5. Photographs showing denser vegetation cover on N-facing scarps (left) than on S-facing scarps (right). The lower photographs are of high scarps, where vegetation differs the most. The upper photographs are of low scarps, where vegetation differences are more subtle.

MORPHOLOGICAL ANALYSIS USING THE DIFFUSION-EQUATION METHOD

The rate of downslope transport (R) can be expressed as:

$$R = kx^m \left(\frac{\partial y}{\partial x} \right)^n, \quad (1)$$

where k , m , and n are constants and x and y are horizontal and vertical distances. For many slope processes, here called "Group A processes" (Table 1), the rate of downslope transport is directly proportional to surface gradient, so that $m = 0$ and $n = 1$. For these processes, combination of equation 1 with continuity relations yields an equation identical to that for diffusion:

$$\frac{\partial y}{\partial t} = c \frac{\partial^2 y}{\partial x^2}, \quad (2)$$

where t is time, and c is a rate coefficient, assumed here not to vary with position or time. We refer to this diffusion equation with a constant rate coefficient simply as the diffusion equation. For discussion of derivations

and assumptions regarding equation 2, see Culling (1960, 1963, 1965), Souchez (1964), Hirano (1968), Kirkby (1971), Nash (1980a, 1984), Colman and Watson (1983), Hanks and others (1984), Mayer (1984), Trofimov and Moskovkin (1984), and Andrews and Hanks (1985).

We assume a rectilinear starting profile at the angle of repose (Nash, 1980a, 1984). We use an analytical solution for equation 2 (Colman and Watson, 1983, note 11).

$$c = \left(\frac{h}{4t^h \tan \alpha \operatorname{erf}^{-1}(\tan \theta / \tan \alpha)} \right)^2, \quad (3)$$

where h = scarp height, α = starting angle (33.53°), $t = 15,000$ yr, erf^{-1} = inverse error function, and θ = maximum slope angle. This solution yields results identical to Nash's numerical solution.

Other slope processes, here called "Group B processes" (Table 1), are more complex, because downslope movement is not proportional simply to the surface gradient (to the first power). For these processes, m may range from 0 to 2.5, and n may range from 1 to 3 in equation 1 (Kirkby, 1971). Kirkby (1971, p. 26) suggested that for soil wash without gully, $m = 1$, and $n = 1-2$, whereas for soil wash with gully, $m = 2$, and $n = 2$.

TABLE 1. COMPARISON OF GROUP A PROCESSES (EQUATION 2, OR EQUATION 1 WITH $m = 0$, $n = 1$) AND GROUP B PROCESSES (EQUATION 1 WITH $m = .5-2$, $n > 1$)

Process	References
<i>Group A: Downslope movement directly proportional to surface gradient and therefore modeled by diffusion equation</i>	
Soil creep. Expansion and contraction due to freezing and thawing, wetting and drying, and temperature changes. Disturbances by animal burrowing and locomotion, and by growth, decay, and wind movement of plants.	Davaon (1889); Mitchell (1976); Souchez (1964); Culling (1963, 1965); Schumm (1967); Carson and Kirkby (1972); Young (1972).
Raindrop impact. Rain splash on slopes results in net downslope movement.	De Ploey and Savat (1968); Young (1972, p. 66).
<i>Possibly Group A</i>	
Soilification. Important at high latitudes and high altitudes. More dependent on moisture than slope. Proportional to surface gradient for sites moist throughout year.	Washburn (1980, p. 205); Young (1972, p. 61).
<i>Group B: Downslope movement a function of distance or surface gradient to a power greater than one, and therefore not modeled by diffusion equation</i>	
Soil wash (sloperwash). Both without gullying ($m = 0.3-1$) and with gullying ($m = 1-2$). Most effective where ground surface is exposed.	Kirkby (1971); Carson and Kirkby (1972); Schumm (1956); Zingg (1940); Young (1972, p. 62-70); Smith and Washmoer (1962).
Cohesion-limited creep. "Efficiency" of creep process a function of the surface gradient, so $n > 1$ (see Fig. 15).	Figure 15, this paper. Emory's observations suggest that n is not > 1 ; see Carson and Kirkby (1972, p. 286-291); Harris (1973, Fig. 8).

For soil creep where $m = 0$, soil cohesion may cause n to be greater than 1; such creep processes may be Group B processes rather than diffusion-equation-modeled Group A processes.

The profile of a scarp degraded by Group A processes would, from the base up, increase in slope to the mid-point and then decrease in slope to the top (Fig. 6). The form of a scarp degraded by Group B processes, if dominated by soil wash, is a profile with an increase in gradient toward the top of the scarp (Fig. 6). If the two groups of processes operate with equal over-all effect, a composite slope profile results that has a nearly constant surface gradient for about one-half of the scarp height (Fig. 6).

The scarps in the study area were similar to this composite profile (Fig. 6) in that their middle half has an essentially constant slope. Synthetic diffusion-equation profiles based on maximum angle and scarp height

commonly differ slightly from the surveyed profiles by having less material eroded from the crest and less material deposited at the base than modeled by the diffusion equation using θ (Fig. 3). The meaning of these departures may in part be due to uncertainty in measurement. For example, Dave Nash (1985, written commun.) provided a synthetic profile that is a very close fit to the actual profile (x 's in Fig. 3) by making the following changes: a 0.7° rather than a horizontal slope for the upper and lower surfaces, a 7% increase in θ , and a 3% increase in h . These changes cause only a 5% decrease in the calculated value of c .

As the maximum angle is a simple parameter that can be accurately measured, and because it represents both a large part of the scarp and the part of the scarp where transport rates are greatest, we use maximum angle in our analysis, following the work of Nash (1980a, 1984).

EFFECT OF HEIGHT AND ORIENTATION ON SCARP DEGRADATION (RESULTS)

This analysis makes the following assumptions: (1) that starting angles are the same for all heights and orientations of scarps, (2) that the scarps are approximately the same age, (3) that lateral planation forming the scarps was great enough to result in the entire scarp being steepened to the angle of repose (starting angle), (4) that scarp height does not change significantly through time (upper and lower slopes horizontal in profile), (5) that degradation of these scarps may be considered a closed system, (6) that the lithology of the gravels and the effects of loess deposition are not significantly different among the scarps, (7) that regional climate within the study area is essentially constant, and (8) that runoff across the scarps comes only from the catchment area of the scarp. We think these assumptions are reasonable either on grounds already discussed, or because we do not know of evidence to the contrary.

A useful way to present scarp morphology data is the method of Bucknam and Anderson (1979). For six sets of scarps of different ages in Utah, they found a strong empirical correlation between θ and $\log h$. For the N-, S-, and W-facing Idaho scarps (Appendix), linear regressions of θ against $\log h$ have coefficient of determination (r^2 of >0.90) (Fig. 7). For a given scarp height, S-facing scarps have degraded to slopes two-thirds those on N-facing scarps (Table 2).

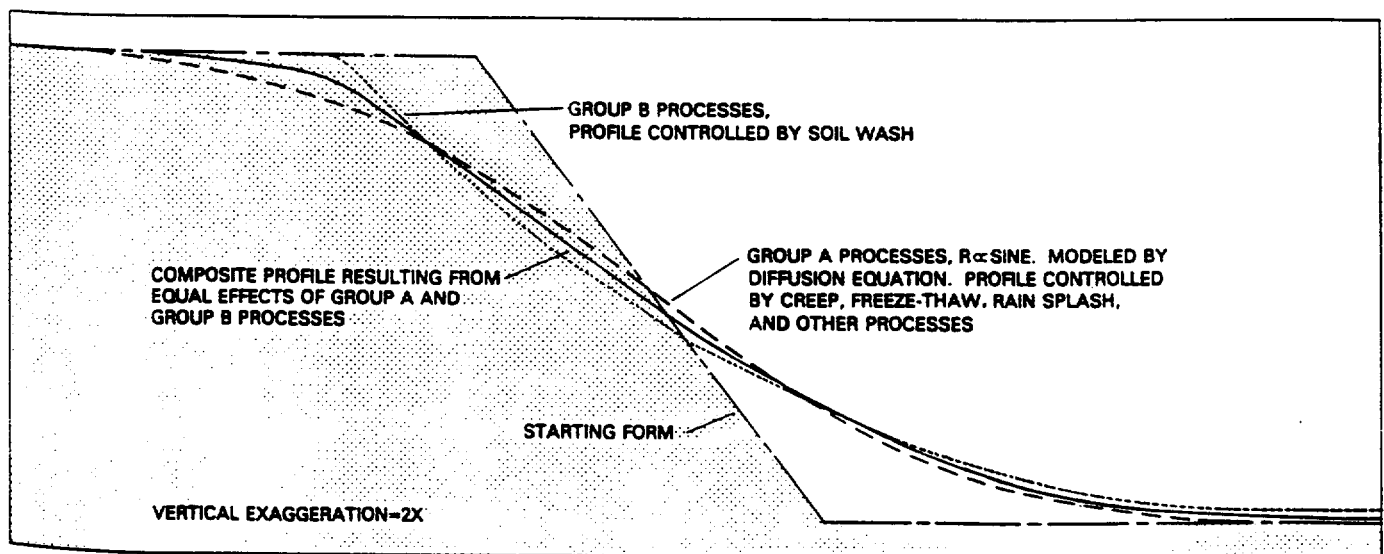


Figure 6. Shapes of scarp profiles formed by Group A and Group B processes (after Kirkby, 1971). Solid line is a visual compromise between lines A and B, and it approximates profile where Group A and B processes produce equal effects.

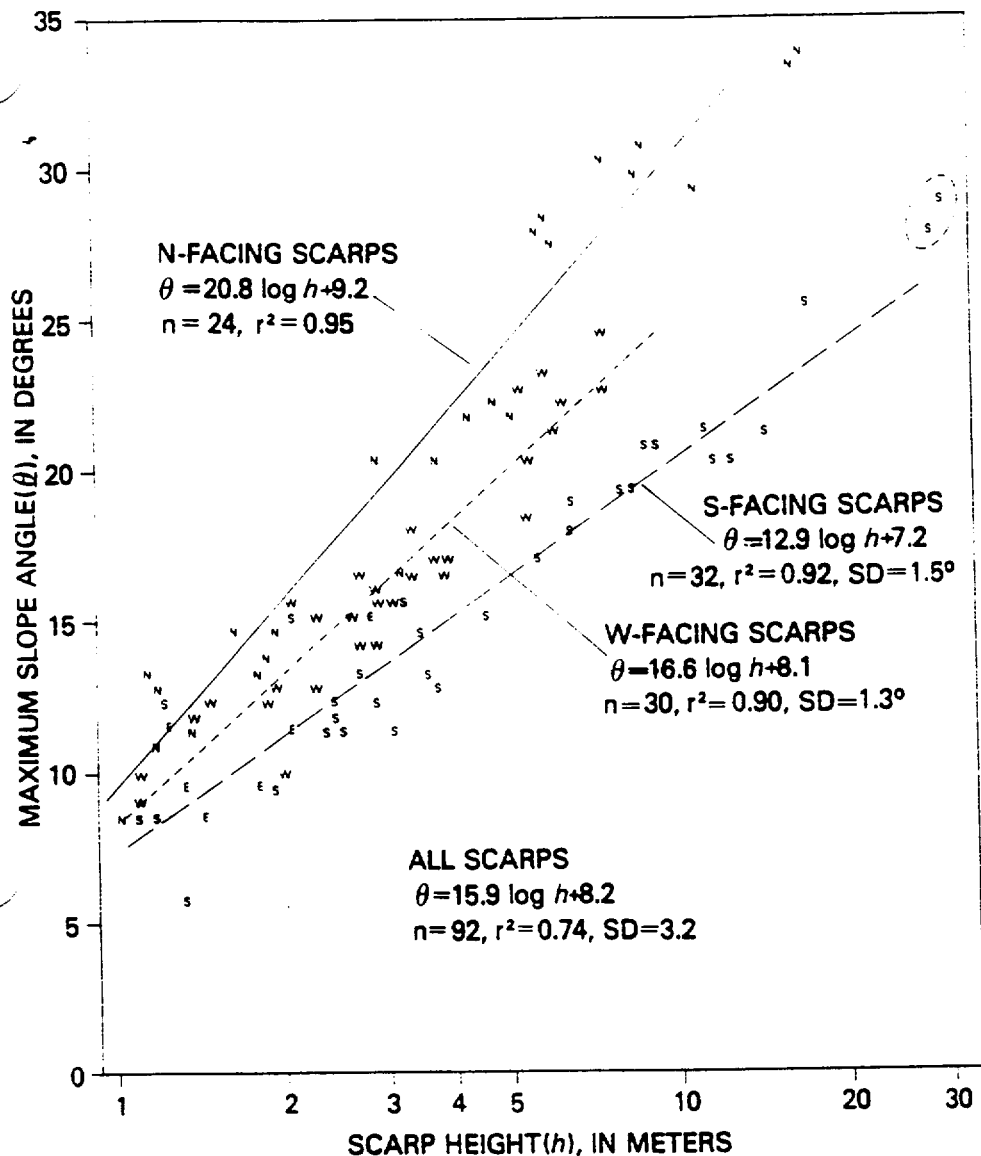


Figure 7. Relation between maximum scarp angle (θ) and scarp height (h , on log scale) for N-, S-, and W-facing scarps. Scarps of a given height have degraded to increasingly lower angles in the following order: N-, W- and S-facing scarps. For regression analyses, n is the number of scarps in a group, r^2 is the coefficient of determination adjusted for degrees of freedom, and SD is the standard deviation of y about the regression line. The two highest S-facing scarps (circled) are excluded from regression analysis, because they may be younger than the others (see text).

TABLE 2. AVERAGE VALUES AND RATIOS FOR S-FACING AND N-FACING SCARPS OF (1) MAXIMUM SLOPES (θ), (2) VOLUMES TRANSPORTED AND MOVED ACROSS SCARP MID-POINTS, AND (3) AVERAGE RATES OF MOVEMENT ACROSS MID-POINTS

Scarp height	Measurement	S-facing	N-facing	South: North
2m	Maximum slope (θ , degrees)	11.1	15.5	0.72
	Volume (m^3)	2.8	1.0	2.8
	Average rate ($m^3/1,000$ yr)	0.2	0.07	
5m	Maximum slope (θ , degrees)	16.2	23.7	0.68
	Volume (m^3)	9.1	3.4	2.7
	Average rate ($m^3/1,000$ yr)	0.6	0.2	
10m	Maximum slope (θ , degrees)	20.1	30.0	0.67
	Volume (m^3)	19.7	7.3	2.7
	Average rate ($m^3/1,000$ yr)	1.3	0.5	
15m	Maximum slope (θ , degrees)	22.4	33.7	0.66
	Volume (m^3)	30.3	11.3	2.7
	Average rate ($m^3/1,000$ yr)	2.0	0.8	

Note: Maximum slopes from regression values from Figure 7. Volumes based on a 1-m-wide belt and regression values from Figure 11. Rates based on scarp age of 15,000 yr (see text). The differences in average rates between N- and S-facing scarps are less than the differences in the rate coefficients c (see text).

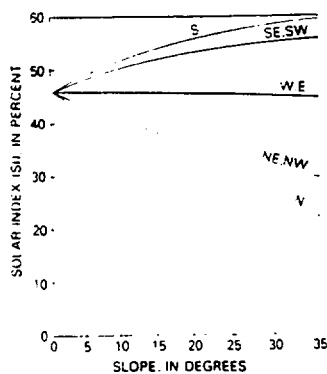
Relation between Maximum Angle and Scarp Height

For scarps of the same age, Bucknam and Anderson (1979) showed that maximum angle steepens with increasing scarp height. We restrict this section to W-facing scarps where microclimate, as reflected by solar insolation, is nearly constant for different inclinations of W-facing slopes (Fig. 8).

As c will be constant if the rate of downslope movement is directly proportional to the surface gradient, the diffusion-equation model predicts the relation between θ and h (Fig. 9, "S"-shaped lines). For W-facing scarps, however, c increases with scarp height (Fig. 9). This means that, using values of c determined for low scarps, the diffusion equation predicts that higher scarps should be steeper than they actually are.

The terrace scarps show a strong, linear relation between c (degradation-rate coefficient, equation 3) and h , such that c increases by $1.5 \times 10^{-4} m^2$ with each metre increase in h (Fig. 10). For processes modeled by the diffusion equation (downslope movement a linear function

Figure 8. Change in solar radiation index (SI) with both scarp orientation and surface gradient at lat. 44°N (from Frank and Lee, 1966). This index is the percentage of potential direct solar-beam radiation that could fall on a surface of the given orientation and inclination and does not account for cloudiness, topography, and diffuse solar radiation.



of surface gradient. Table 1), c should not change with scarp height. Because c is not constant with changing scarp height, we designate our degradation rate coefficient as c^* .

Owing to this unexpected finding that c^* depends on h , we also calculated c^* values for the Bonneville shoreline scarps, assuming a starting angle of 33.5° (Bonneville data from R. C. Bucknam, 1983, written commun.). The Bonneville scarps are also formed in alluvial-fan gravels under a semiarid climate, are ~15,000 yr old (Scott and others, 1983), and are similar in orientation (E-facing and W-facing). The strong dependence of c^* on h for both the Bonneville and Idaho scarps (Fig. 10) demonstrates that the diffusion equation does not completely model degradation of either set of scarps.

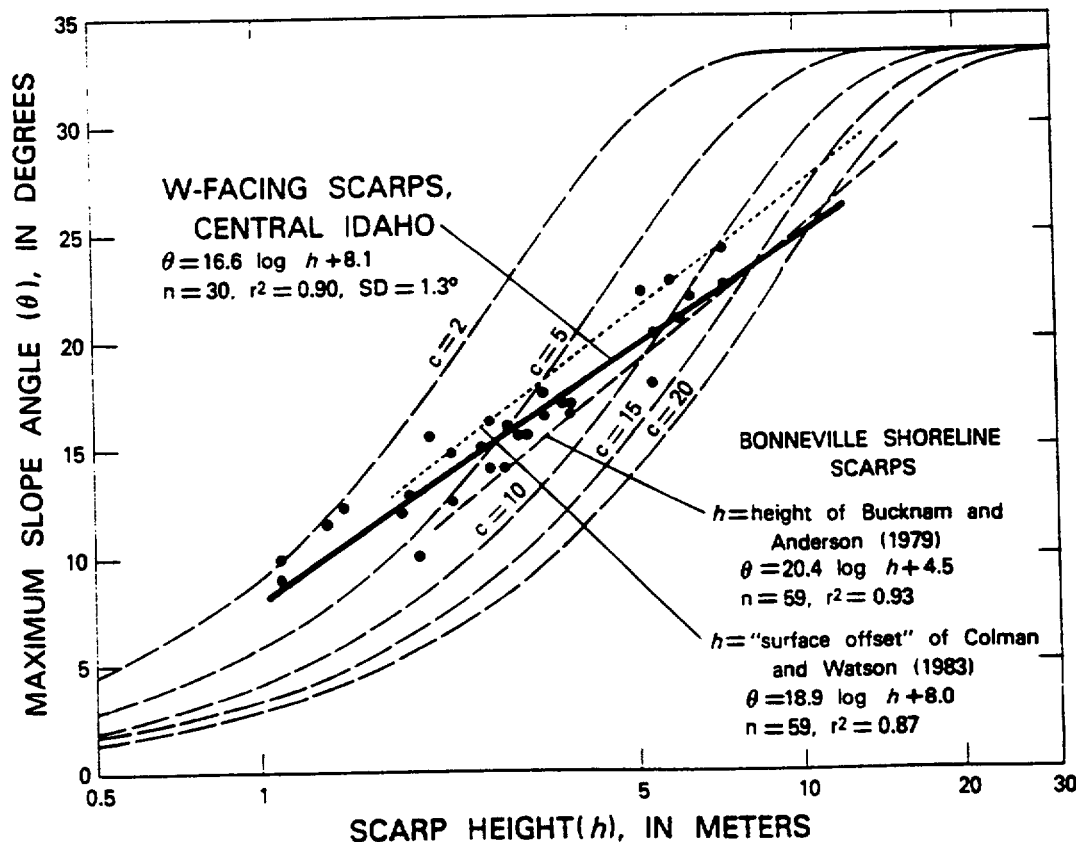
The dependence of c^* on h is sensitive to the starting angle: gentler angles diminish the dependence, and steeper angles accentuate it. Nash

(1980a) found that a 25° starting angle produced the best constant c fit to the Drum Mountains data. Colman and Watson (1983) sought to eliminate the dependence of c on h by reducing the starting angle, yielding starting angles of 30° for Bonneville scarps and 28° for Drum Mountains fault scarps. Hanks and others (1984) noted that c depended on h , assuming a 90° starting angle, but they minimized this relation by assuming starting angles of 31° or lower for the Bonneville and 26° for Drum Mountains scarps.

We think the starting angle is related to the angle of repose and is best determined from consideration of the materials involved and field measurements of vegetated scarps at or near the angle of repose (Nash, 1984), rather than by selection of a starting angle that minimizes the dependence of c on h (Colman and Watson, 1983; Hanks and others, 1984). As noted previously, several vegetated N-facing Idaho scarps are steeper than 33°. Although the Bonneville scarps are now gentler than 29.5°, none surveyed both face north and are as high as the steepest Idaho scarps. A starting angle of 33.5° better fits the Bonneville data, because it halves the standard deviation of tc about h (our value is 3.2 m², versus 5.9 m² of Colman and Watson, 1983).

The dependence of c^* on h indicates that Group B processes, most likely soil wash (slope wash), are involved. Although the dependence of c^* on h indicates that the diffusion equation does not completely model the processes operating on the scarp, we find c^* a useful quantification of scarp degradation rates and tc^* of total degradation amounts. Comparison of scarp degradation in terms of either c^* or tc^* has two advantages over other methods. It accounts for (1) the reduced absolute rates of transport as the surface gradients decrease and (2) volume differences based on the correct relation between height and volume (for scarps of different h but the same θ , the volumes moved are proportional to the ratio of their heights squared).

Figure 9. Departure of W-facing Idaho scarps from relation between θ and h (on log scale) predicted by diffusion-equation model for 5 degradation-rate coefficients (dashed lines, $c \times 10^{-4}$ m²/yr for a 15,000-yr-old scarp). W-facing Idaho scarps (W) define the regression line (solid) that transects constant values of c such that with a fivefold increase in h , c shows an apparent increase of about fivefold. A similar increase in c with h is shown by the Bonneville shoreline scarps. (Bonneville data from R. C. Bucknam, 1983, written commun.).



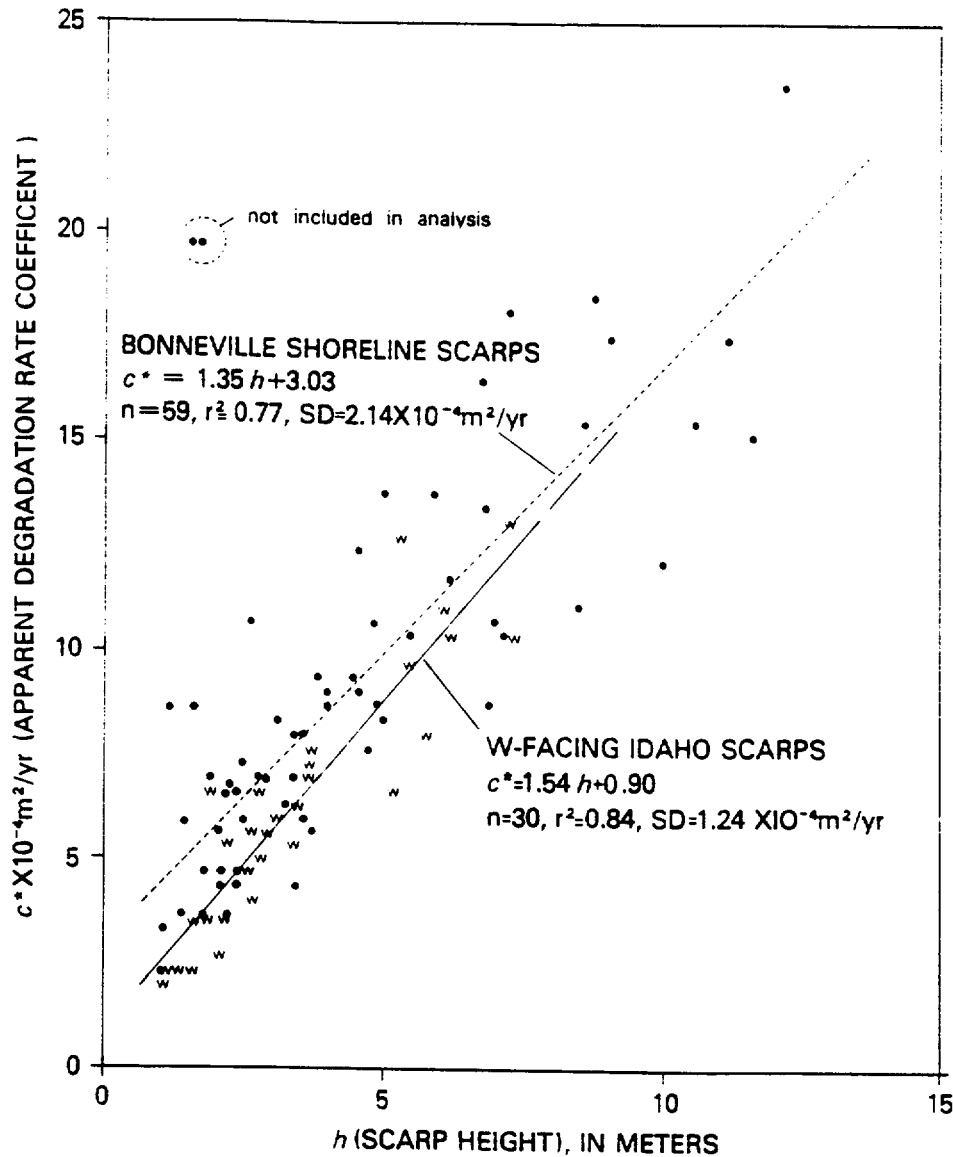


Figure 10. Dependence of the apparent degradation-rate coefficient (c^*) on h for W-facing central Idaho scarps (W). Also shown are Bonneville shoreline scarps that face west or east (solid dots). For the Bonneville shoreline scarps, calculations of c^* use "surface offset" rather than height, so as to account for the effect of the fan slopes above and below the scarps. (Bonneville data from R. C. Bucknam, 1983, written commun.).

Climatic Effects of Orientation

Differences in degradation between N- and S-facing scarps (Fig. 3) may be quantified by estimating the volume of material removed from the top and deposited at the base of a scarp, as determined by planimetry of the area between the present scarp profiles and the inferred original rectangular form (Figs. 1 and 3; Appendix). About three times more material has been removed from the upper parts of S-facing than N-facing scarps of the same height (Fig. 11). Total volume moved, or mean rate of transport, across the scarp mid-point differs by thirtyfold from 2-m-high, N-facing scarps and 15-m-high, S-facing scarps (Fig. 11; Table 2). As the S-facing scarps have degraded to lower slopes, and rate depends on surface gradient, differences in mean rate (Table 2) underestimate the actual contrast between N-facing and S-facing slopes.

Using the diffusion-equation model, S-facing scarps have c^* values that increase greatly with h , whereas c^* values for N-facing scarps increase much less with h (Fig. 12; Table 3). The relations between c^* and h for different orientations (Fig. 12) show both a height effect in addition to that modeled by the diffusion equation and an orientation or microclimatic effect. Solar radiation is probably important to the different slopes of c^*

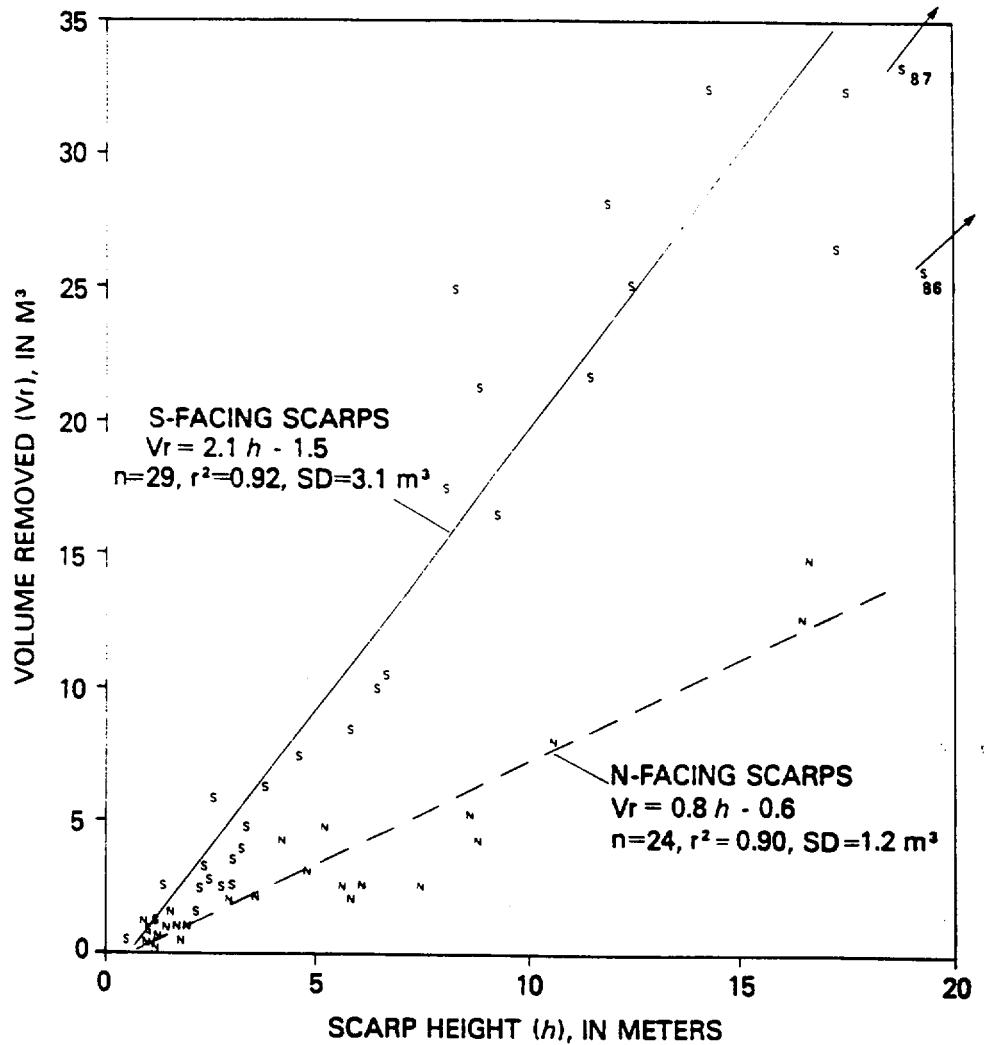
versus h regression lines (Fig. 12), for it increases with steepness (and height) for S-facing scarps but decreases with steepness for the N-facing scarps.

Potential solar-beam radiation is an important and available determinant of microclimate for the different orientations and inclinations of scarps (Fig. 8). For the Idaho scarps, differences in solar radiation affect snow cover, number of freeze-thaw cycles, soil moisture, and vegetative cover. An additional climatic factor is a prevailing southwesterly wind that dries scarps facing south and west and drifts snow onto scarps facing north and east.

For a given latitude, solar index (SI) is the percentage of potential solar-beam radiation on a slope of given orientation and inclination (θ used for inclination) compared to that on a surface kept perpendicular to the sun's rays throughout the day (Fig. 8 and Appendix, interpolated from Frank and Lee, 1966). The index does not account for scattering or blockage by clouds and topography.

To examine the climatic effect of solar radiation on degradation rates, two procedures are used: (1) regression analysis of SI and h on c^* and (2) removal of height effect on c^* and then comparison of the residual with SI .

Figure 11. Relation between volume removed from the upper half of the scarp and scarp height for N- and S-facing Idaho scarps (from Appendix). Arrows show direction to data points for two high scarps (S-86, loc. 86; S-87, loc. 87). These two scarps are excluded from regression analysis because they may be younger than the other scarps (see text).



The dependence of c^* on SI and h is first evaluated by stepwise regression analysis, which shows h has a greater effect on c^* than does SI . F-statistics for the stepwise regression, however, indicate that the contribution of SI to the regression is large and highly significant.

Step 1.

$$c^* = 2.91 h - 2.9$$

$$(r^2 = .77, SD = 8.4 \times 10^{-4} \text{m}^2/\text{yr}). \quad (4)$$

Step 2.

$$c = 2.75 h + 0.67 SI - 31.1$$

$$(r^2 = .90, SD = 5.4 \times 10^{-4} \text{m}^2/\text{yr}). \quad (5)$$

The second procedure removes the height effect from c^* by normalizing all scarps to W-facing ones, where SI does not change with surface inclination (Fig. 8). The regression line for the W-facing group (Fig. 10) approximates this normalizing line, except that the average orientation of the W-facing group is 36° north of due west (Fig. 4). A normalizing line for due-west-facing scarps would therefore have a steeper slope than the line for the W-facing group in Figure 10. To construct a normalizing line approximating c^* versus h for due-west-facing scarps, a line with values of c^* halfway between those of N-facing and S-facing scarps of the same height was defined (Fig. 12).

For each scarp, c^* was subtracted from the normalizing line, yielding residual c^* . For S-facing scarps, residual c^* is positive and increases with height; for N-facing scarps, residual c^* is negative and becomes more negative with height (Fig. 13). These trends parallel the changes in the solar index for N- and S-facing slopes (Fig. 8). The regression line for the W-facing scarps has a negative slope one-third as great as that for N-facing scarps (Fig. 13), compatible with the former's average orientation 36° north of due west (Fig. 4).

A plot of residual c^* on solar index (SI) shows a clear positive dependence (Fig. 14). Linear regression (Fig. 14, equation 1) has a poor correlation coefficient, largely because of the S-shaped distribution. A cubic equation (Fig. 14, equation 2) does better, but an unlikely negative slope occurs in the middle of the range, and the standard deviation remains rather large.

The very high and low values of residual c^* relate to special circumstances noted in the field. The two N-facing scarps in this group have maximum slopes that are so close to the estimated starting angle of 33.5° that they are very sensitive to the exact value chosen. If a 35° starting angle is chosen, they plot much closer to the other points.

The 8 S-facing scarps with high residual c^* values are the only ones higher than 11 m (Fig. 14). Residual c^* for these scarps averages ten times that for smaller S-facing scarps with similar SI . Such large differences in calculated rate coefficients suggest that a geomorphic threshold has been

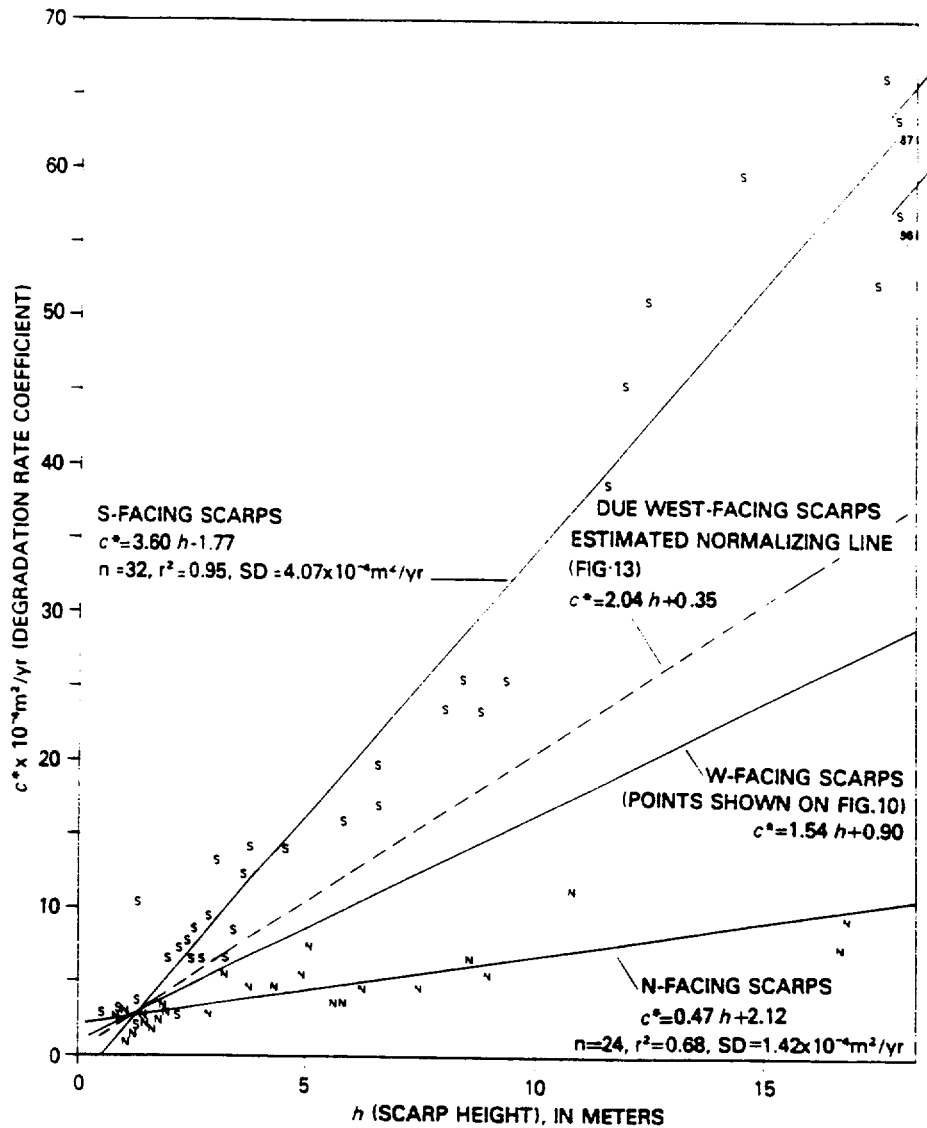


Figure 12. Relations showing that c^* increases much more with h for S-facing than for N-facing scarps. For S-facing scarps, solar radiation increases with increasing surface inclination; for N-facing scarps, it decreases (Fig. 8). For E- or W-facing scarps, solar radiation does not change with surface inclination (Fig. 8). The average orientation of the W-facing group is 36° north of due west (Fig. 4), and so the dashed line for due-W-facing scarps was constructed using values of c^* halfway between those for N-facing and S-facing scarps. For arrows, see Figure 11.

exceeded. For these high S-facing scarps, high residual c^* values probably result from accelerated soil wash. The rate of transport by soil wash depends on slope length, which closely correlates with scarp height. Factors favoring the importance of soil wash for these scarps are the following: (1) they are the highest, longest, steepest scarps and have the greatest amount and velocity of runoff; (2) they have the least vegetative cover; (3) they show abundant evidence of downslope movement such as colluvial mounds decimetres high uphill from bushes; (4) small fans of debris occur at the base of these scarps; and (5) following an intense storm in the summer of 1983, decimetre-wide and -deep rills were cut into these scarps.

Deletion of the eight S-facing and two N-facing scarps from the regression analysis results in improved linear-regression values (Fig. 14, equation 3). A cubic equation (Fig. 4, equation 4) accounts for the obvious S-shaped distribution of points and yields the best results ($r^2 = 0.82$, $SD = 1.7 \times 10^{-4} \text{ m}^2/\text{yr}$, $n = 84$). The height-normalized rates of scarp degradation (res. c^*) thus correlate well with the simple climatic variable solar index, in spite of the following known deficiencies of this analysis, that (1) additional climatic effects such as wind are involved, (2) the diffusion-equation incompletely models the degradation of these scarps, (3) the normalizing procedure for determination of residual c^* is crude, and (4) potential rather than actual solar radiation is used.

DISCUSSION AND IMPLICATIONS

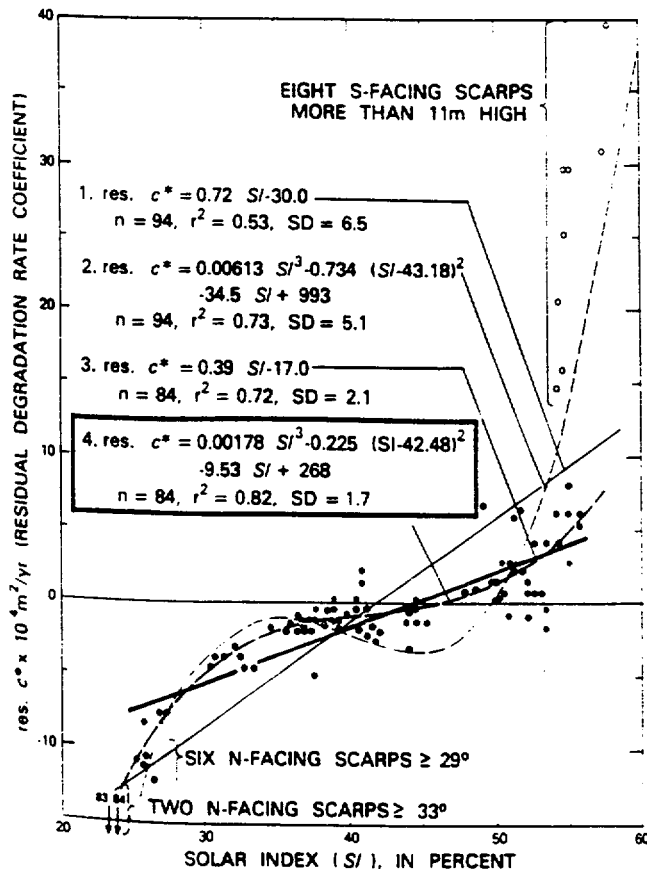
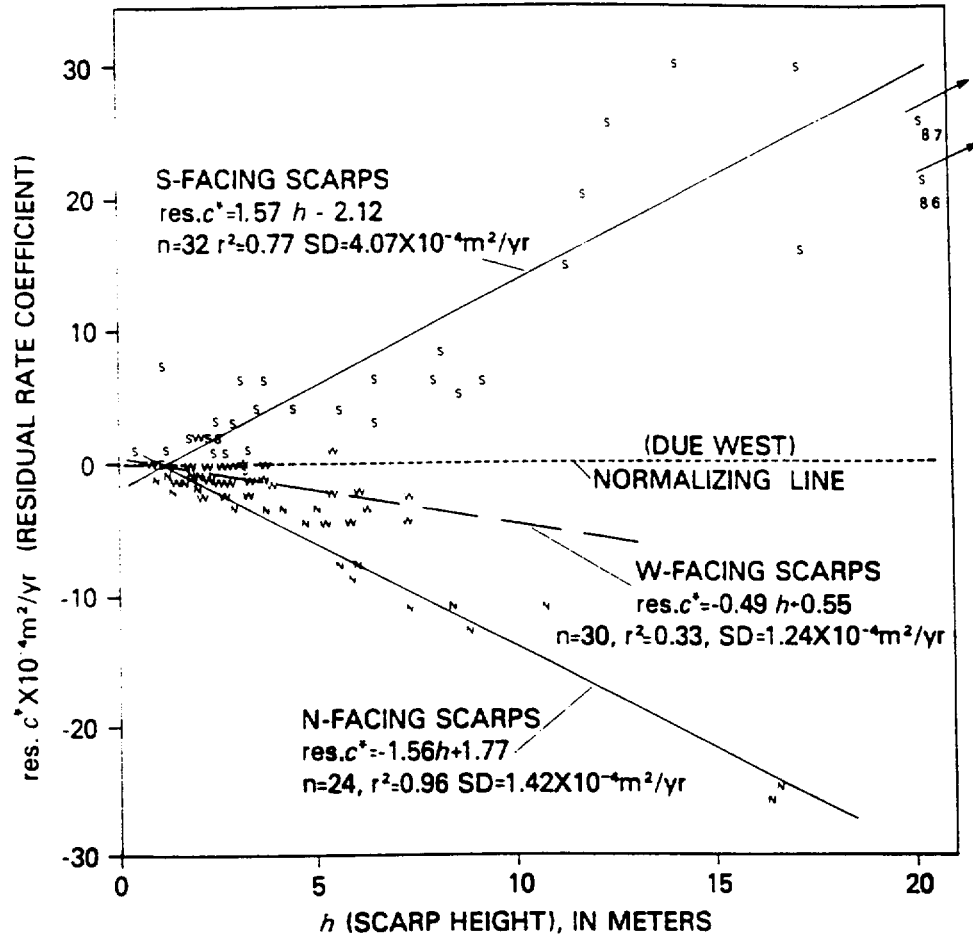
This study has several implications regarding geomorphic processes, slope evolution, valley asymmetry, slope-process modeling, and morphologic dating of fault and terrace scarps. Discussion addresses, first, the implications of the height effect in addition to that modeled by the diffusion equation, then morphologic dating, and, finally, the effect of climate on slope degradation.

TABLE 3. CHANGE IN DEGRADATION RATE COEFFICIENT ($c^* = 10^{-4} \text{ m}^2/\text{yr}$), WITH FIVE HEIGHTS OF N- AND S-FACING SCARPS

Scarp height	S-facing	N-facing	South : North =	South - North =
2	5.4	3.1	1.8*	2.4
5	16.2	4.5	3.6*	12.
10	34.	6.8	5.0*	27.
15	52.	9.2	5.7*	43.
20	70.	12.*	6.1*	59.*

Note: change was determined from regression equations (Fig. 12) for each height.
*Highest N-facing scarp is only 16.5 m; value for 20 m based on projection of regression line.

Figure 13. Plot showing that residual c^* for S-facing scarps is positive and increases with h , whereas residual c^* for N-facing scarps is negative and becomes more negative with h . Residual c^* calculated by normalizing c^* values to those estimated for due-W-facing scarps (Fig. 12). The average orientation of W-facing scarps is north of due west, and thus this group plots between N- and due-W-facing scarps. For arrows, see Figure 11.



Height Effect in Addition to That Predicted by the Diffusion-Equation Model

For the diffusion equation (equation 2) to fully model scarp degradation, the degradation-rate coefficient c should be independent of scarp size, but it changes as a function of height by about tenfold both for W-facing Idaho scarps and for W- or E-facing Bonneville shoreline scarps. If one assumes an initial angle of $<30^\circ$, this dependence on height can be reduced or eliminated, but stable, vegetated scarps as steep as 33.25° to 35° require starting angles no less than 33.5° . Angles of repose of 33.5° or greater are appropriate for sand and gravel, and they become steeper as porosity is decreased by addition of fines, such as loess. The diffusion equation thus incompletely models the degradation of these scarps.

Processes that may contribute to the relation between c^* and height or orientation are listed and ranked in Table 4. Soil wash is probably the main factor responsible for the increase in c^* with scarp height, because (1) soil-wash rates depend on slope length (Zingg, 1940; Carson and

Figure 14. Relation between residual c^* and solar index (SI) showing the effect of local climate on scarp degradation. As the solar index increases, the scarps are subject to both more freeze-thaw cycles and greater drying. Both of these climatic effects result in higher residual c^* (height-normalized degradation rate coefficient). The lowest r^2 and SD value are for equation 4, in which the 8 S-facing scarps higher than 11 m (empty circles) and the N-facing scarps steeper than 33° (below graph) were not included in the regression analysis (see text). Units for standard deviation (SD) are $10^{-4}m^2/yr$.

TABLE 4. SCARP HEIGHT (OR SIZE) AND ORIENTATION (MICROCLIMATE) ATTRIBUTES THAT PROBABLY AFFECT THE APPARENT DEGRADATION-RATE COEFFICIENT c^*

Height (size) attributes	Orientation (microclimate) attributes
Soil wash increases with slope length (and height)	Soil wash more effective on more southerly, drier, less-vegetated slopes
Efficiency of creep may increase with surface gradient (Fig. 15)	Freeze-thaw cycles greater on steeper, more southerly slopes
Lesser infiltration and greater runoff on steeper slopes	Cohesion resistance to creep less on drier, less-vegetated slopes
	Winter snowpack protects more northerly slopes from winter erosion and freeze-thaw and enhances soil moisture and hence vegetation cover
	Steeper slopes drier because they intercept less precipitation per unit horizontal area

Note: attributes listed in order of estimated importance.

Kirkby, 1972; Young, 1972); (2) the effects of soil wash are observed on the Idaho scarps; and (3) soil wash is a logical factor to explain the over-all increase in c^* from well-vegetated N-facing, through W-facing, to poorly vegetated S-facing scarps. In addition, soil wash *with gullying* is the most logical factor to explain the very high c^* values on highest S-facing scarps.

Nash (1980b, 1984) did not recognize a dependence of c on h for wave-cut scarps near Lake Michigan or for fault scarps in the West Yellowstone area. Soil wash does not appear to be important in the degradation of these forested scarps. The presence or absence of a dependence of c on h supports the inference that an additional process, such as soil wash, strongly affects the nonforested Idaho scarps.

Nonlinear creep might also result in a dependence of c on h (equation 1, $n > 1$). Expansion processes such as freezing lift material in a direction normal to the surface (Fig. 15). Upon contraction, vertical settling would result in downslope movement " V_{pd} ," but soil cohesion due to clay, plant roots, surface tension of water, interlocking of grain edges, and other

factors reduces this amount by a retrograde vector " V_r " (Davison, 1889; Young, 1972, p. 51). With increases in surface gradient and V_{pd} , deformation will disrupt the soil, and cohesion, especially that resulting from interlocking grains, will be lessened and efficiency increased (Fig. 15, V_{ad}/V_{pd}). Creep processes in which "efficiency" increases with surface gradient are not modeled by the diffusion equation with a constant rate coefficient.

Another way to regard this efficiency factor is in terms of movement from one stable position to another across an intervening threshold requiring an input of energy (Mitchell, 1976). As represented by rolling a cubic boulder down surface gradients of increasing steepness, the greater the surface gradient, the larger the difference in energy state of the different positions and the lesser the threshold between the two positions.

Either the efficiency or threshold-state model suggests that the increase in rate of downslope creep may depend on the surface gradient to a power exceeding unity. Such a power function would result in a scarp with less material removed from the top and deposited at the base than predicted by the diffusion equation based on θ . Figure 3 and four other simulations of N-facing scarps show this kind of departure of surveyed profiles from diffusion-equation simulations.

Although the simple assumption of the diffusion-equation model, that the rate of downslope movement is a linear function of the surface gradient, is not fully warranted for the Idaho and Utah scarps, the model is still quite useful. The model accounts for the decrease in rate as surface gradients decrease through time, as well as for correctly scaling volume relations between scarps of different heights.

Morphologic Dating of Scarps

Mayer (1984) analyzed the variation in morphologic parameters for several fault scarps in the southwestern United States. He concluded that

EXPLANATION

- V_n Expansion vector normal to scarp surface
- V_{ps} Potential vertical settling vector for cohesionless material
- V_a Actual settling vector due to cohesion between soil particles
- V_{pd} Potential downslope vector for cohesionless material
- V_{ad} Actual downslope vector for cohesive material
- V_r Retrograde vector
- $\frac{V_{ad}}{V_{pd}}$ Efficiency of process

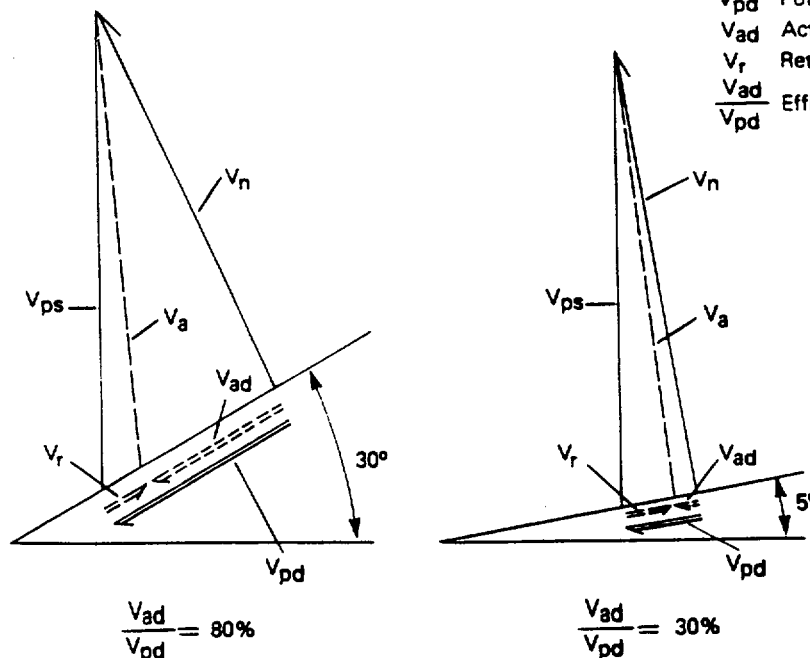


Figure 15. Vector diagram illustrating how interrelations between cohesion and surface gradient may alter the efficiency of creep processes resulting from expansion and contraction. With the increase in surface gradient from 5° to 30°, the value of V_{ad} changes more than does V_r (see text).

the scatter in morphologic data indicates large uncertainties for morphologic age estimates. Factors affecting morphologic variation of scarps are (1) age, (2) lithology, (3) climate and climatic history, (4) orientation, (5) height, (6) erosion by drainages crossing the scarp, (7) scarp burial by alluvial or eolian deposition, and (8) for multiple-event fault scarps, amount, and timing of offsets. Lithology can have a large effect. Along a fault scarp in Nevada, Dodge and Grose (1980) showed that θ is 6° to 10° less for lake clays than for fan gravels. Factors 6 and 7 can be avoided or at least recognized by appropriate field selection of profiling sites. Factor 8 presents difficult problems, but multiple-event scarps may be recognized by such features as abrupt steepening on the scarp, offsets changing with the stratigraphic age of offset unit, and fault scarps higher than those reasonably associated with a single faulting event.

If age-independent sources of variation can be accounted for, more reliable estimates of age may be obtained. In the following example, we modify the diffusion-equation model and estimate the age of an undated scarp by comparing it with a dated scarp. The undated Drum Mountains fault scarps and the dated Bonneville shoreline scarps occur in the same area where similar lithologies have degraded under similar climates on scarps facing either east or west. Using scarp-offset, maximum-slope, and fan-slope data from the Drum Mountains scarps (R. C. Bucknam, 1983, written commun.), and assuming a starting angle of 33.5° , our methods lead to a regression equation:

$$tc^* = 1.16 h + 2.69$$

$$(n = 49, r^2 = 0.40, SD = 2.1 \times 10^{-4} \text{ m}^2/\text{yr}). \quad (6)$$

Given the 15,000-yr age of the Bonneville scarps (Scott and others, 1983), the age of the Drum Mountains scarps can be estimated using c^* values from the two areas, estimated from the regression equations at the same height (Table 5). The dependence of c^* on h is weak for the Drum Mountains scarps ($r^2 = 0.4$), in large part because the range in h is low, but the standard deviation (SD) of c^* about h is actually less than that for the Bonneville scarps. For the Drum Mountains scarps, we place a higher confidence than $r^2 = 0.4$ for the dependence of c^* on h , because r^2 values of 0.84 and 0.77 are determined where the range in h is greater on Idaho and Bonneville scarps.

This method estimates an age of $\sim 9,000$ yr for the Drum Mountains scarps (Table 5). Judging from the scatter of data points about the regression lines for the two scarp heights, we estimate the error limits to be about $\pm 25\%$. Other diffusion-equation dating of the Drum Mountains scarps is 4,800 yr (Colman and Watson, 1983) and 3,600–5,700 yr (Hanks and others, 1984). These estimates compare Drum Mountains scarps averaging 2.4 m high with Bonneville scarps averaging 4.6 m high. Owing to the increase in c^* with h documented in this paper, the twofold difference in h explains why previous ages are about one-half our estimate. An age of $\sim 9,000$ yr is more compatible with the early Holocene age (7,000 to

10,000 yr) estimated by Crone (1983) for the Drum Mountains fault scarp on the basis of local stratigraphy and soil development calibrated using the 15,000-yr-old Bonneville shoreline.

Orientation also needs to be held constant or accounted for in using the morphology of a dated scarp to estimate the age of an undated one. Correction for orientation could be estimated, if the local effects of orientation or solar radiation are known (Figs. 7, 10, 12, and 14). The greatest rates of change in solar radiation and, thus, microclimate with angular changes in orientation occur for easterly and westerly orientations (Fig. 8). Scarp orientations of $\pm 30^\circ$ from due east or west might result in significant scatter of scarp morphology data. For example, Bonneville scarps facing northeasterly generally have values above the average line, whereas scarps facing southwesterly generally have values below it (Figs. 8 and 10; orientation data from R. C. Bucknam, 1983, written commun.).

The W-facing central Idaho terrace scarps are degraded an amount similar to that of the Bonneville shoreline scarps (Figs. 9, 10), dated as 15,000 yr old. Assuming climatic differences are minor, Figure 10 indicates the central Idaho scarps are also $\sim 15,000$ yr old.

Usefulness of θ versus $\log h$ Plot. For most studied scarps, the simple θ versus $\log h$ relation has lower coefficients of determination or standard deviations than those calculated from diffusion-equation analysis (Figs. 7, 9, 10, 12; Bucknam and Anderson, 1979; Colman and Watson, 1983). Regressions of θ on $\log h$ predict unrealistic extremes of negative slopes for very low scarps, as well as slopes greater than the angle of repose for very high scarps (Nash, 1980a). For common heights of fault, terrace, and shoreline scarps, however, $\theta/\log h$ plots are still a useful relative-age method for comparing scarps. Figure 9 shows $\theta/\log h$ plots to have a linear fit to scarp data not modeled by the constant " c " assumption of the diffusion equation. Hanks and others (1984, Fig. 11) showed that plots of tangent θ against scarp height are useful for displaying such data in a format appropriate to the diffusion-equation model, but such plots are nonlinear for the Bonneville data (starting angle = 33.5°).

Dating by the $(h_1/h_2)^2$ Relation. For scarps having the same maximum angle, Nash (1980a) showed that their ages are proportional to the ratio of their heights squared $(h_1/h_2)^2$, if factors other than age are constant, and if the diffusion equation applies. For $\theta/\log h$ regression lines of the Drum Mountains compared to the Panguitch fault scarps, Mayer (1982) showed that Nash's $(h_1/h_2)^2$ relation predicted greater age ratios with greater height of scarps. The Panguitch scarps are mainly multiple-event fault scarps; such scarps have $\theta/\log h$ regression lines displaced to the right and have lesser slopes than scarps representing only the last event (Colman and others, 1981; Machette and McGimsey, 1982, p. 5–8). This is at least part of the explanation of why dating by the $(h_1/h_2)^2$ relation gives too old an age for high, most likely multiple-event fault scarps.

For the single-event Idaho terrace and Utah shoreline scarps, the "height effect in addition to that modeled by the diffusion-equation" also causes a problem in dating by the $(h_1/h_2)^2$ relation. For the two ages of scarps, this method will overestimate actual age differences by mistaking an increase in c^* with h for an increase in age.

Effects of Climate on Scarp Degradation

Greater degradation of slopes facing the equator has been commonly noted, but quantification of this observation in terms of material moved, rates, and rate coefficients generally has not been possible (Carson and Kirkby, 1972, p. 385–389). For central Idaho scarps, S-facing scarps have degraded to slopes 65% to 75% as steep as N-facing scarps, and about 3 times more material has been moved (Table 2). The volumetric differences underestimate the differences in rate coefficients (c^*), because the surface gradients of S-facing scarps are now less. A similar orientation effect is

TABLE 5. AGE ESTIMATES OF DRUM MOUNTAINS FAULT SCARPS BASED ON COMPARISON WITH BONNEVILLE SHORELINE SCARPS OF SAME HEIGHT (SURFACE OFFSET)

Scarp height (offset)	Location	c^* m ²	$10^{-4} c^*$ m ² /yr	t yrs
2 m	Bonneville	8.6	5.7 [†]	15,000
	Drum Mountains	5.0	5.7 [‡]	8,800 [§]
5 m	Bonneville	14.77	9.8 [†]	15,000
	Drum Mountains	8.5	9.8 [‡]	8,700 [§]

Note: See equation 6 for c^* . Drum Mountains scarps.
[†] Calculated using known age (t) of 15,000 yr (Scott and others, 1983)
[‡] Calculated assuming the same c^* as Bonneville shoreline scarps.

apparent for Pleistocene Lake Bonneville scarps in Utah (R. C. Bucknam, 1985, written commun.), where 5 recently profiled S-facing scarps have degraded to slopes 80% of those of E- or W-facing scarps.

The velocity of colluvial movement across the mid-points of the Idaho scarps and the kind of accuracy needed if one wanted to measure modern slope movements can be estimated, assuming a linear increase in velocity above a depth of 20 cm (Carson and Kirkby, 1972, p. 286). For the 6-m-high scarps in Figure 3, the velocity of the ground surface averaged 1.5 mm/yr for the N-facing scarp and 5.6 mm/yr for the S-facing scarp.

Diffusion-Equation Model and Orientation (Microclimate) Differences. S-facing scarps degrade faster than do N-facing ones by amounts that increase with scarp height (Fig. 12; Table 3). Microclimatic changes with orientation are similar to regional climatic differences: vegetation on 15-m-high, N-facing scarps has the morphologic appearance of a prairie grassland, whereas that on the S-facing scarps has the appearance of a shrub desert. For 15-m-high scarps in sandy gravel, the vegetation character and associated degradation rates for S- and N-facing Idaho scarps might be used to infer that scarps in Nevada covered with a sparse shrub desert might degrade about five times faster than scarps in Nebraska covered with a dense prairie grassland.

For N- to S-facing scarps in central Idaho, c^* values range by nearly two orders of magnitude (Fig. 12). This range encompasses values of c determined in semiarid areas for E- or W-facing scarps in Utah, Idaho, and New Mexico and scarps in forested areas near West Yellowstone, Montana (Nash, 1980a, 1984; Colman and Watson, 1983; Hanks and others, 1984; and M. N. Machette, 1984, written commun.).

Values of c faster than any of the Idaho terrace scarps have been determined. Scarps 20 m high in a forested area of Michigan have c values near $120 \times 10^{-4} \text{ m}^2/\text{yr}$ (Nash, 1980b), and scarps 30 m high along the well-vegetated central California coast have c values of $100 \times 10^{-4} \text{ m}^2/\text{yr}$ (Hanks and others, 1984). Notably, these Michigan and California scarps are higher than the Idaho scarps and occur in finer-grained material under a moister climate.

For S-facing central Idaho scarps higher than 11 m, c^* ranges from ~ 40 to $100 \times 10^{-4} \text{ m}^2/\text{yr}$. These rapid degradation-rate coefficients appear to result from soil wash with gullying (equation 1, $m = 2$, $n = 3$; see Kirkby, 1971). These high rates reflect the vulnerability of surficial materials to rill wash when heavy rains fall on poorly vegetated slopes having catchment areas large enough for runoff to become concentrated in small channels.

Solar radiation is the main climatic variable among the terrace scarps in semiarid central Idaho (Table 4). Greater solar radiation results in higher degradation-rate coefficients (c^*) by reducing soil moisture, minimizing vegetation and root stabilization, increasing freeze-thaw cycles, and reducing snow cover. Removal of the "scarp height effect in addition to that modeled by the diffusion equation" results in a strong relation between residual c^* and solar radiation (Fig. 14, equation 4, $r^2 = 0.82$).

In central Idaho, climate is such that variation in scarp orientation results in pronounced vegetation differences. In wetter and perhaps also in drier areas, vegetation differences and associated differences in degradation rates may not be as pronounced.

Russell (1909) noted that slope asymmetry in the United States was more prominent north of the January freezing isotherm and suggested that this asymmetry was caused by more numerous freeze-thaw cycles on S-facing slopes and a greater duration of snow cover on N-facing slopes,

two of the four orientation effects (Table 4) that we consider important for central Idaho. A layer of stone-free silt below a surface stony layer on S-facing Idaho scarps shows that frost heaving and segregation are strong enough to dynamically maintain this sorting in spite of other processes mixing the two layers.

Microclimatic differences do not always result in greater degradation of S-facing slopes at temperate latitudes in the Northern Hemisphere. Near the Utah-Nevada border, R. E. Anderson (1983, oral commun.) noted steeper S-facing slopes of valleys incised into basin-fill deposits; the steeper S-facing slopes may result from a cement of soil carbonate stabilizing the drier, S-facing slopes. In central Utah, a different process results in slope asymmetry. R. Fleming (1984, oral commun.) noted that in areas of moderate precipitation, N-facing slopes underlain by the North Horn Formation are gentler than S-facing slopes. The North Horn Formation is rich in swelling clays, and greater soil moisture caused by lesser solar radiation on N-facing slopes may enhance soil creep.

CONCLUDING STATEMENT

Geologic studies such as this can rather simply quantify slope degradation by integrating over thousands of years the effects of slow geomorphic processes. Modern slope measurements yielding results comparable to this study would be expensive and require years of observations. They would require depth-integrated measurements of slope movements in the 1 mm/yr range for many tens of scarps and be compromised by "atypical" processes associated with possible overgrazing and trampling of slopes by cattle.

Additional studies of scarps of different heights and orientations in areas with different climates, vegetation, and materials should lead to a more fundamental general understanding of slope processes and their rates and of the evolution of slopes through time and under changing climates.

ACKNOWLEDGMENTS

We thank Mike Winter for field, computer, and drafting assistance; Andrew Pierce, Fred Hawkins, and Daniel Pierce for field help; and Linda Pierce for editorial help. Hal Malde, Tony Crone, Larry Mayer, and an anonymous reviewer gave helpful reviews. Our understanding of this topic has benefited from discussions with Mike Machette, Bill Scott, Tony Crone, Bob Bucknam, Ernie Anderson, and especially Dave Nash.

REFERENCES CITED

- Andrews, D. J., and Hanks, T. C., 1985, Scarp degraded by linear diffusion: Inverse solution for age: *Journal of Geophysical Research*, v. 90, p. 10,193-10,208.
- Bucknam, R. C., and Anderson, R. E., 1979, Estimation of fault-scarp ages from a scarp-height-slope-angle relationship: *Geology*, v. 7, p. 11-14.
- Carrara, P. E., Mode, W. N., Rubus, Meyer, and Robinson, S. W., 1984, Deglaciation and postglacial timberline in the San Juan Mountains, Colorado: *Quaternary Research*, v. 21, no. 1, p. 42-55.
- Carson, M. A., and Kirkby, M. J., 1972, *Hillslope form and process*: London, England, Cambridge University Press, 475 p.
- Colman, S. M., and Watson, Ken, 1983, Ages estimated from a diffusion equation model for scarp degradation: *Science*, v. 221, p. 263-265.
- Colman, S. M., McCauley, James, and Osteraa, D. A., 1981, Morphology of fault scarps in the Rio Grande Rift, Colorado, as an indicator of age of faulting: *Colorado Geological Survey Special Publication* 19, p. 34-35.
- Crone, A. J., 1983, Amount of displacement and estimated age of a Holocene surface faulting event, eastern Great Basin, Millard County, Utah, in Gurgel, K. D., ed., *Geologic excursion in neotectonics and engineering geology in Utah*: Utah Geological and Mineral Survey Special Studies, v. 62, p. 49-55.
- Culling, W. E. H., 1960, Analytical theory of erosion: *Journal of Geology*, v. 68, p. 336-344.
- , 1963, Soil creep and the development of hillside slopes: *Journal of Geology*, v. 71, p. 127-161.
- , 1965, Theory of erosion on soil-covered slopes: *Journal of Geology*, v. 73, p. 230-254.
- Davison, Charles, 1889, On creeping of the soil-cap through the action of frost: *Geological Magazine*, Decade 3, v. p. 255-261.
- De Ploey, J., and Savat, J., 1968, Contribution à l'étude de l'érosion par le splash: *Zeitschrift für Geomorphologie*, v. 1, p. 174-193.

- Dodge, R. L., and Grise, L. T., 1980. Tectonic and geomorphic evolution of the Black Rock Fault, northwestern Nevada. *in* Andrus, P. C., compiler, Earthquake hazards along the Wasatch Sierra-Nevada frontal fault zones: U.S. Geological Survey Open-File Report 80-801, p. 494-508.
- Dohrenwend, J. C., 1978. Systematic valley asymmetry in the central California Coast Ranges: *Geological Society of America Bulletin*, v. 89, p. 891-900.
- Frank, E. C., and Lee, Richard, 1966. Potential beam irradiation on slopes: Tables for 30° to 50° latitude: Fort Collins, Colorado, U.S. Forest Service Research Paper RM-18, Rocky Mountain Forest and Range Experiment Station, 116 p.
- Gilbert, G. K., 1877. *Geology of the Henry Mountains*: Washington, D.C., U.S. Geological and Geographical Survey, 160 p.
- Gile, L. H., Peterson, F. F., and Grossman, R. B., 1966. Morphological and genetic sequences of carbonate accumulation in desert soils: *Soil Science*, v. 101, p. 347-360.
- Hanks, T. C., Bucknam, R. C., Lajoie, K. R., and Wallace, R. E., 1984. Modification of wave-cut and faulting-controlled landforms: *Journal of Geophysical Research*, v. 89, no. B7, p. 5771-5790.
- Harris, S. A., 1973. Studies of soil creep, western Alberta, 1970 to 1972. *Arctic and Alpine Research*, v. 5, no. 3, pt. 2, p. A-171-A-180.
- Hessner, C. J., 1983. Vegetational history of the northwestern United States including Alaska. *in* Porter, S. C., ed., *The Late Pleistocene*. *in* Wright, H. E., Jr., ed., *Late Quaternary environments of the United States*. Volume 1: Minneapolis, Minnesota, University of Minnesota Press, p. 239-258.
- Hirano, M., 1968. A mathematical model of slope development—An approach to the analytical theory of erosional topography: *Journal of Geosciences, Osaka City University*, v. 11, p. 13-52.
- Kirkby, M. J., 1971. Hillslope process-response models based on the continuity equation. *in* Brunsden, D., ed., *Slopes: Form and process*: Institute of British Geographers Special Publication 3, p. 15-30.
- Knapp, C. L., Stoffel, T. C., and Whitaker, S. D., 1980. *Insolation data manual*: Solar Energy Research Institute, SERI-SP-755-789, 282 p.
- Machette, M. N., and McGimsey, R. G., 1982. Quaternary and Pliocene faults in the Socorro and western part of the Fort Sumner 1° x 2° quadrangles, New Mexico: U.S. Geological Survey Miscellaneous Field Studies Map MF-1465-A with 12 p. pamphlet.
- Mayer, Larry, 1982. Quantitative tectonic geomorphology with applications to neotectonics of northwestern Arizona (Ph.D. dissertation): Tucson, Arizona, University of Arizona, 213 p.
- , 1984. Dating Quaternary fault scarps formed in alluvium using morphologic parameters: *Quaternary Research*, v. 22, p. 300-313.
- Melton, M. A., 1960. Intravalley variation in slope angles related to microclimate and erosional environment: *Geological Society of America Bulletin*, v. 71, p. 133-144.
- Mitchell, J. K., 1976. *Fundamentals of soil behavior*: New York, Wiley, 422 p.
- Nash, D. B., 1980a. Morphologic dating of degraded normal fault scarps: *Journal of Geology*, v. 88, p. 353-360.
- , 1980b. Forms of bluffs degraded for different length of time in Emmet County, Michigan, U.S.A.: *Earth Surface Processes*, v. 5, p. 331-345.
- , 1980c. Morphologic dating of fluvial terrace scarps and fault scarps near West Yellowstone, Montana: *Geological Society of America Bulletin*, v. 95, p. 1413-1424.
- Pierce, K. L., 1985. Quaternary history of faulting on the Arco segment of the Lost River fault, central Idaho. *in* Stein, R. S., and Bucknam, R. C., eds., Conference 28 on the Borah Peak earthquake. Proceedings: U.S. Geological Survey Open-File Report 85-290, p. 195-206.
- Pierce, K. L., and Scott, W. E., 1982. Pleistocene episodes of alluvial-gravel deposition, southeastern Idaho. *in* Bonnicksen, Bill, and Breckenridge, R. M., eds., *Cenozoic geology of Idaho*: Idaho Bureau of Mines and Geology Bulletin 26, p. 685-702.
- Pierce, K. L., Fosberg, M. A., Scott, W. E., Lewis, G. C., and Colman, S. M., 1982. Loess deposits of southeastern Idaho: Age and correlation of the upper two loess units. *in* Bonnicksen, Bill, and Breckenridge, R. M., eds., *Cenozoic geology of Idaho*: Idaho Bureau of Mines and Geology Bulletin 26, p. 717-725.
- Porter, S. C., Pierce, K. L., and Hamilton, T. D., 1983. Late Wisconsin mountain glaciation in the western United States. *in* Porter, S. C., ed., *The late Pleistocene*. Volume 1. *in* Wright, H. E., Jr., ed., *Late Quaternary environments of the United States*: Minneapolis, Minnesota, University of Minnesota Press, p. 71-111.
- Rahn, P. H., 1969. The relationship between natural forested slopes and angles of repose for sand and gravel: *Geological Society of America Bulletin*, v. 80, p. 2123-2128.
- Russell, R. J., 1909. Geomorphic evidence of a climatic boundary: *Science*, v. 74, p. 484-485.
- Schumm, S. A., 1956. The role of creep and rainwash on the retreat of badland slopes: *American Journal of Science*, v. 254, p. 693-706.
- , 1967. Rates of surficial rock creep on hillslopes in western Colorado: *Science*, v. 155, p. 560-561.
- Scott, W. E., 1982. Surficial geologic map of the eastern Snake River Plain and adjacent areas, 111° to 115° west, Idaho and Wyoming: U.S. Geological Survey Miscellaneous Geologic Investigations Series Map I-1372, 2 sheets, scale 1:250,000.
- Scott, W. E., McCoy, W. D., Shroba, R. R., and Ruben, Meyer, 1983. Reinterpretation of the exposed record of the last two lake cycles of Lake Bonneville, western United States: *Quaternary Research*, v. 20, p. 261-285.
- Scott, W. E., Pierce, K. L., and Hart, M. H., Jr., 1985. Quaternary tectonic setting of the 1983 Borah Peak Earthquake, central Idaho: *Bulletin of the Seismological Society of America*, v. 75, p. 1053-1066.
- Smith, D. D., and Wachsmier, W. H., 1962. Rainfall erosion: *Advances in Agronomy*, v. 14, p. 109-148.
- Souches, R., 1964. Viscosité, plasticité, et rupture dans l'évolution de versants: *Ciel and Terre*, v. 80, p. 3-24.
- Statham, Ian, 1974. The relationship of porosity and angle of repose to mixture proportions in assemblages of different sized materials: *Sedimentology*, v. 21, p. 149-162.
- Szabo, B. J., and Rosholt, J. N., 1982. Surface continental sediments. *in* Ivanovich, M., and Harmon, R. S., eds., *Uranium series disequilibrium: Applications to environmental problems*: Oxford, England, Clarendon Press, p. 246-269.
- Trofimov, A. M., and Moskovkin, V. M., 1984. Diffusion models of slope development: *Earth Surface Processes and Landforms*, v. 9, p. 435-453.
- U.S. Weather Bureau, 1959. *Climates of the States—Idaho*: Climatology of the United States, no. 60-10, 16 p.
- Visher, S. S., 1954. *Climatic atlas of the United States*: Cambridge, Massachusetts, Harvard University Press, 403 p.
- Wallace, R. E., 1977. Profiles and ages of young fault scarps, north central Nevada: *Geological Society of America Bulletin*, v. 88, p. 1267-1281.
- Washburn, A. L., 1980. *Geocryology*: New York, John Wiley & Sons, 406 p.
- Young, A., 1972. *Slopes*: Edinburgh, Oliver and Boyd, 288 p.
- Zingg, A. W., 1940. Degree and length of land slope as it affects soil loss in runoff: *Agricultural Engineering*, v. 21, p. 59-64.

MANUSCRIPT RECEIVED BY THE SOCIETY APRIL 8, 1985

REVISED MANUSCRIPT RECEIVED FEBRUARY 19, 1986

MANUSCRIPT ACCEPTED FEBRUARY 20, 1986

EOS

Transactions, American Geophysical Union
Vol. 71 No. 43 October 23, 1990



Identification of the surface and subsurface soil conditions at the same site has been accomplished through visual inspection and laboratory tests on soil specimens which have been obtained from borings or through other soil sampling techniques, as well as from data acquired from soil moisture measuring devices.

It is the explicit goal of this effort to develop field experimental techniques that can be utilized in point-, plot-, and basin-scale studies conducted for the purpose of aggregating, in a physically based manner, large-scale processes related to the hydrologic cycle, in conjunction with digital terrain analysis, geographic information systems and remote sensing.

H52A-15 1330h POSTER

An Unusual Playa Scraper at Double Lakes, TX

C. C. Reeves Jr (Department of Geosciences, Texas Tech University, Lubbock, TX 79409; 806-742-3115) (Sponsor: Stanley Cebull)

Examples of "grooving" of sediments and rock by overlying moving objects are common in glacial and arid areas. However, controversy concerning the cause/method of movement has been centered on the playa scrapers of the western United States.

Whereas movement was first attributed to wind for California scrapers, very heavy (300 lb) scrapers led Stanley (1955) to suggest wind-blown ice floes. Sharp (1960) subsequently provided a theoretical study showing that scrapers could be propelled across a muddy playa only by winds of unusual velocity (125 mph), and then only if a sufficiently high pore pressure existed beneath the objects. Motts (1969) found considerable evidence on several California playas for moving ice floes, but Sharp and Carey (1979) concluded that the stone scrapers on Racetrack Playa (CA) had been moved by the wind and that "...ice sheets are not required."

The recent discovery of a heavy steel water tank plya scraper and track conclusively shows that 1) movement has been intermittent, 2) that the most recent event moved the tank about 400 feet, 3) that the tank did not roll during movement but remained in a fixed position, 4) that the tank was oriented normal to the prevailing direction of movement (normal to wind direction), and 5) that the tank was subsequently rotated 90° after last movement. All of the above is consistent with the tank having been frozen in a drifting ice floe.

H52A-16 1330h POSTER

USING COSMOGENIC NOBLE GASES TO ESTIMATE EROSION RATES

J. Poths and F. Goff (Both at: Los Alamos National Laboratory, Los Alamos, NM 87545)

We have analyzed for He and Ne in quartz and sanidine separates from 3 samples of Bandalier Tuff on the Pajarito plateau near Los Alamos, New Mexico. Two are surface samples from different locations on a single mesa, and the third is a shielded sample taken from a road cut. Both minerals from the exposed samples show clear signals of cosmogenic Ne-21. There is no excess Ne-21 in the shielded sample, implying that "background" nuclear reactions are negligible. The ratio of cosmogenic Ne-21 in sanidine/quartz is 1.8 ± 0.4 . Using a surface Ne-21 production rate (currently known only within a factor of two) of 150 atoms/gm-yr for sanidine at the Los Alamos location, a density of 1.25 g/cm^3 for tuff, and an attenuation length for production of cosmogenic Ne-21 of 160 gm/cm^2 , the two samples yield erosion rates of 1.8 ± 0.5 and $2.8 \pm 0.5 \text{ cm/1000 yrs}$ (analytical uncertainties only). This rate is similar to those measured at Hawaii of $0.8-1.1 \text{ cm/1000 yrs}$ (1), and lower than the rate for erosion in stream beds in the Bandalier Tuff of 200 cm/1000 yrs (2). Better calibration of the Ne-21 production rate will make this a very viable and useful technique for estimating erosion rates on surfaces developed in a variety of rock types. In contrast, all samples show little or no cosmogenic He-3 (<5% of that expected based on Ne-21), reiterating Cerling's result (3) that cosmogenic He is readily lost from quartz and feldspar. Refs: (1) M. Kurz, Geochim. Cosmochim. Acta 50, 2855-2862, 1986; (2) F. Goff & L. Shevenell, Geol. Soc. Am. Bull. 92, 292-302, 1987; (3) T. Cerling, Quatern. Res. 33, 148-156, 1990. Support provided by BES/Geosciences.

H52A-17 1330h POSTER

Rapid Long-Term Rates of Erosion in NW Pakistan

D.W. Burbank and R.A. Beck (Dept. of Geological Sciences, Univ. of Southern California, Los Angeles, CA 90089-0740)

Chronologic control derived from numerous magnetic polarity stratigraphies, in combination with stratigraphic control from measured sections and detailed mapping, permits minimum long-term erosion rates during the past 6 Myr to be calculated for portions of the Himalayan foreland basin in northern Pakistan. The simplified stratigraphy of the foreland comprises a wedge of fluvial sandstones and overbank sediments that is 3-6 km thick and overlies a predominantly carbonate succession of ~1 km thickness. In several different areas, the timing of the initiation and cessation of uplift can be closely constrained based on the stratigraphic and structural signature of deformational events that is preserved within the foreland strata. These events include development of a box fold, initial translation of a hanging wall up a frontal ramp, and later translation across the adjacent thrust flat. Mean rates of uplift, averaging 2-15 mm/yr, were sustained over intervals of 0.2-1.6 Myr. Given the resolution of the available time constraints, the rate of denudation of the uplifted fluvial strata closely approaches the rate of uplift. Within the Soan Syncline, a mean thickness of 3 km across an area of >80 km² was removed in <0.3-0.2 Myr. Two episodes of deformation are discernible in the Salt Range. During the first, a mean of ~1.5 km of fluvial strata were removed over an interval of ~0.5 Myr from an area likely to exceed 300 km², whereas in the second, 2.5-3.0 km of strata were eroded during the past 1.6 Myr from an area exceeding 1500 km². Rates of denudation appear to have dropped dramatically when predominantly carbonate strata were being exposed to erosion. These observations suggest that 1) moderately to weakly cemented fluvial strata are highly susceptible to erosion when uplifted; 2) rapid rates of thrust motion and uplift may produce relatively subdued topography when fluvial strata are involved; 3) due to erosional stripping of an allocthon, significant crustal subsidence directly attributable to the emplacement of a thick hanging wall may not occur, although the redistribution of the eroded sediment load would be expected to cause more distributed subsidence to occur, and 4) in contrast to several previous studies, long-term rates of erosion can approach rates of uplift under special conditions.

H52B CA: 414 Fri 1330h Groundwater Hydrology II Presiding: T C J Yeh, Univ of Arizona

H52B-1 1330h

A Steady-State Solution for Flow to a Finite-Diameter Well in a Multiaquifer Groundwater System

N. Hsu and T. Chang (Both at: Department of Civil Engineering, National Taiwan University, Taipei, Taiwan, Republic of China)

In this paper, a steady-state solution for flow to a finite-diameter well in a multiaquifer groundwater system is given. Aquifer and aquitard properties may vary from one layer to the next but are assumed to be isotropic and homogeneous in the horizontal direction. Normally, the solution of a generalized eigenvalue problem is required for the numerical evaluation of the problem. However, the solution developed in this paper is more general and can be reduced to the special case in which the diameter of the well is approaching zero. If pumping is from a number of aquifers, an iterative algorithm is proposed to calculate the pumping rates from these aquifers. Numerical examples are provided to calculate the solutions for a hypothetical multiaquifer groundwater system. The sensitivity of the diameter of the well to the solution is further investigated.

H52B-2 1345h

The Use of Vertical Interpolation Functions for Modeling Leaky Aquifer Problems

J. M. McCartney and A. Buikis (Both at: Dept. of Physics and Mathematics, Latvia University, 226098 Riga, Latvia, USSR)

Vertical interpolation functions are assumed to represent the vertical head distribution for the aquifers and aquitard of a leaky aquifer system. Coefficients for the interpolation functions are chosen to conserve mass and satisfy the boundary conditions in the vertical direction. Using this representation of the vertical head distribution, it is quite easy to integrate over depth and obtain a modified version of the classical leaky aquifer problem. This modification is easily implemented and provides a number of important advantages over the classical approach, including:

- 1) No model modification is necessary when the depth of the separating aquitard approaches zero.
- 2) A good approximation to the vertical head distribution can easily be generated using the vertical interpolation functions and the modified solution to the classical leaky aquifer problem.

H52B-3 1400h

An Evaluation of Parallel-Processing Algorithm Efficiency for Large Scale, Three-Dimensional, Unconfined Groundwater Flow Simulations

M.M. Hughes, C.T. Miller, and A.S. Mayer (Department of Environmental Sciences and Engineering, 105 Rosenau Hall, CB# 7400, University of North Carolina, Chapel Hill, NC 27599-7400; 919-966-2643)

The simulation of transient, three-dimensional, saturated groundwater flow problems is performed routinely. However, accurate simulation of typical heterogeneous systems can lead to discretization patterns with 100,000 or more degrees of freedom. While problems of this size can be simulated with available computing resources, it is desirable to reduce the computational burden below the level required by popular finite-difference models. Previous research has demonstrated that algorithms that exploit vector and parallel processing hardware can significantly reduce computational requirements.

This research involves the comparison of Picard, Newton-Raphson, and Broden iterative methods for resolving the nonlinearities associated with unconfined flow—within the construct of a parallel solution algorithm. Iterative and direct matrix-vector solvers also are analyzed with respect to computational efficiency. A predictor-corrector finite-element approximation is employed in space, while a variable time-weighted finite-difference approximation for temporal derivatives is used. This approach uncouples a three-dimensional problem into, first, a parallel set of two-dimensional problems, and second, a parallel set of one-dimensional problems. Comparisons are made between the parallel finite-element model and a commonly-used finite-difference model, for a series of large-scale simulations. Solution results are shown as a function of vector and parallel processing implementation under two hardware platforms: a Convex C240 and a Cray Y-MP. The results reinforce the importance of proper algorithm and code design to exploit emerging computer architectures.

H52B-4 1415h

Convergence and Accuracy of Numerical Solutions to the Richards Equation

T.-C. Jim Yeh and Rajesh Srivastava (Both at: Department of Hydrology and Water Resources, University of Arizona, Tucson, Arizona 85721)

Analytical solutions describing the transient soil-water pressure distributions during one-dimensional, vertical infiltration toward the water table through homogeneous and two-layer soils are derived. Exponential functional forms are used to represent the hydraulic conductivity and pressure relation and the soil-water release curve. Steady-state profiles are used as initial conditions. Hydraulic behaviors of the soils during wetting and drainage scenarios are simulated.

Numerical models using Picard, Modified Picard, and Newton-Raphson iteration schemes are constructed. Simulated pressure and moisture content profiles in homogeneous and layered soils, using these models are compared to those obtained from the analytical solutions. Accuracy of the numerical models is examined. The criterion for selecting the time-step size: ensuring the convergence of the numerical solutions is derived. Generally, the time-step size is proportional to the element size and moisture capacity, and is inversely proportional to the infiltration rate.

H52B-5 1430h

Two-phase Flow Simulations in Porous Media: Mass Conservation and Phase Velocities

Michael A. Celia and Philip Binning (Water Resources Program, Dept. of Civil Eng., Princeton University, Princeton, NJ 08544, 609-258-5425 and 609-258-4660, Email: CELIA@KARST.PRINCETON.EDU and PHILIP@KARST.PRINCETON.EDU)

Richard E. Ewing (Dept. of Mathematics, University of Wyoming, Laramie, WY 82071, 307-766-4933)

Simulation of multiphase flow in porous media involves many important steps, including careful development of numerical simulation methods. The resulting simulator should, at a minimum, respect the conservation principles inherent in the governing equation, including conservation of mass and any inherent maximum principle. Simulators with these attributes may then be used to conduct numerical experiments from which certain physical responses may be observed and studied.

A mass-conservative numerical simulator has been developed to solve the equations of two-phase flow in porous media. This simulator uses a simultaneous solution algorithm with the unknowns being iteration increments of the two fluid pressures. The algorithm has been applied to a variety of two-phase systems, including the simultaneous flow of air and water in unsaturated soils. Such air/water simulations may be used to study fundamental behaviors of the unsaturated zone, including velocity distributions of each fluid phase. Simulation results indicate that under certain infil-

Rock Stripes on Sierra Nevada Foothills

FRESNO AND TULARE COUNTIES

By

N.P. PROKOPOVICH, Engineering Geologist
U.S. Bureau of Reclamation, Mid-Pacific Region
Sacramento, California

The following information is a byproduct of engineering-geological studies conducted by the U.S. Bureau of Reclamation along the Friant-Kern Canal in California's San Joaquin Valley (Anonymous, 1981). During these studies, a brief investigation was made of peculiar rock stripes or "flows" on the Sierra Nevada foothill slopes facing the valley. The rock stripes seem to provide some paleoclimatological data which may be of general geologic interest...*editor*.

REGIONAL SETTING

The study area is located at the western base of the well defined, steep Sierra Nevada foothills, along the eastern margin of central part of the San Joaquin Valley in Fresno and Tulare counties, California (Figure 1). Elevations of the valley floor along the Friant-Kern Canal, near the foothills, are on the order of 400 feet while the tops of the foothills close to the valley have elevations up to 1,000 to 2,000 feet.

The present climate is semiarid with hot, dry summers and cool, wet, foggy winters (Elford, 1970). Mean annual precipitation in Fresno is 11.14 inches (Kahrl, 1978-79).

Native vegetation was represented originally by California Prairie, and at the Kings River by the Valley Oak Savanna (Küchler, 1977). At the present time, the steep foothill slopes are grass covered and are used as cattle ranges, while the valley floor is blanketed by irrigated fields and orchards.

The foothills are underlain mostly by Mesozoic granitic rocks and locally by basic Mesozoic intrusive rocks (Matthews and Burnett, 1965), whereas the valley floor is blanketed by thick alluvial fill frequently composed of highly plastic, red-brown clays (Huntington, 1971; Stephens, 1982).

The average angle of hill slope varies. Based on an interpretation of published 7½ minute USGS topographic quadrangle maps in the Stokes Mountain area, the average hill slopes dip 17 to 20°. Most of the barren, grass covered hillslopes here frequently show three fairly well defined units: (1) upper steep slopes with numerous bedrock outcrops and a rather thin clayey colluvium; (2) a somewhat less steep colluvium blanketed middle portion of the slope with no or very few bedrock outcrops; and (3) a relatively flat colluvial apron at the base of the foothill slope.

DESCRIPTION OF ROCK STRIPES

Peculiar, very prominent striations in the form of echelons of narrow, downward oriented rock stripes on the colluvium blanketed hill slope below the steep upper slope with numerous rock outcrops

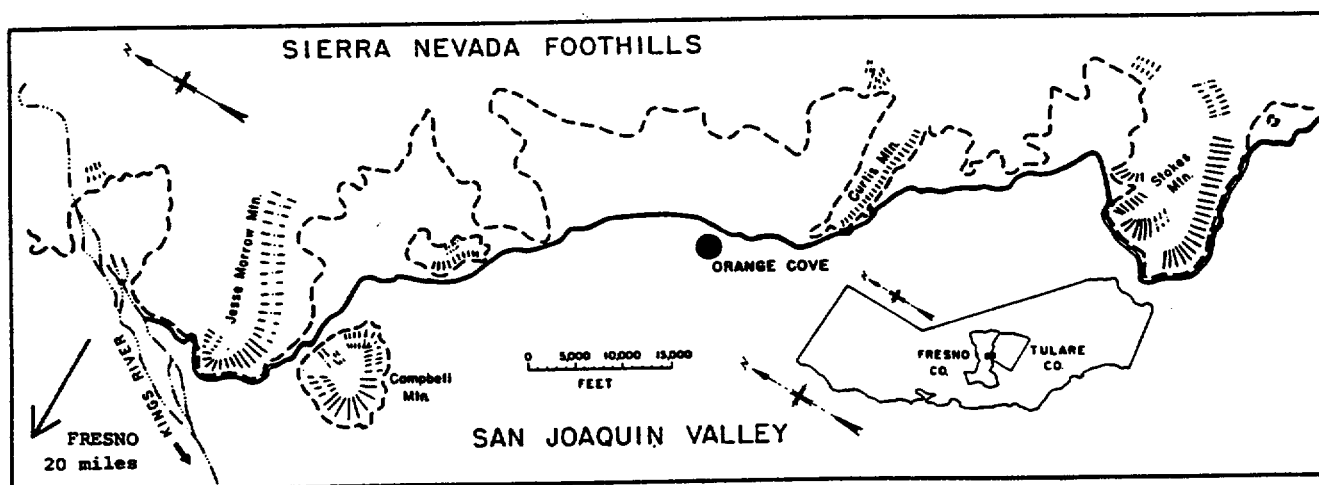


Figure 1. Location map showing the study area and generalized distribution of rock stripes on the western slope of the Sierra Nevada foothills.

- | | |
|---|--|
| <p>1. Friant-Kern Canal of the U.S. Bureau of Reclamation</p> <p>2. Generalized position of the base of the Sierra Nevada foothills</p> | <p>3. Area with observed rock stripes</p> <p>4. Presence of the stripes as noted from aerial photography. Some stripes may be present in other (not explored) areas between the Kings River and Stokes Mountain.</p> |
|---|--|

were noted in several places on the foot-hill front and on two partially isolated bed-rock knobs between the Kings River and Stokes Mountain (Figure 1; Photos 1, 2, and 3). Particularly good striations occurred on the slope of Stokes Mountain in sections 14, 22, and 27, T16S, R25E (Photos 1, 2, and 3), and on the western slope of Campbell Mountain—a partially isolated bedrock knob in Sections 23, 25, and 26, T24S, R23E.

Only a few stripes extended into the belt of rock outcrop above the colluvium blanketed slope. Practically no stripes were noted on the relatively gentle slope on the surface of the colluvial apron at the base of the foothills. Some individual stripes are over 2,200-foot long. Small stripes are only 5- to 6-foot wide, larger stripes are 15-foot to 100-foot wide, and the average width of stripes on Stokes Mountain is about 40 feet. Many stripes become wider toward the bottom. Some of the stripes have the shape of a vertically oriented "Y" and appear to be developed by a junction of two originally separated tributary stripes. A few other stripes have the shape of an "inverted Y."

Several stripes start at loosely "jointed" or fractured outcrops of otherwise fresh, hard intrusive rocks. At the downslope end, the rock stripes rapidly disappear into a blanket of colluvial clay. A close inspection of several rock stripes on Stokes Mountain indicated that the stripes occupied gentle, 2- to 3-foot deep, downward oriented depressions on the colluvial apron, which are filled with large, angular to semiangular, fresh blocks of very hard, massive granitic rock which are up to 2 to 3 feet and larger (Photo 4). Edges on many rocks are sharp. No rust stains or other traces of intense chemical weathering were noted on rocks. In cross-section, the enveloping rock surfaces of the stripes are not flat but appear to be slightly convex.

Individual rock flows are separated by belts of "normal" grass covered slopes, 60- to 100-foot and more wide, with relatively few or no loose rocks or outcrops.

Rock outcrops at the head of a few rock stripes were inspected. In all cases they were composed of loosely fractured, fresh, very hard intrusive, medium-grained, massive granitic rocks (Photo 5). Some loose rocks were 3- to 5- and more feet long. No rust stains or other evidence of chemical weathering were noted on rock surfaces and minor questionable weathering here was less than 1 mm thick.

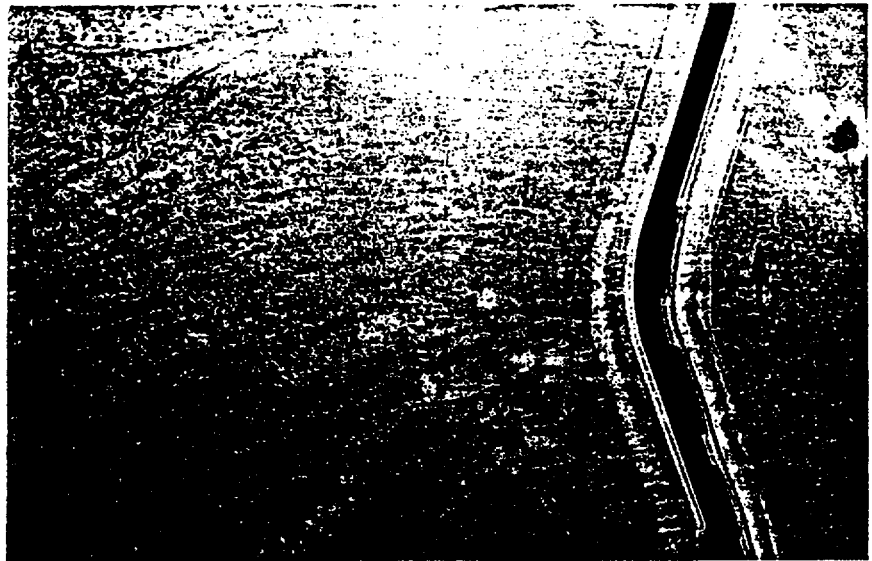


Photo 1. Aerial photograph of the Friant-Kern Canal showing a portion of Stokes Mountain with numerous rock stripes. Arrow indicates direction of the canal flow. The canal is about 83 feet wide.



Photo 2. General northerly view of rock stripes on the western slope of Stokes Mountain. The Friant-Kern Canal is in the foreground; orange orchards occupy valley floor in front of Stokes Mountain. Rock stripes appear light colored because of the higher grass cover.

Excavations of red, highly plastic, colluvial clay at the Friant-Kern Canal at the base of the foothills, encountered numerous semiangular and more or less worn fragments of hard, mostly granitic rock types embedded in the colluvial clay. The presence of these rocks interfered with past lime treatment operations of the canal lining, which were conducted to stabilize canal banks in the vicinity of Stokes Mountain.

ORIGIN OF ROCK STRIPES

There is no doubt that the scattered bedrock outcrops on the steep upper portion of the foothill slopes are the source for the rocks in the rock stripes. The angularity of the loosely fractured intrusive rocks in the outcrops (Photo 5) and rock flows indicate rather short distances of transportation for the rocks in the rock stripes. The freshness of the hard, massive

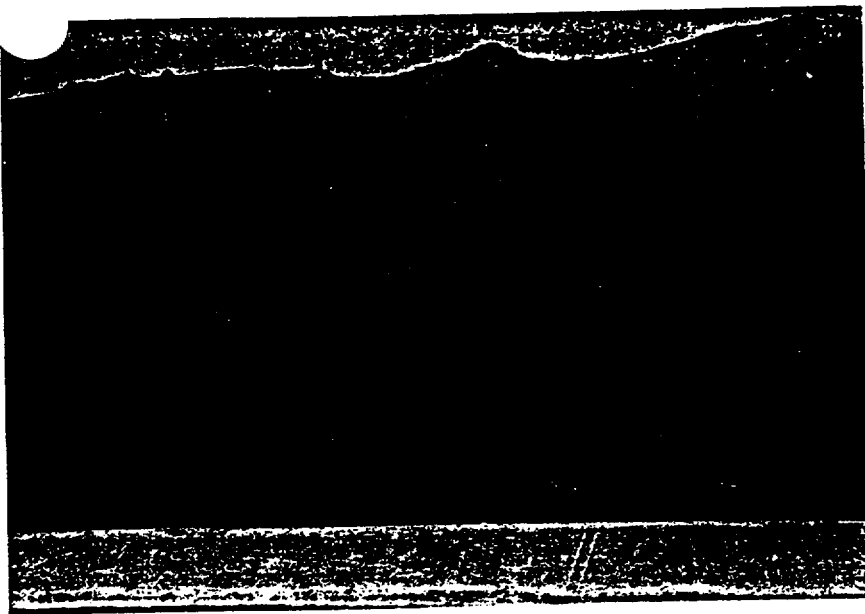


Photo 3. Southern front of Stokes Mountain showing prominent rock stripes which disappear in the clayey colluvial apron at the base of the foothills. The hill slope along the "striped belt" has a clayey colluvial cover. Numerous rock outcrops are visible on the steep hillslope above the rock stripes.

in outcrops and in the rock stripes, the absence of chemical weathering (including rust stains), indicate mechanical weathering as the main factor in the formation of rocks in the rock stripes. Such conditions characterized by an intense frost weathering are common in the local periglacial areas (Washburn, 1973).

The Pleistocene glaciation of the Sierra Nevada, particularly of Yosemite Valley (Bailey, 1966), is an internationally famous example of mountain glaciation. The study area is located near this previously glaciated area. The existence of a severe periglacial paleoclimate in the study area is, therefore, more than a possibility. Intense frost weathering and ice formation under such conditions could easily fracture and break outcrops of hard, massive, intrusive rock into large, sharp edged, loose blocks. Sliding of such rocks by solifluction, which is typical in periglacial areas (Washburn, 1973), could have created the observed rock stripes. The movement could be accelerated by the presence of snow and ice. In such cases, the rock stripes somewhat resemble present day rock glaciers (Washburn, 1973, p. 195). The main difference between rock stripes and rock glaciers is the absence in rock stripes of typical glacial cirques. Very similar rock stripes have been described in eastern England (Williams, 1964), in Idaho (Malde, 1961; 1964), and elsewhere.



Photo 4. A closeup downslope view of a rock stripe on the southern slope of Stokes Mountain. The angular and semiangular rocks are closely packed.

CONCLUSION

Peculiar rock stripes on slopes of some Sierra Nevada foothills southeast of the City of Fresno are probably relict micro-landscape forms created in an ancient Pleistocene periglacial zone by intense frost weathering and mass-wasting.

REFERENCES

- Anonymous, 1981, Project Data, United States Water and Power Resources Service-A Water Resources Technical Publication: U.S. Government Printing Office, Denver, CO, 1,463 p.
- Bailey, Edgar H., editor, 1966, Geology of northern California: California Division of Mines and Geology, Bulletin 190, 508 p.
- Elford, C. Robert, 1970 (revised), Climate of California: U.S. Department of Commerce, Environmental Data Service, Climatography of the United States No. 60-4, U.S. Government Printing Office, Washington, DC, 9 p.
- Huntington, Gordon L., 1971, Soil survey eastern Fresno area, California: U.S. Department of Agriculture, Soil Conservation Service, U.S. Government Printing Office, Washington, DC, 323 p.
- Kahl, W.L., 1978-79, The California water atlas: Governor's Office of Planning and Research in cooperation with the California Department of Water Resources, Sacramento, CA, 113 p.
- Küchler, A.W., 1977, Natural vegetation of California (map): Department of Geology, University of Kansas, Lawrence, KS, scale 1:1,000,000.

Malde, Harold E., 1961, Patterned ground of possible solifluction origin at low altitude in the western Snake River plain, Idaho: U.S. Geological Survey Research, Short Papers in the Geologic and Hydrologic Sciences, Article no. 71, U.S. Government Printing Office, Washington, DC, p. B-170 to B-173.

Malde, Harold E., 1964, Patterned ground in the western Snake River plain, Idaho, and its possible cold-climate origin: Geological Society of America Bulletin, v. 75, p. 191-208.

Matthews, Robert A., and Burnett, John L., compilers, 1965, Geologic map of California, Fresno sheet: California Division of Mines and Geology, Sacramento, CA, scale 1:250,000.

Stephens, Floyd G., 1982, Soil survey of Tulare County, California, Central Part: U.S. Department of Agriculture, Soil Conservation Service and U.S. Department of the Interior, Bureau of Indian Affairs, U.S. Government Printing Office, Washington, DC, 165 p.

Washburn, A.L., 1973, Periglacial processes and environments: Edward Arnold Ltd., London, 320 p.

Williams, R.B.G., 1964, Fossil patterned ground in eastern England: *Buletyn Peryglacjalny*, no. 14, p. 337-349.



Photo 5. Close up view of an outcrop of highly fractured, fresh, massive granitic rock at the head of the rock stripe shown in Photo 4. The San Joaquin Valley and Friant-Kern Canal are in the background; X marks the Friant-Kern Canal. 

Memorial

CORDELL DURRELL

Cordell Durrell, Professor Emeritus of Geology, University of California, Davis, died on October 12, 1986 after a brief illness.

Durrell was born in 1908 in San Francisco and grew up around Oakland. He received his A.B. and Ph.D. degrees in Geology from the University of California, Berkeley in 1931 and 1936, respectively. He was an instructor in geology at UC Berkeley in 1936-37, and a geologist for Richfield Oil Corporation in Los Angeles in 1937-38. In 1938 he became an instructor in geology at the University of California, Los Angeles, beginning an association that lasted for 25 years. In 1943 he received a two-year leave of absence from UCLA to work for the U.S. Geological Survey helping to assess United States resources in barite and optical-quality calcite. He returned to UCLA in 1945 with the rank of Assistant Professor, and re-

ceived promotions to Associate Professor in 1946 and Professor in 1951.

Durrell began his geologic work in the Sierra Nevada near Visalia in 1933. In 1938 he began work on the Blairsden quadrangle in the northeastern Sierra Nevada, a study that continued the rest of his professional career. During the course of this work, he became the principal authority on the Cenozoic geology of the Sierra Nevada and surrounding regions. A book containing the main results of his life-long work will be published by the University of California Press.

In 1963 Durrell went to the University of California, Davis as Professor and Chairman of Geology to oversee the planned growth of the Department, then small, into a first-rank research and teaching group. During his Chairmanship (1963-67) he laid the foundation for Departmental expansion and planned a new

building, which was occupied in 1971. He remained an active and influential member of the department until his retirement in 1976. Even after retirement he came to the Department daily.

Durrell was a member of the American Geophysical Union and the American Association of Petroleum Geologists, and a Fellow of the Geological Society of America, as well as of the Sociedade Brasileiro de Geologia.

Professionally, Durrell was known as an outstanding and dedicated educator and as an expert in Sierra Nevada geology. As an educator he inspired hundreds of graduate and undergraduate students at both UCLA and UC Davis, many of whom have gone on to distinguished geological careers in industry, government service, and in academic communities.

...Department of Geology,
University of California, Davis. 

Chapter 1

Introduction

Roger B. Morrison

Morrison and Associates, 13150 West Ninth Avenue, Golden, Colorado 80401

Grove Karl Gilbert, in his classic monograph on Lake Bonneville (1890, p. 1), succinctly described for all geologists the importance of the Quaternary:

When the work of the geologist is finished and his final comprehensive report is written, the longest and most important chapter will be on the latest and shortest of the geological periods.

This book reviews the Quaternary geology of the contiguous United States beyond its glacial limits. Knowledge of the Quaternary has become increasingly important because it applies to many facets of paleoclimatology, engineering, and environmental geology, hydrogeology, and neotectonics.

We focus chiefly on Quaternary stratigraphy, not geomorphology. Geomorphic processes and systems that have operated in various regions of North America are discussed in Graf (1987). We also avoid discussing glacial geology as much as possible, although glacial relations are mentioned in areas adjoining glaciated ones. Richmond and Fullerton (1986) provide a recent synthesis of the glacial stratigraphy of the United States. Our volume also partly subordinates the Holocene and late Wisconsin records because Wright and Porter (1984) describe these records; also, Ruddiman and Wright (1987) cover part of this time span.

This book has two parts (see Table of Contents for details of coverage). The first part has short reviews of topics of general interest to students of the Quaternary: Quaternary paleoclimatology, dating methods applicable to the Quaternary, Quaternary volcanism, and Quaternary tephrochronology. Quaternary tectonism is treated in Slemmons and others (1991). Nonetheless, many of the regional chapters in this volume describe neotectonism within their region.

The second part of the book, more than three-quarters of its length, contains syntheses of Quaternary nonglacial geology of major regions of the contiguous United States. Chapters in this part are arranged to cover successive north-south strips from the Pacific to Atlantic coasts (Fig. 1 and Contents). The boundaries of these chapters generally conform to the outlines of the physio-

graphic provinces of Fenneman (1930), with minor adjustments. The regional chapters provide general overviews for each region, augmented with summaries of detailed studies that give representative samples of the region. Consequently, the regional section has some gaps in its coverage of the unglaciated contiguous United States (Fig. 1). Most of this book covers regions west of the Mississippi River because of the generally better degree of accumulation and preservation of nonglacial Quaternary sediments there, and because fewer definitive studies have been made of equivalent deposits in the eastern United States. We have tried to synthesize the most up-to-date research, much of it previously unpublished, which results in conclusions often agreeing with, but in other places very different from, those given 25 years ago in Wright and Frey (1965).

WHY THE QUATERNARY PERIOD IS EXCEPTIONAL IN GEOLOGIC TIME

Climatic change is the outstanding characteristic of Quaternary time. Starting about 2.5 m.y. ago, the amplitude of climatic cycles increased greatly (Fig. 2), causing frequent large changes in the rates and types of deposition in both marine and terrestrial environments, to a degree that makes the better Quaternary stratigraphic records exceptional in geologic time. Fairbridge (1962, p. 111) commented:

Seen from the vantage point of the whole geologic time scale . . . we must say: *the present climatic, oceanographic, structural, and sedimentological picture of the Earth is abnormal.* If we use the Lyellian philosophy of assuming the present is the direct key to the past we run a grave danger of being wrong. There is nothing wrong with that basic logic, but processes and relative factors are liable to great changes in velocity, scope, volume, etc.

Homo sapiens evolved in the late Pleistocene, and began to change from a hunting-gathering to a farming society 10,000 to 9,000 years ago, beginning human "civilization" soon after the start of the Holocene. From this perspective it is easy to understand why knowledge of the climatic, tectonic, and erosional/

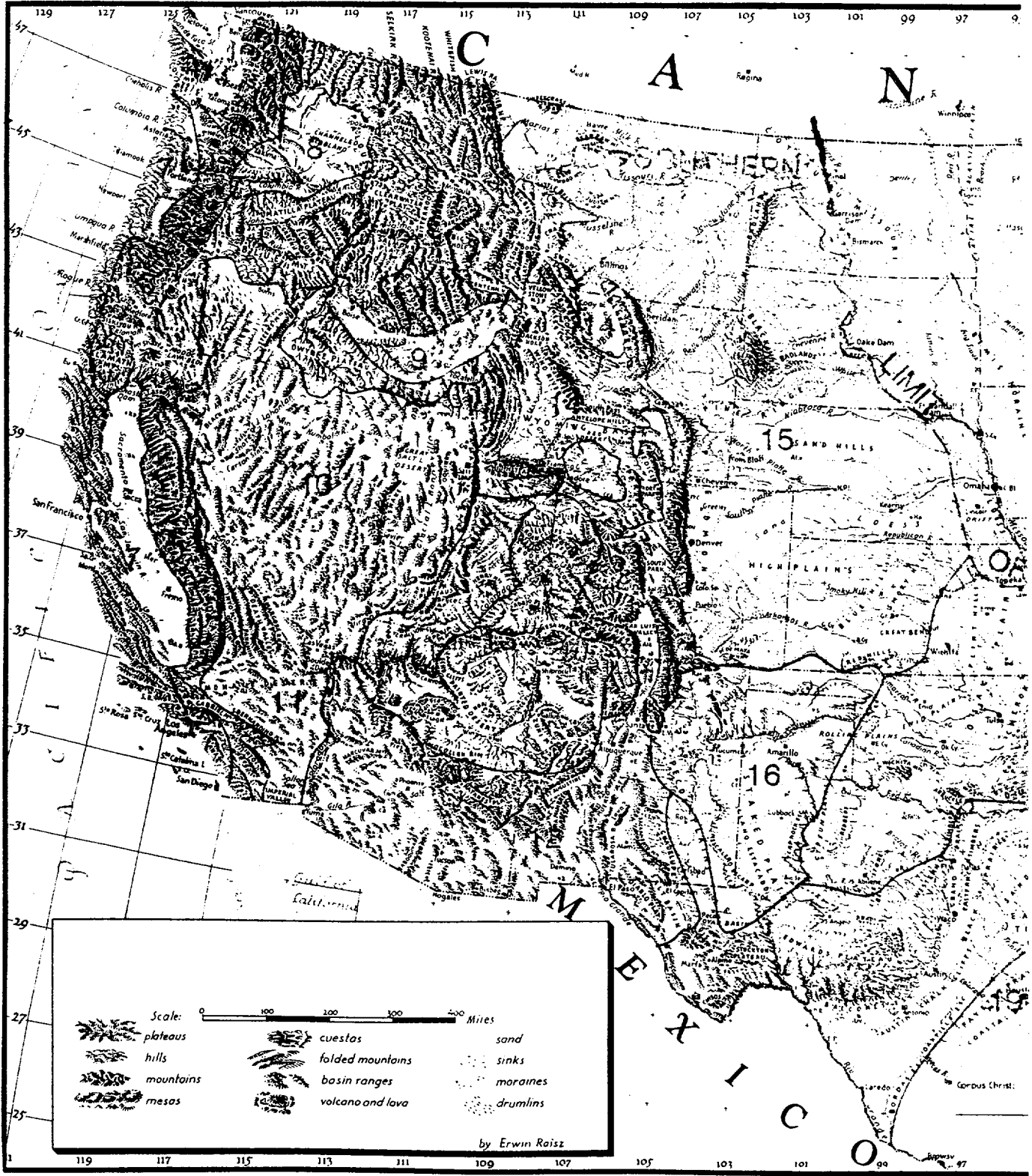
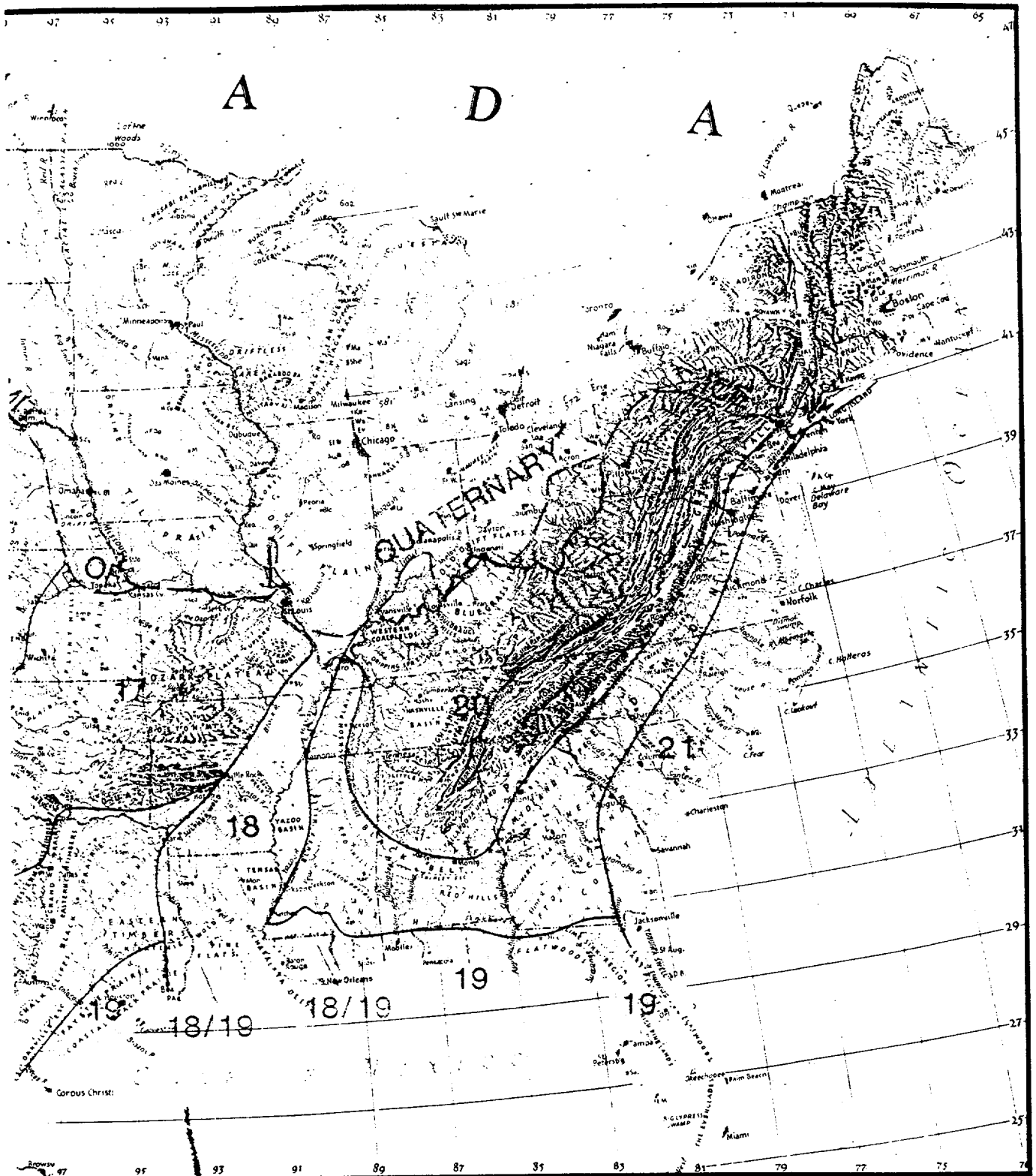


Figure 1. Landforms of the United States (by Erwin Raisz, published with permission of Kate Raisz). Dashed color line shows the maximum southern extent of the Laurentide and Cordilleran ice sheets; generally this is the pre-Wisconsin ice margin. The solid color lines outline the coverage by the various regional chapters in this book, designated by their chapter numbers. Dotted color lines indicate overlapping coverage between adjacent chapters.



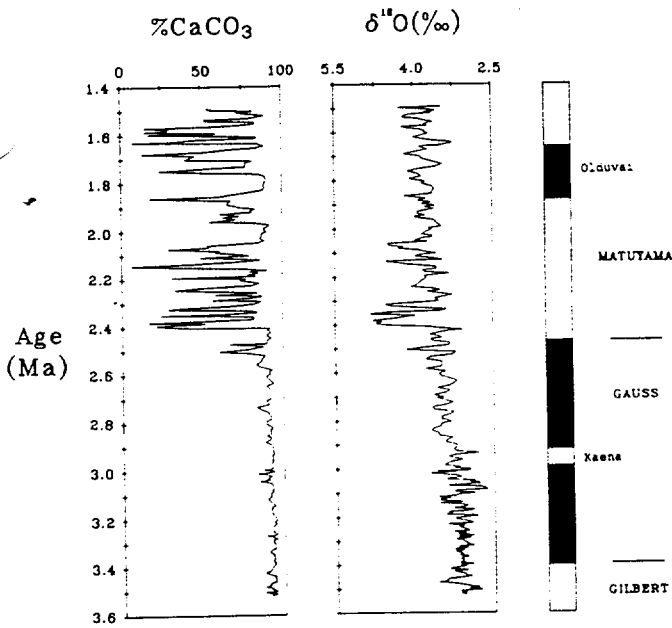


Figure 2. Late Pliocene and early Pleistocene records of percent CaCO_3 and $\delta^{18}\text{O}$ (from benthic foraminifera) in a deep-sea core from the North Atlantic Ocean. The abrupt increases in CaCO_3 near 2.55 Ma and especially 2.4 Ma mark the onset of ice rafting into the North Atlantic brought about by appearance of moderate-sized ice sheets in North America and Europe, after more than 1 m.y. of stable warm climate. (From Ruddiman and Wright, 1987a; after Shackleton and others (1984) and Zimmerman and others (1985); core site 552 at $56^\circ 03' \text{N}$, $23^\circ 14' \text{W}$.)

depositional history of the Quaternary Period is important in order to comprehend our changing environment and to predict our future.

Well-documented summaries of the development of concepts about the Quaternary and Pleistocene are given in Flint (1957, chapter 1; 1971, chapter 2). The Pleistocene was first defined (Lyell, 1839) on the basis of fossil mollusks. Later it became equated to widespread glaciation (the Great Ice Age) and also to the appearance of humanoids (the Age of Man) and certain other vertebrates. Modern research shows that these criteria (and biostratigraphic criteria such as microfossil assemblages) are too imprecise in chronostratigraphic definition to be internationally acceptable for marking the boundary between the Tertiary and Quaternary Periods (see Fig. 5). At present, two boundary levels are being considered, at about 1.65 and 2.5 Ma (see below), but a formal decision about this boundary and selection of an internationally acceptable boundary stratotype have not yet been achieved either by the International Association for Quaternary Research (INQUA) or by the International Geological Congress.

The deep-ocean core record

The most comprehensive record of late Cenozoic climatic change on a global scale is the oxygen-isotope ($\delta^{18}\text{O}/^{16}\text{O}$) record from deep-ocean cores (Figs. 2, 3, and 4) (Emiliani, 1955,

1967, 1970, 1972; Shackleton, 1969; Hays and others, 1969, 1976; Shackleton and Opdyke, 1973, 1976; Shackleton and others, 1984; Johnson, 1982; Imbrie and others, 1984; Ruddiman and Kidd, 1986; Ruddiman and Wright, 1987b). This record chiefly shows changes in the volume of ice stored on the continents during glaciations, and subordinately, temperature changes in the ocean-surface layer (Mix, 1987; Shackleton, 1969).

The oxygen-isotope record from deep-ocean cores has become a standard for Quaternary chronology, even among geologists who study terrestrial deposits, because the best deep-ocean cores provide far more complete sequences, with fewer time gaps than any terrestrial records. The deep-ocean record correlates strongly with long loessial records from central Europe (Fig. 3) (Kukla, 1975, 1977; Fink and Kukla, 1977) and China (Kukla, 1987, 1989; Kukla and others, 1988; Kukla and An, 1989). The marine oxygen-isotope cycles also correlate strongly with astronomical Earth-orbital cycles (Fig. 4), suggesting that Earth-orbital mechanisms were "pacemakers" for Quaternary climatic cycles (Hays and others, 1976; Johnson, 1982; Imbrie and others, 1984; Ruddiman and Wright, 1987a).

These records lead to the following four conclusions:

1. At least 17 complete interglacial-glacial cycles have occurred since the end of the Olduvai normal-polarity Subchronozone (about 1.65 Ma), and perhaps as many as 44 such cycles after the 2.48-Ma Gauss-Matuyama magnetic reversal (Gauss-Matuyama magneto-chronozone boundary) are recognizable in the loess sequences in China (Kukla and An, 1989; Kukla, 1989). The seven completed interglacial-glacial cycles during the past 620,000 years lasted between 88 and 118 k.y. apiece (Fig. 4, Table 1), an average duration of 100,000 years. Therefore, they were similar but not identical in duration. Also, they commonly differed in amplitude. Some cycles had stronger maxima and/or minima than others during their glacial and/or interglacial phases (Figs. 3, 4).

2. Five major interglacial intervals occurred during the past 529,000 years. Three of these were composed of two or three interglacial episodes separated by one or two cooler episodes (Table 1, Fig. 4). Interglacial episodes are defined here as times when the $\delta^{18}\text{O}$ values in deep-ocean-core data (from Imbrie and others, 1984, Table 7) were consistently at or below Holocene interglacial (since 9 ka) values; the $\delta^{18}\text{O}$ value of -0.05 is used here as a cutoff between interglacial and subglacial conditions.

On this basis, for the five completed interglacial-glacial cycles during the last 529,000 years, the interglacial episodes lasted from 28 to 49 k.y., or 27 to 42 percent of a given interglacial-glacial cycle (Fig. 4 and Table 1). This means that, including the Holocene, interglacial conditions prevailed for 39 percent of the last 529,000 years.

Interglacial and glacial intervals clearly have been somewhat erratic in occurrence and magnitude and have not been identical in duration. The last pre-Holocene interglacial interval, comprising all of O-isotope stage 5, lasted 55 k.y., albeit with two cool episodes (O-stages 5b and 5d; Figs. 3 and 4) in its later part. Its first part, O-stage 5e (Sangamon in the strict sense), was some-

what stronger than the Holocene and lasted about 18,000 years—longer than the Holocene. The three interglacial episodes within stage 5 occupied a total of 89 percent of stage 5 and 42 percent of the whole O-stage 2-5 interglacial-glacial cycle.

3. Ice accumulation accelerated greatly at the O-stage 5 to 4 transition; between 68 and 77 ka there was a 2-fold increase in the $\delta^{18}\text{O}$ ratio in deep-ocean cores. The Wisconsin/Würm glaciation peaked during oxygen-isotope stages 4 and 2 (stage 3 was a

weak interstadial), and climaxed at 18 to 20 ka during O-stage 2. Deglaciation began about 15 to 14 ka and was almost complete about 9 ka, starting the interglacial phase of the Holocene.

4. Projecting this record into the future, it appears virtually certain that the Holocene interglacial will be followed by a long glacial phase. Such a cold phase will cause crises in food and energy supplies far more severe than any since civilized man developed. We are privileged to live in an exceptional time by paleoclimatic standards.

There are no certain paleoclimatic means of predicting exactly when the change from the present interglacial conditions to a much cooler climate will occur (note the erratic distribution and time spans of previous interglacials in Fig. 4 and Table 1). However, the past records provide a frame of reference that indicates possibilities. First, it is important to recognize that Earth now has progressed past an interglacial maximum into a somewhat cooler phase. If the Holocene resembles the last interglacial (which is rather unlikely), we Earthlings will soon (within hundreds to a few thousand years) come to the end of a warm episode like O-stage 5e, to enter a few thousand years of oscillating climate, with one or more subglacial cold episodes alternating with one or more near-Holocene-interglacial warm episodes. Then comes the onslaught of a long, severe major glacial phase lasting tens of thousands of years. The "Greenhouse Effect" warming is an aberration lasting perhaps several hundred years—and badly timed. It is too bad that it can't be postponed until it would help mitigate the inevitable next cooling phase, which will be beyond human control.

Correlations of deep-ocean oxygen-isotope records with other terrestrial sedimentary and paleoclimatic records

Although the deep-ocean oxygen-isotope record correlates strongly with loess records in central Europe and China (Fig. 4) (Kukla, 1975, 1977, 1987, 1989; Fink and Kukla, 1977; Kukla

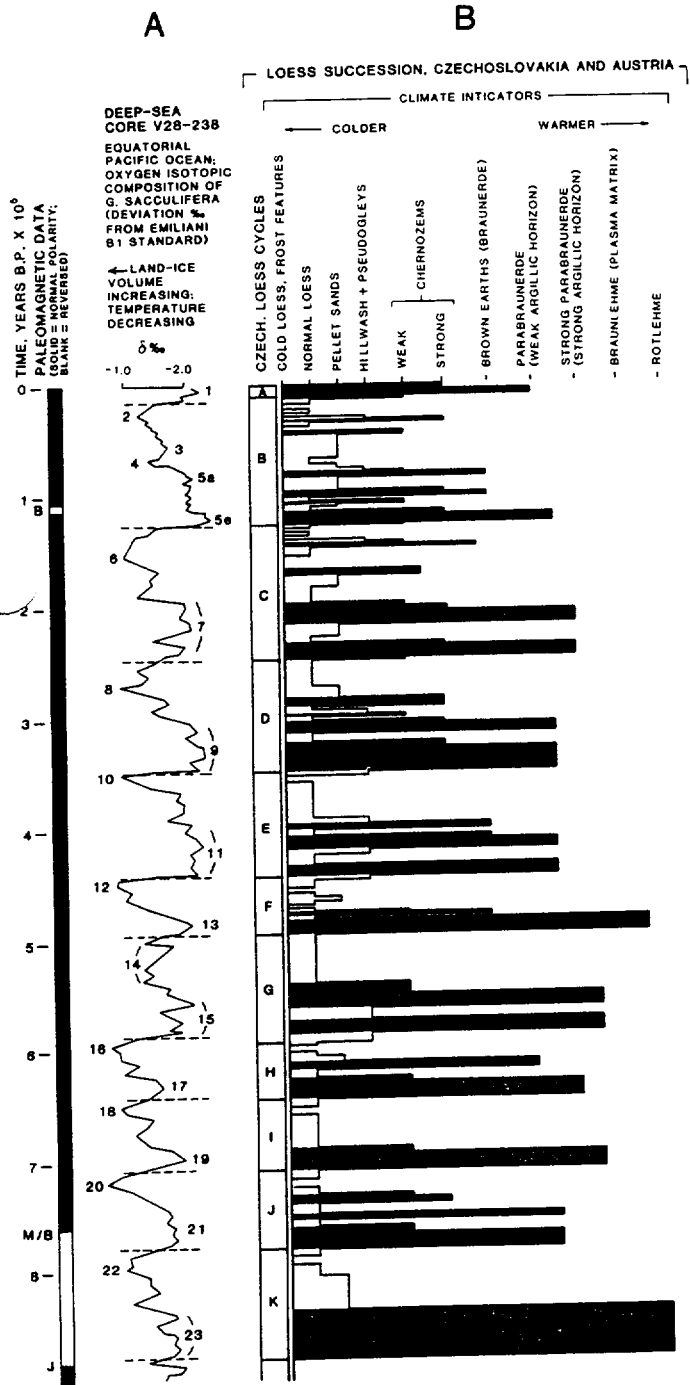


Figure 3. Comparison of the deep-sea and central-European loess records for the last 900,000 years (from Morrison, 1978). A, the interglacial-glacial cycles represented by an important core from the Equatorial Pacific Ocean. Oxygen-isotope stage numbers are in color. The even numbers at the left indicate glacial maxima, and the odd numbers on the right denote interglacials. Also, in black horizontal dashed lines, are Terminations (T 1 to T 11) in the O-isotope record; these are the midpoints of the sudden transitions from glacial to interglacial conditions. B, a synthesis of the paleoclimatic record from key loess sequences in Czechoslovakia and Austria (Kukla, 1970, 1975, 1977). The horizontal axis represents semiquantitatively the indications of climate, from very cold glacial at far left to warm interglacial at far right, determined from snail faunas, sedimentologic, and pedologic criteria. The paleosols (shown in color) formed during the interstadials and interglacials. The black parts of the paleomagnetic data column represent normal polarity and the white parts, reversed polarity; B, indicates the Blake reversed polarity event; M/B, indicates the Matuyama-Brunhes Chronozone reversal (shown somewhat too young because it was based on 1977 data); J, indicates the Jaramillo normal-polarity Subchron.

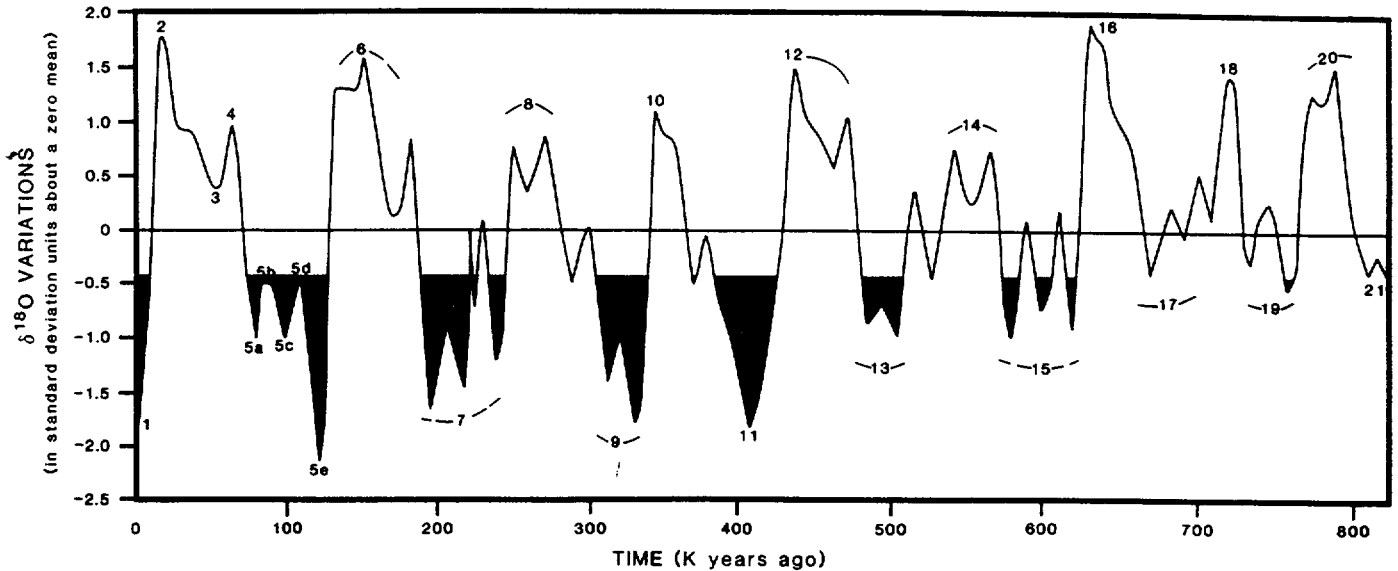
VARIATIONS $\delta^{18}/^{16}\text{O}$ 

Figure 4. Record of $^{18}\text{O}/^{16}\text{O}$ variations in five deep-sea cores, tuned to each other and to earth-orbital parameters, as a function of time, plotted from Table 7 data in Imbrie and others (1984). Color shows the interglacial episodes, based on a cutoff at -0.5 $\delta^{18}\text{O}$ oxygen-isotope values (equivalent to Holocene interglacial values). The numbers along the graph indicate oxygen-isotope stages; the even-numbered peaks (at top) are glacial maxima, and odd-numbered troughs are interglacial minima. Note: The portions of this graph older than 620 ka are here regarded as somewhat too young, and the portions older than 475 ka are believed to suppress excessively the oxygen-isotope minima for interglacial stages 13 through 21 (see text).

and others, 1988; Kukla and An, 1989); correlations with other terrestrial records commonly are less clear. Early investigators of terrestrial sequences tended to recognize only the more pronounced, larger amplitude manifestations of climatic change, essentially megacycle sets composed of more than a single interglacial-glacial cycle in the marine record.

The differences of opinion on correlation between marine and various terrestrial Quaternary sequences are due partly to the fragmentary character of nearly all terrestrial sequences (glacial, alluvial, lacustrine, volcanic, etc.) because of: (a) episodic deposition, with disconformities or diastems that represent small to large time-gaps in the geologic record; (b) disjunct records at various sites (natural/artificial exposures, drillholes, etc.) due to local erosion or nondeposition of units or concealment by younger deposits; and (c) many terrestrial records being diachronic/asynchronous within regional areas. Also, as paleoclimatic proxies to the deep-ocean record, the climate-cycle manifestations on land commonly were out of phase with the deep-sea record, being modified by time lags in the responses of various ocean/terrestrial systems to given climatic changes, by global differences in weather patterns, and by local orography, tectonism, and other factors.

The effects of glaciation were felt far beyond the glaciated areas. Along the coastal margins, glacioeustatic changes in sea level (commonly more than 100 m between glacials and intergla-

cial) controlled not only the patterns of marine regressions and transgressions, as recorded by coastal marine terraces and platforms, but also controlled cycles of fluvial entrenchment and alluviation of coastal valleys, as well as episodic development of coastal dunes (Chapters 7, 19, and 21, this volume).

Unfortunately, some workers who make paleoclimatic models still propose "finger-matching" correlations between the deep sea and various terrestrial records. For example, many models date the last pleniglacial at 18 to 20 ka because it is the maximum of marine oxygen-isotope stage 2. However, the end moraines that record the maximum southward extent of the Laurentide ice sheet during the last glaciation range in age from about 22 to 14 ka in various places (Richmond and Fullerton, 1986). Also, the highest late Wisconsin pluvial-lake strandlines in the Great Basin range in age from about 18 to 13 ka. Earlier pluvial lakes in the Great Basin were at times out of phase with each other and with Sierra Nevada glaciations by tens of thousands of years (Morrison, Chapter 10, this volume).

Despite problems in sea versus land correlation for determining global or continental paleoclimatic models, there is no doubt that repeated climatic cycles of several orders of magnitude characterized the Quaternary. On land, these climatic cycles resulted in terrestrial-process cycles of similar orders of magnitude, causing repeated cyclic changes in the rates of all surficial processes (fluvial, eolian, mass-wasting, pedogenic, etc.), at times to

TABLE 1. COMPARATIVE DURATIONS OF INTERGLACIAL EPISODES VERSUS WHOLE GLACIAL-INTERGLACIAL CYCLES OF THE MARINE RECORD*

Oxygen-isotope interglacial-glacial cycle (O-isotope stages)	Age of whole cycle	Age of interglacial episode(s)	Percent of interglacial vs glacial time
2-5	10-128 (118)	73-85 (12) 91-110 (19) 110-128 (18)	(49) 42
6-7	129-245 (116)	188-219 (31) 233-243 (10)	(41) 35
8-9	245-338 (93)	302-337 (35)	38
10-11	338-426 (88)	391-424 (33)	33
12-13	426-529 (103)	478-506 (28)	27
14-15	529-620 (91)	572-580 (8) 592-602 (10) 612-618 (6)	(24) 37

*Ages listed are in thousands of years; durations of various episodes follow in parentheses. Imbrie and others' (1984) Table 7 is the source of the ages as well as the $\delta^{18}\text{O}$ values from which the various oxygen-isotope cycle boundaries, maxima and minima, and interglacial episodes are based.

Interglacial episodes are defined here as those with $\delta^{18}\text{O}$ values of minus 0.5 or less, comparable to or less than those of the interglacial part of the Holocene, after 9 ka (see Fig. 3).

such a degree as to cross an important geomorphic threshold, changing the dominant *type* of process in a given area. Nowhere on Earth have surficial processes acted at a steady state throughout the Quaternary!

Using the Great Plains as an example, I (Morrison, 1987) illustrate the results of the crossing of various levels of geomorphic thresholds, to induce erosion-deposition-landscape stability cycles of four orders of magnitude: (a) microcycles lasting in the 10- to 100-yr order of magnitude; (b) mesocycles of a 1,000- to 10,000-yr magnitude; (c) macrocycles lasting 95 ± 25 k.y.; and (d) megacycles that lasted 400 to 500 k.y. The macrocycles were approximately equivalent to, but not necessarily coeval with, the interglacial-glacial cycles of the marine record. The megacycles correspond to four or five interglacial-glacial cycles in this record and exhibit the strongest expression of four successive dominant-process stages: typically, (1) widespread downcutting, (2) lateral erosion, (3) alluviation, and (4) landscape stability and soil development.

CHRONOSTRATIGRAPHIC DIVISION OF THE QUATERNARY

Table 2 shows the chronostratigraphic divisions of the Quaternary used in this volume and the current best estimates of their boundary dates. The divisions are chiefly those used by Rich-

mond and Fullerton (1986). The boundary dates are based mostly on correlations between oxygen-isotope data from deep-ocean cores and astronomical data on Earth-orbital variations (Berger, 1987), as discussed below.

Formerly, the Pleistocene was divided on the basis of glaciations, the most striking manifestations of climatic change in the terrestrial stratigraphic record. The "classic" divisions in North America and Europe were based on the few then-recognized glaciations and interglaciations, and these divisions commonly were used akin to chronostratigraphic units. Now, as a result of more advanced research, many more glaciations (and interglaciations, stadials, and interstadials) are recognized throughout the Northern Hemisphere (Sibbala and others, 1986). Also understood is the fact that the boundaries of the physical units in glaciated areas (tills, outwash deposits, etc.) are strongly time transgressive (Richmond and Fullerton, 1986, p. 6, 8, 183-184, Chart 1).

Consequently, Quaternary workers are moving toward defining major chronostratigraphic boundaries on the basis of geologically isochronous units, such as tephra layers and geomagnetic reversals (Fig. 5). Tephra layers have limited areal extent, but magnetostratigraphic chronozone and subchronozone boundaries are recognizable throughout the world and therefore are now more frequently used internationally. This is illustrated by the recommendation of the INQUA 1987 Congress that the

TABLE 2. DIVISIONS OF THE QUATERNARY AND THEIR BOUNDARY DATES AS USED IN THIS VOLUME*

Present	
Holocene (Oxygen-isotope stage 1)	
16 to 12 ka	
Late Pleistocene	Late Wisconsin (Oxygen-isotope stage 2)
	~28 ka
	Middle Wisconsin of Richmond and Fullerton (1986) (O-isotope stages 3 and 4)
	~71 ka
	Late Sangamon (Early Wisconsin and Eowisconsin of Richmond and Fullerton, 1986; O-isotope stages 5a-5d)
~115 ka	
	Sangamon of Richmond and Fullerton (1986) (O-isotope stage 5e)
~128 ka†	
Middle Pleistocene	Late-Middle Pleistocene (Illinoian of Richmond and Fullerton, 1986; O-isotope stages 6-8)
	~300 ka
	Middle-Middle Pleistocene of Richmond and Fullerton (1986) (O-isotope stages 9-15)
	~620 ka§
	Early-Middle Pleistocene (Richmond and Fullerton, 1986) (O-isotope stages 16-19) (Matuyama-Brunhes Chronozone boundary)
750-775 ka**	
Early Pleistocene	
-----	Upper boundary of Olduvai Subchron
-----	1.65 Ma
----- or -----	Gauss-Matuyama Chron boundary
-----	2.48 Ma
Pliocene	
5.0-5.5 Ma‡	
Miocene	

Notes: *See text for supporting arguments.

†Corals from the highest strandlines of the last interglacial on Barbados and Curacao gave mean ages of 125 to 126 ka by high-precision uranium-thorium dating (Bard and others, 1989).

§Richmond and Fullerton (1986) use the Lava Creek B tephra layer, dated 620 ka by K-Ar and fission-track (G. A. Izett, U.S. Geological Survey, personal communication, 1987) to identify this boundary in much of the western U.S. This is the approximate age of the boundary between oxygen-isotope stages 15 and 16 (Figs. 1 and 2).

**INQUA's Subcommittee on Subdivisions of the Pleistocene in 1987 recommended that the Matuyama-Brunhes paleomagnetic Chronozone boundary be adopted internationally as marking the boundary between the lower and middle Pleistocene.

‡The Miocene-Pliocene boundary currently is dated 5.0 to 5.5 Ma (Odin, 1982)

Matuyama-Brunhes Chronozone boundary be adopted internationally as the boundary between the lower and middle Pleistocene. Also, both the upper boundary of the Olduvai Subchronozone and (preferably) the Gauss-Matuyama Chronozone boundary currently are candidates for marking the Pliocene-Pleistocene (Tertiary/Neogene-Quaternary) boundary internationally (see below).

Age of the Pleistocene-Holocene boundary

Unfortunately, there is no magnetostratigraphic chronozone or subchronozone boundary at or close to the preferred position of the Pleistocene-Holocene boundary. Based on the deep-sea record, the Pleistocene-Holocene boundary should be placed at the boundary between O-isotope stages 2 and 1 (Termination I,

Fig. 3), commonly given as about 11 to 12 ka (e.g., Ruddiman and Wright, 1987a; Imbrie and others, 1984, Tables 6 and 7). However, in deep-sea cores from around the world this boundary is time transgressive between about 9 and 13 ka. Its various terrestrial litho- and biostratigraphic representations in North America and western Europe average about 10 ka (Fairbridge, 1972), albeit with much diachronism. Hopkins (1975) proposed an arbitrary age of 10,000 years as a compromise for divergent opinions based on land data. However, this proposal does not meet the requirement of the International Stratigraphic Code that a chronostratigraphic boundary of this rank be based on an internationally acceptable stratotype. Richmond and Fullerton (1986) accept 10,000 years as a provisional date for the Pleistocene-Holocene boundary; however, they note (p. 186) that it is a geochronometric boundary without a stratigraphic basis; it does not date the termination of continental glacial activity in the United States, and it has no significance in the overall record of glaciation in the United States. Neither INQUA nor the International Geological Congress have decided on a suitable stratotype and date for this boundary.

The Sangamon-Wisconsin boundary

For more than two decades, leading workers in Quaternary geology in the midwestern United States have placed the lower boundary of the Wisconsin(an) at 70 to 75 ka (e.g., Willman and Frye, 1970). This age corresponds to the boundary between marine oxygen-isotope stages 5 and 4, and would make O-stage 5 entirely interglacial. However, Richmond and Fullerton (1986) regard the O-stage 5d to 5a interval to be part of the Wisconsin glaciation and designate it "Eowisconsin" and "Early Wisconsin." This is because they correlate moderate glacial advances on

the Yellowstone Plateau, Wyoming (as well as in Alaska and perhaps eastern Canada), with O-isotope stages 5b and 5d. Nonetheless, there is no reliable documentation in Europe or Asia of glacial advances correlative with O-stages 5b or 5d (Sibrava and others, 1986). Therefore, many students of terrestrial and marine records still regard the whole of O-stage 5 as a single, albeit modulated, interglacial.

Age of the Matuyama-Brunhes Chronozone boundary

The Matuyama-Brunhes (M/B) magnetostratigraphic Chronozone boundary has been proposed by the INQUA Commission on Subdivisions of the Pleistocene (1987) as the most acceptable marker for the boundary between the lower and middle Pleistocene. However, the age of this magnetostratigraphic boundary cannot be ascertained directly; like all geomagnetic reversals it must be determined by dating underlying and overlying strata by isotopic, fission-track, or other methods at many localities. The best approximation of the age of the M/B chronozone boundary appears to be about midway between the estimates of Mankinen and Dalrymple (1979), Imbrie and others (1984), and Johnson (1982) (730 ± 11 , 734 ± 5 and 788 ka, respectively), for the following two reasons.

1. Johnson's (1982) date of 788 ka is somewhat too old, because it does not allow enough time between the M/B chronozone boundary and the end of the Jaramillo Subchronozone (well dated at 890 ka), as evinced by deposition rates in many deep-sea cores (G. J. Kukla, personal communication, 1989). Nonetheless, Richmond and Fullerton (1986) accept Johnson's date as a provisional age for the M/B boundary.

2. On the other hand, the ages for the M/B reversal used by Mankinen and Dalrymple (1979) and by Imbrie and others

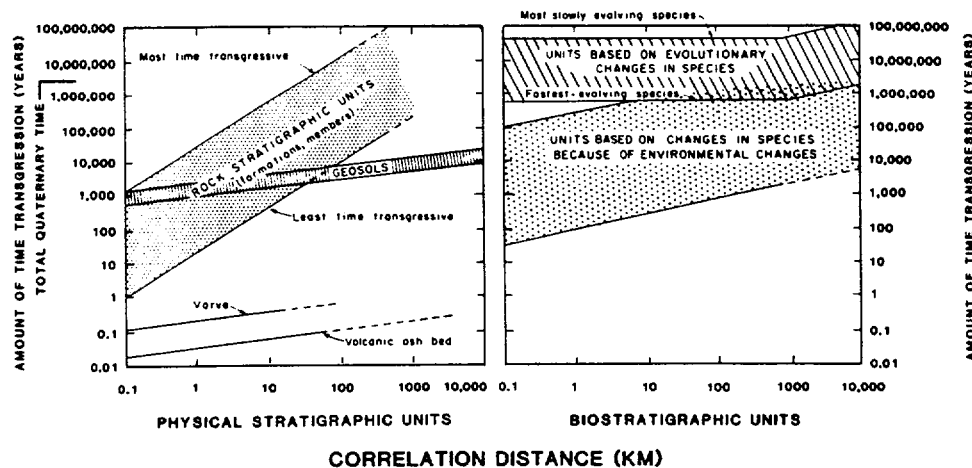


Figure 5. Amount of time transgression with correlation distance for various kinds of stratigraphic units (from Morrison, 1968). Note the logarithmic scales; also that the least time-transgressive units are varves, volcanic ash beds, magnetozone and chronozone/subchronozone boundaries/reversals, and geosols. Varves have the least geographic extent, but geomagnetic chronozone/subchronozone reversals are global. (The band designated "geosols" also represents these paleomagnetic reversals, which have similar time spans; the geosols considered here represent only a single interglacial or interstadial, not compound pedocomplexes.)

(1984) clearly are too young because they are younger than the Bishop Ash, which has normal polarity. Glen Izett (U.S. Geological Survey, personal communication, 1989; Izett and others, 1988) redetermined the age of this tephra layer, obtaining 738 ± 3 ka as a weighted mean of 15 dates on sanidine (14 ^{40}K - ^{40}Ar dates and one ^{39}Ar - ^{40}Ar date). The Bishop ash lies 3 m above the M/B reversal in a Lake Bonneville (Utah) sequence cored at the southern edge of the Great Salt Lake, and a strongly developed paleosol lies just below the ash layer; the M/B reversal is estimated from deposition rates to be between 15 and 40 k.y. older than the Bishop Ash, giving an age of 753 to 778 ka for the reversal (Eardley and others, 1973, Fig. 1 and p. 212). Also, in two borehole cores near Bakersfield, California, the M/B boundary was identified in lacustrine clay 3.7 and 4.9 m below the Bishop Ash; the average deposition rate including diastems is 11.7 cm/1,000 yr, making the approximate age of the M/B boundary about 775 Ma (Davis and others, 1977). Furthermore, on the basis of K-Ar ages from a volcanic sequence in the Jemez Mountains, New Mexico, the age of the M/B reversal is estimated to be about 770 ka (G. A. Izett, personal communication, 1984).

Because of the above considerations, the Matuyama-Brunhes Chronozone boundary is tentatively dated at 750 to 775 ka in this volume. The Bishop tephra layer is a key marker < 1 m to rarely > 3 m above the M/B reversal in remnants scattered widely over the western United States (Chapters, 5, 6, 7, 10, 13, 14, this volume).

Correlation of the deep-ocean-core and astronomical earth-insolation chronologies

Many deep-sea core-record chronologies were presented before Johnson (1982) published the first attempt to correlate the deep-sea oxygen-isotope and Earth-orbital records by statistical analysis, using oxygen-isotope data from a core from the central-western Pacific Ocean. Toward the same goal, Imbrie and others (1984) used more sophisticated statistical techniques to correlate data from this and four other deep-sea cores (from the Southern Atlantic, Indian, and Southern Oceans, and Caribbean Sea), and to correlate the core records with astronomical earth-orbital parameters (Berger, 1984). Three of the cores penetrated the M/B chronozone boundary. Imbrie and others initially used two calibration points: 127 ka for the O-stage 5/6 boundary, and 730 ka (from Mankinen and Dalrymple, 1979) for the M/B chronozone boundary. After the oxygen-isotope curves were "tuned" to the precessional parameters and averaged, the final ages of these calibration points were 128 and 734 ka, respectively.

However, the 734-ka age for the M/B chronozone boundary is too young, as explained above; a better estimate is between 750 and 775 ka. From the present back to about 620 ka the deep-sea O-isotope data not only are fine-tuned to close agreement with astronomical data but also agree well with terrestrial data; however, earlier than 620 ka the ages given by Imbrie and others become discordant, particularly with terrestrial data such as European and Chinese loess sequences (G. J. Kukla, written and oral communication, 1989). For example, O-isotope stage 19

is only 10,000 years long in Imbrie and others (1984), yet on land it is represented by a polygenetic paleosol comparable to all paleosols in the whole of O-isotope stage 5. Moreover, starting with interglacial O-stage 13 and continuing through interglacial stages 15, 17, 19, and 21, the $\delta^{18}\text{O}$ minima are not nearly low enough; these minima indicate only weak interglacial to subglacial conditions (compare Figs. 3 versus 4). In contrast, the central European and Chinese loess records (Fig. 2) show by degree of paleosol development and snail faunas that O-stage 13 was one of the Pleistocene's stronger interglacials, and that O-stages 15, 17, 19, and 21 were as strong or stronger than the Sangamon.

Because of these problems, I regard the portion of Imbrie and others' (1984, Table 7) data pertaining to ages older than 620 ka as somewhat too young; also, back beyond about 745 ka the oxygen-isotopic data strongly suppress the true amplitudes of interglacial minima.

Age of the Pliocene-Pleistocene boundary

Two quite different stratigraphic levels/ages currently are proposed for the Pliocene-Pleistocene boundary: (1) the end of the Olduvai normal-polarity Subchronozone, dated about 1.65 Ma; and (2) the 2.48-Ma Gauss-Matuyama magneto-chronozone boundary.

Placing the Pliocene-Pleistocene boundary at the end of the Olduvai Subchronozone. This is the provisional boundary selected in 1981 by joint resolution of the Working Group of the International Geological Correlation Program Project 41 (Neogene-Quaternary Boundary) and the International Union for Quaternary Research (INQUA) Subcommittee 1-d on the Pliocene-Pleistocene Boundary (International Commission on Stratigraphy Working Group on the Pliocene-Pleistocene Boundary). Nevertheless, the end of the Olduvai subchron is seriously unsuitable as a candidate for this geologic-period boundary, for the following reasons.

1. Aguirre and Pasini (1985) propose that the international stratotype for the Pliocene-Pleistocene boundary be designated as the top of the Olduvai normal-polarity Subchronozone in the Vrica section, southern Italy. However, the proposed stratotype area is much deformed and faulted, with many tectonic and erosional hiatuses; even the Vrica section is truncated. Moreover, the paleomagnetic, tephrochronologic, biostratigraphic, and chronologic data are ambiguous and may be in serious error (Kukla, 1987, p. 214-216). Identification of the Olduvai Subchron here is questionable; the normal-polarity strata may represent an older subchronozone such as the Reunion (Arrias and Bonnadona, 1987).

2. The relatively short Olduvai Subchronozone cannot be identified paleomagnetically in many Pliocene-Pleistocene marine and terrestrial sequences, and identification of the precise position of its upper boundary is even less common.

3. Neither the Olduvai Subchronozone nor its upper boundary marks a substantial climatic event on a global basis; they are not marked by a distinctive worldwide litho- or biostratigraphic discontinuity.

Published comments adverse to placing the Plio-Pleistocene boundary at the top of the Olduvai Subchronozone include Richmond and Fullerton (1986, p. 186), who state,

... there are no criteria by which the Pliocene-Pleistocene boundary thus defined can be located accurately in the stratigraphic sequences in the U.S.A. . . . The Pliocene-Pleistocene boundary thus defined has no significance in the stratigraphic and chronologic framework of glaciation in the United States. . . . It has no significance with respect to the dispersal of microtine rodents . . . or other vertebrate faunas . . . that distinguish the North American land mammal ages; . . . no clear significance with respect to climatic or environmental changes in North America based on biotic criteria.

In addition, G. I. Smith (Chapter 11, this volume) observes, regarding the deep-core record at Searles Lake, California,

... the 1.6 Ma "beginning of Quaternary time" falls near the middle of a virtually uninterrupted intermediate hydrologic regime that lasted about 0.75 m.y.

Kukla (1987) comments that the proposed Pliocene-Pleistocene boundary at the top of the Olduvai Subchronozone has no lithostratigraphic or biostratigraphic representation in the loess sequences of China.

Geologists working with offshore core and seismic data in the Gulf of Mexico generally cannot recognize this boundary on stratigraphic or paleomagnetic grounds; they almost uniformly prefer a more distinguishable boundary.

The Gauss-Matuyama Chronozone boundary as a candidate for the Pliocene-Pleistocene boundary. Mounting evidence indicates that the 2.48-Ma Gauss-Matuyama Chronozone boundary would be a more suitable candidate for the Pliocene-Pleistocene boundary (Ruddiman and Wright, 1987b; Kukla, 1987, 1989; Kukla and An, 1989). Arguments on behalf of placing the Pliocene-Pleistocene boundary at the Gauss-Matuyama magnetic reversal are as follows.

1. The Gauss-Matuyama magnetic reversal was close in time to a sudden cooling of the Earth and the initiation of moderate-sized ice sheets in North America and Europe, between 2.55 and 2.4 Ma (Fig. 2), after several million years without significant glaciation. This cooling ended a Pliocene warm period whose climatic cycles were much smaller in amplitude than those of the Pleistocene and never became colder than the Pleistocene interglacials, even at high latitudes (Matthews and Poore, 1981). This climatic shift—the true beginning of the "Great Ice Age"—is recorded in cores from the subpolar North Atlantic and the Labrador and Norwegian Seas by a marked increase in ^{18}O , a decrease in percent CaCO_3 (Fig. 3), and an increase in ice rafting (Backman, 1979; Shackleton and others, 1984; Zimmerman and others, 1985; Ruddiman and Kidd, 1986; Eldholm and Thiede, 1987; Srivastava and Arthur, 1987; Ruddiman and Wright, 1987a).

2. This drastic climatic change is well represented by lithologic and biostratigraphic discontinuities in marine and terrestrial sequences throughout the world (e.g., by the start of loess deposi-

tion in Europe and China (Kukla, 1987, 1989; Kukla and An, 1989).

3. The Gauss-Matuyama polarity reversal can be identified unambiguously in terrestrial and marine sequences throughout the world, much better than the top of the Olduvai Subchronozone.

4. Placing the Pliocene-Pleistocene boundary at the 2.48-Ma Gauss-Matuyama Chronozone boundary will accommodate the two classic concepts of the Quaternary, of it being "The Great Ice Age" and also that it is "The Age of Man" (the earliest humanoids evolved near this time).

Some significant revisions in Pleistocene terminology

Much of the "classical" terminology for designating the age of Pleistocene deposits is now revised throughout the Northern Hemisphere (Sibrava and others, 1986). Geologists in the United States should note the recommendations that terms such as Yarmouth(ian), Kansan, Afton(ian), and Nebraskan be abandoned (Richmond and Fullerton, 1986, p. 6–7, 183–184) because they have been widely misused as chronostratigraphic names. These names were originally based on litho- and pedomatigraphic units, but they oversimplify a complex stratigraphic record and have led to much miscorrelation of units. Other classical terms, including Sangamon, Illinoian, and parts of the Wisconsinian are more narrowly redefined; Richmond and Fullerton (1986) also recommend that the names Wisconsinian and Sangamonian (which have chronostratigraphic connotations) also be abandoned.

REFERENCES CITED

- Aguirre, E., and Pasini, G., 1985, The Pliocene-Pleistocene boundary: Episodes, v. 8, p. 116–120.
- Arrias and Bonnadona, 1987: Ottawa, INQUA 12th Congress Abstracts, p. 67.
- Backman, J., 1979, Pliocene biostratigraphy of DSDP Sites 111 and 116 from the North Atlantic Ocean and the age of the Northern Hemisphere glaciation: Stockholm Contributions to Geology, v. 32, p. 115–137.
- Bard, E., Hamelin, B., Lao, Y., Anderson, R. F., and Fairbanks, R. G., 1989, Dating of the last interglacial period by U/Th mass spectrometry of Caribbean corals [abs.]: International Correlation Program 3 Meeting 1989, Cambridge, United Kingdom.
- Berger, A. L., 1984, Milankovitch theory and climate: Reviews of Geophysics, v. 26, p. 624–657.
- Davis, P., Smith, J., Kukla, G. J., and Opdyke, N. D., 1977, Paleomagnetic study at a nuclear power plant site near Bakersville, California: Quaternary Research, v. 7, p. 380–397.
- Eardley, A. J., and 6 others, 1973, Lake cycles in the Bonneville basin, Utah: Geological Society of America Bulletin, v. 84, p. 211–216.
- Eldholm, O., and Thiede, J., eds., 1987, Proceedings of the Ocean Drilling Program, Part A (Leg 104): Washington, D.C., U.S. Government Printing Office, 783 p.
- Emiliani, C., 1955, Pleistocene paleotemperatures: Journal of Geology, v. 63, p. 538–578.
- , 1967, The Pleistocene record of the Atlantic and Pacific Ocean sediments, correlations with the Alaskan stages by absolute dating, and the age of the last reversal of the geomagnetic field: Progress in Oceanography, v. 4, p. 219–224.
- , 1970, Pleistocene paleotemperatures: Science, v. 168, p. 822–825.
- , 1972, Quaternary hypsithermals: Quaternary Research, v. 2, p. 270–273.
- Fairbridge, R. W., 1962, World sea level and climatic changes: Quaternaria, v. 6, p. 111–134.

- , 1972, Climatology of a glacial cycle: *Quaternary Research*, v. 2, no. 2, p. 283–302.
- Fenneman, N. M., 1930, Physical divisions of the United States: U.S. Geological Survey Map, scale 1:7,000,000.
- Fink, J., and Kukla, 1977, Pleistocene climates in central Europe; At least 17 interglacials after the Olduvai event: *Quaternary Research*, v. 7, p. 363–371.
- Flint, R. F., 1957, *Glacial and Pleistocene geology*: New York, John Wiley and Sons, 553 p.
- , 1971, *Glacial and Quaternary geology*, New York, John Wiley and Sons, 892 p.
- Gilbert, G. K., 1890, Lake Bonneville: U.S. Geological Survey Monograph 1, 438 p.
- Graf, W. L., ed., 1987, *Geomorphic systems of North America*: Boulder, Colorado, Geological Society of America, Centennial Special Volume 2, 643 p.
- Hays, J. D., Imbrie, J., and Shackleton, N. J., 1976, Variations in the Earth's orbit; Pacemaker of the ice ages: *Science*, v. 194, p. 1121–1132.
- Hays, J. D., Saito, T., Opdyke, N. D., and Burckle, L. H., 1969, Plio-Pleistocene sediments of the equatorial Pacific; their paleomagnetic, biostratigraphic, and climatic record: *Geological Society of America Bulletin*, v. 80, p. 1481–1514.
- Hopkins, D. M., 1975, Time-stratigraphic nomenclature for the Holocene Epoch: *Geology*, v. 3, p. 10.
- Imbrie, J., and 8 others, 1984, The orbital theory of Pleistocene climate: Support from a revised chronology of the marine delta ¹⁸O record, in Berger, A. L., and others, eds., *Milankovitch and climate, Part 1*: Dordrecht, D. Reidel Publishing, p. 269–305.
- Izett, G. A., Obradovich, J. D., and Mehnert, H. H., 1988, The Bishop ash bed (middle Pleistocene) and some older (Pliocene and Pleistocene) chemically and mineralogically similar ash beds in California, Nevada, and Utah: *U.S. Geological Survey Bulletin* 1675, 37 p.
- Johnson, R. G., 1982, Brunhes-Matuyama magnetic reversal dated at 790.00 yr BP by marine-astronomical correlations: *Quaternary Research*, v. 17, p. 135–147.
- Kukla, G. J., 1970, Correlations between loesses and deep-sea sediments: *Geologiska Foreningen i Stockholm Forhandling*, v. 92, pt. 2, p. 148–180.
- , 1975, Loess stratigraphy of central Europe, in Butzer, K., and Isaac, G. L., eds., *After the Australopithecines: The Hague*, Mouton, p. 99–188.
- , 1977, Pleistocene land-sea correlations: *Earth-Science Reviews*, v. 13, p. 307–374.
- , 1987, Loess stratigraphy in central China: *Quaternary Science Reviews*, v. 6, p. 191–219.
- , 1989, Long continental records of climate: An introduction: *Palaeogeography, Palaeoclimatology, Palaeoecology*, v. 72, p. 1–9.
- Kukla, G., and An, Z., 1989, Loess stratigraphy in central China: *Palaeogeography, Palaeoclimatology, Palaeoecology*, v. 72, p. 203–225.
- Kukla, G., and 5 others, 1988, Pleistocene climates in China by magnetic susceptibility: *Geology*, v. 16, p. 811–814.
- Lyell, C., 1839, *Nouveaux elements de geologie*: Paris, Pitois-Levrault, 648 p.
- Mankinen, E. A., and Dalrymple, G. B., 1979, Revised geomagnetic polarity time scale for the interval 0–5 m.y. B.P.: *Journal of Geophysical Research*, v. 84, no. B2, p. 615–626.
- Matthews, R. K., and Poore, R. Z., 1981, Tertiary delta ¹⁸O record and glacio-eustatic sea-level fluctuations: *Geology*, v. 8, p. 501–504.
- Mix, A. C., 1987, The oxygen-isotope record of glaciation, in Ruddiman, W. F., and Wright, H. E., Jr., eds., *North America and adjacent oceans during the last deglaciation*: Boulder, Colorado, Geological Society of America, *The Geology of North America*, v. K-3, p. 111–135.
- Morrison, R. B., 1968, Means of time-stratigraphic division and long-distance correlation of Quaternary successions, in Morrison, R. B., and Wright, H. E., Jr., eds., *Means of correlation of Quaternary successions*; Proceedings INQUA 7th Congress, v. 8: Salt Lake City, University of Utah Press, p. 1–113.
- , 1978, Quaternary soil stratigraphy; Concepts, methods, and problems, in Mahaney, W. C., ed., *Quaternary soils: Norwich, United Kingdom*, Geoabstracts, p. 77–108.
- , 1987, Long-term perspective; Changing rates and types of Quaternary surficial processes; Erosion-deposition-stability cycles, in Graf, W. R., ed., *Geomorphic systems of North America*: Boulder, Colorado, Geological Society of America, Centennial Special Volume 2, p. 167–176.
- Odin, G. S., ed., 1982, *Numerical dating in stratigraphy*, 2 vols.: New York, John Wiley and Sons, 1,040 p.
- Richmond, G. M., and Fullerton, D. S., 1986, eds., *Quaternary glaciations in the United States of America*, in Sibrava, V., Bowen, D. Q., and Richmond, G. M., eds., *Quaternary glaciations in the Northern Hemisphere*: Oxford, Pergamon Press, p. 3–200.
- Ruddiman, W. F., and Kidd, R., eds., 1986, *Initial reports of the Deep Sea Drilling Project*: Washington, D.C., U.S. Government Printing Office, v. 94, 1261 p.
- Ruddiman, W. F., and Wright, H. E., Jr., 1987a, Introduction, in Ruddiman, W. F., and Wright, H. E., Jr., eds., *North America and adjacent oceans during the last deglaciation*: Boulder, Colorado, Geological Society of America, *The Geology of North America*, v. K-3, p. 1–12.
- , eds., 1987b, *North America and adjacent oceans during the last deglaciation*: Boulder, Colorado, Geological Society of America, *The Geology of North America*, v. K-3, 501 p.
- Shackleton, N. J., 1969, The last interglacial in the marine and terrestrial records: *Royal Society of London Proceedings, series B*, no. 174, p. 135–154.
- Shackleton, N. J. and Opdyke, N. D., 1973, Oxygen isotope and paleomagnetic stratigraphy of equatorial Pacific core V27-238; oxygen isotope temperatures and ice volumes in a 10⁵ and 10⁶ year scale: *Quaternary Research*, v. 3, p. 39–55.
- , 1976, Oxygen-isotope and paleomagnetic stratigraphy of Pacific Core V28-239; Late Pliocene to latest Pleistocene, in Cline, R. M., and Hays, J. D., eds., *Investigation of Late Quaternary paleoceanography and paleoclimatology*: Geological Society of America Memoir 145, p. 449–464.
- Shackleton, N. J., and 16 others, 1984, Oxygen isotope calibration of the onset of ice-raftering and history of glaciation in the North Atlantic region: *Nature*, v. 307, p. 216–219.
- Sibrava, V., Bowen, D. Q., and Richmond, G. M., eds., 1986, *Quaternary glaciations in the Northern Hemisphere*; *Quaternary Science Reviews*, v. 5: Oxford, Pergamon Press, 511 p.
- Slemmons, D. B., Engdahl, E. R., Blackwell, D., and Zoback, M. D., eds., 1990, *Neotectonics of North America*: Boulder, Colorado, Geological Society of America, *Decade of North American Geology Map Volume* (in press).
- Srivastava, S., and Arthur, M. A., 1987, *Proceedings of the Ocean Drilling program, Part A (Leg 105)*: Washington, D.C., U.S. Government Printing Office, 917 p.
- Willman, H. B., and Frye, J. C., 1970, Pleistocene stratigraphy of Illinois: *Illinois Geological Survey Bulletin* 94, 204 p.
- Wright, H. E., Jr., and Frey, D. G., 1965, *The Quaternary of the United States*: Princeton, New Jersey, Princeton University Press, 922 p.
- Wright, H. E., Jr., and Porter, S. C., eds., 1984, *Late Quaternary environments of the United States*, 2 vols.: Minneapolis, University of Minnesota Press, v. 1, 407 p., v. 2, 277 p.
- Zimmerman, H., and others, 1985, History of Plio-Pleistocene climate in the northeast Atlantic, Deep sea Drilling Project Hole 552A, in Roberts, D., and others, eds., *Initial reports of the Deep sea Drilling Project*: Washington, D.C., U.S. Government Printing Office, v. 81, p. 861–875.

MANUSCRIPT ACCEPTED BY THE SOCIETY APRIL 3, 1990

ACKNOWLEDGMENTS

I am indebted to the following geologists for reviewing preliminary versions of this chapter: Whitney Autin, Jules DuBar, William Dupré, Thomas Gustavson, Vance Holliday, George Kukla, Harold Malde, Richard Madole, Martin Mifflin, Pete Palmer, Marith Reheis, and Andre Sarna-Wojcicki. Their comments helped greatly. I also thank Aileen Jeffries for the computer printout of Figure 4.